SBUF

2018

FEM case study on
existing reinforced concrete buildings

Influence of cutout openings size in reinforced concrete walls

LULEÅ UNIVERSITY OF TECHNOLOGY

European Network for Durable Reinforcement and Rehabilitation Solutions

SKANSKA

Cristian SABAU, Cosmin POPESCU, Gabriel SAS, Luleå University of Technology
Thomas BLANKSVÄRD, Skanska Sverige AB

1 Abstract

New openings are nowadays often required to allow improvements in existing buildings, interior functionality and operational efficiencies. However, these new openings reduce the structural performance, prompting the need for strengthening. While new openings are created in walls, beams and slabs have been shown to significantly reduce their performance, the influence of new openings at the structural level has rarely been studied and for structural walls is mostly focused on the seismic performance.

Recently, new strengthening solutions for reinforced concrete walls with cutout openings using composite materials have been investigated with promising results in experimental tests carried out in half-scale wall panels (Popescu et al. 2017; Sabau et al. 2018; SBUF 13246 2018). Due to uncertainties related to the influence of cutout openings at the structural level, it is not immediately obvious that such solutions are viable in practice.

This report presents a case study on an existing 11-storey reinforced concrete residential building performed through a numerical analysis by the finite element method (FEM) using the commercial software Atena (Cervenka Consulting 2018). The report first describes the verification of the FEM modelling approach against experimental tests. Further, the studied building is modelled to investigate the considered parameter, namely the size of cutout openings that are created in structural walls. Furthermore, combinations of openings having different sizes at two consecutive stories is investigated. The results obtained from the FEM analysis are used to quantify the influence of openings on the service limit state determined by deflections and crack openings according to ACI 318 (2011), and the ultimate limit state of the building in determined by concrete crushing and yielding of steel reinforcement according to EC 2 (2005). Finally, the need for interventions and possible strengthening solutions using composite materials are discussed.

This work represents a phase in the SBUF 13246 (2018) project, namely Phase 5, in which the influence of cutout openings at a structural level was evaluated. On overview of the entire project is given bellow. In Phase 1 existing studies on the RC walls with opening as well as studies for possible strengthening methods have been reviewed. In Phase 2 an experimental study that employed a non-contact digital image correlation monitoring system was carried out to peer into the structural behaviour of reinforced concrete walls with cutout openings. In Phase 3, strengthening solution for axially loaded walls were experimentally investigate and in Phase 4 a design method for FRP strengthened walls was developed.

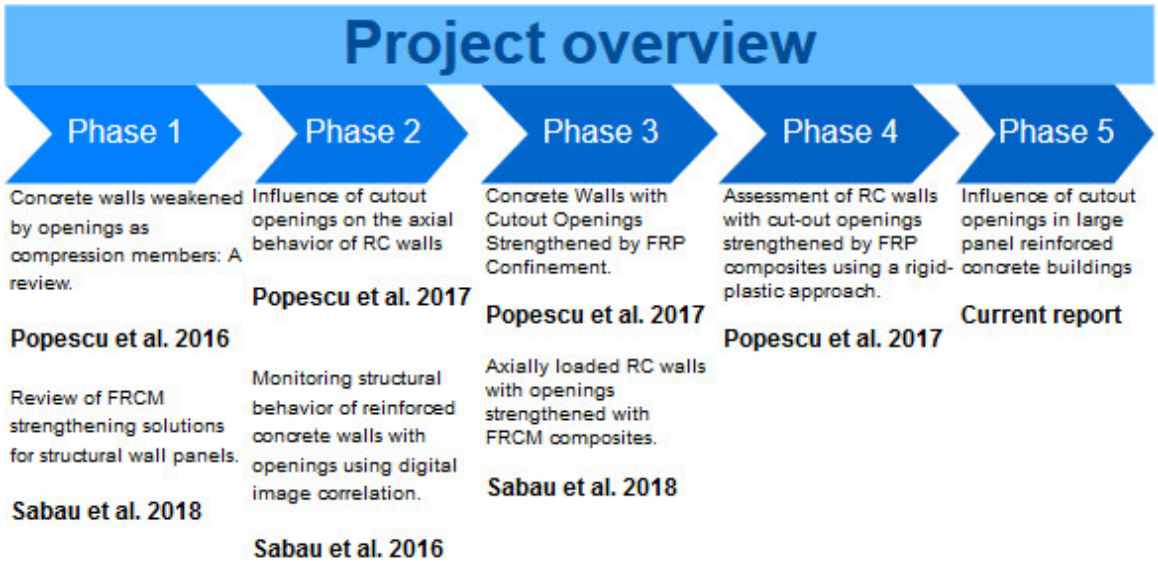

Keywords: non-linear FEM, reinforced concrete, building, walls, openings, assessment

2 Sammanfattning

Håltagning i befintliga konstruktioner är någon som är vanligt förekommande i betongkonstruktioner nu för tiden. Anledningarna är många men i de flesta fall beror detta på att förutsättningarna ändras med tiden och därmed förutsätter att den befintliga utformningen förändras. Den här typen av håltagningar kan i många fall förändra den strukturella funktionen och genomförandet av sådana förändringar kräver ofta reparations- eller förstärkningsåtgärder. Hur den strukturella funktionen påverkas i större sammanhang för en hel byggnad har inte studerats i någon större utsträckning i samband med håltagning.

Nyliga experimentella studier på förstärkningssystem i samband med håltagning i väggar och hur dessa kan förstärkas har genomförts vid Luleå Tekniska Universitet. Dessa studier omfattar väggelement i halv skala med och utan håltagning, (Popescu et al. 2017; Sabau et al. 2018; SBUF 13246 2018). Dessa studier visar att det går att förstärka betongväggar i samband med håltagning. Dock är det inte helt uppenbart att se hur en eventuell håltagning, lokalt, påverkar det strukturella systemet i en byggnad, globalt.

Den här rapporter redovisar en fallstudie på ett 11-våningshus i armerad betong som simulerats med finita element metod (FEM) och då särskilt genom mjukvaran Atena (Cervenka Consulting 2018). Först beskrivs en verifiering av FEM modelleringen mot de experimentella studierna och sedan simuleras en hel byggnad och hur denna påverkas i samband med håltagning. Fallstudien är byggd som en parameterstudie där olika utformningar på håltagningar i bärande väggar undersökts tillsammans med variationen om håltagningarna sker på olika våningsplan. Resultaten från FEM simuleringarna används för att kvantifiera hur håltagningar påverkar bruksgränstillstånd, nedböjning och sprickvidd, samt brottgränstillstånd, flytning i armering. Slutligen diskuteras olika behov av åtgärder i samband med håltagning och möjliga reparations- och förstärkningsåtgärder kopplat till de experimentella studierna.

Den här rapporten representerar en av faserna i SBUF projekt 13246, nämligen fas 5. Denna fas undersöker alltså hur håltagning påverkar en byggnad som ett sammansatt konstruktionssystem. En överblick över hela SBUF projektet är redovisat nedan. Fas 1 består av en genomförandestudie på betongväggar i samband med håltagning samt möjliga reparations- och förstärkningssystem. Fas 2 omfattar experimentella studier för att undersöka icke-berörande mätmetoder för att kunna mäta väggelementens strukturella beteende på en större skala, de metoder som undersökt är fotometrisk töjnings och deformations mätning (Digital Image Correlation, DIC). Fas 3 omfattar experimentella studier på axiellt belastade väggar med och utan håltagning samt olika reparations- och förstärkningsmetoder av väggelement i samband med håltagning. Fas 4 omfattar en teoretisk modell för dimensionering av betongväggar i samband med FRP förstärkning.

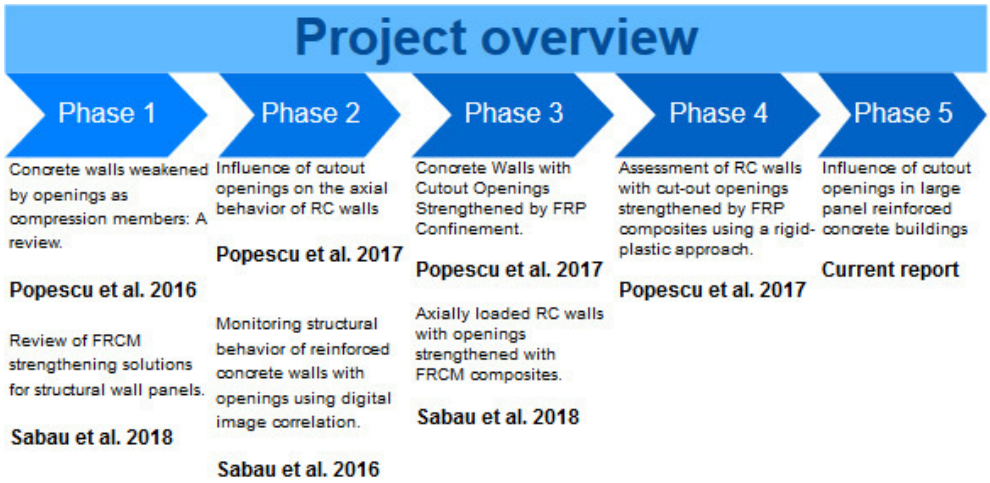

Nyckelord: icke-linjär FEM, armerad betong, väggar, håltagning, tillståndsbedömning

3 Notations

Latin upper case letters

A_c	Cross section area (m^2)
A_0	Cross section area of an opening (m^2)
E_{cm}	Secant modulus of elasticity of concrete (MPa)
E_c	Modulus of elasticity of concrete (MPa)
E_s	Modulus of elasticity of reinforcement (MPa)
F_T	tensile strength (MPa)
F_C	Compressive strength (MPa)
G_F	Fracture energy (N/m)
H	Height of the wall (m)
H_0	Height of an opening (m)
L	Length of the wall (m)
L_0	Width of an opening (m)

Latin lower case letters

a_g	Aggregate size (mm)
c_{ts}	Tension stiffening factor (-)
e	Eccentricity of the load (mm)
f_{cm}	Mean cylinder compressive strength for concrete (MPa)
$f_{cm,cube}$	Mean cube compressive strength of concrete cubes(MPa)
f_y	Mean yield strength for reinforcement (MPa)
f_u	Mean tensile strength in the reinforcement (MPa)
f_y	Yield strength of steel reinforcement (MPa)
f_c	Concrete compressive strength (MPa)
f_t	Concrete tensile stress of concrete (MPa)
f_{c0}	Onset of crushing (MPa)
w_d	Critical compressive displacement (m)
$f_{c,reduct}$	Reduction of compressive strength (-)
X,Y,Z	Coordinates (mm)

Greek lower case letters

ε_c	Strain in the concrete (-)

ε_{cu}	ultimate concrete compressive strain (-)
ε_{y}	Mean yield strain in the reinforcement (-)
ε_{cp}	Concrete plastic strain (-)
ø	Diameter of reinforcement bar (m)
Δ_1	instant deflection limit under load (mm) (ACI 318 2011)
Δ_2	deflection limit under quasi-permanent loads (mm) (EC 2 2005)

4 Abbreviations

ACI	American Concrete Institute
AS	Australian Standard
BS	British Standard
EC 1	Eurocode 1 - EC 1 (2002)
EC 2	Eurocode 2 - EC 2 (2005)
EC 3	Eurocode 3 - EC 3 (2004)
FEM	Finite element method
FEA	Finite element analysis
RC	Reinforced concrete
SHS	Square hollow section
SLS	Serviceability limit state
ULS	Ultimate limit state
FRCM	Fabric reinforced cementitious matrix composite
FRP	Fibre reinforce polymer
COD	Crack opening displacement

Table of Contents

1 Introduction

1.1 Background

Reinforced concrete (RC) walls are one of the most reliable load resisting structural systems used for buildings. Concrete has good mechanical properties in terms of resistance, rigidity (particularly compression) and durability, therefore use of concrete for walls in tilt-up construction, shear walls and concrete core in buildings has increased over the years. In addition, RC walls provide increased lateral stiffness that adds stability to high rises structures, thus providing higher resistances to later forces generated by wind and earthquakes compared to RC frame structures. Currently a consistent share of the building stock is consists of reinforced concrete buildings and it is common that functional modifications need to be made on the building to adapt to the development of the society. Examples of such modifications could be that apartments are old and a modernization is needed or that the function of the building can be changed, for example a residential building is converted to an office building or a modern heat recovery ventilation systems is retrofitted to the building to increase the energy efficiency Figure 1. It is more beneficial both from an economical and environmental perspective to modify an existing buildings than to demolish and replace them with new buildings. These modifications lead to new openings being necessary to be made in the buildings load bearing elements.

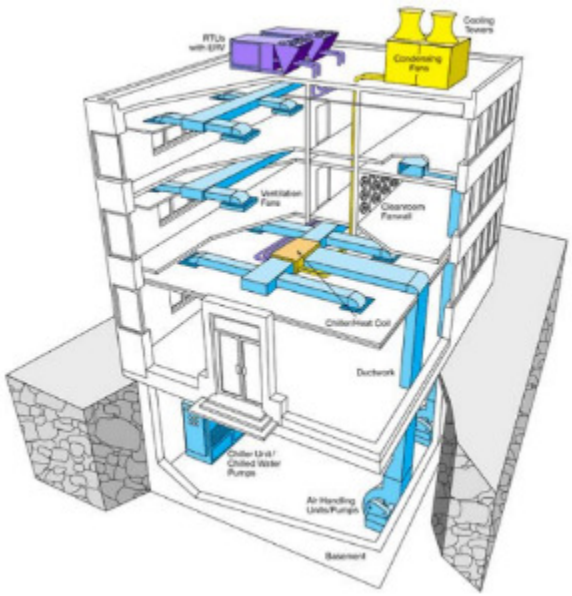

Figure 1 Example of HVAC system retrofiting plans (Willwerth 2013)

Openings can be divided into three types, already existing openings, existing openings that have been enlarged and newly created openings (Popescu et al. 2015). Openings in a RC wall were shown to affect the load bearing capacity and failure mode of the wall (Fragomeni et al. 2012; Lee et al. 2008; Popescu et al. 2016; Saheb and Desayi 1990). However, the influence cutout openings have at the structural level has yet to be investigated. The design of RC walls with openings is done explicitly considering the size and location of the openings, such that additional reinforcement is provided in the spandrel and at the corners of the openings (EC 2 2005). However, this is not the case for RC walls with a cutout openings. When a cutout opening is created the existing reinforcement is cut off at the edges of the new opening. As the structural capacity and stress distribution in RC walls are changed when a cut out opening is made the wall need to be upgraded and traditionally two methods have been used to strengthen these types of walls. The methods are either to create a frame around the opening with either steel or RC members or to increase the cross-sectional thickness. These methods increase the weight of the wall and also limiting the use of the structure during repairs.

No design method for cut-out openings in RC walls exist in current design codes. Design methods for openings in newly built walls exist (EC 2 (2005), ACI 318 (2011), AS 3600 (2009) and BS 8110-1 (1997)), however are relatively succinct. For example, according to EC 2 (2005) RC walls with openings are designed similarly to a solid RC wall, by dividing the wall with openings into two solid elements each considered as a solid element. For solid elements, a simplified empirical design method for ultimate capacity and a method based on column theory that can be used to also determined deflection are provided. The simplified method becomes more limited when lateral loads needs to be considered. The column method provides a more accurate results (Popescu et al. 2016).

The size and location of the opening affects the stress distribution and structural capacity of the wall (Guan et al. 2010; Lee et al. 2008). It is generally believed that small openings can be neglected in the design of structural walls, while large opening have a significantly influence the structural capacity. EC 2 (2005) and AS 3600 (2009) provide limits for when an opening can be neglected and be designed as a solid concrete wall, however, there are no agreed limits between large and small opening exists in the scientific literature (Popescu et al. 2016).

The majority of the previous research was focused on the behaviour of solid walls and walls with openings as isolated structural members. These studies concluded that several factors can affect the behaviour of RC walls, such as boundary conditions, reinforcement, and load eccentricity. For example, for lateral restraints of provided by adjacent RC panels are replaced by steel frames in experimental tests and the loading is usually applied through a steel round bar and contact steel plates (Popescu et al. 2016). These simulated restrains, were observed to replicate reasonably well the expected failure modes and cracking pattern, however represent at best an idealisation of the actual condition. No studies have yet to address the influence of cutout openings in panels as part of complete structure and or the influence of cutout opening at the structural level.

This report presents the results of the structural assessment of a typical building structure through FEM (finite element method) analysis. The FEM-model of the building is used to evaluate the influence of a the cutout opening and their size on the behaviour of the structural panel as part of the structure.

1.2 Goal and objectives

The goal was to assess the influence of cutout openings created in structural RC walls as part of a buildings structure, and to assess the influence of the new opening on the global behaviour of the structure. The following steps were taken to achieve these goal:

- Verify that FEM-models of tested RC walls panels predict the experimentally obtained ultimate loads within ±10%.
- Create a FE-model of an existing RC building with RC walls structural system.
- Serviceability assessment of the modelled structures
- Assessment of the service limit capacity of the modelled structure
- Assessment of the ultimate capacity of the modelled structures

1.3 Limitations

This study is based on results from finite element simulation. The model is a detailed simulation of an existing building based on construction drawings. However, the model does not explicitly take into account any possible deviations and errors pertaining to the construction of the building, as well as time dependent effects, such as creep, shrinkage and degradation. The material properties used in the building model were derived using the prescription of EC 2 (2005) based on classes indicated in available drawings. Actual values for an existing building might vary. Further simplifications and assumption that were made in modelling process include: rigid connection were considered between adjacent solid elements; the reinforcement in tie beams and intersections was smeared over the entire elements volume; perfect bond was considered between steel reinforcement and concrete; reinforcement lap splices were not explicitly considered; and only the subassembly of the full structure where the cutout openings were created was modelled with non-linear elements, the rest of the building was modelled using linear elastic elements.

2 Finite Element Method (FEM)

Finite element method (FEM) is a numerical method for solving a differential or integral equation of engineering and mathematical physics also known as finite element analysis (FEA). Useful for problems with complicated geometries, loadings, and material properties where analytical solutions cannot be obtained. The method essentially consists of assuming the piecewise continuous function for the solution and obtaining the parameters of the functions in a manner that reduces the error in the solution.

The model body is divided into an equivalent system of many smaller bodies or units (finite elements) interconnected at points common to two or more elements (nodes) and boundary surfaces. To describe and interpolate the behaviour between the nodes a shape linear or quadratic shape function is used. The choice of shape function influences the accuracy of the solution (Ottosen and Petersson 1992). However, a linear shape functions provide good results provided that the body is divided in sufficient elements (i.e. small enough element size).

A non-linear FEA can simulate a more realistic behaviour of a structure compared to a linear analysis as it can consider the nonlinearities in material behaviour. The non-linear FEM is usually used as an analysis method, and not a design method. For example, RC structures can be modelled to account for tension cracking, non-linear behaviour of concrete in compression and reinforcement yielding. Models that account for those parameters can simulate a successive reduction of rigidity and a rearrangement of forces and stresses (Svenska Betongföreningen 2010). Material parameters and dimensions are defined using mean strength values in the FE model to generate a more accurate analysis (Svenska Betongföreningen 2010).

In a non-linear FEA, the load is applied gradually in so called load steps. A set of algebraic equations are obtained that are solved for unknown first nodal quantity, displacement. Secondary quantities (stresses and strains) are expressed in terms of nodal values of primary quantity. This procedure will be repeated until convergence is reached in the load step (Svenska Betongföreningen 2010), that is, equilibrium in terms of displacement, forces, energy, is achieved with acceptable error.

To reach convergence in the load step, the Newton-Raphson method is most commonly used, see Figure 2. The subsequent load steps are based on the slope of the curve at previous load step. This method is suitable when the response is steadily increasing, however it can face difficulties in determining the solution when the load response presents a snap-back behaviour.

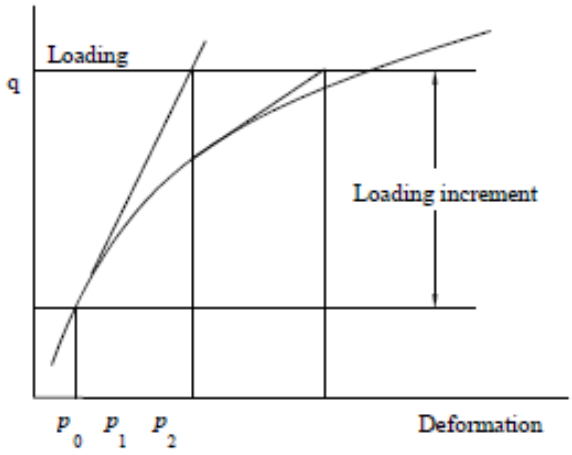

Figure 2 Newton Raphson method (Atena Theory Manual).

The Arc-Length method, see Figure 3, searches the next approximation of the solution at a radius of an arc from the last point. Thus to converge the solution both the load step increment and displacement are adjusted. However, usually the Arc-Length method is more computational demanding.

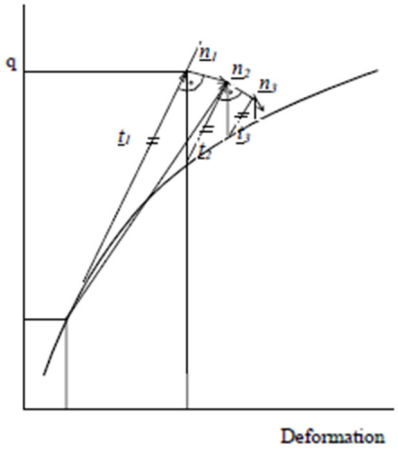

Figure 3 Arc-Length method (Atena Theory Manual)

3 Verification of FEA approach

3.1 Experimental test results

A more detailed description of the experimental test is described in (Popescu et al. 2016). The results of the experimental tests were used to verify the FEM modelling approach of the walls in the FEA software Atena (Cervenka Consulting 2018).

3.1.1 Geometry

The experimental tests were conducted on three RC walls with two different opening configurations. The three walls were designed to represent wall panels in residential buildings and they were designed in half scale and had all the same height, length and thickness. They were 1800 mm long, 1350 mm tall and 60 mm thick.

One wall was designed as a solid wall with no opening, one with a small symmetric opening (450 mm x 1050 mm) and one with a large symmetric opening (900 mm x 1050 mm). The solid wall was named I-C, the small opening wall I-S and the large opening wall I-L. In all three walls strain gauges and displacement sensors were installed according to Figure 4. The openings were introduce before casting the panels, however the reinforcement details was done considering the case of cut-out opening. The lateral displacement along the sides edges were also measured in one point 500 mm from the top of the wall and were called A1 and A2.

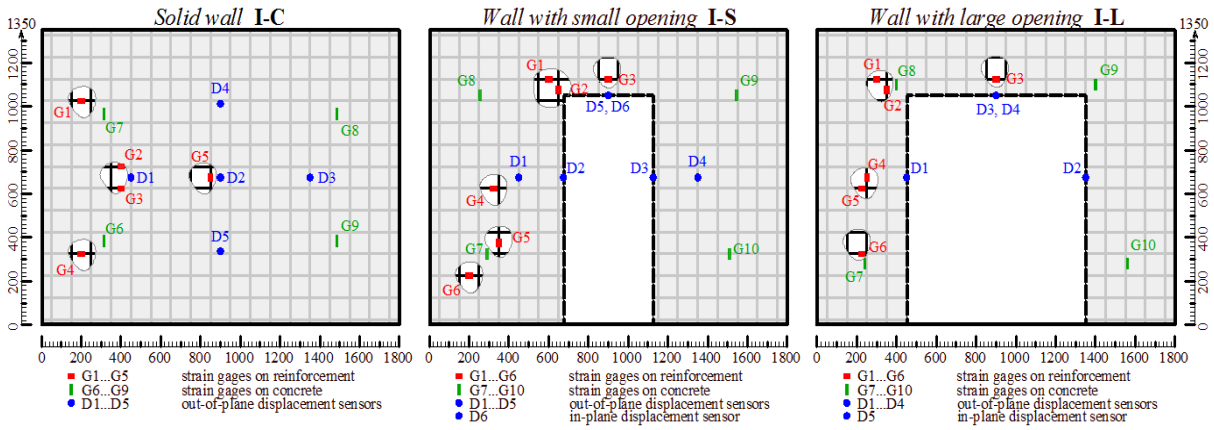

Figure 4 Instrumentation scheme and geometry of the walls, (Popescu et al. 2016).

3.1.2 Materials

3.1.2.1 Concrete

The concrete was mixed so that concrete class C32/40 was aimed for. In Table 1 is the mix proportion for the concrete mix is shown.

Table 1 Mix proportion of the concrete (Popescu et al. 2016)

Concrete class	w/c	Cement	Aggregate size		Additives
			1-4 mm	8-16 mm	
	-	(kg)	(kg)	(kg)	(%) of cement weight
C32/40	**0.55**	380	1030	630	**2.6**

From this concrete mix five concrete cubes were cast and tested. The average cubic strength $(f_{cm,cube})$ of the concrete was determined to be 62.8 MPa. Five concrete beams were tested to determine the fracture energy of the concrete, and the mean fracture energy (G_F) was decided to 168 N/m.

3.1.2.2 Steel Reinforcement

The internal reinforcement was provided by a welded steel mesh with bars of 5 mm in diameter and the spacing is 100 mm in both vertical and horizontal direction. From the reinforcement mesh five coupons were taken and their stress-strain properties were tested. The mean yield strength (f_y) was 632 MPa and the mean strain at this point (ε_y) was 0.28 %. Their mean tensile strength (f_u) was 693 MPa and the mean strain at this point (ε_u) was 4.87 %.

3.1.3 Test set-up

A steel reaction frame was designed to apply the load and restrain the walls. The frame was built up so that the top and bottom edges of the wall were supported as a hinged support along the whole edge. The supports along the side edges were built up so that the side edges of the wall were supported as a clamped support along the whole edges.

The wall was loaded with an eccentricity of one sixth of the walls thickness $(t_w/6)$ to simulate effects of imperfections that occur in normal construction practices and are accounted for in standards. To simulate this eccentricity a steel bar with a diameter of 22 mm was welded on the steel beams at the top and bottom of the loading frame, see Figure 5 below. The load was applied by four hydraulic jacks that act at the steel beam at the top of the wall.

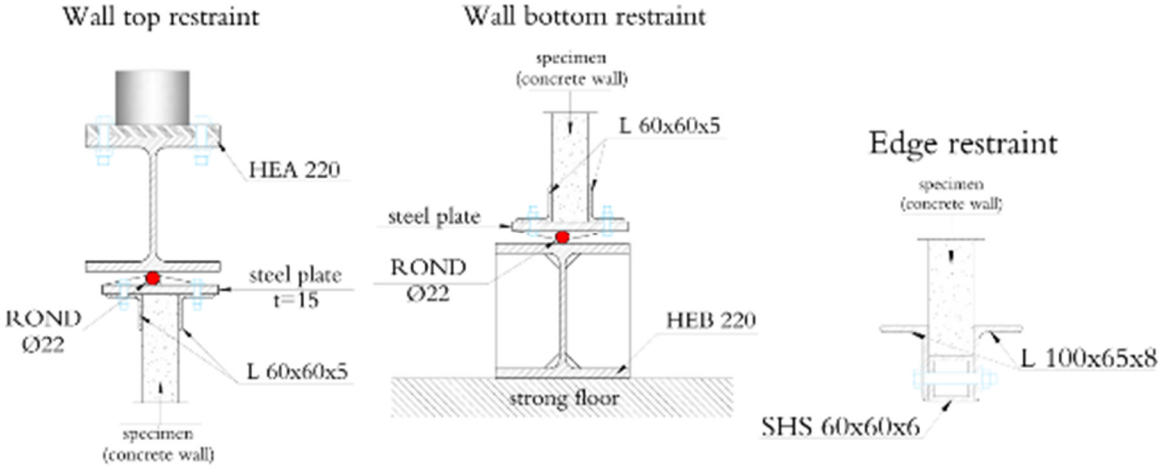

Figure 5 Supports at top and bottom and side edges of the wall, (Popescu et al. 2016).

The configuration with the steel rod allows the wall to rotate around the horizontal axis at the top and bottom edges and the steel beams prevent it from lateral translation. The strong floor prevents the bottom support from translation in vertical direction. A steel plate is placed between the steel rod and top and bottom edge of the concrete wall to prevent contact between concrete and steel rod.

To simulate the clamped support along the side edges of the wall an L-beam 100x65x8 was attached to an SHS 60x60x6. See Figure 5**.** The side support had to be made with sufficiently rigidity to prevent excessive out-of-plane deformations.

3.1.4 Test result

3.1.4.1 Solid wall

The failure of the solid wall occurred at 2.36 MN. The experimentally obtained results are presented in Figure 6. Out-of-plane displacements and reinforcement strains at failure are shown in Table 2. The maximum out of plane displacement occurred in D2 and was 19.0 mm. Compression strains at the measuring point G5 in the vertical reinforcement increased linearly up to failure load and showed a value of 0.4 ‰. The horizontal measuring points, G1-G4, showed linear tensile strains up to 60-70 % of the failure load. They were after this pronounced with yielding at failure and the maximum value at this point was 4.4 ‰. The gauges measuring compressive strains in the concrete showed a maximum of 3.0 ‰ in compressive strain at failure.

Table 2 Displacements and strains at failure for the experimental test, (Popescu et al. 2016).

Points	Value [mm]	Points	Value [mm/m]	Symmetry points	Mean value
D1	16.7	**G1**	4.4	**D1-D3**	16.4
D2	19.0	**G2**	3.1	**D4-D5**	12.3
D3	16.1	**G3**	3.0	**G7-G8**	-2.5
D4	11.9	**G4**	2.6	**G6-G9**	-2.8
D5	12.8	**G5**	0.4	**A1-A2**	-3.2
A1	-3.1	**G6**	-3.0		
A2	-3.3	**G7**	-2.5		
		G8	-2.4		
		G9	-2.5		

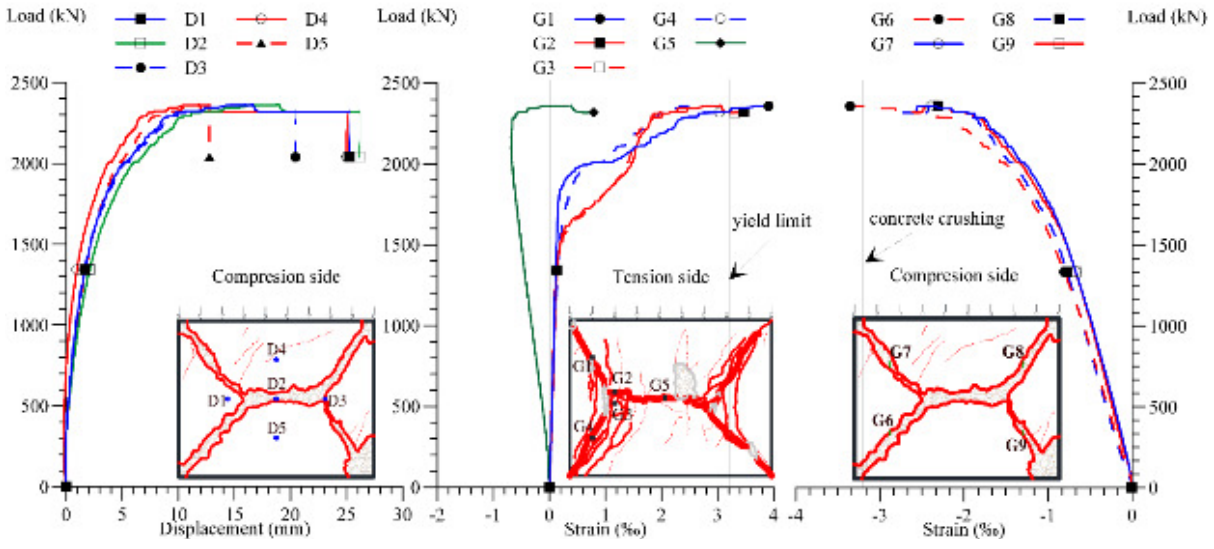

Figure 6 Responses of the solid wall (SW): a) load-displacement; b) Strain in steel reinforcement; c) Strain in concrete. D1-5 and G1-9 refer to displacement sensors and strain gauges, respectively at indicated positions, (Popescu et al. 2016).

The wall had a brittle failure due to crushing of concrete. Crack pattern for both tension and compression sides were as predicted for a wall restrained at all four sides, see Figure 7. Also several secondary tensile cracks were developed parallel to each other around the major tensile cracks which indicates that the reinforcement played an active role in de redistribution of the stresses in the concrete.

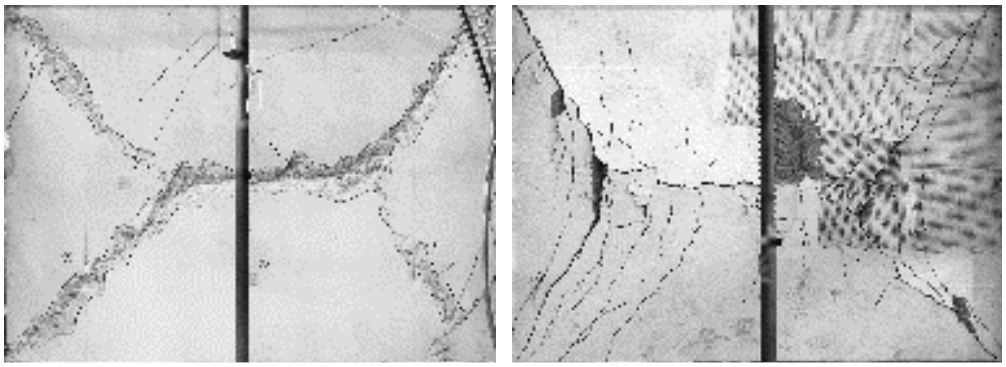

Figure 7 Crack pattern and failure mode of the solid wall. Compression side to the left and tension side to the right (Popescu et al. 2016)

3.1.4.2 Wall with small opening

The failure of the wall with small opening occurred at 1.50 MN. Out of place displacements and reinforcement strains at failure are shown in Table 3. The experimentally obtained results are presented in Figure 8. The maximum out of plane displacement was in D2 and it was 26.8 mm. The displacement were lower and developed more slowly in the left pier compared to the right pier. Moreover, failure primarily occurred in the right pier, immediately followed by the failure of the left pier. Vertical reinforcement strains were recorded by G2 and G5. The maximum reinforcement compressive strain at failure was 1.2 ‰ at location G2. Reinforcement strains recorded by G2 increased linear up to 90 % of failure load. All horizontal bars were subjected to tensile strains but the strains recorded in the strain gauges were relatively small up to 90 % of the failure load. Reinforcement yielding was recorded by G5 and G6, in the bars at failure with maximum strains of 2.6 and 3.0 ‰, respectively. The recorded strains increased linearly up to 85-90% of failure load at locations G1 and G4, and up to 40% of failure load at G3. At location G6 the strains were at first compressive strains and at about 70% of failure load they switched to tensile stresses. The maximum concrete compressive strain 2.7 ‰ was recorded at location G8. The recorded concrete strains were below the limit of concrete crushing, suggesting that the wall failed by loss of stability. However, strain gage readings have a local nature, and might not have recorded the maximum strain of the element.

Table 3 Displacements and strains at failure for the experimental test

Points	Value [mm]	Points	Value [mm/m]	Symmetry points	Mean value
D1	22.9	**G1**	0.6	**D1-D4**	18.8
D2	26.8	**G2**	-1.2	**D2-D3**	22.7
D3	18.6	**G3**	1.4	**G8-G9**	-2.5
D4	14.7	**G4**	2.6	**G7-G10**	-0.6
D5	14.6	**G5**	0.1	**A1-A2**	-2.9
D6	6.6	**G6**	3.0		
A1	-3.3	**G7**	-0.7		
A2	-2.6	**G8**	-2.7		
		G9	-2.4		
		G10	-0.6		

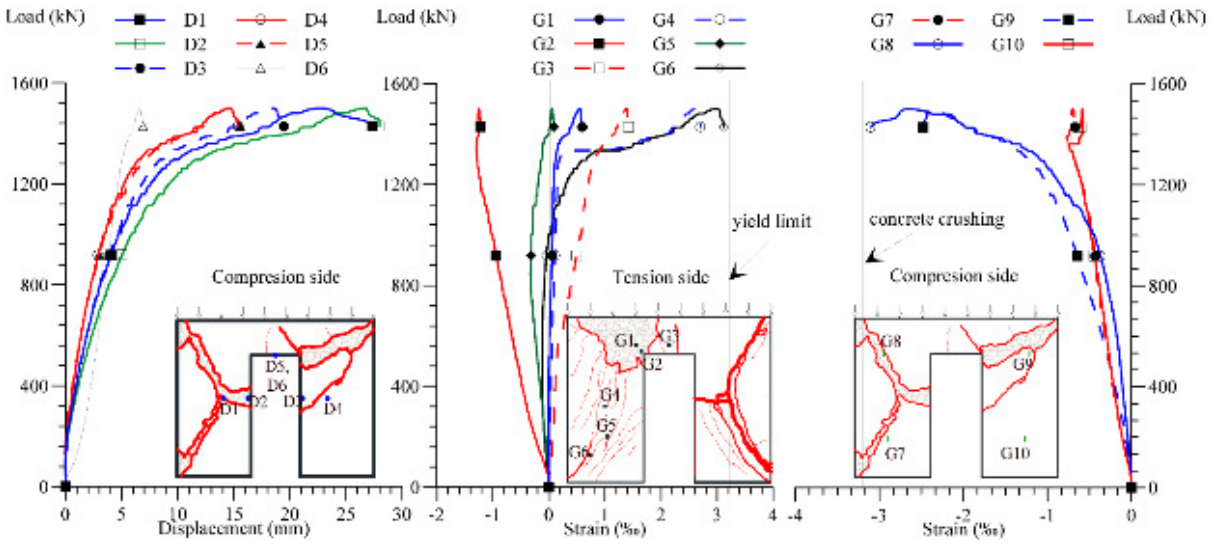

Figure 8 Responses of the wall with a small opening (SO): a) load-displacement; b) strain in steel reinforcement; c) strain in concrete. D1-6 and G1-10 refer to displacement sensors and strain gauges, respectively at indicated positions.

The wall had a brittle failure due to crushing of concrete with spalling and reinforcement buckling. This occurred along the line between the corner of the opening and the corner of the wall. The pier on the other side of the opening failed immediately after with a typical crack pattern as for walls restrained on three sides, see Figure 9.

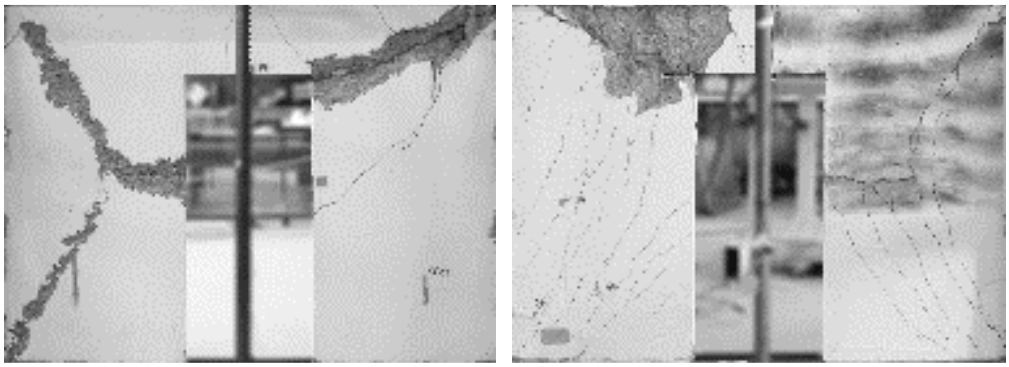

Figure 9 Crack pattern and failure mode of the wall with small opening. Compression side to the left and tension side to the right, (Popescu et al. 2016).

3.1.4.3 Wall with large opening

The failure of the wall with large opening occurred at 1.18 MN. Out of plane displacement and reinforcement strains at failure are shown in Table 4. The experimentally obtained results are presented in Figure 10. The maximum out of plane displacement of 11.4 mm was recorded at location D2. Failure occurred in the left pier, immediately followed by the failure of the right pier. Vertical reinforcement strains were recorded by G2 and G4. A maximum compressive strain of 1.7 ‰ was recorded by G2 at failure. The strain increased linearly up to failure. All horizontal bars were subjected to tensile strains. Yielding was recorded at location G3 with strains of 3.2 ‰. Strains increased linearly up to 80-90% of failure load except for G3 where the strains started to increase rapidly at 45% of failure load. The maximum concrete compressive strain 3.9 ‰ was recorded at location G8. The recorded concrete strains were below the limit of concrete crushing, suggesting that the wall failed by loss of stability. However, strain gage readings have a local nature, and might not have recorded the maximum strain of the element.

Table 4 Displacements and strains at failure for the experimental test

Points	Value [mm]	Points	Value [mm/m]	Symmetry points	Mean value
D1	8.7	**G1**	0.6	**D1-D2**	10.0
D2	11.4	**G2**	-1.7	**A1-A2**	-2.6
D3	9.5	**G3**	3.2	**G8-G9**	-2.3
D4	7.4	**G4**	-0.9	**G7-G10**	-1.3
A1	-1.7	**G5**	1.9		
A2	-3.5	**G6**	2.5		
		G7	-1.1		
		G8	-3.9		
		G9	-0.7		
		G10	-1.6		

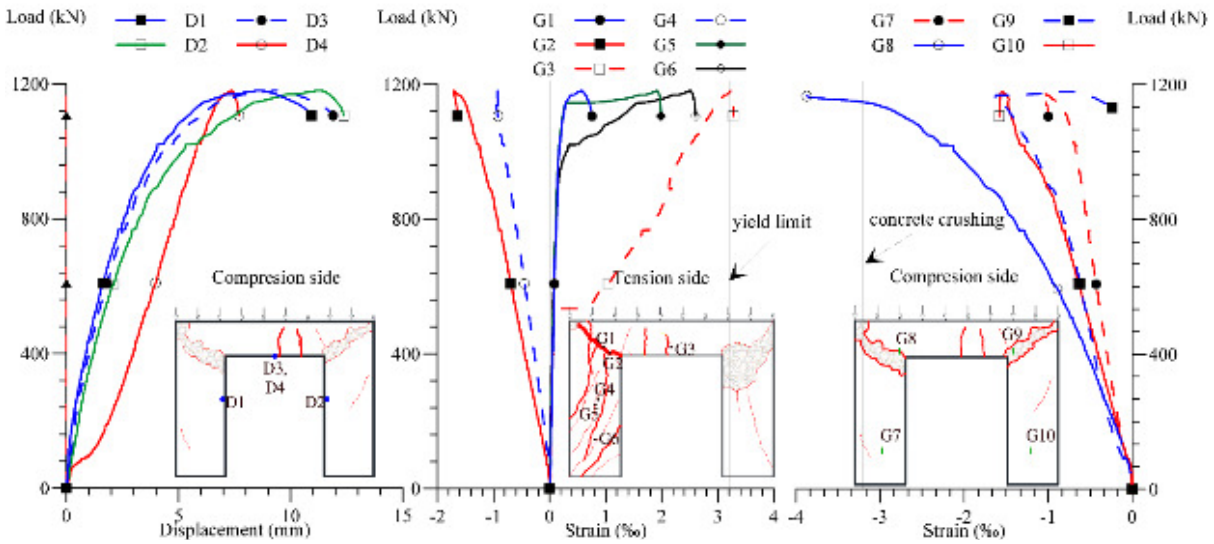

Figure 10 Responses of the wall with a large opening (LO): a) load-displacement; b) strain in steel reinforcement; c) strain in concrete. D1-4 and G1-10 refer to displacement sensors and strain gauges, respectively at indicated positions, (Popescu et al. 2016).

The wall had a brittle failure due to crushing of concrete with spalling and reinforcement buckling, see Figure 11. This occurred along the line between the corner of the opening and the corner of the wall as in the wall with small opening.

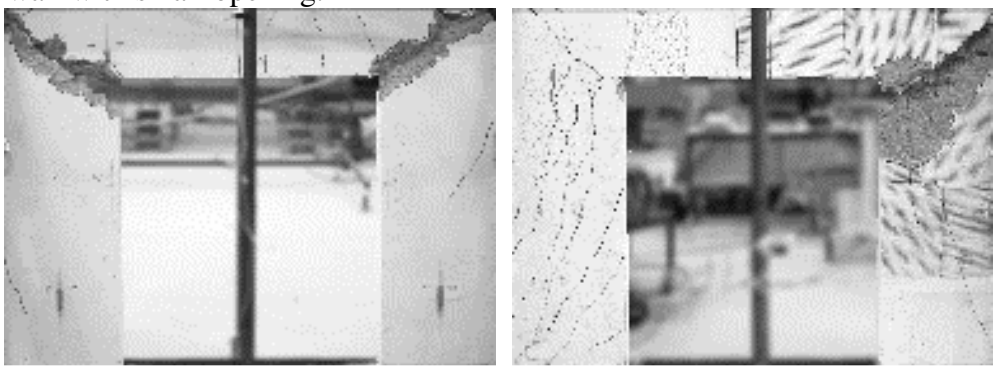

Figure 11 Crack pattern and failure mode of the wall with large opening. Compression side to the left and tension side to the right, (Popescu et al. 2016)

3.2 FEA of tested wall panels

3.2.1 Model formulation in ATENA

To obtain an accurate FEM-model a first benchmark process was performed (Jansson and Svensson 2016). The process was further refined by updating boundary conditions to more accurately represent the actual conditions during testing. The refinement process was aided by full field strain and displacement obtained using digital image correlation available in Sabau et al. (2016) and Popescu et al. (2016). The FEA software used in this process was ATENA Science (Cervenka Consulting 2018). ATENA Science is an advanced program for non-linear analysis of reinforced concrete structures. This product can simulate structural behaviour in statics, dynamics, creep and thermal and moisture transport. ATENA Science consists of two parts, GiD and ATENA Studio. GiD (CIMNE 2018) is a universal, adaptive and user-friendly pre-processor for numerical simulations in science and engineering. ATENA Studio is simple and intuitive user interface for ATENA solution core. It is unified environment for all analysis types: 2D, 3D, statics, dynamic, creep, heat & moisture transport.

3.2.1.1 Geometry

The walls were modelled using 3D solid elements since out-of-plane deformations that cannot be captured by a 2D analysis were expected. To reduce the computational effort, only half the walls geometry was modelled as permitted by the elements symmetry. The used finite element size, also known as mesh size, was 10:20:20 mm. This was chosen based on results of Jansson and Svensson (2016) where a mesh sensitivity study was carried out.

The solid panel was modelled with 6 volumes as shown in Figure 12. The wall with small opening was obtained by removing the volume corresponding volume, indicated in Figure 12 with yellow colour. The wall with large opening was obtained by removing the two volumes corresponding to the small and large opening, volumes indicated in Figure 12 with yellow and blue colours. The load was applied trough a 5mm steel plate. Fixed contacts between the surface of the steel plates and the concrete volumes were defined, and are further described in Section 3.2.1.2 “Boundary conditions”. The width of the plate was equal to the thickness of the wall. The load applied at considering an eccentricity relative to the centre of the concrete section of 10mm ($t_w/6$), as considered in the experimental tests.

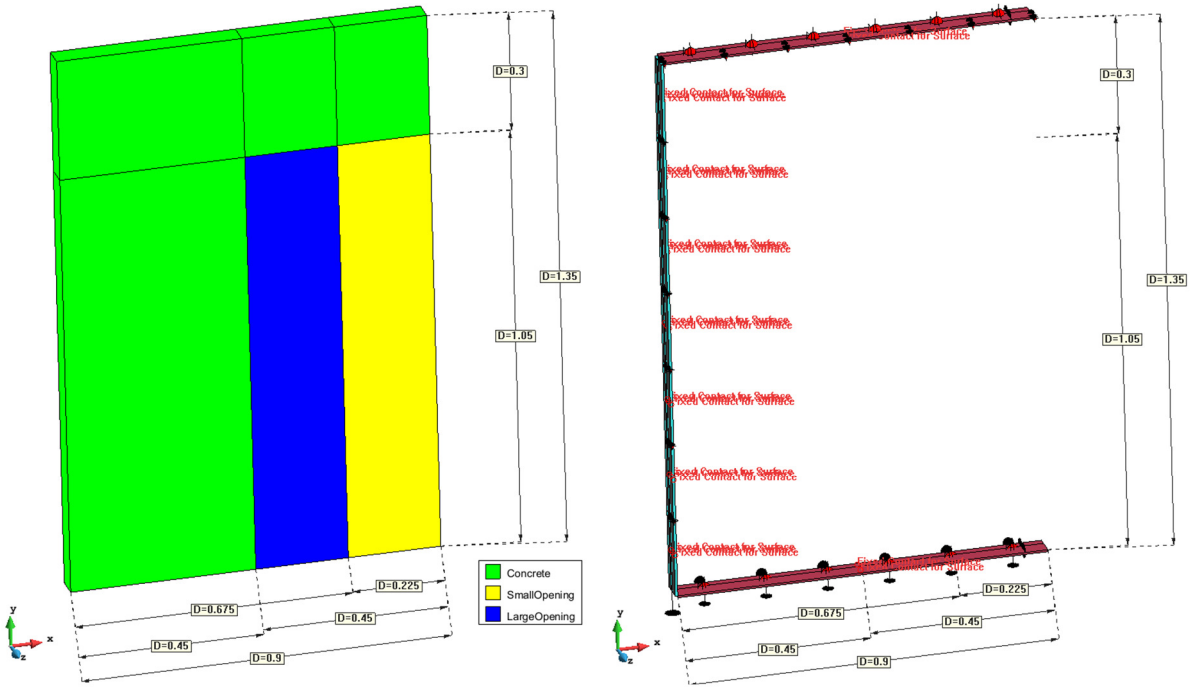

Figure 12 Geometry of wall models, concrete volumes (left) and steel plates and boundary conditions (right).

The wall has centric reinforcement in both horizontal and vertical direction, Figure 13. The reinforcement bars are modelled as lines assigned with 1D-properties, thus they only can take axial forces. The distance between the bars and the diameter of the bars are similar to tested walls.

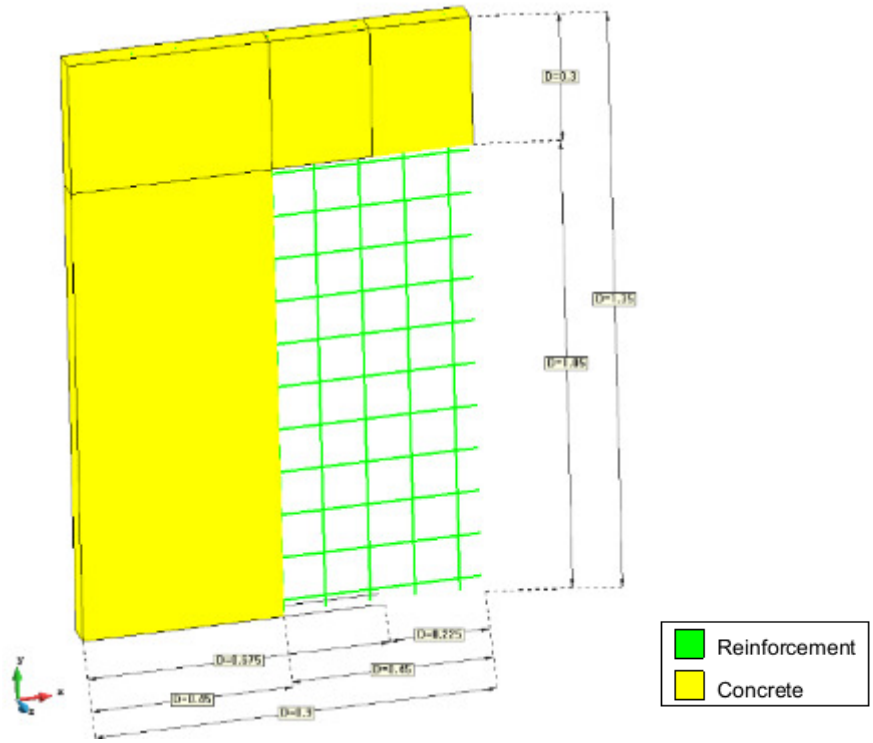

Figure 13 Reinforcement bars in horizontal-and vertical direction.

3.2.1.2 Boundary conditions

Solid volume plates of 5 mm thickness are connected to the three edges of the concrete volumes (except for the symmetry axis) using fixed contact for surface conditions in the Z and Y direction (i.e. the sliding of the wall along the top and bottom support is permitted). The side support plate is connected to the concrete volume using a fixed contact for surface in the Z and X direction (i.e. sliding of the wall relative to the lateral support is permitted, as observed experimentally).

The top and bottom steel plates are constrained along the load application line representing the support bar. The out of plane displacement (Z) are restrained at the top and bottom support plates, and the vertical in plane displacement and the out of plane displacement (Y and Z, respectively) are restrained at the bottom support.

The side support is restrained using 8 “spring for point” conditions applied on the outer side and in the middle of the plate. All springs were assigned the same stiffness value. The value of the stiffness was calibrated to match the average out-of-plane displacement measured on the test rig (A1 and A2). At the symmetry line a surface constraint in the X direction was applied for the concrete volume and the steel volumes.

The load was applied as an incremental vertical displacement in y-direction. The displacement steps used were 0.1 mm and a maximum number of 100 step were applied to ensure the failure of the modelled walls. The chosen solution method was Newton-Raphson. By applying the load in displacement rather than load control, allowed the use of the Newton-Raphson solution method to also obtain the behaviour of the modelled panel even after the maximum capacity was achieved (i.e. post peak behaviour).

3.2.1.3 Materials

To specify the concrete material properties, the CC3DNonLinCementitious2 material model was used. This material prototype is fully incremental (Cervenka Consulting 2018). The constitutive models for tensile (fracturing) and compressive (plastic) behaviour of concrete are combined in the fracture-plastic model that is used. This model is based on the classical orthotropic smeared crack formulation and crack

band model (Cervenka et al. 2014). The model is based on the Rankine failure criterion (Rankine 1857) and exponential softening (Cervenka et al. 1995). The model can be used for fixed or rotated crack model. The hardening/softening plasticity model is based on Menétry-Willam failure surface (van Mier 1986). A return-mapping algorithm is used for the integration of constitutive equations that can treat the combination of the two models. The algorithm also works when physical changes occur such as crack closure. The material model can simulate concrete cracking, crushing under high confinement and crack closure due to crushing in other material directions.

De Borst (1986) referred in Cervenka et al. (2014) developed a method of strain decomposition that could combine fracture and plasticity models. That method guarantees a solution for all magnitudes of strain increment. The algorithm that combines both models cannot reach convergence in certain cases for example for softening and dilating materials. The algorithm is therefore extended by a variation of the relaxation method (iterative) to stabilize convergence, Cervenka et al. (2014).

The values for the material properties are based on experimentally obtained properties mechanical properties. However, they were adjusted to account for the conditions observed for the tested members and are presented in Table 5 . The material parameters were the same as describe in Jansson and Svensson (2016),where a detailed explanation for each value parameter is given, a summary is available in Table 5 and Table 6.

Table 5 Concrete model material input parameters

Description	Notation and value	Details
Elastic modulus	$E_c = 32000\ MPa$	$E_c = \left(6000 - 15.5 f_{cm,cube}\right)\sqrt{f_{cm.cube}}$
Tensile strength	$F_t = 1.9\ MPa$	$F_t = \left(\frac{1}{2}\right)^{*} 0.24 f_{cm.cube}^{2/3}$
Compressive strength	$F_c = -53.4\ MPa$	$F_c = -0.85 f_{cm.cube}$
Fracture energy	$G_F = 4.74 \cdot 10^{-5}\ MN/m$	$G_F = 0.000025 F_t$
Plastic strain	$\varepsilon_{cp} = -0.00167$	$\varepsilon_{cp} = F_c / E_c$
Onset of crushing	$f_{c0} = -3.98\ MPa$	$f_{c0} = min\left\{-2.1 F_t; \frac{2}{3} F_c\right\}$
Critical compressive displacement	$w_d = -0.0008\ m$	Value recommended by software developer
Reduction factor of compressive strength	$f_{c,reduct} = 0.2$	Recommend value based on the modified compression field theory
Aggregate size	$a_g = 16\ mm$	According to the concrete mix used
Poisson's ratio	$\upsilon = 0.2$	Recommended value for normal concrete
Tension stiffening factor	$c_{ts} = 0.01$	Recommend value for lightly reinforced concrete

*50% reduced tensile strength to consider concrete shrinkage

Table 6 Reinforcement model material input parameters

Description		Notation and value
Mean yield strength	➔	$f_y = 632\ MPa$
Mean yield strain	➔	$\varepsilon_y = 0.0028$
Mean tensile strength	➔	$f_u = 693\ MPa$
Mean tensile strain	➔	$\varepsilon_u = 0.0487$
Elastic modulus	➔	$E_s = f_y / \varepsilon_y = 226\ GPa$

3.2.2 FEA compared to experimental test

. Displacement monitors were defined and named according to the experimental test program see Figure 4. In the experimental test program there were symmetry points, thus experimental displacement measurements were on both sides with respect to the walls' symmetry line. Therefore, the FEA results are compared to all out-of-plane displacement measurements.

3.2.2.1 Solid wall

In Figure 14 the load-displacement response at point D1 is presented. The ultimate load for the solid wall in the experimental test was 2.36 MN compared to 2.18 MN from FEA. Thus, FEA gives a 7.4 % lower ultimate load compared to the one obtained experimentally.

Table 7 Table 6: Displacements from experimental test and FEM-analysis for the solid wall.

Displacements	D1	D3	D2	D4	A1	A2
Experimental test [mm]	16.7	16.1	19.0	11.9	-3.1	-3.3
FEM-analysis [mm]	8.38		9.37	9.11	-4.1	
Difference [%]	-39.2	-36.9	-39.7	-28.8	9.5	2.0

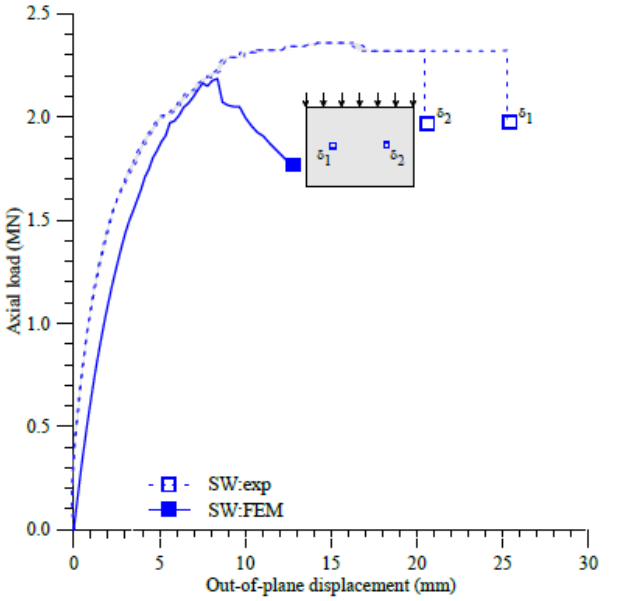

Figure 14 Load-displacement response in point D1 both for experimental test and FEM-analysis for the solid wall.

The difference for the displacement at points D1, D2, D3 and D4 are between 28.8% and 39.7% lower for FEA than for the experimental test. The difference in points A1 and A2 are 9.5% and 2.0% higher respectively in the FEM-analysis. Moreover, up to about 80% of failure load, the experimentally load displacement response differs from the one FEA obtained response, such that it shows an initially higher stiffness. However, close to the maximum capacity the experimental and FEA response coincide. After this point, experimental measurements show large out-of-plane displacements while the load is relatively constant from the experimental curve, whereas the FEA shows that after maximum, the applied load steadily decreases with the increase in the deflection. This suggest that experimentally, a loss of stability of a failure mode occurred, with sudden out-of-plane displacements at the moment of failure. The experimentally obtained response indicates a ductile failure mode with the element maintaining its load bearing capacity at higher out-of-plane displacements. However, this observation might be misleading. The FEA was not able to capture the dynamic part of the, failure mode in the same way. Although the observed post peak behaviour is different, the FEM model is able to predict with good accuracy the maximum load and the out-of-plane deflection corresponding to the maximum load.

3.2.2.2 Wall with small opening

In Figure 15 the load-displacement diagram for D1 is presented. The ultimate load for the wall with small door opening in the experimental test was 1.5 MN compared to 1.63 MN from FEA. Thus, FEA gives an 8.8% higher ultimate load compared to the one obtained experimentally.

Table 8 Table 7: Displacements from experimental test and FEM-analysis for the small opening wall.

Displacements	D1	D4	D2	D3	A1	A2
Experimental test [mm]	22.9	14.7	26.8	18.6	-3.3	-2.6
FEM-analysis [mm]	9.24		10.7		-4.85	
Difference [%]	-59.7	-37.1	-65.5	-50.3	50.0	86.5

The difference for points D1, D2, D3, and D4 are between 37.1% and 65.5% lower for the FEM-analysis than for the experimental test. The difference in points A1 and A2 are 50% and 86% higher respectively in the FEA.

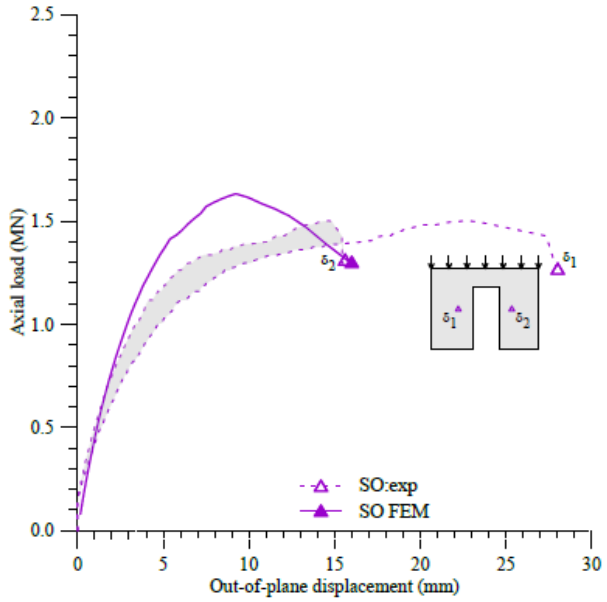

Figure 15 Load-displacement response in point D1 both for experimental test and FEM-analysis for the small opening wall.

Up to about 70% of failure load, the FEA and experimental response are very similar, in particular that of the right pier. However, the experimental plots show an initial higher stiffness compared to the FEA. The stiffness of the panel is overestimated in the FEA compared to the experimentally observed stiffness close to the maximum load. After maximum load the experimental results show large out-of-plane displacements accompanied by a gradual decrease of the applied load. The FEA results show a similar behaviour; however, the decrease is more pronounced. The observed post peak behaviour is slightly different, and the higher stiffness of the FEM model compared to the experiments, however the FEM model is able to predict with relatively good accuracy the maximum load.

3.2.2.3 Wall with large opening

In Figure 16 load-displacement diagram for D1 is shown. Ultimate load for the wall with large door opening in the experimental test was 1.18 MN compared to 1.32 MN from the FEM-analysis. Thus, FEA gives 12% higher ultimate load compared to the one obtained experimentally.

Table 9 Table 8: Displacements from experimental test and FEM-analysis for the large opening wall

Displacements	**D1**	**D2**	**A1**	**A2**
Experimental test [mm]	8.7	11.4	-1.7	-3.5
FEM-analysis [mm]	10.0		-5.34	
Difference [%]	-14.9	-12.3	214	52.6

The differences for points D1 and D2 are between 14.9 and 12.3% lower for the FEM-analysis than for the experimental test. Point A1 has 214% higher deformation in the FEM-analysis and point A2 has 52.6% lower deformation in the FEM-analysis.

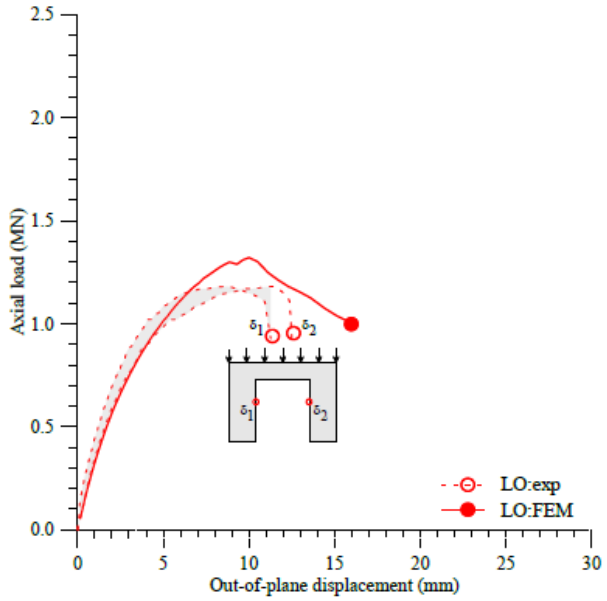

Figure 16 Load-displacement response in point D1 both for experimental test and FEM-analysis for the large opening wall.

The experimental test and FEA response curves are similar. The stiffness of the FEM model matches the stiffness obtained experimentally up to about 70% of failure load. After this point, the experimental response shows higher out-of-plane displacements and a slightly lower capacity. After the peak load, the experimentally measured response, shows large out-of-plane displacements are observed accompanied by a gradual decrease of the applied load. The FEA shows a similar behaviour; however, the decrease is more pronounced. The observed post peak behaviour is slightly different; however, the stiffness of the FEM model is very similar compared to the experiments. The FEM model is able to predict with relatively good accuracy the maximum load and the stiffness of the experimental tests.

3.3 Summary

To check performance of the FEM modelling, the load-displacement responses obtained from FEA were compared with ones experimentally determined, as shown in Figure 14, Figure 15, and Figure 16. Two symmetrically placed linear displacement transducers were used to monitor out-of-plane displacements (δ) of each tested specimen. Due to material randomness, possible variations of support condition at the sides supports, a difference is observed between the symmetrical points. It is therefore difficult to capture this behaviour in a FEA following a deterministic approach. Thus, it will be considerate as having an adequate model if in terms of maximum load, the error is less than 10%. An average ratio between the numerical and experimental ultimate loads of 0.96 (being less than 5% error) was obtained.

4 Structural FEA of full scale building

The previous chapter presents the behaviour of structural wall elements simulated using FEA compared to experimental results. The boundary conditions of these FEA models were defined to replicate the supports of the experimental tests and are idealisations of the actual support conditions in a real structure. In this chapter, a FE model of a RC building is used to study the behaviour of RC wall panels with cutout openings. This approach is believed to provide more realistic support conditions (i.e. walls, slabs or columns) for the studied wall compared to the ones used in the presented experimental tests. While this may eliminate the supports problem, the increased complexity of the model may introduce additional errors. Such an example is modelling errors due to the idealisation of some structural elements (needed for decreasing computational times). Also, stress concentration that can arise at contacts between adjacent

elements can be an additional source of error. However, if treated with caution these results can offer hints for further experimental studies.

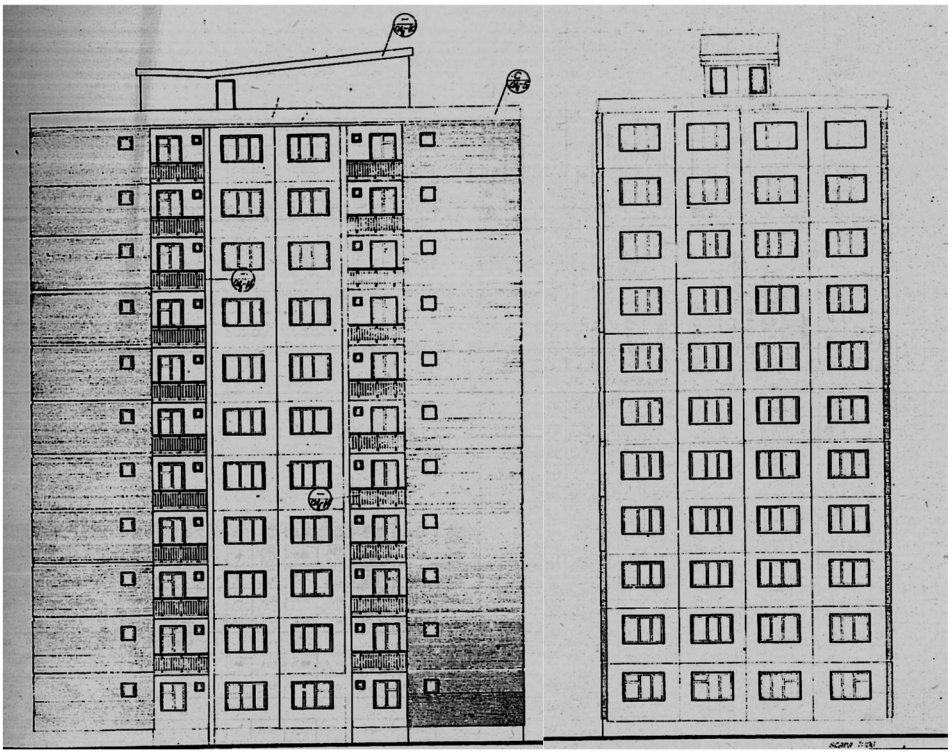

Figure 17 Building Facades

Additionally, this approach permits an evaluation of the state of structure when cutout openings are introduced through a global analysis. Considering that, due to the high complexity of hyperstatic nature of RC concrete buildings, simple analytical calculations are usually not enough for checking the reliability of a given structure, design codes offer the possibility to perform a load test. A load test on a real structure usually involves many financial resources and limits the use of structure. The modelling and loading approach in this case was developed to simulate the proof loading of an actual structure in the first stage to evaluate the serviceability of the structure. Afterwards, the magnitude of the load is increased to investigate the actual service and the ultimate limits of the modelled structure. This second stage cannot normally be performed in real life due to economical and safety reasons, thus if treated with caution these results can provide additional insight into the structural response of existing RC buildings.

4.1 Building description

A large portion of the multi storey residential building stock in Sweden is represented by so called “Punkthus” and “Lamellhus” (tower blocks and lamellar blocks) built between 1960 and 1980 (Björk et al. 1983). According to Björk et al. (1983), the construction of lamellar block began in 1930s, however the majority were built between 1946 and 1975 (e.g. >220.000 units with more than 5 stories) and by 1960 many were up to 9 stories high . Tower block were built since 1940s with most buildings built in the 50s and 60s (e.g. >80.000 units with more than 5 stories). In this period most buildings were between 8 and 10 stories high. The analysed structure is an existing 11-storey residential building Figure 17, located in Romania. This block of flats consisting of large-panels is a typical structure across Europe, where for example, represents 40%, 49% and 45% of the residential building stock in Slovakia, Poland and Estonia, respectively (Csoknyai et al. 2016). This type of building has the same structural system as tower blocks built in Sweden, for example between 1961 and 1975, when normal or light concrete was used to cast in place or prefabricate the structural wall panels.

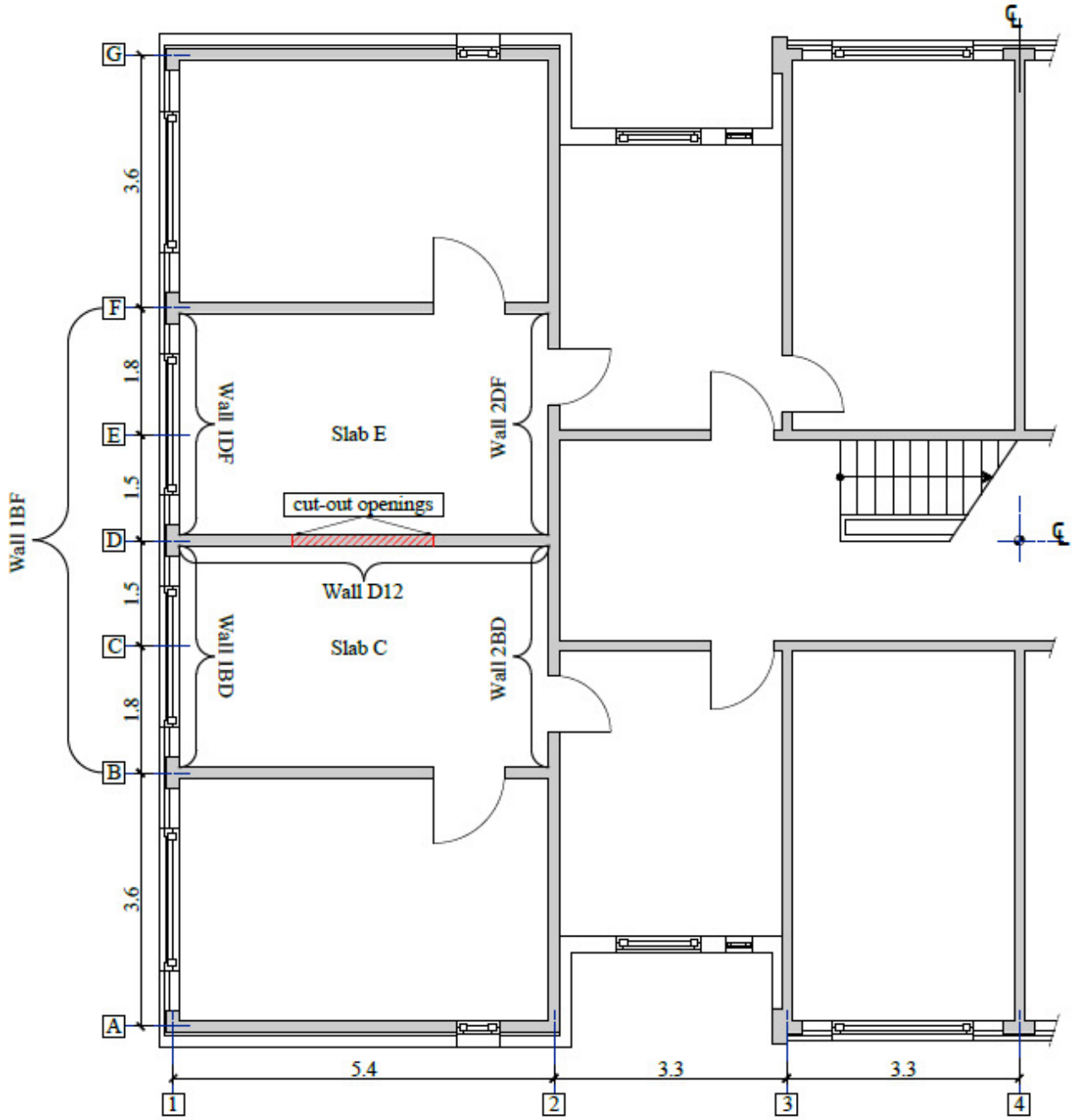

Figure 18 First storey plan (according to drawings)

The structural system comprises an integral wall system in which load-bearing walls run in both longitudinal and transversal direction of the building. Structural simplicity was achieved by a regular floor layout which run from the foundation to the top of the building. The first storey layout is shown in Figure 18. The geometric characteristics are given below:

a) **Walls**. Two types of load-bearing walls are carrying the loads: cast-in-situ RC walls and prefabricated sandwich panels. The 150-mm-thick monolithic RC walls are used as interior walls ending with a 170-mm-thick flange towards its edge. The flange was cast in a second stage to make the connection with prefabricated walls (see Figure 21). The prefabricated wall is a 3-layer panel (including 70 mm protective concrete layer, 60 mm insulating material and 140 mm structural concrete) used to close the building envelope (see Figure 21).

b) **Floors**. The floor panels are prefabricated with a thickness of 120 mm (see Figure 20a).

c) **Joints and intersections**. Shear stresses are transferred by the joints between external and internal walls through shear keys and welded lap splices. At the junction wall-floors the stresses are transferred by a tie-beam (see Figure 21). Additionally, original drawings are given in Annex A5.

The first storey rests above an uninhabitable basement, which was not explicitly modelled in the current analysis. Fixed boundary conditions were considered at the contact between the first storey and the basement.

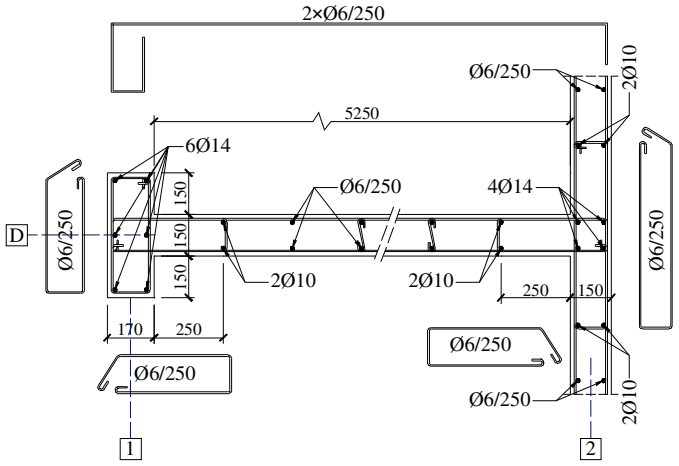

Figure 19 Reinforcement details of the cast-in-situ RC wall (units in mm)

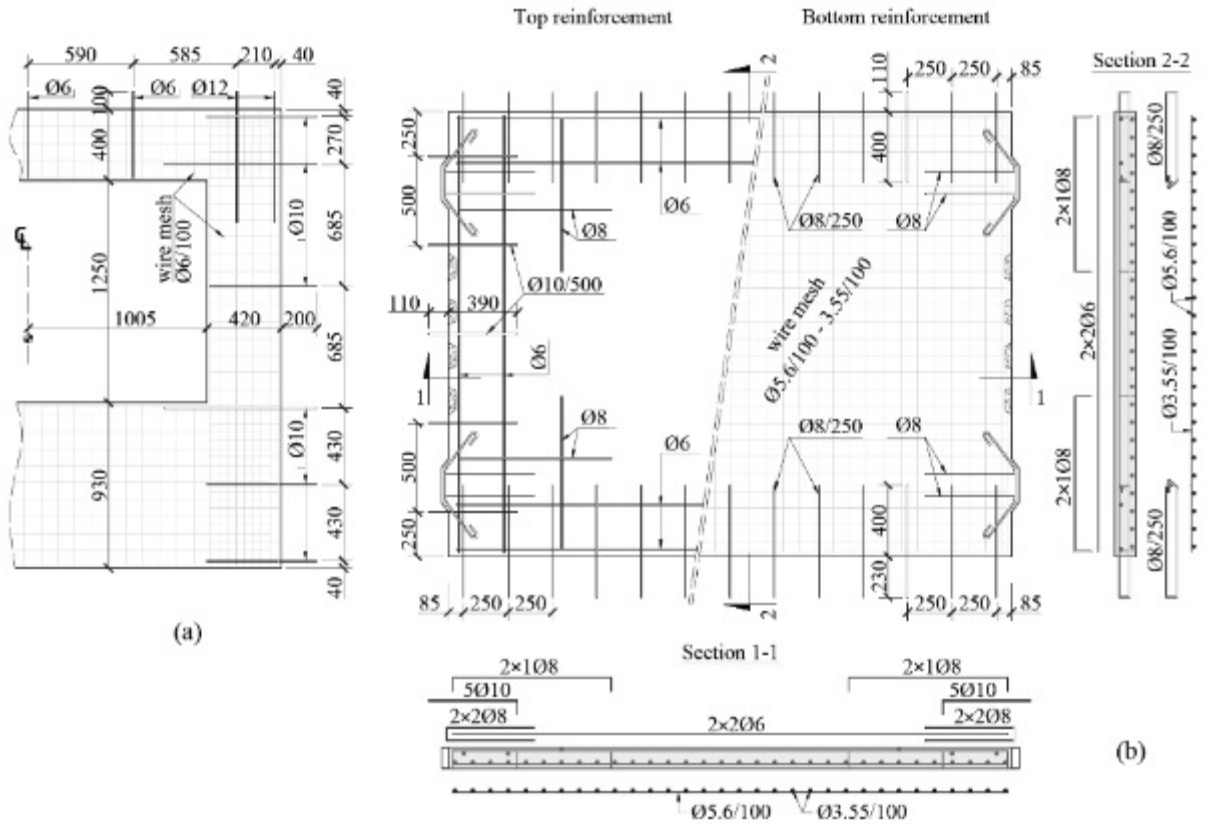

Figure 20 Reinforcement details of the prefabricated RC elements: (a) outer wall; (b) floor panel (units in mm)

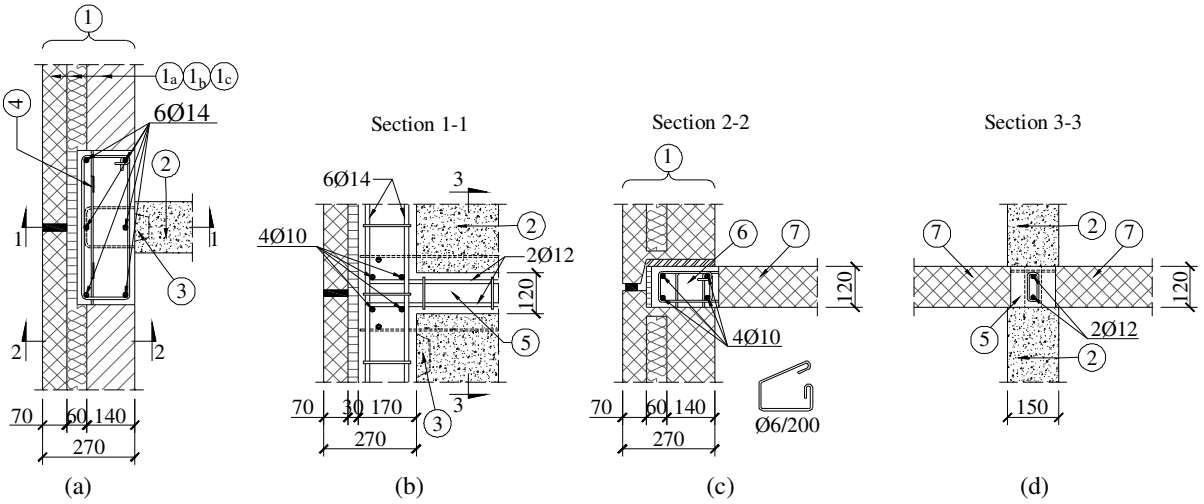

1 - prefabricated panel for outer walls (1_a - protective layer, 1_b - insulating material, 1_c - structural wall); 2 - cast-in-situ RC wall; 3 - shear key; 4 - lapped splices (dowels); 5 - tie-beam for inner walls; 6 - tie-beam for outer walls; 7 - prefabricated RC floor panel

Figure 21 Joint details: (a) inner – outer walls (horizontal section); (b) inner – outer walls (vertical section); (c) prefabricated floor – wall panel (vertical section); (d) prefabricated floor – cast-in-situ RC wall (units in mm)

4.2 Building FEM model description

The FE model was generated in ATENA (Cervenka Consulting 2018) according to the geometry described above and following the reinforcing detail available in Annex A5. The modelling was also done following the recommendations for FEM modelling of concrete structures in plastic domain given by Hendriks et al. (2016), which advises on the choice of material properties, choice of constitutive models, finite element discretization, loads and analysis.

In order to reduce the computational time, symmetry was considered due to regularity of the building in both plan and elevation. Furthermore, the analysis was carried out in two phases.

4.2.1 Phase 1

In the first phase a single storey of the building was modelled to: (1) evaluate the distribution of the reaction forces (due to dead- and live-load); (2) to observe the critical load bearing elements in the studied bay; (3) perform a finite element size sensitivity study for the critical load bearing elements.

The critical load bearing elements, depending on the size of the cutout opening, were found to be the analysed wall, D12, the transversal walls, 1BD, 1DF, 2DB, and 2DF, and the slabs C and E as indicated schematically in Figure 18.

The critical elements were assign structured finite elements with an aspect ratio of 1:2:2 (thickness : length : height), using a minimum of 5 finite elements over the thickness of the structural element (Cervenka Consulting 2018; Hendriks et al. 2016) to avoid “shear locking”. Because the bending stiffness of the rest of the structure was not considered critical, only one finite element per thickness was used.

The reinforcement of walls D12, 1BF (referring to both 1BD and 1DF), slabs C and E, was modelled discretely according to the plans in Annex A5. For the rest of non-linear elements, the reinforcement was smeared over the modelled volumes based on the reinforcement ratios obtained from reinforcing plans.

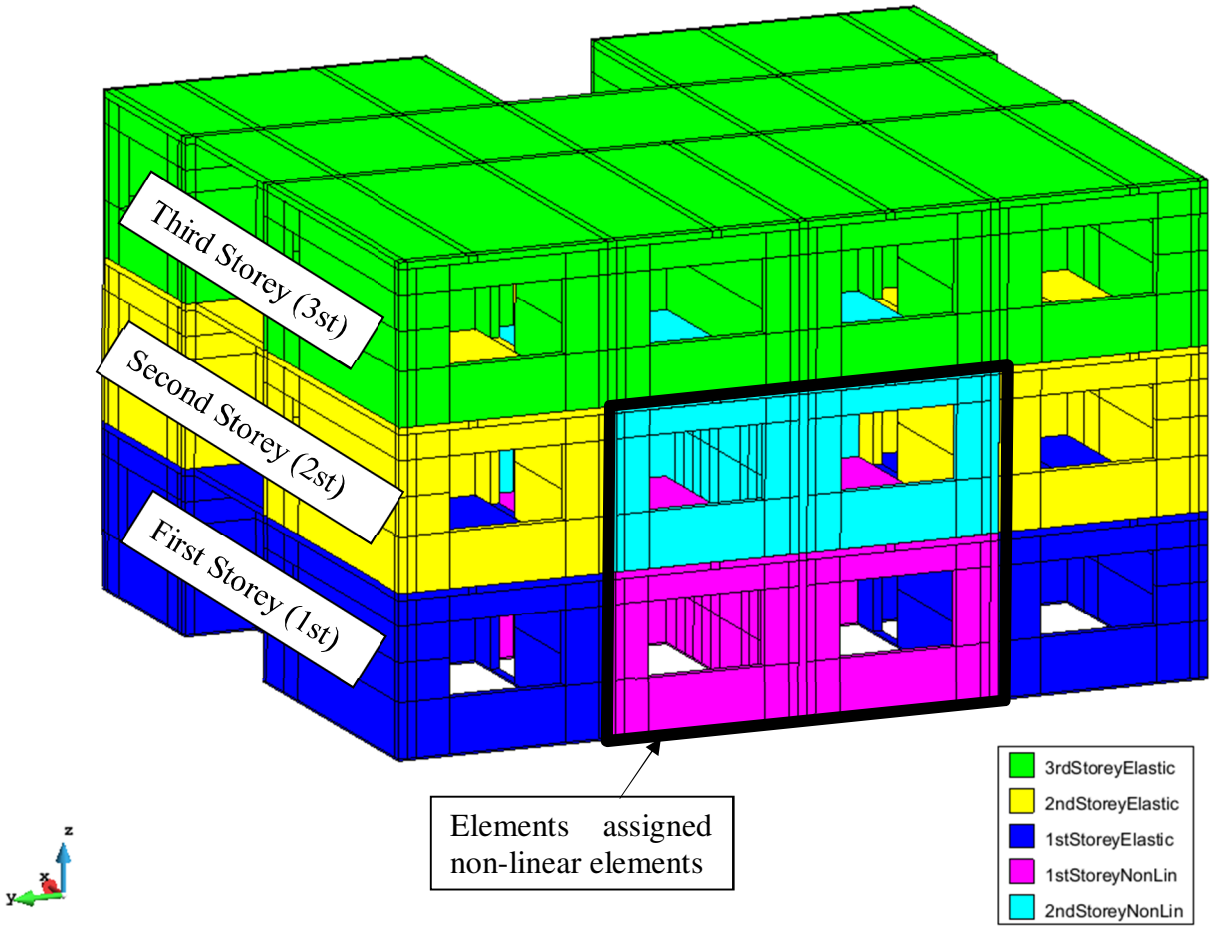

Figure 22 Schematic representation of material types used for modelling the building

4.2.2 Phase 2

In the second phase the first three storeys were modelled considering the building in the original unaltered state (i.e. no cut-out openings) from here on referred to by the term AsBuilt, see Figure 22. Dead, imposed, and live loads applied were applied to all storeys. The loads applied to the third storey were multiplied by factor of 9 representing the number of storeys excluded from the analysis. This approach was preferred to only modelling the first two stories and applying the load as a uniformly distributed line load on the walls as was done in the first phase.

Cutout openings were only created in wall D12 and only at the first two stories, therefore, only critical structural elements adjacent to wall D12 at the first and second storeys were modelled considering a non-linear behaviour, the rest of the building was modelled using linear elements in order to save computation time. Figure 22 shows which building elements were modelled considering a non-linear material and which were modelled considering only a linear material behaviour. Material qualities for each of the structural elements are given in Table 10. The third storey was modelled considering the building in the unaltered state only.

Table 10 Material characteristics

Structural element	Material quality	
	Concrete class[a)]	Reinforcement type[b)]
Prefabricated walls	B250 (C16/20)	OB38 and STM (S235 and S400)
Cast-in-situ walls (web)	B200 (C12/15)	OB38 (S245)
Cast-in-situ walls (flange)	B300 (C20/25)	OB38 (S235)
Prefabricated floors	B250 (C16/20)	OB38 and STM (S235 and S400)
Joints and intersections	B300 (C20/25)	OB38 (S235)

[a)] B200, B250 and B300 (f_{ck}≈12.5, 16.6 and 20.5 MPa, respectively) where f_{ck} is the characteristic compressive cylinder strength, equivalent concrete classes according to EC 2 (2005) are given in brackets

[b)] OB38 (plain bars with f_{yk}≈235 MPa); STM (welded wire (plain) mesh with f_{yk}≈440 MPa), equivalent stell classes according to EC 3 (2004) are given in brackets

The analysed panel (D12) and the neighbouring panels (1BF and 2BF) of the second storey were offset by 25 mm (t_w/6) perpendicular to their respective axis direction to simulate effects of imperfections (i.e. misalignment) that can occur in normal construction practices.

The FE model of the entire building is constructed based on the same principles as the ones presented in Section 3.2 “FEA of tested wall panels”, with the following differences:

- The chosen solution method was Newton-Raphson for dead weight and live load up to a predefined load level, and afterwards was switched to Arc-Length. The switch was necessary to obtain the post peak behaviour of the structure since load application was done in force control, in order to ensure the failure of the structure is achieved;
- The walls were supported continuously along their bottom surface simulating the basement (represented in magenta, see Figure 23);
- The lateral supports were replaced by transverse walls and floors under as-built conditions;
- Perfect plasticity and perfect bond with no hardening was assumed for reinforcement.
- The loading to failure was done by increasing the uniformly distributed load on the slabs C and E at each storey, see Figure 18

A parametric study was performed where the size of new openings varies from 0.9 × 2.1 m up to 4.4 × 2.1 m. The width of the opening was varied in steps shown in Table 11.

Table 11 Opening size summary

Assigned number	Opening size
0	No opening (solid wall)
1	0.9 m x 2.1 m
2	1.8 m x 2.1 m
3	3.1 m x 2.1 m
4	4.4 m x 2.1 m

Openings were introduced in wall D12 at the first and second storey, named 1st and 2st, respectively, see Figure 22. The size and location of the openings are indicated using the convention Oxy, where x and y representing the size of the opening created at the first and second storey, respectively, taking values from 0 to 4 as indicated in Table 11.

Table 12 shows the naming system used to identify the models considering the combination of openings crated in wall D12. For example, O23 refers to a building model having O2 (1.8x2.1m) cut-out opening at the first storey and O3 (3.1x2.1m) at the second storey. A graphical representation of openings size and configuration can be seen in Annex A1 and A2.

Table 12 Model naming matrix with respect to opening configuration

	Solid	**Ox1**	**Ox2**	**Ox3**	**Ox4**
Solid	AsBuilt (O00)	O01	O02	O03	O04
O1y	O10	O11	O12	O13	O14
O2y	O20	O21	O22	O23	O24
O3y	O30	O31	O32	O33	O34
O4y	O40	O41	O42	O43	O44

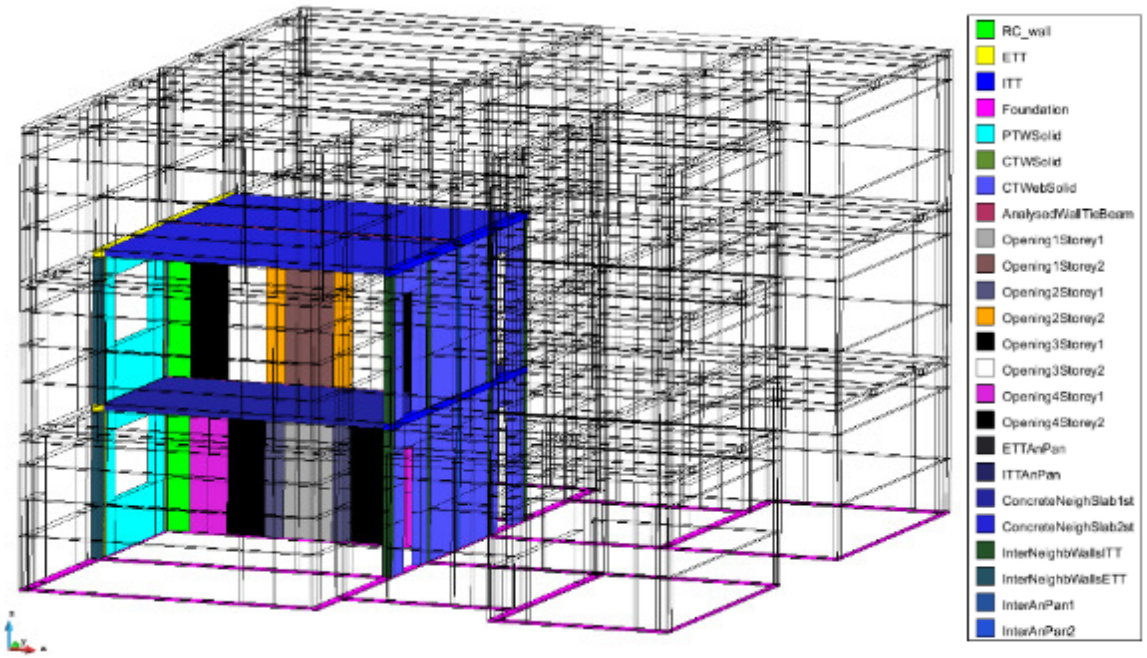

Figure 23 Schematic representation of the main analysed bay with type of materials assigned to elements

The total base reaction of the building was monitored, as well as reactions of walls 1BD, 1DF, 2BD, 2BF, and D12 that were monitored independently during the FEM analyses. The sum of reactions 1BD, 1DF, 2BD, 2DF, and D12 represents the total load distributed to the analysed bay, referred to as the MainBay. Figure 23 illustrates the main analysed bay near the cut-out opening relative to rest of the FEM model, outlined by thin black lines. All volumes in the main bay were assigned non-linear materials of different properties as indicated in the original design documentation.

4.3 Loading strategy

The loads in the current analysis (shown in Table 13) were evaluated according to EC 1 (2002), although they might differ from previous standards used to design the building.

Table 13 Loads

Loads	Intensity
Dead load	
Self-weight	Default[a)]
Flooring	1.0 kN/m^2
Imposed load	
Live load	2.0 kN/m^2 or 5.0 kN/m^2
Roof live load	0.4 kN/m^2
Variable loads	
Snow	3.0 kN/m2

[a)] The density of normal weight concrete was given in the software as 24 kN/m^3 and increased by 1.0 kN/m^3 to account for reinforcement

Analyses were conducted considering the hypothetical load cases for the live load of 5.0 kN/m^2 assuming a change in use from apartment to office spaces. That is, initially a distributed live load of 2 kN/m^2 was applied to all slabs, in addition to all other dead and permanent loads. Subsequently, a cutout opening was introduced in wall D12 (see Figure 18), an additional live load of 3.0 kN/m^2 was applied after the creation of the openings. Thus, the total applied load was 5.0 kN/m^2. Subsequently, to obtain the serviceability and ultimate limit loads, an additional uniformly distributed load was applied in increments of 2.0 kN/m^2 to the slabs adjacent to wall D12 at each storey.

A procedure to determine if a building is allowed to remain in service is given in ACI 318 (2014). The total test load *P:*

$$P = 1.15D + 1.5L + 0.4(L_r \text{ or } S \text{ or } R) \quad (1)$$

where, D is the dead load, L is the imposed load, L_r is the roof live load, S is the snow load and R is the rain load. It should be noted that all load were factored with the coefficients shown in Equation 1.

4.4 Service and ultimate limit-state criteria

4.4.1 Serviceability limit state (SLS)

A general acceptance criterion for the behaviour of a structure under loading is that it does not show evidence of failure. Evidence of failure includes cracking, spalling, or deflection of such magnitude and extent that the observed result is obviously excessive (ACI 318 2014). Crack widths are good indicators of the state of the structure and should be observed to help determine whether the structure is satisfactory. ACI 318 recommends the displacement of structural elements to be limited to:

$$\Delta_1 = \frac{l_t^2}{20000h} \quad (2)$$

with l_t the span of member and h is the thickness of a member. Considering the geometries of slabs C and E, Δ_1 is 4.1 mm.

According to EC 2, the appearance and general utility of a structure could be impaired if the deflection of structural components exceeds the span/250, however EC 2 also suggest that an appropriate limit for elements deflection after construction under quasi-permanent loads can be calculated as: $\Delta_2 = l_t/500$. Considering the geometries of slabs C and E, Δ_2 is 6.3 mm. The ACI 318 provides in this case a more conservative limit compared to EC 2. The ACI 318 limit ($\Delta_1 = 4.1\ mm$) will further be used to determine the serviceability limit.

According to ACI 533 (2011), where it is stated that under normal service conditions cracks up to 0.3 mm wide are structurally acceptable in precast wall panels. This limitation is in line with the provision provided in EC 2 for most exposure classes with the exception of classes X0 and X1 for which the limit is 0.4 mm. A 0.3 mm crack opening size will be further used as crack opening serviceability limit.

4.4.2 Ultimate limit state (ULS)

The ultimate limit state concerns the safety of people and of the structure to carry the imposed loads. According to EC 2, limit states prior to structural collapse can be considered in place of the collapse itself and may be treated as the ultimate limit state. Relevant limit states that need to be verified for a structure or part of a structure are loss of equilibrium, failure by excessive deformation or rupture. Excessive deformations for concrete are considered for those above the value associated with concrete crushing. In this study for wall elements, the ultimate total strain of concrete in compression is ε_{cu}=1484 μm/m determined based on the concrete class. Excessive deformation for the reinforcement steel are considered values above that associated with yielding, ε_y=1231 μm/m according to the material properties for reinforcement used.

5 Structural FEA results

5.1 Influence of openings on the load redistribution to the foundations

Previous experimental tests have shown that the capacity and the stiffness of solid concrete panels is considerably reduced when cut-out openings are created (Popescu et al. 2016). At a structural level, such changes can alter the path of loads in the structures and can lead to higher loads distributed to elements not designed accordingly.

The influence of openings on the axial load distribution between the vertical wall panels is quantified based on the changes in the bottom reaction forces (i.e. loads transmitted to the foundation by the wall panels).

Figure 24 shows the comparison of the reaction coefficients for walls 1BD, 1DF, 2BD, 2BF, and D12 (i.e. the reaction of wall 1BD, 1DF, 2BD, 2BF, and D12, divided by the total reaction in the

MainBay, respectively) as a function of opening configuration Figure 24 shows the influence of enlarging an opening of the first storey when the wall on the second storey is solid or with openings of different sizes, respectively. It can be seen that the reaction force transmitted by wall D12 decrease with the increase in the size of the opening. Simultaneously the load in the adjacent wall is increased. For example, in the case Building O40 the reaction of wall D12 is decreased by approximately 62% compared the AsBuilt Building while the reaction force in wall 1BD is increased by the about 60%. This indicates that with the creation of openings and the change in the wall axial rigidity loads are proportionally redistributed to adjacent members. Thus, in the case of such interventions the conditions of the foundations would require investigation, however, this is out of the scope of this study.

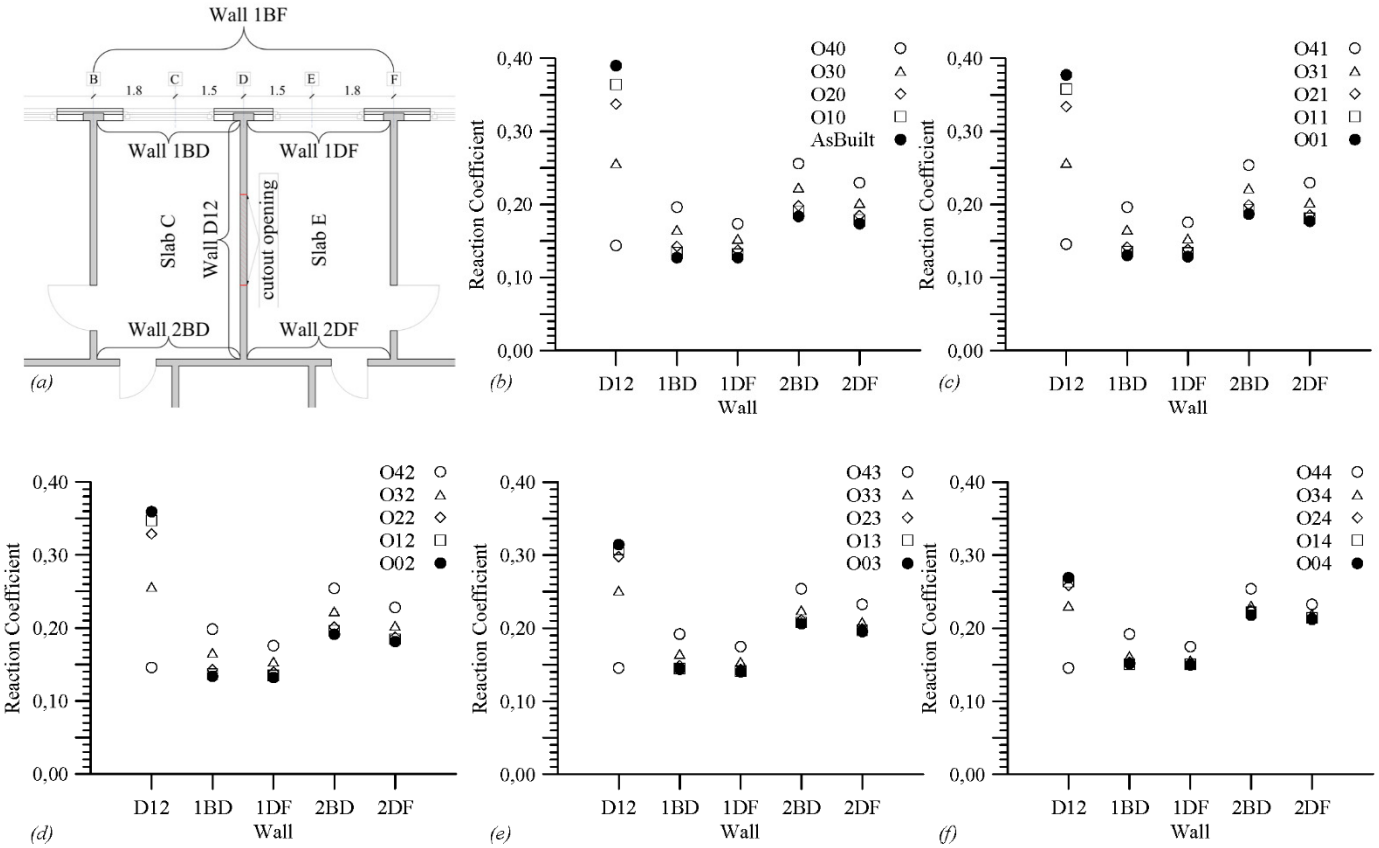

Figure 24 Comparison of wall reaction coefficients a) ground floor schematic of the MainBay b) 2nd storey solid wall, c) 2nd storey wall O1, d) 2nd storey wall O2, e) 2nd storey wall O3, f) 2nd storey wall O4.

5.2 Serviceability under simulated loading

The following performance checks are done considering a live load of 5 kN/m^2. All loads are factored according to Eq. 1.

5.2.1 Deflection checks

The variation of slabs' maximum vertical deflection and the deflection of the D12 wall spandrel are presented in Figure 25. It should be noted that only the vertical deflection components are indicated. For solid walls, the spandrel deflection represents the vertical displacement of the solid wall in the middle of the wall and 2.1 m relative the level storey elevation. In location of the maximum deflection was automatically determined.

It can be observed that in all cases the actual deflection limits are well below the recommended limit. A 0.25 mm increase in the maximum displacements of the slabs at the first storey can be observed from the AsBuilt to the O44 building. This represents a 50% increase relative to the AsBuilt conditions.

It can be observed that the eccentricity of wall D12 influences the maximum slab displacements. For example, in the case of the AsBuilt building a slight difference is observed between the two slabs at the same storey (i.e. 1stDisplSlabC and 1stDisplSlabE), a similar observation can be made for the second

storey. The influence of eccentricity is reduced with the size of the openings created, irrespective of the storey. For example, Buildings O40, O04 and O44 show the same maximum deflection values for slabs C and E of the same storey.

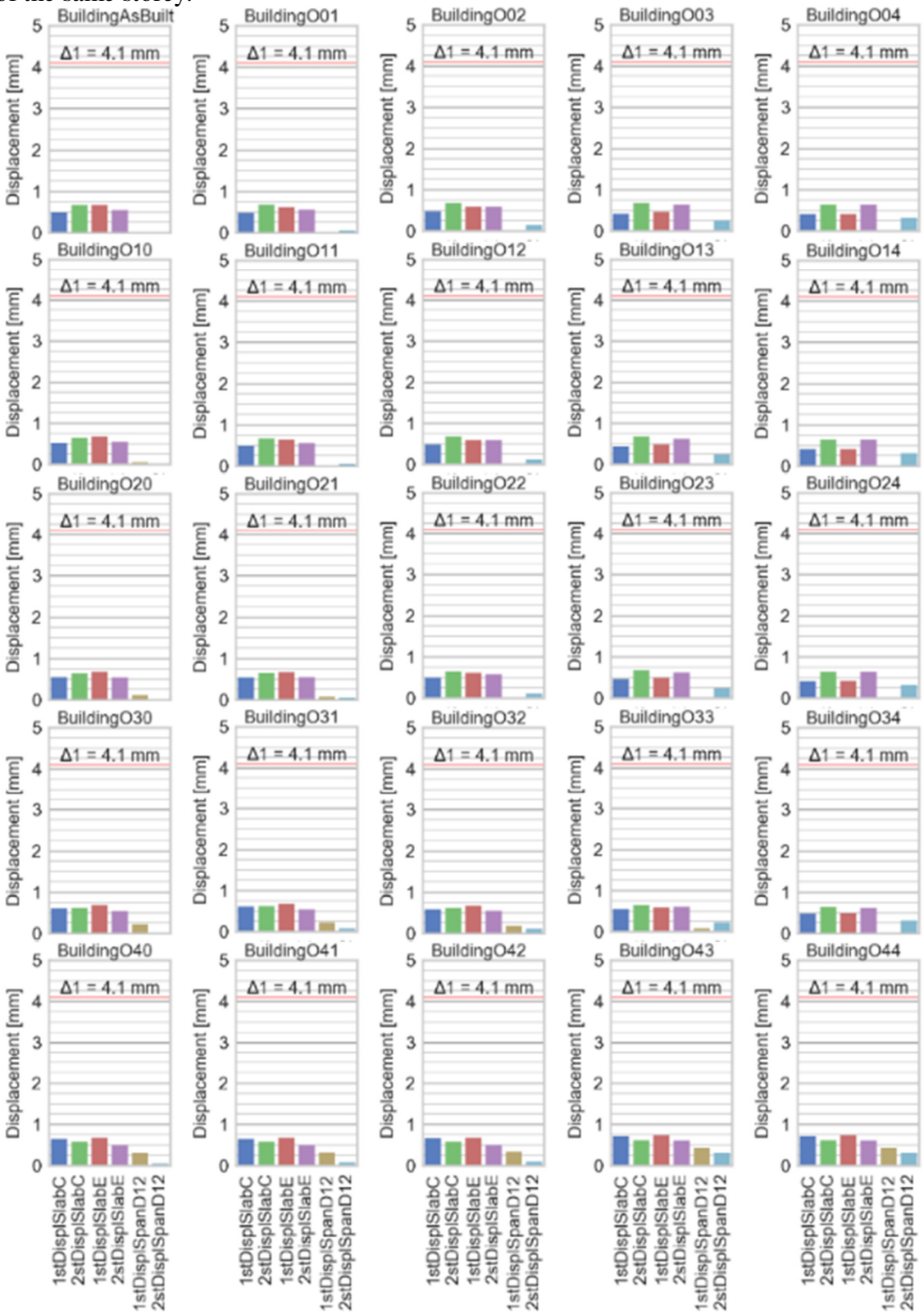

Figure 25 Variation of vertical deflections of slabs and spandrels relative to allowable deflections

Figure 26 Variation of maximum crack opening displacements (COD) relative to allowable crack openings (wc)

5.2.2 Crack opening checks

The results shown in Figure 26 indicate that in all cases the cracks in the evaluated elements are below the limit. It can be observed that the creation of openings has small or little effect on the maximum crack

of slab elements and in some cases the influence is positive (i.e. the maximum crack opening is reduced). For example, it can be observed that the crack opening size in the slabs (particularly the slab over the first storey) decreases with the increase in opening size at the second storey, see Figure 26 diagram from BuildingAsBuilt to BuildingO04. Due to the cutout opening created at the second storey, the slabs support condition change. Thus for the case with the largest opening, has larger rotational capacity that translates into smaller cracks. In addition, the spandrel of the walls accommodating cutout openings have small cracks appearing in at midspan. Crack patterns are given in Annex A1 for the ultimate limit state of the building.

In all cases, the solid walls do not show any cracks. Creating openings in all cases induces cracks in the wall where the opening is created, on the other hand adjacent walls with openings (i.e. 1BF) do not present cracks in either of the cases. This is due to the fact that these walls were designed to accommodate openings, while wall D12 was designed as a solid (i.e. no reinforcement around the opening). The maximum crack opening of 0.036 mm is observed for wall D12 of Building O42.

5.3 Serviceability limit state (SLS)

After the simulated loading the load applied to slabs C and E (adjacent to wall D12, the wall with the cutout opening) was increased in increments of 2 kN/m^2 to verify the actual serviceability and ultimate state limits of the building. The maximum vertical displacement of Slabs C, Slab E, the spandrel above the cutout opening and the maximum crack opening of Slabs C and E, walls D12 and walls 1BF at each level were monitored, respectively. The responses of each displacement and crack-opening monitor to the applied load are given in Annex A3 and A4, respectively.

Annexes A3 and A4 show the full load response for each displacement and crack opening monitor and for each modelled building up to failure. A different response can be observed depending on the size and configuration of the openings. Table 14 and Table 16 summaries the maximum load that can be uniformly applied to slabs C and E at each storey that satisfies the previously mentioned serviceability criteria (i.e. maximum slab displacement 4.1 mm and maximum crack opening 0.3 mm)

Table 14 shows the maximum service load from the deformation condition. Interestingly the maximum service load is not obtained for the AsBuilt building, instead Building O20 (i.e. having a 1.8 x 2.1 m opening at the first floor has the maximum service limit, although, compared to the AsBuilt and O10 Buildings is only marginally higher. The lowest service limit was obtained for Building 43.

Table 14 Service load (kN/m^2) from displacement condition

	Solid	**Ox1**	**Ox2**	**Ox3**	**Ox4**
Solid	27.9	27.8	26.9	26.9	26.1
O1y	28.0	27.9	27.0	26.9	26.2
O2y	28.1	28.0	27.2	27.0	26.2
O3y	27.4	27.3	27.1	26.5	26.1
O4y	26.8	26.4	24.4	22.2	23.6

Table 15 presents the change of the maximum service limit load in percentage relative to the AsBuilt building. Positive value indicate an increase and negative values indicate a decrease. Small changes can be observed for combinations of O1 and O2 at the first and second floor, decreasing the service limit up to 3.5 %. The highest decrease in load was observed as expected for the building with the largest cut-out openings, in particular when openings are created at the first storey (i.e. O42, O43, O44).

Table 15 Change in service load (%) due to cutout openings from displacement condition

	Solid	**Ox1**	**Ox2**	**Ox3**	**Ox4**
Solid	Ref.	-0.3	-3.5	-3.7	-6.3
O1y	0.3	0.1	-3.4	-3.6	-6.1
O2y	0.6	0.4	-2.7	-3.4	-6.1
O3y	-1.7	-2.3	-2.9	-5.1	-6.3
O4y	-3.9	-5.6	-12.6	-20.3	-15.6

Table 16 shows the maximum service load from the crack opening condition. Also in this case, the maximum service load is not obtained for the AsBuilt building, instead Building O20 (i.e. having a 1.8 x 2.1 m opening at the first floor has the maximum service limit, although, compared to the AsBuilt Building is only slightly higher. The lowest service limit was obtained for Building 43.

Table 16 Service load (kN/m2) from crack opening condition

	Solid	**Ox1**	**Ox2**	**Ox3**	**Ox4**
Solid	22.1	22.1	19.0	21.3	20.1
O1y	23.0	22.1	18.8	21.3	20.4
O2y	23.1	22.1	22.2	21.3	20.1
O3y	22.4	22.4	22.3	20.7	20.3
O4y	21.8	22.4	19.2	14.0	17.8

Table 17 presents the change of the maximum service limit load in percentage relative to the AsBuilt building. Positive values indicate an increase and negative values indicate a decrease in the maximum service load. Small changes can be observed for combinations of O1 at the first and second floor, increasing the service limit up to 4.1 %. In this case it was observed that creating an O2 opening at the second storey decreases the service limit load by 13.6% and in combination with a O1 opening at the first storey, by 14.7%. The highest decrease in load was observed as expected for the building with the largest cut-out openings, in particular when openings are created at the first storey (i.e. O42, O43, O44) but also for (O02 and O12).

Table 17 Change in service load (%) due to cutout openings from crack opening condition

	Solid	**Ox1**	**Ox2**	**Ox3**	**Ox4**
Solid	Ref.	0.0	-13.6	-3.7	-9.0
O1y	4.1	0.2	-14.7	-3.7	-7.7
O2y	4.4	0.2	0.6	-3.6	-8.9
O3y	1.5	1.3	0.9	-6.3	-8.1
O4y	-1.3	1.7	-12.8	-36.8	-19.5

Table 18 shows the maximum service load from both the displacement and crack opening conditions. It can be seen that the crack opening is the condition that governs serviceability in all cases, and the observations previously made for crack opening conditions are valid overall. The load at the service limit state for the AsBuilt and O44 buildings was found to be 160% and 100% higher, respectively, compared to the proof load.

Table 18 Service limit load (kN/m2)

	Solid	**Ox1**	**Ox2**	**Ox3**	**Ox4**
Solid	22.0	22.1	19.1	21.3	20.1
O1y	23.0	22.1	18.8	21.3	20.4
O2y	23.0	22.1	22.2	21.3	20.1
O3y	22.4	22.3	22.3	20.7	20.3
O4y	21.8	22.4	19.2	14.0	17.8

Table 19 presents the difference between the maximum service loads determined from crack opening and displacement conditions. The difference is given in percentage for each building relative to service limit load from the crack opening condition. It can be seen that the deflection limit load is between 17.4 and 59.4 % with an average of 28.3 % higher than the crack opening limit load.

Table 19 Difference in service load (%) between displacement and crack opening conditions

	Solid	Ox1	Ox2	Ox3	Ox4
Solid	26.5	26.1	41.2	26.4	30.3
O1y	21.8	26.3	43.1	26.5	28.7
O2y	21.8	26.6	22.3	26.6	30.4
O3y	22.5	22.0	21.7	28.2	28.8
O4y	23.1	17.4	26.8	59.4	32.6

5.4 Ultimate limit state (ULS)

The full load response for each concrete and reinforcement strain monitor and for each modelled building up to failure are given in Annexes A5 and A6, respectively. Table 20 summarizes the maximum ultimate load from concrete crushing condition in the concrete walls. From the concrete crushing condition, the AsBuilt building shows the maximum ultimate capacity. However, the maximum capacity of the structure is limited by the capacity of the slabs and no concrete crushing is observed in the monitored walls. The lowest ultimate capacities were obtained for the cases with the largest opening areas Building O43 and O44.

Table 20 Ultimate load (kN/m2) from walls concrete crushing condition

	Solid	Ox1	Ox2	Ox3	Ox4
Solid	52.84*	43.76	36.52	28.46	30.19
O1y	43.26	43.92	36.53	28.48	30.21
O2y	41.77	44.00	35.98	28.54	30.22
O3y	33.10	30.46	30.27	27.29	30.03
O4y	30.61	28.6	25.84	21.54	22.73

* failure of slabs before concrete crushing

Table 21 presents the change of the ultimate limit load in percentage relative to the AsBuilt building. The highest decrease in load was observed as expected for the building with the largest cutout openings, in particular when openings are created at the first storey (i.e. O41, O42, O43, O44). In this case, also creating openings O3 and O4 at the second storey, substantially influences the ultimate capacity of the structure (43–59% decrease).

Table 21 Change in ultimate load (%) due to cutout openings from concrete crushing condition

	Solid	Ox1	Ox2	Ox3	Ox4
Solid	Ref.	-17.2	-30.9	-46.1	-42.9
O1y	-18.1	-16.9	-30.9	-46.1	-42.8
O2y	-21.0	-16.7	-31.9	-46.0	-42.8
O3y	-37.4	-42.4	-42.7	-48.4	-43.2
O4y	-42.1	-45.9	-51.1	-59.2	-57.0

Table 22 shows the maximum ultimate load from the reinforcement yielding condition. As expected the AsBuilt building shows the maximum ultimate capacity, for which the ultimate limit is given by the yielding of the reinforcement in adjacent walls with openings (walls 1BF). In all other cases the ultimate limit is given by the by the reinforcement yielding in the walls accommodating the cutout openings. The lowest ultimate capacity was obtained for Building O43. The ultimate limit of the structure was observed to decrease with the opening size, although not proportionally. However for cases with O2 cutout opening at the second storey (column Ox2 in Table 22), a higher limit load was observed when the openings of the same size are introduced (i.e. opening O2 at both stories) compared to cases when first storey has a solid wall or a smaller cutout opening. This would suggest that vertical consistency can provide a better structural response.

Table 22 Ultimate load (kN/m2) from yielding of reinforcement condition

	Solid	Ox1	Ox2	Ox3	Ox4
Solid	35.2	31.9	28.5	28.5	24.5
O1y	33.7	32.8	28.5	28.5	24.6
O2y	33.0	32.9	28.0	27.8	24.6
O3y	30.7	24.9	25.0	21.5	23.7
O4y	28.4	20.7	18.5	14.0	17.1

Table 23 presents the change of the ultimate limit load in percentage relative to the AsBuilt building. The highest decrease in load was observed as expected for the building with the largest cutout openings, in particular when openings are created at the first storey (i.e. O41, O42, O43, O44). It was observed that O2 has a more significant influence on the ultimate capacity when introduced at the second storey.

Table 23 Change in ultimate load (%) due to cutout openings from reinforcement yielding condition

	Solid	Ox1	Ox2	Ox3	Ox4
Solid	Ref.	-9.5	-19.1	-19.2	-30.4
O1y	-4.3	-6.9	-19.1	-19.1	-30.2
O2y	-6.4	-6.7	-20.6	-21.2	-30.2
O3y	-12.9	-29.3	-29.7	-38.8	-32.7
O4y	-19.4	-41.4	-47.3	-60.4	-51.3

Table 24 shows the maximum ultimate load from both concrete crushing and reinforcement yielding conditions. It can be seen that yielding of the reinforcement is the condition that governs the ultimate limit in all cases, and the observations previously made for yielding of reinforcement conditions are applicable overall.

Table 24 Ultimate limit load (kN/m2)

	Solid	Ox1	Ox2	Ox3	Ox4
Solid	35.2	31.9	28.5	28.5	24.5
O1y	33.7	32.8	28.5	28.5	24.6
O2y	33.0	32.9	28.0	27.8	24.6
O3y	30.7	24.9	24.8	21.5	23.7
O4y	28.4	20.7	18.5	14.0	17.1

Table 25 presents the difference of the maximum ultimate load between the concrete crushing and reinforcement yielding conditions. The difference is given in percentage for each building relative to ultimate limit load from the reinforcement yielding condition. It can be seen that concrete crushing limit load is between 0 and 61 % with an average of 28.2 % higher than the reinforcement yielding limit load.

Table 25 Difference in ultimate load (%) between concrete crushing and reinforcement yielding conditions

	Solid	Ox1	Ox2	Ox3	Ox4
Solid	50.1	37.4	54.2	0.0	23.1
O1y	28.4	34.0	61.7	0.0	23.0
O2y	26.8	33.9	28.7	2.8	23.0
O3y	7.9	22.4	22.3	26.7	26.7
O4y	7.8	38.5	39.4	54.4	32.7

Table 26 shows the change in ultimate load for openings at the first storey relative to the ultimate load of buildings with all opening sizes at the second storey. For example, the first column of Table 26 shows the decrease (negative values) of the ultimate load compared to the building having a solid panel at the second storey, whereas the fourth column shows the decrease of the ultimate load compared to the building having a O4 cutout opening at the second storey. The results suggest that if the opening at the second storey is larger than the cutout opening at the first storey, the size of the opening at lower level

does not affect the capacity of the structure. However, if the opening at the first level, exceeds the size of the opening at the upper level, depending on the size of the opening an additional 15 to 50% decrease in capacity can be expected depending on the size of the openings.

Table 26 Change in ultimate load (%) between buildings having cutout opening at the adjacent upper storey

	Solid	Ox1	Ox2	Ox3	Ox4
Solid	0,0%	0,0%	0,0%	0,0%	0,0%
O1y	-4,3%	2,9%	0,0%	0,1%	0,2%
O2y	-6,4%	3,2%	-1,9%	-2,5%	0,2%
O3y	-12,9%	-21,9%	-13,2%	-24,3%	-3,3%
O4y	-19,4%	-35,2%	-34,9%	-51,0%	-30,1%

5.5 Comparison of limit states

According to EC2, for a structure to be fit for use, no limit state should be exceeded when design load values are used in the models. Table 27 shows the difference between the load at SLS and ULS in percentage. Positive values indicate that the ULS limit is higher that SLS, and negative values indicate the ULS is reached before the SLS. It can be seen that for the AsBuilt building there is a safe margin between SLS and ULS (15.9%). This implies that cracks and deflections will be evident in the structure before the failure of the structure or the element. With the creation of cutout openings, the margin between SLS and ULS is reduced such that in the case of openings larger than O2 (i.e. 1.8x2.1m) the ULS is likely to be reached without warning in the form of cracks or noticeable deflections.

Table 27 Difference in load (%) between service and ultimate limit states considering factored live loads

	Solid	Ox1	Ox2	Ox3	Ox4
Solid	15.9	3.2	-12.5	-5.1	-14.6
O1y	4.8	6.5	-16.1	-5.0	-15.9
O2y	1.8	6.8	-12.0	-8.0	-14.6
O3y	-2.9	-24.0	-24.1	-29.8	-19.1
O4y	-8.2	-39.9	-36.5	-33.3	-36.4

6 Discussions

6.1 Simulated loading and load distribution to foundations

From the analysis of the building under simulated loads (following the recommendations of ACI 318), no excessive deformations or crack openings were observed. This suggests that no strengthening is necessary when increasing the live load by 3kN/m^2 and introducing any opening configuration considered in this study. It should be noted that ACI 318 only requires the verification of displacements criteria against prescribed values while leaving the other criteria such as crack opening size to the choice of the responsible engineer, in which case other standards such as ACI 533 (2011) or EC 2 (2005) can be consulted. The proof loading procedure indicated in ACI 318, requires residual deformations (i.e. after removing the applied load) to be measured. Depending on the duration of the load and pre-existing cracks in the structure, crack widths and deformations can be significantly higher. However, in the current study the effects of creep and shrinkage were not included in the analysis thus the residual deformations cannot be measured.

Despite the fact that the creation of large openings in concrete panels significantly reduces their capacity (Popescu et al. 2016) it was observed in this study that the wall with the cutout opening (i.e. wall D12) does not show any significant increase in crack opening or deflections. This can be explained by the fact that creating an opening in a solid wall also decreases its axial rigidity, thus less load is transferred trough the wall. This is demonstrated in Figure 24 where the total load transferred by the wall with cutout

openings to the foundations is reduced progressively with the increase of the opening size. Simultaneously the load transmitted to the foundation of the adjacent walls is increased.

6.2 Serviceability limit state

In section 4.5.3 it was shown that in all studied cases the serviceability limit was governed by the crack opening condition. Annex A4, shows that with the exception of the AsBuilt building where cracks larger than 0.3 mm are observed first in the slabs, cracks larger than 0.3 mm are observed in the walls with cutout openings (D12), usually at the midspan of the spandrel, and in the slabs at approximately the same load level.

Table 20 indicates that creating opening ranging from O1 (0.9x2.1m) to O4 (4.4x2.1m) at the first storey, while the second storey panel is solid, does not decrease the service limit load of the structure. This can be explained by the fact the wall at the second storey acts like deep beam redistributing the loads from the upper structure to the adjacent members. This beam behaviour can be observed in Annex A1 where typical bending-shear cracks can be observed for the solid panel at the second storey, particularly for larger openings at the first storey. Similarly, when the wall at the first and third storey is solid, Table 20 indicates no decrease in the structures serviceability limit for the range of opening sizes investigated. Moreover, considerable reductions in the serviceability limit load were observed for combinations of openings larger than O2 at the first and second storey. This indicates that the presence and size of cutout openings in walls at adjacent storeys, has an important influence the serviceability limit state of the structure.

However, combination of openings type O1 (0.9x2.1m) at the two storeys did not show any influence on the serviceability capacity of the structure. This indicates that O1 (0.9x2.1m), could represent a possible a limit for opening size bellow which the opening does not significantly affect the capacity of the structure.

6.3 Ultimate limit state

Section 5.4 “Ultimate limit state (ULS)” showed that cutout openings significantly influence the capacity of the structure associated to the ultimate limit conditions. In particular, yielding of the tensile reinforcement was found to first occur in the spandrel of the newly created openings.

The experimental tests and the FEA simulation of the experimental tests indicated that an approximately 36 and 50% decrease in ultimate capacity is associated with small and large cutout openings, respectively. The small and large cutout openings investigated experimentally correspond to the size of O1 (0.9x2.1m) and O2 (1.8x2.1m) openings in the building FEA. Based on the results of the building FEA, the ultimate load decrease associated with openings O1 and O2 at the first storey, was about 4 and 6%, respectively, and at the second storey about 10 and 33%. The difference between cases when cutout openings are present at the first storey and the second storey, can be attributed to the eccentricity introduced for second storey walls. However, both cases, the influence of openings based on the FEA analysis is considerably lower than the one observed based on the experimental studies.

It was observed (Table 24) that the size of the openings have a significant influence on the ultimate load. For example, ULS capacity of Building O44 (4.1x2.1m openings at the first and second storey) is reduced by 51% lower compared to the AsBuilt Building, whereas the capacity of Building O11 (0.9x2.1m openings at the first and second storey) is only reduce by about 7%.

It is widely accepted that so called ‘small’ openings do not have an influence on the elements and the structures capacity, while so called ‘large’ opening have a considerable effect. Small openings are usually considered, openings created for passing pipes or ventilation ducts, while windows and door are generally considered large openings. However, a clear threshold to classify openings based on their size is not available. EC 2 (2005) states that effects of an opening on a wall’s axial strength can be neglected if the wall is restrained on all sides, while ratio of the opening’s area and height to the wall’s total area and height the are less than 0.1 and 0.33, respectively. In this study all openings were above the limit suggested by EC 2. For example, the ratios between the openings area and height to the wall’s total area and height for O1 are 0.13 and 0.77 and for O4 are 0.8 and 0.77.

For combinations of openings larger than O2 (i.e. opening to wall area ration higher than 0.26), a large decrease in ultimate capacity was observed, whereas for combinations of O1 (i.e. opening to wall area ration of 0.13), the ultimate load was only reduced by approximately 4 to 10%. Moreover, in Section 5.5

"Comparison of limit states" it was shown that in cases when combinations of O1 cutout openings were created, the SLS associated limit loads were found to be lower than the ULS. This would suggest that the influence of openings of size O1 (0.9x2.1m) is practically limited even though O1 openings exceed the limits suggested by EC 2.

6.4 Strengthening recommendations

6.4.1 Strengthening for serviceability conditions

Table 19 suggests that a strengthening solution aimed at reducing the size of the cracks, can provide a 17 to 30% increase of the service load when cutout openings need to be created. Externally bonded FRP (fibre reinforce polymers) and FRCM (fabric reinforced cementitious matrix) strengthening solutions have been shown to substantially delay the openings of cracks and decrease the size of cracks when applied to RC walls (Popescu et al. 2017; Sabau et al. 2018), slabs (Bruckner et al. 2006; Floruţ et al. 2014; Michels et al. 2014), and beams (Blanksvärd 2009; Sas et al. 2014) Thus, applying additional FRP and FRCM reinforcement to the slabs would reduce the crack or delay the opening of cracks and increase the service limit load to that imposed by the deflections. The amount of additional FRP or FRCM reinforcement should result from an additional analysis.

If the service capacity needs to be increased above the limit imposed by deflection, externally bonded or near surface mounted pre-stressed FRP solutions, have been shown to simultaneously increase the capacity and the rigidity of RC beams (Nordin and Täljsten 2006) and slabs (Correia et al. 2015). However, a disadvantage of these techniques compared to the above mentioned solutions is considered to be the mechanical anchorage systems necessary to transfer the pre-stressing force that can be time consuming and cumbersome to install.

6.4.2 Strengthening for ultimate limit conditions

For all openings arrangements the ultimate limit state was given by the reinforcement yielding condition in the walls with cutout openings. This suggest that strengthening solutions should consist of applying additional reinforcement to prevent the yielding of the element's internal steel reinforcement. Suitable strengthening solutions that can be considered in this case were investigated in (Sabau et al. 2017) Sabau et al. (2018) using FRCM composites and Popescu et al. (2017) using FRP composites. In both cases it was shown that that the strengthening solutions decreased the maximum strain in the internal steel reinforcement below the yielding limit compared to un-strengthened concrete walls (Popescu et al. 2016) considering the same load levels.

For some opening configurations (i.e. O13 and O23) the reinforcement yielding limit state coincides with the concrete crushing limit state. For these cases, an effective strengthening solution would imply the increase in concrete compressive strength simultaneously with the addition of tensile reinforcement. The strengthening solution proposed in (Popescu et al. 2016) has a better applicability in these cases, as the FRP composites have the double role of providing a confinement to the concrete elements and providing additional tensile reinforcement. The choice of strengthening solution and the amount of reinforcement used for either of the strengthening systems should result from an additional analysis.

A heuristic approach to optimize the strengthening method for concrete walls is presented in Figure 27. The scheme illustrates the steps taken in the analyses presented in this report starting from the initial analysis to the identification of structural deficiencies and the choice of strengthening more suitable for each case.

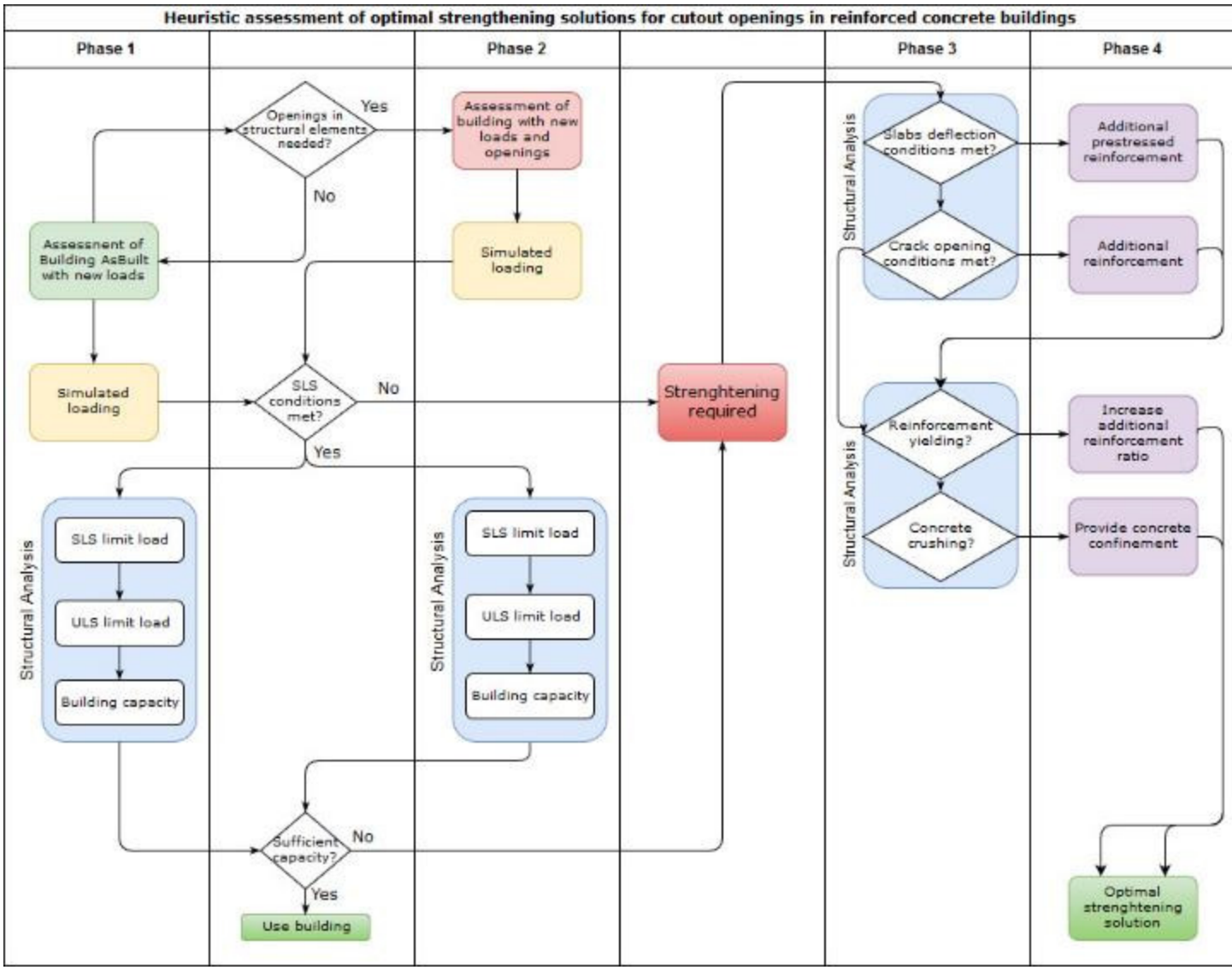

Figure 27 Proposed scheme for choosing an optimized strengthening method

7 Conclusions

The results presented in this report are based on the non-linear finite element modelling of an 11-storey residential building with the structural system of reinforced concrete walls. First, the FEM modelling approach is described. The FEM model is first verified by comparison with experimental test on reinforced concrete walls with openings tested to failure (Popescu et al. 2016). The boundary conditions (i.e. the connection between the studied wall and the adjacent elements) was found to have an important influence on the wall's load response. The FE models were able to predict the strength of the tested walls satisfactorily when the boundary conditions were defined to allow deformations similar to those observed experimentally.

Subsequently, a similar modelling approach was used to study the influence of cutout openings on reinforced concrete walls as part of a building, thus simulating boundary conditions that are more similar to the reality. The report presents the results of a parametric study in which the influence of the size and location of openings was investigated. The results of the parametric study were used to assess possible strengthening solution using composite material that could be effectively used for the studied cases.

The FEA pointed out:

- an increase in live load of 3 kN/m^2 associated to a change in the building's function from residential to office building could possibly be made for any opening configuration considered in this study, without exceeding deflection and crack openings limitation provided in design guidelines;
- the presence of cutout openings in adjacent stories influences the ultimate capacity of the structure, causing an additional 15% to 50% decrease in capacity if the cutout opening is larger than the one at the storey above;
- cutout openings reduce the axial stiffness and capacity of solid reinforced concrete panels changing the distribution of loads to the foundations, leading to up to 60% higher loads on in adjacent members. No cracks or excessive deformations were observed for adjacent members in this study, however, in case of such an intervention, verifications should also consider the adjacent wall panels and their foundations;
- the maximum capacity for buildings with small door cutout openings (i.e. openings size 0.9x2.1m) was obtained from serviceability limit conditions, whereas for buildings with large door cutout openings (i.e. openings size larger than 1.8x2.1m) was obtained from ultimate limit conditions for building with larger cutout door openings;
- for buildings with small openings (i.e. openings size 0.9x2.1m), externally bonded FRP and FRCM strengthening solution can be used to increase the service limit load by 17 to 30% by reducing the crack opening size in slabs and walls, this measures should also provide an increases in ultimate limit load by reducing the strain in the internal steel reinforcement thus raising the yield limit;
- for buildings with large openings, strengthening solution that increases the concrete strength or ultimate strain can represent a more effective alternative.
- the influence of cutout openings observed in the experimental tests, as well as the FEA simulation of the experimental tests, was observed to be higher compared to that obtained in the FEA of the entire building structure

8 Future research

The current study is based on finite element analysis of a particular of structure. Therefore, results and should not be extrapolated to other cases. However, if treated with care, these results can guide practicing engineers to evaluate more effectively the need for strengthening for in other existing structures. Future full-scale tests on decommissioned or in service structures could be useful to confirm the findings of this study. Additionally, future numerical studies should address a number of other parameters such as the location of the openings within the wall, as well as the effects of shrinkage, creep and thermal loading

as well as the influence of long-term loading and potential effects of shrinkage on the performance intersection between walls. The effectives of FRP and FRCM strengthening solutions at the global level should further be investigated.

Acknowledgements

The authors would like to thank Dr. Sorin Codruţ Floruţ for providing the original design drawings of the building. The authors would like to acknowledge the Development Fund of Swedish Construction Industry (SBUF), Skanska AB, the Research Council of Norway (RFF) and the European Commission (Contract number MC-ITN-2013-607851) for financing the presented and associated work.

9 References

American Concrete Institute. (2011) "Building Code Requirements for Structural Concrete." Farmington Hills, MI 48331.

American Concrete Institute. (2011) "Guide for Precast Concrete Wall Panels." ACI 533R-11, Farmington Hills, MI.

Standards Australia. (2009) "Concrete structures." CAN/CSA-A23.3, Sydney, Australia.

Björk, C., Kallstenius, P., and Reppen, L. (1983). *Sä byggdes husen 1880-1980*, Stockholms stadsbyggkontor och Statens råd för byggnadsforsking, Stockholm, Sweden.

Blanksvärd, T. (2009). "Strengthening of concrete structures by the use of mineralbased composites." PhD. Doctoral, Luleå University of Technology, Universitetstryckeriet, Luleå.

Bruckner, A., Ortlepp, R., and Curbach, M. (2006). "Textile reinforced concrete for strengthening in bending and shear." *Mater Struct*, DOI 10.1617/s11527-005-9027-2, 39(8), 741-748.

British Strandards Institution. (1997) "Structural use of concrete." London, United Kingdom.

Cervenka Consulting (2018). "Atena version 5.6." (08.01.2018).

Cervenka, V., Jendele, L., and Cervenka, J. (2014). "ATENA Program Documentation Part 1. Theory. ." Cervenka Consulting., Prauge, Czech Republic.

Cervenka, V., Pukl, R., Ozbolt, J., and Eligehausen, R. "Mesh sensitivity effects in smeared finite element analysis of concrete fracture." *Proc., Fracture Mechanics of Concrete Structures*, AEDIFICATIO Publishers, Freiburg, Germany, 1995.

CIMNE (2018). "GiD v11." (2018).

Correia, L., Teixeira, T., Michels, J., Almeida, J. A. P. P., and Sena-Cruz, J. (2015). "Flexural behaviour of RC slabs strengthened with prestressed CFRP strips using different anchorage systems." *Composites Part B: Engineering*, https://doi.org/10.1016/j.compositesb.2015.07.011, 81(Supplement C), 158-170.

Csoknyai, T., Hrabovszky-Horváth, S., Georgiev, Z., Jovanovic-Popovic, M., Stankovic, B., Villatoro, O., and Szendrő, G. (2016). "Building stock characteristics and energy performance of residential buildings in Eastern-European countries." *Energy and Buildings*, https://doi.org/10.1016/j.enbuild.2016.06.062, 132, 39-52.

De Borst, R. (1986). "Non-linear analysis of frictional materials."

European Committee for Standardization (CEN). (2002) "Eurocode 1: Actions on structures." Bruxelles, Belgium.

European Committee for Standardization (CEN). (2005) "Eurocode 2: Design of concrete structures." EC 2, Brussels, B-1050, Belgium.

European Committee for Standardization (CEN). (2004) "Eurocode 3: Design of steel structures." Bruxelles, Belgium.

Floruţ, S.-C., Sas, G., Popescu, C., and Stoian, V. (2014). "Tests on reinforced concrete slabs with cut-out openings strengthened with fibre-reinforced polymers." *Composites Part B: Engineering*, 10.1016/j.compositesb.2014.06.008, 66, 484-493.

Fragomeni, S., Doh, J. H., and Lee, D. J. (2012). "Behavior of Axially Loaded Concrete Wall Panels with Openings: An Experimental Study." *Advances in Structural Engineering*15(8), 1345-1358.

Guan, H., Cooper, C., and Lee, D.-J. (2010). "Ultimate strength analysis of normal and high strength concrete wall panels with varying opening configurations." *Engineering Structures*, 10.1016/j.engstruct.2010.01.012, 32(5), 1341-1355.

Hendriks, M. A. N., de Boer, A., and Belletti, B. (2016). *Guidelines for Nonlinear Finite Element Analysis of Concrete Structures.*, Rijkswaterstaat Technisch Document (RTD), Delft, Netherlands.

Jansson, J., and Svensson, S. (2016). "Effect of Cut-Out Openings in RC Walls : A Parametric Study with the Finite Element Program ATENA." Independent thesis Advanced level (professional degree) Student thesis. Available at: http://urn.kb.se/resolve?urn=urn:nbn:se:ltu:diva-57256

Lee, Y., Lee, B. Y., Kwon, S. H., Kim, Y. Y., and Kim, J. K. (2008). "Long-term behaviour of a reinforced concrete wall under compressive stress applied to part of the wall's entire width." *Magazine of Concrete Research*, 10.1680/macr.2008.00090, 60(10), 759-768.

Michels, J., Zwicky, D., Scherer, J., Harmanci, Y. E., and Motavalli, M. (2014). "Structural Strengthening of Concrete with Fiber Reinforced Cementitious Matrix (FRCM) at Ambient and Elevated

Temperature - Recent Investigations in Switzerland." *Advances in Structural Engineering*17(12), 1785-1799.
Nordin, H., and Täljsten, B. (2006). "Concrete Beams Strengthened with Prestressed Near Surface Mounted CFRP." *Journal of Composites for Construction*, 10.1061/(ASCE)1090-0268(2006)10:1(60), 10(1), 60-68.
Ottosen, N. S. L., and Petersson, H. L. (1992). *Introduction to the Finite Element Method*, Prentice-Hall.
Popescu, C., Sas, G., Blanksvärd, T., and Täljsten, B. (2015). "Concrete walls weakened by openings as compression members: A review." *Engineering Structures*, 10.1016/j.engstruct.2015.02.006, 89, 172-190.
Popescu, C., Sas, G., Blanksvärd, T., and Täljsten, B. (2017). "Concrete Walls with Cutout Openings Strengthened by FRP Confinement." *Journal of Composites for Construction*, doi:10.1061/(ASCE)CC.1943-5614.0000759, 21(3), 04016106.
Popescu, C., Sas, G., Sabau, C., and Blanksvärd, T. (2016). "Effect of Cut-Out Openings on the Axial Strength of Concrete Walls." *Journal of Structural Engineering*, 10.1061/(ASCE)ST.1943-541X.0001558, 142(11), 04016100.
Rankine, W. (1857). "On the stability of loose earth." *Philosophical Transactions of the Royal Society of London*147.
Sabau, C., Popescu, C., Sas, G., Blanksvärd, T., and Täljsten, B. "Monitoring structural behavior of reinforced concrete walls with openings using digital image correlation." *Proc., 19th IABSE Congress*, International Association for Bridge and Structural Engineering (IABSE), Stockholm, Sweden, 2016.
Sabau, C., Popescu, C., Sas, G., Blanksvärd, T., and Täljsten, B. (2018). "Axially loaded RC walls with openings strengthened with FRCM composites." *Journal of Composites for Construction*Submitted.
Saheb, S. M., and Desayi, P. (1990). "Ultimate Strength of RC Wall Panels with Openings." *Journal of Structural Engineering*, doi:10.1061/(ASCE)0733-9445(1990)116:6(1565), 116(6), 1565-1577.
Sas, G., Dăescu, C., Popescu, C., and Nagy-György, T. (2014). "Numerical optimization of strengthening disturbed regions of dapped-end beams using NSM and EBR CFRP." *Composites Part B: Engineering*, 10.1016/j.compositesb.2014.07.013, 67, 381-390.
SBUF 13246 (2018). "Rehabiliteringsmetoder för håltagning i armerade betongväggar." Skanska Sverige AB.
Svenska Betongföreningen (2010). *Svenska Betongföreningens handbok till Eurokod 2. Volym I.*, Stockholm, Sweden.
van Mier, J. G. M. (1986). "Multiaxial strain-softening of concrete." *Mater Struct*, 10.1007/bf02472034, 19(3), 179-190.
Willwerth, A. (2013). "Grounding HVAC Motor Shafts: Protecting bearings and lowering repair costs." *Construction Canada*, Kenilworth Media Inc., Canada.

10 Annexes

A1 – Principal tensile strain distribution on wall D12

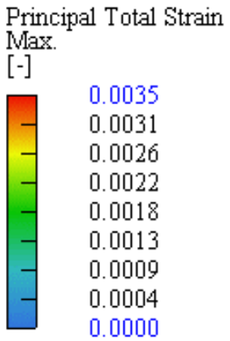

Deformation magnification factor: 70

The shape of the element before deformation is indicated by the black contour lines

Cracks larger than 0.3 mm are indicated with thick black lines

	Solid	Ox1	Ox2	Ox3	Ox4
Applied load =	52.84 kN/m^2	53.09 kN/m^2	52.28 kN/m^2	51.68 kN/m^2	50.02 kN/m^2
Solid	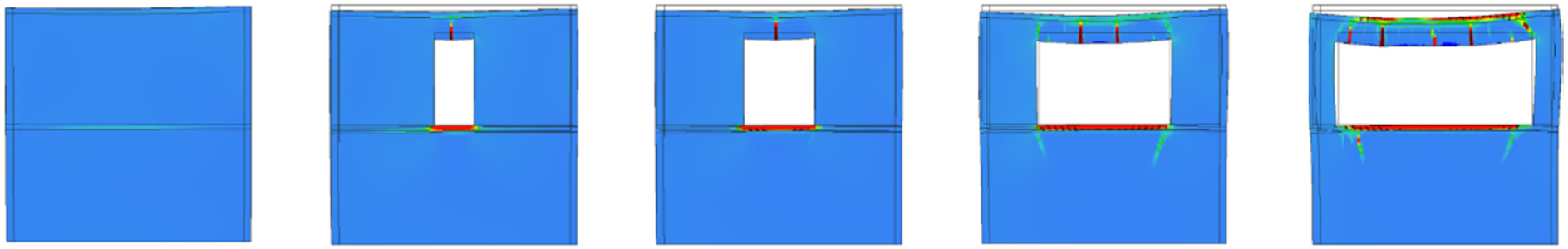				
Applied load =	53.06 kN/m^2	52.78 kN/m^2	52.74 kN/m^2	51.75 kN/m^2	50.33 kN/m^2
O1y	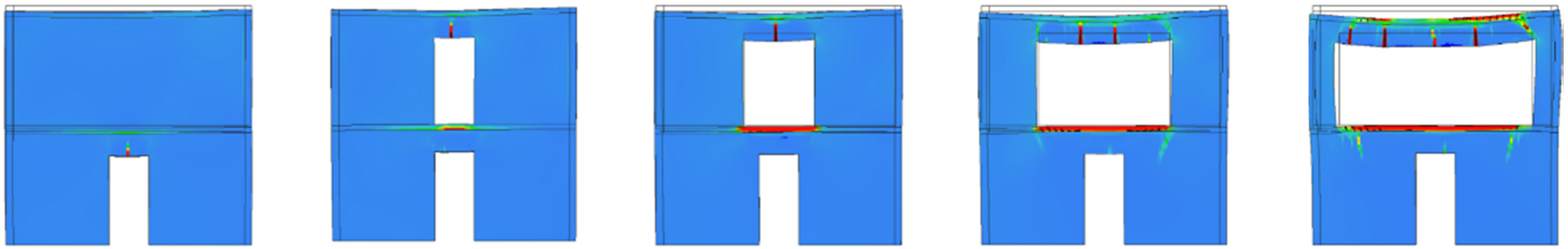				
Applied load =	52.96 kN/m^2	52.73 kN/m^2	52.69 kN/m^2	51.8 kN/m^2	50.09 kN/m^2
O2y	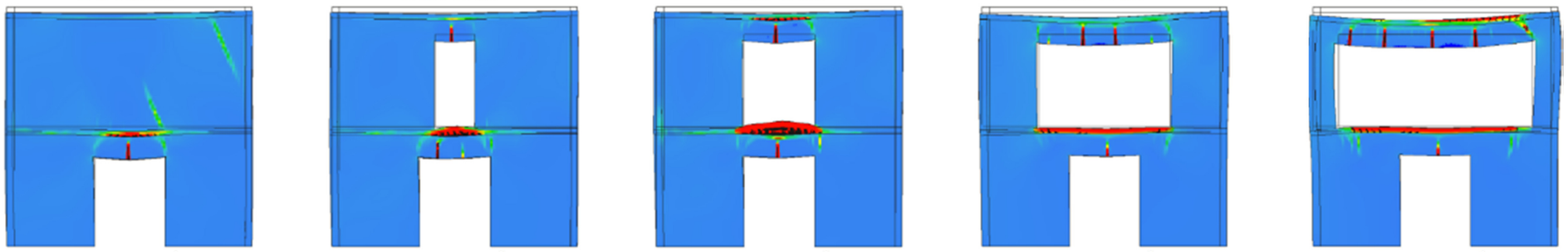				
Applied load =	51.96 kN/m^2	51.96 kN/m^2	52.12 kN/m^2	51.50 kN/m^2	50.14 kN/m^2
O3y	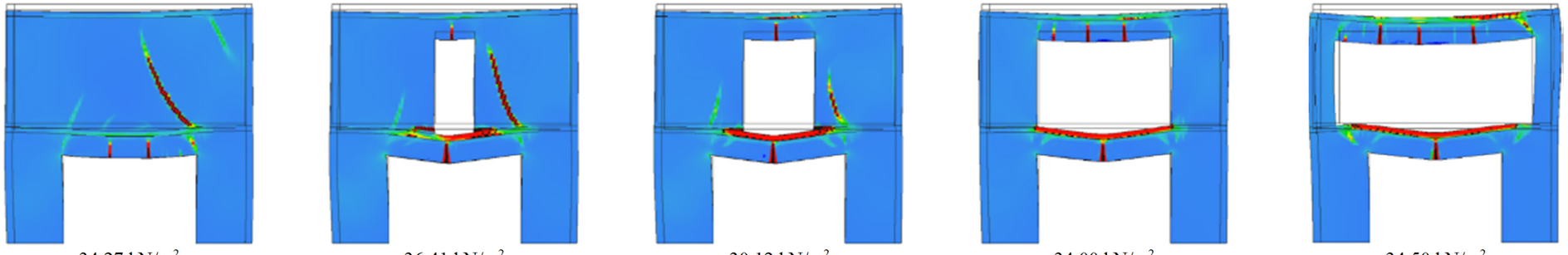				
Applied load =	34.27 kN/m^2	36.41 kN/m^2	30.12 kN/m^2	34.00 kN/m^2	34.50 kN/m^2
O4y	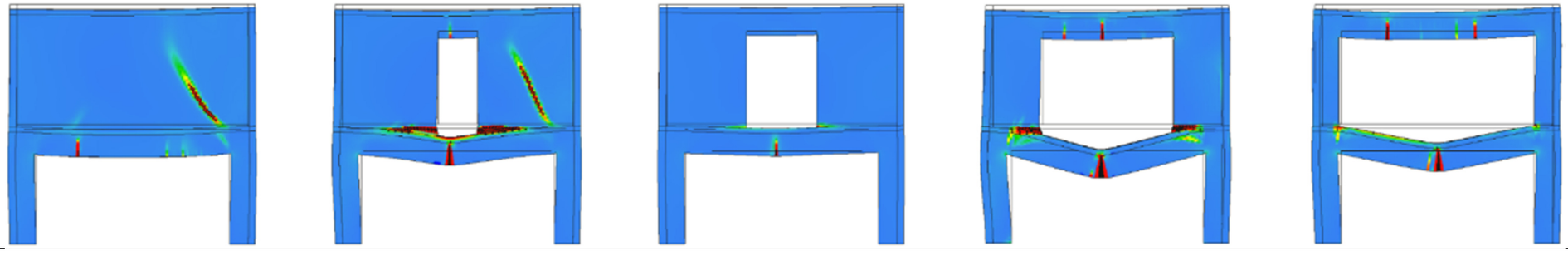				

A2 – Principal compressive strain distribution on wall D12

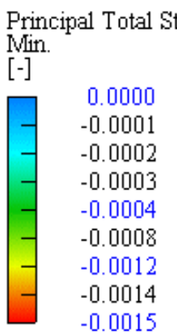

Deformation magnification factor: 70

The shape of the element before deformation is indicated by the black contour lines

Cracks larger than 0.3 mm are indicated with thick black lines

	Solid	Ox1	Ox2	Ox3	Ox4
Applied load =	52.84 kN/m^2	53.09 kN/m^2	52.28 kN/m^2	51.68 kN/m^2	50.02 kN/m^2
Solid	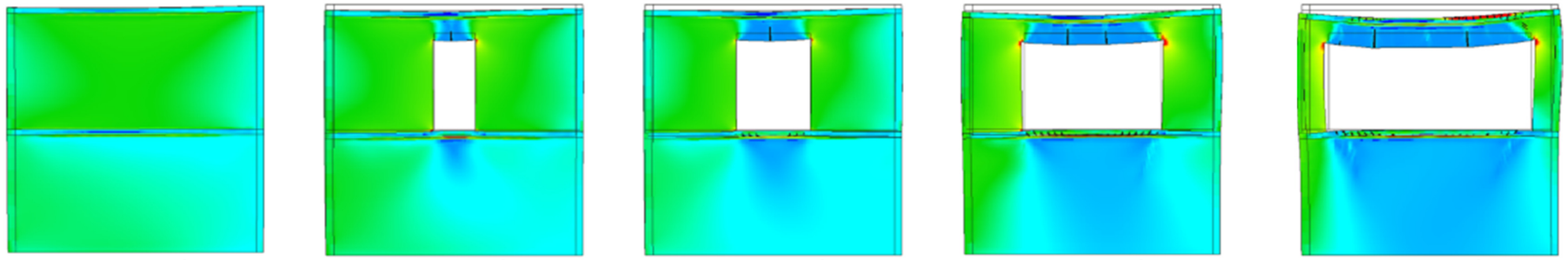				
Applied load =	53.06 kN/m^2	52.78 kN/m^2	52.74 kN/m^2	51.75 kN/m^2	50.33 kN/m^2
O1y	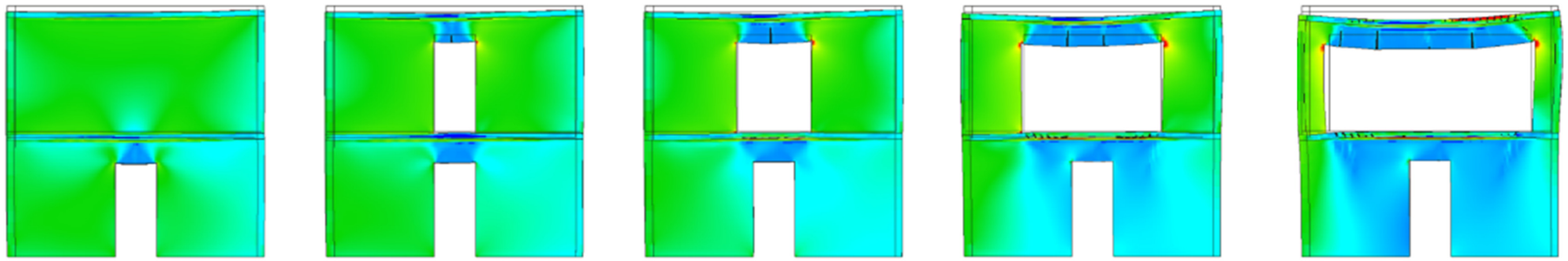				
Applied load =	52.96 kN/m^2	52.73 kN/m^2	52.69 kN/m^2	51.8 kN/m^2	50.09 kN/m^2
O2y	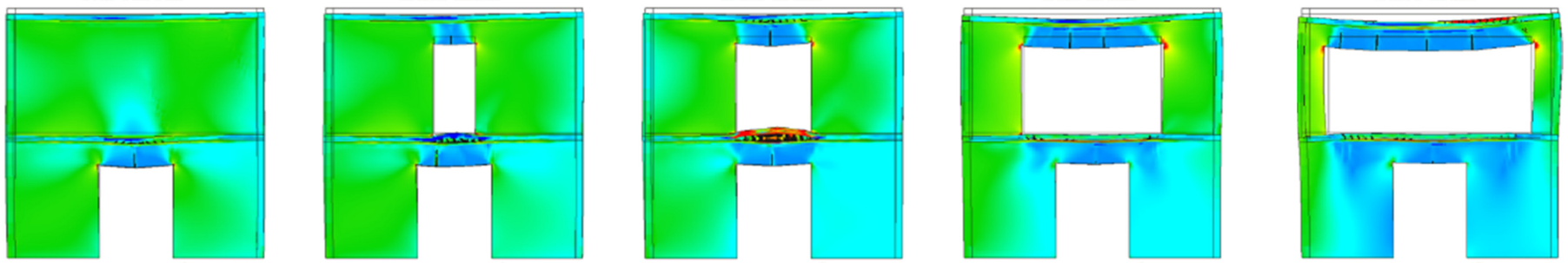				
Applied load =	51.96 kN/m^2	51.96 kN/m^2	52.12 kN/m^2	51.50 kN/m^2	50.14 kN/m^2
O3y	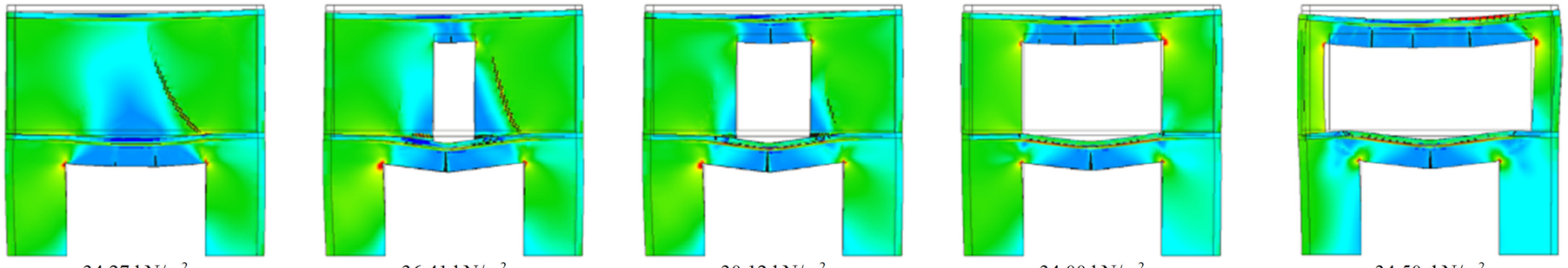				
Applied load =	34.27 kN/m^2	36.41 kN/m^2	30.12 kN/m^2	34.00 kN/m^2	34.50 kN/m^2
O4y	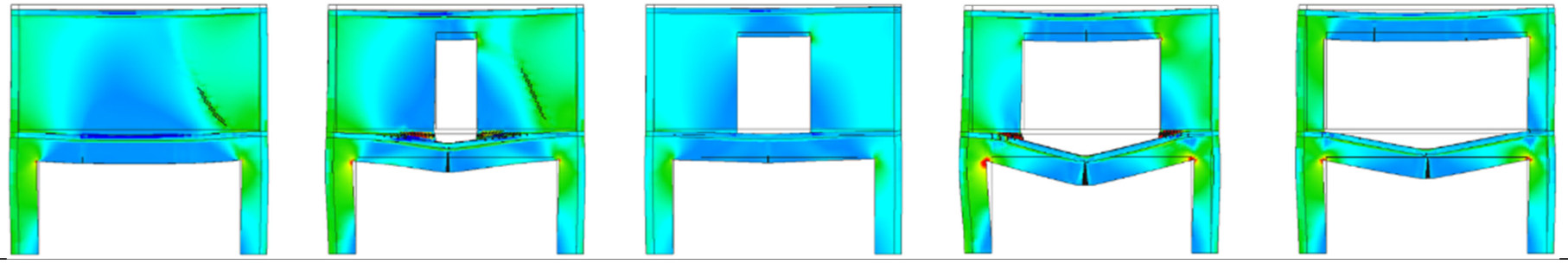				

A3 – Load response diagrams for deflections in critical slabs and spandrel.

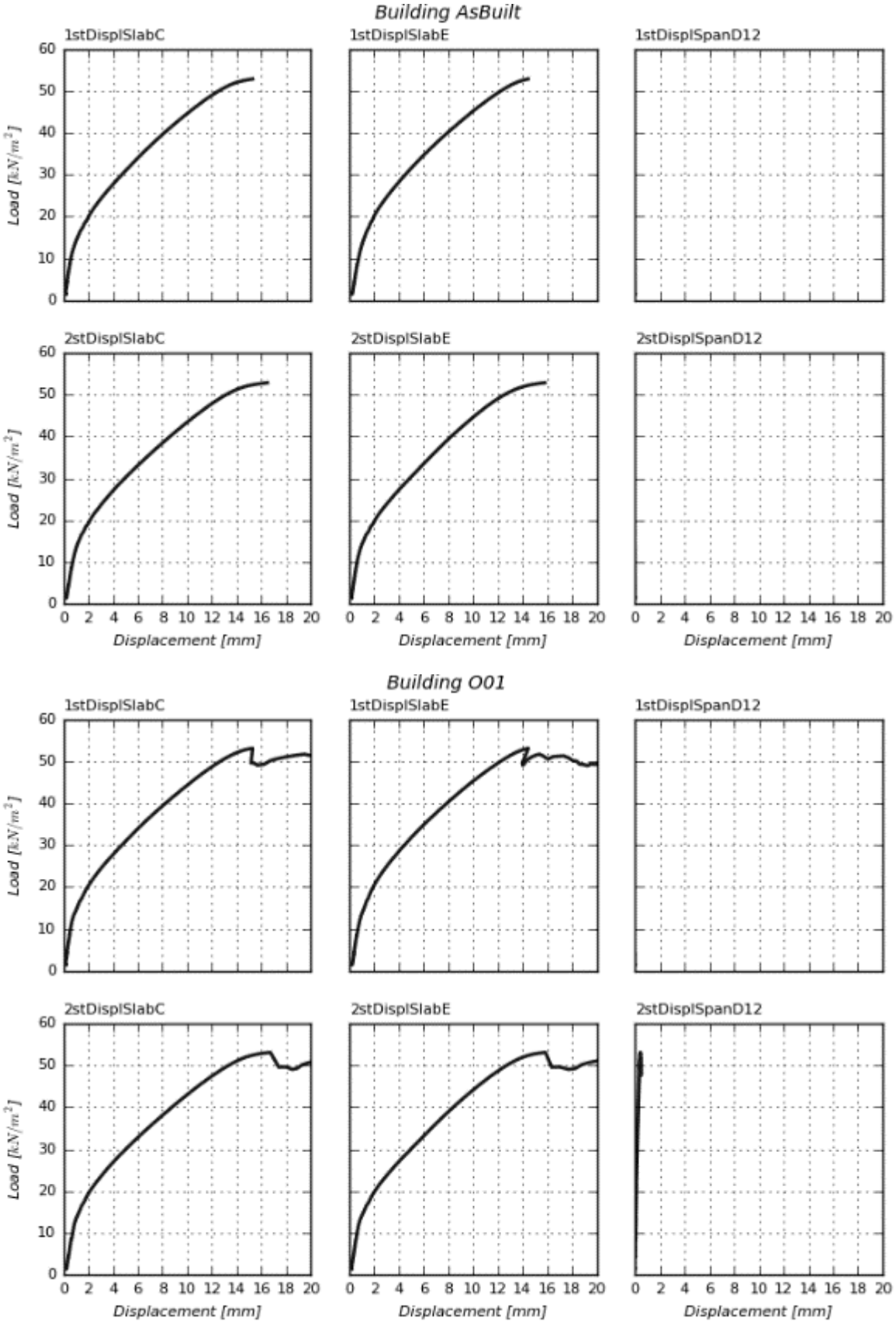

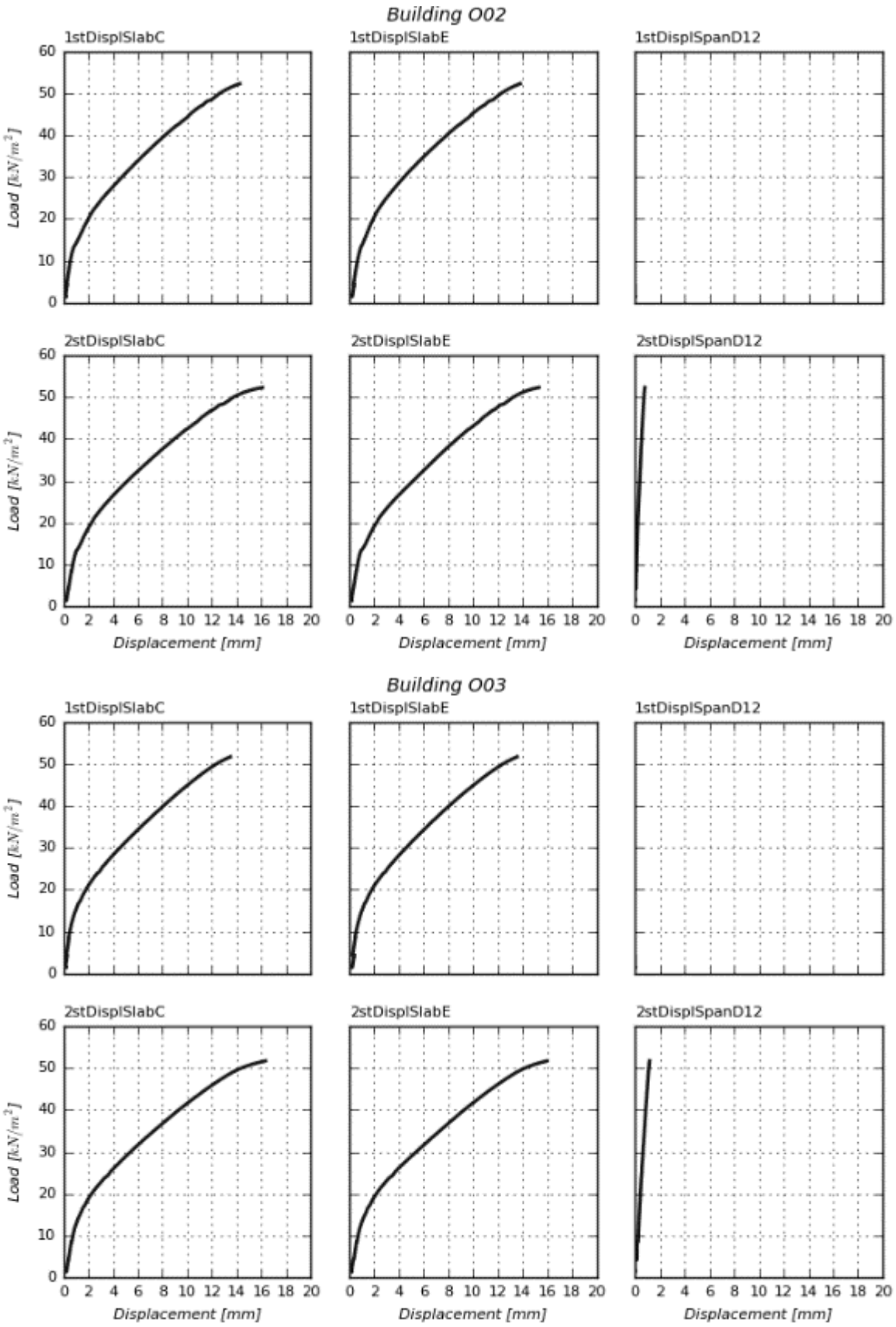
Building O02
1stDisplSlabC
1stDisplSlabE
1stDisplSpanD12
2stDisplSlabC
2stDisplSlabE
2stDisplSpanD12
Load [kN/m²]
Displacement [mm]
Building O03
1stDisplSlabC
1stDisplSlabE
1stDisplSpanD12
2stDisplSlabC
2stDisplSlabE
2stDisplSpanD12
Load [kN/m²]
Displacement [mm]

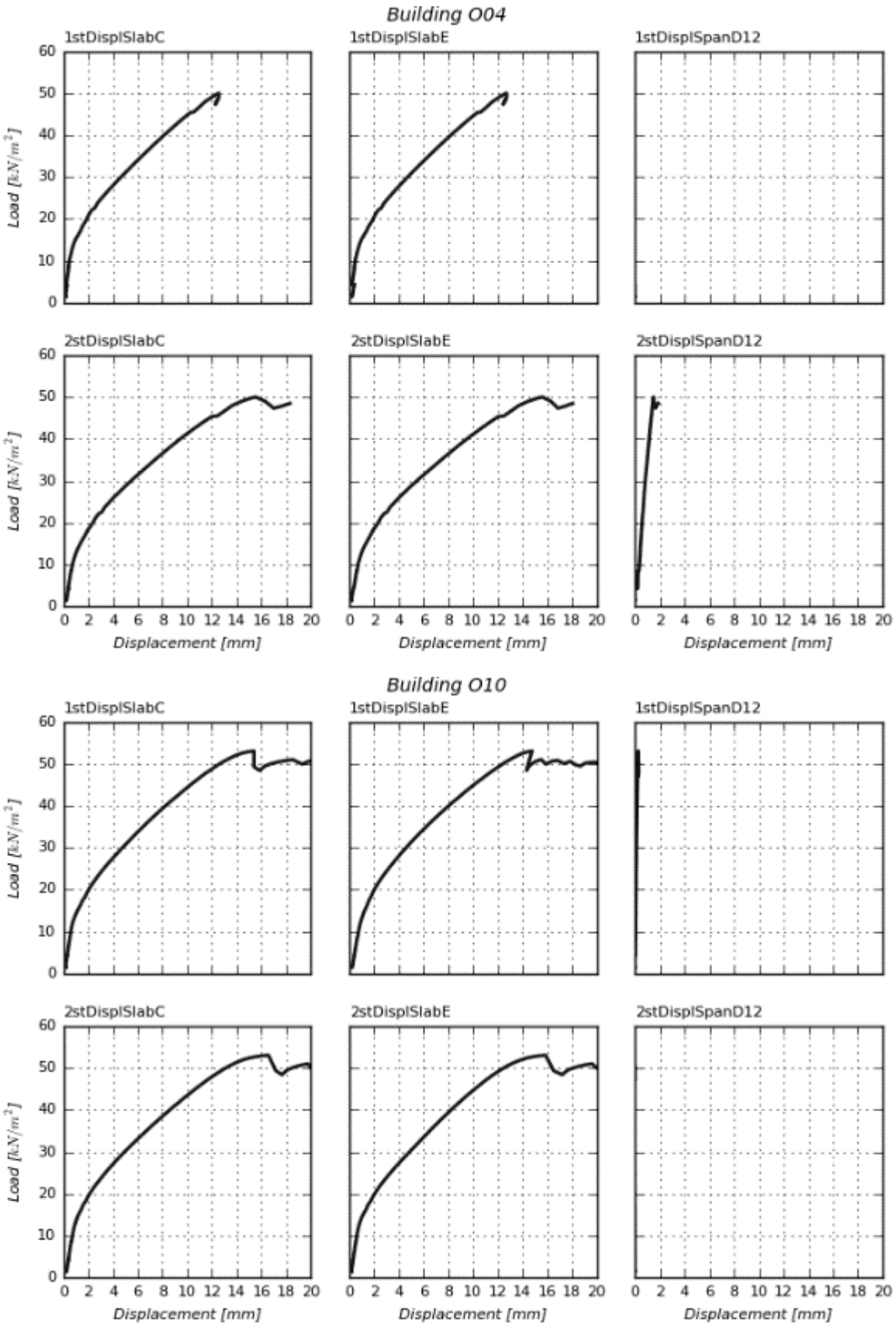
Building O04
1stDisplSlabC
1stDisplSlabE
1stDisplSpanD12
2stDisplSlabC
2stDisplSlabE
2stDisplSpanD12
Load [kN/m²]
Displacement [mm]
Building O10
1stDisplSlabC
1stDisplSlabE
1stDisplSpanD12
2stDisplSlabC
2stDisplSlabE
2stDisplSpanD12
Load [kN/m²]
Displacement [mm]

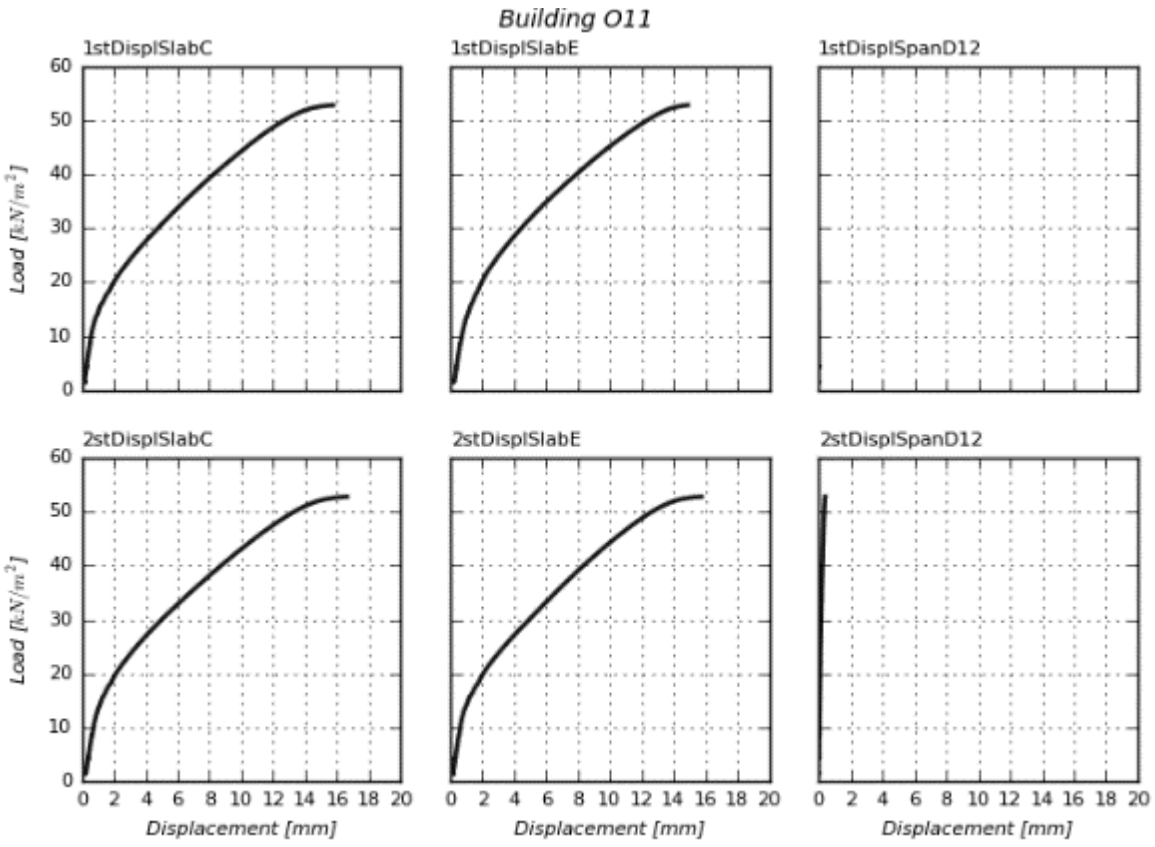
Building O11
1stDisplSlabC
1stDisplSlabE
1stDisplSpanD12
2stDisplSlabC
2stDisplSlabE
2stDisplSpanD12
Load [kN/m²]
Displacement [mm]

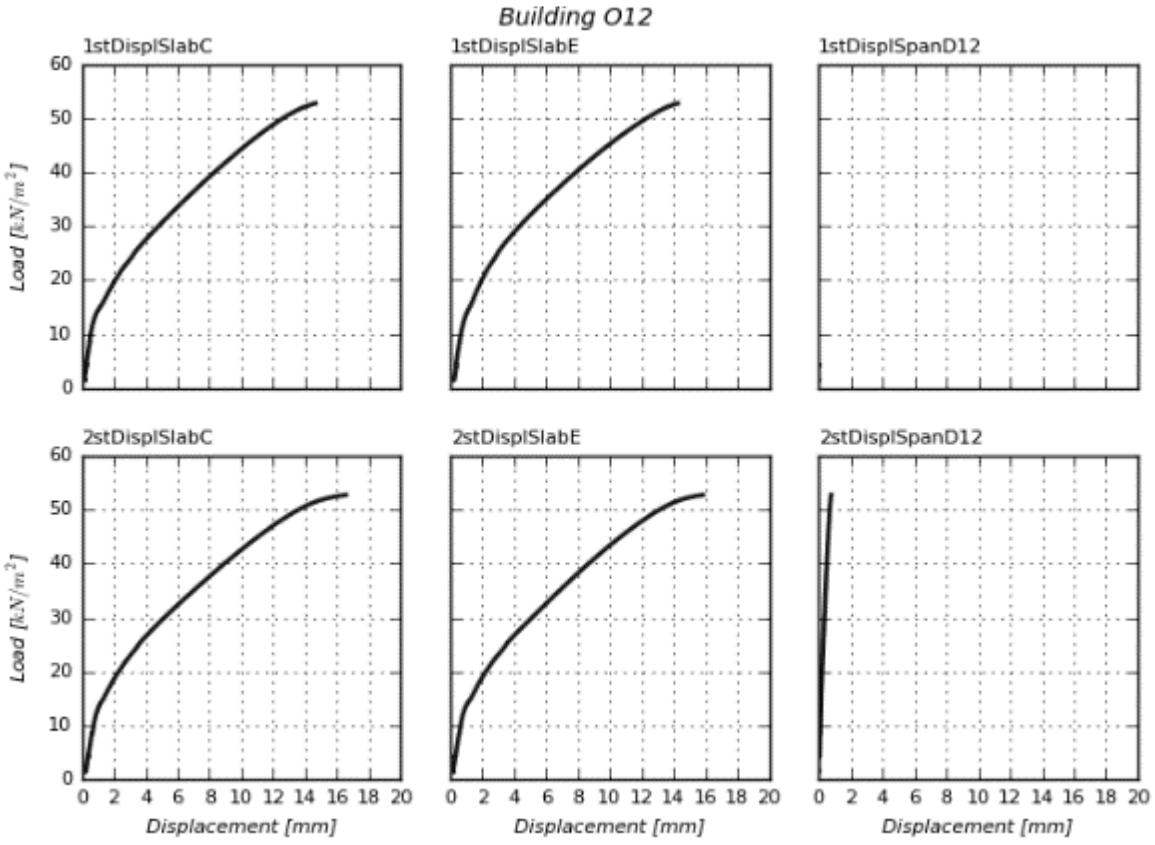
Building O12
1stDisplSlabC
1stDisplSlabE
1stDisplSpanD12
2stDisplSlabC
2stDisplSlabE
2stDisplSpanD12
Load [kN/m²]
Displacement [mm]

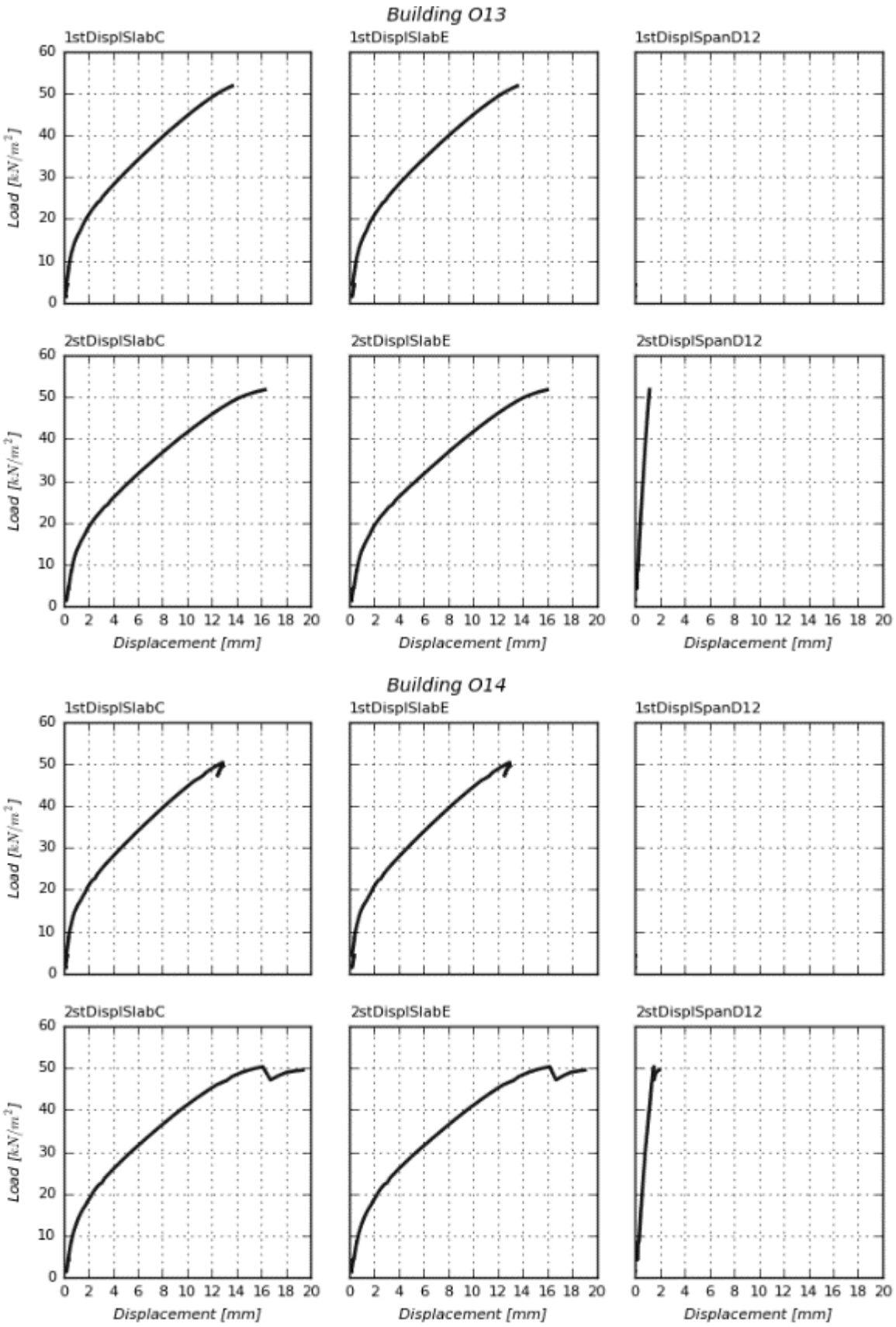
Building O13
1stDisplSlabC
1stDisplSlabE
1stDisplSpanD12
2stDisplSlabC
2stDisplSlabE
2stDisplSpanD12
Load [kN/m²]
Displacement [mm]
Building O14
1stDisplSlabC
1stDisplSlabE
1stDisplSpanD12
2stDisplSlabC
2stDisplSlabE
2stDisplSpanD12
Load [kN/m²]
Displacement [mm]

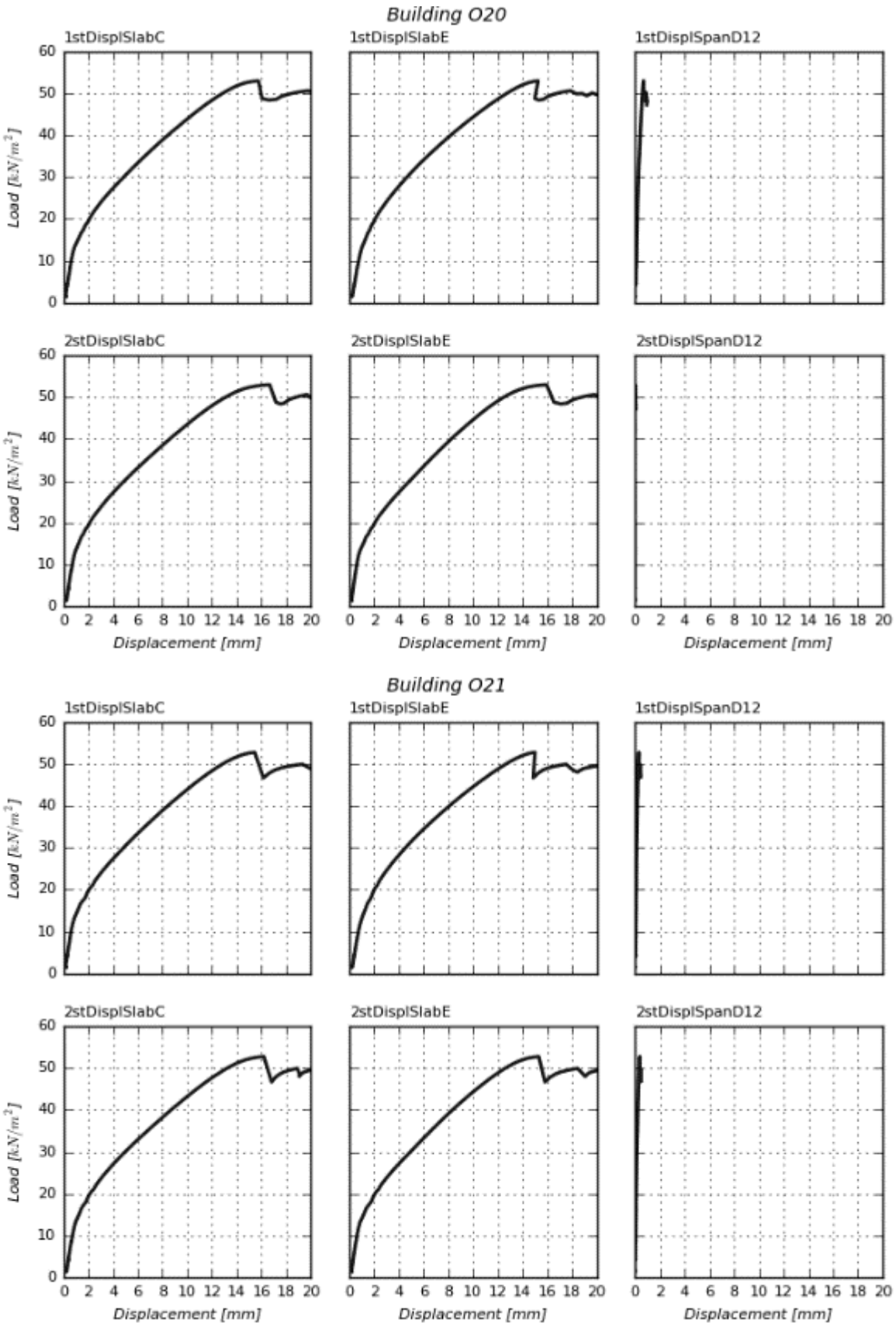
Building O20
1stDisplSlabC
1stDisplSlabE
1stDisplSpanD12
2stDisplSlabC
2stDisplSlabE
2stDisplSpanD12
Load [kN/m²]
Displacement [mm]
Building O21
1stDisplSlabC
1stDisplSlabE
1stDisplSpanD12
2stDisplSlabC
2stDisplSlabE
2stDisplSpanD12
Load [kN/m²]
Displacement [mm]

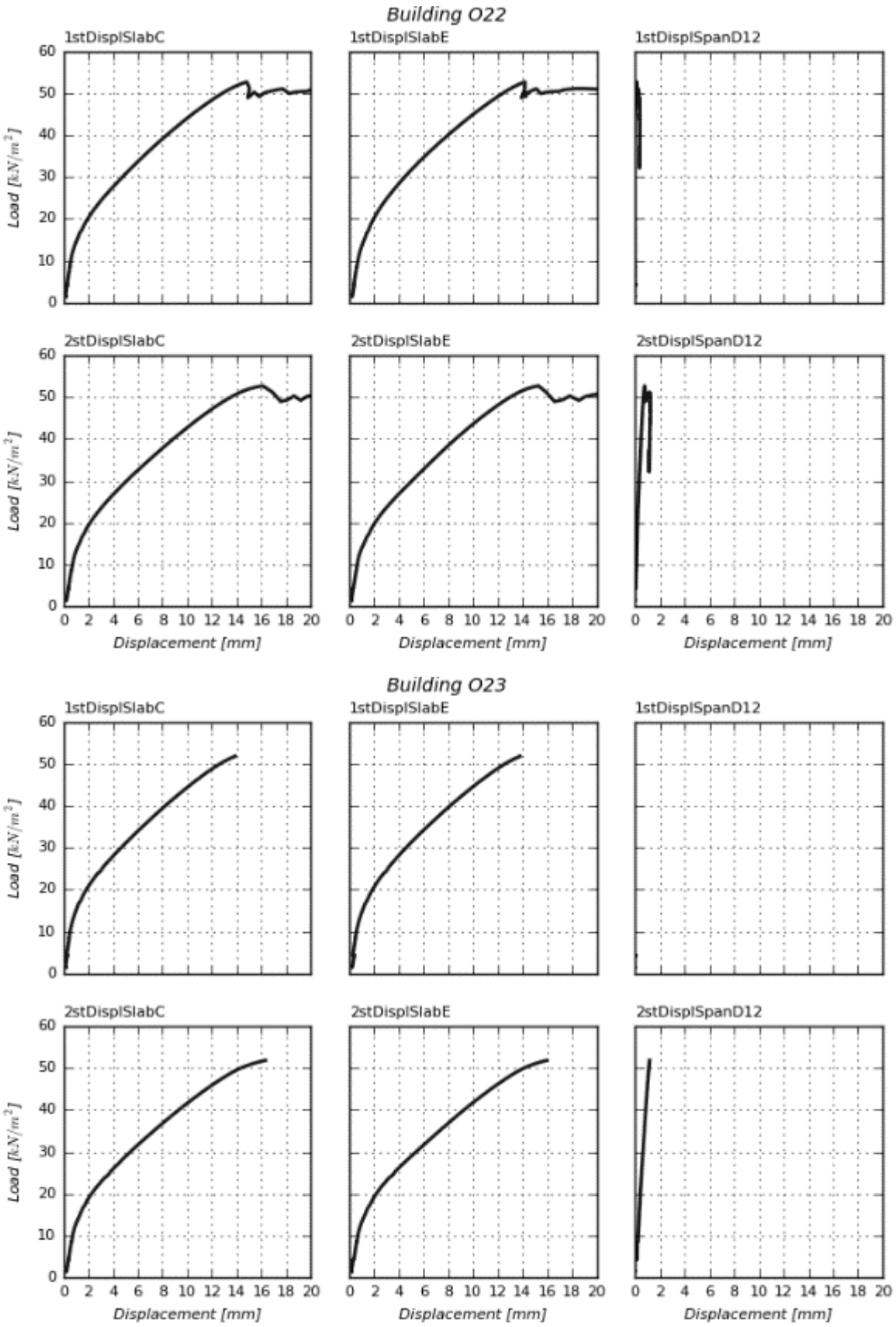
Building O22
1stDisplSlabC
1stDisplSlabE
1stDisplSpanD12
2stDisplSlabC
2stDisplSlabE
2stDisplSpanD12
Load [kN/m²]
Displacement [mm]
Building O23
1stDisplSlabC
1stDisplSlabE
1stDisplSpanD12
2stDisplSlabC
2stDisplSlabE
2stDisplSpanD12
Load [kN/m²]
Displacement [mm]

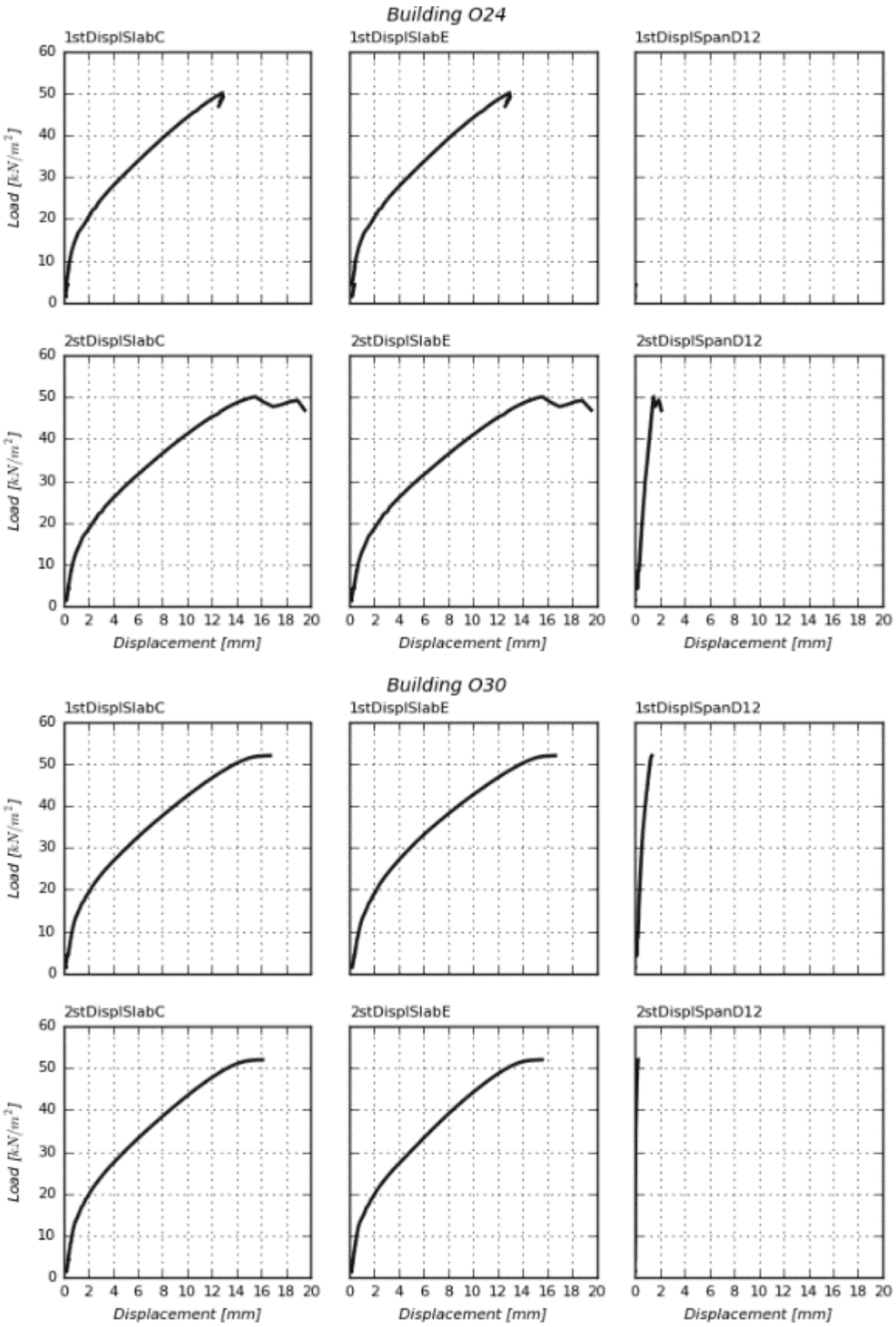
Building O24
1stDisplSlabC
1stDisplSlabE
1stDisplSpanD12
2stDisplSlabC
2stDisplSlabE
2stDisplSpanD12
Load [kN/m²]
Displacement [mm]
Building O30
1stDisplSlabC
1stDisplSlabE
1stDisplSpanD12
2stDisplSlabC
2stDisplSlabE
2stDisplSpanD12
Load [kN/m²]
Displacement [mm]

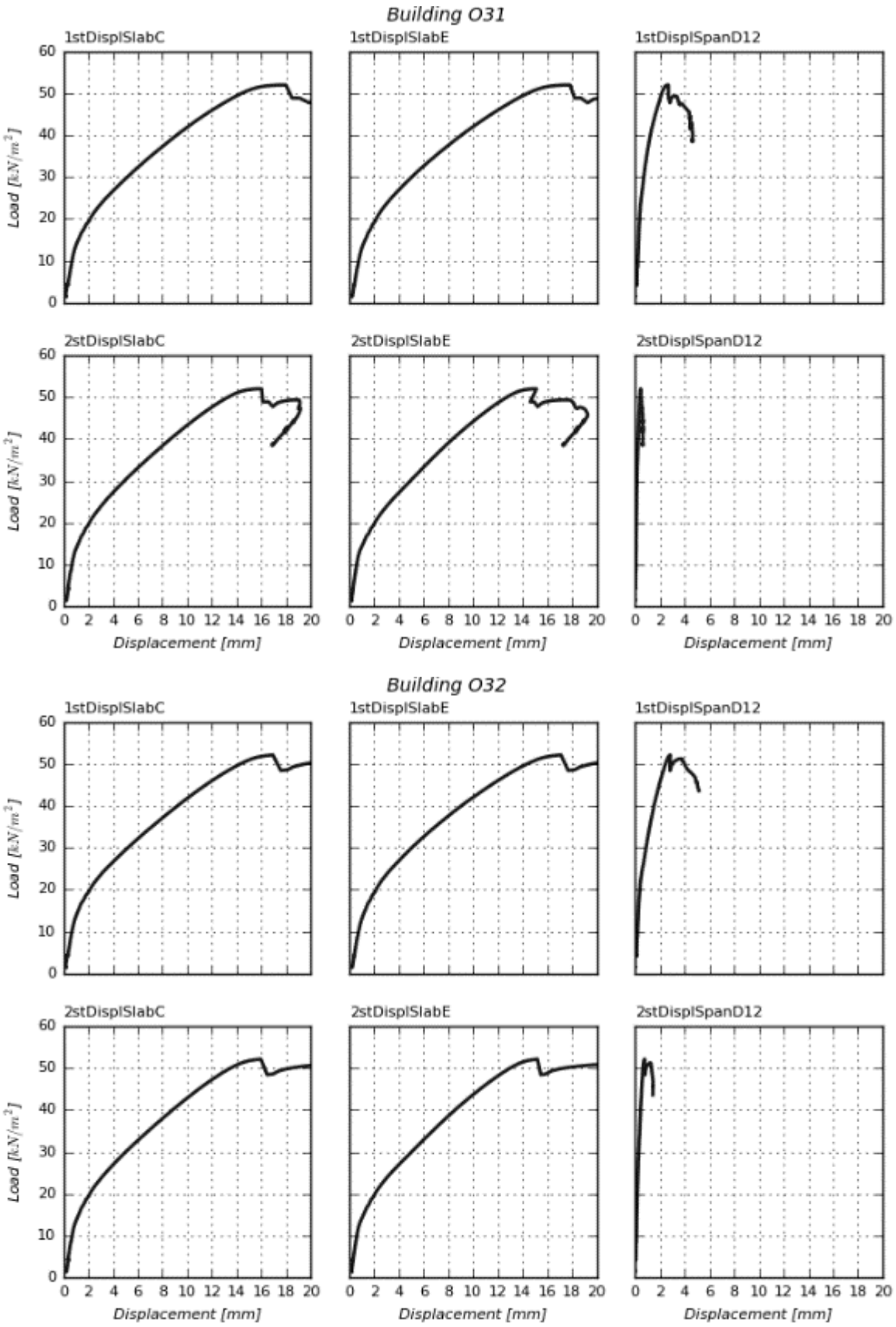
Building O31
1stDisplSlabC
1stDisplSlabE
1stDisplSpanD12
2stDisplSlabC
2stDisplSlabE
2stDisplSpanD12
Load [kN/m²]
Displacement [mm]
Building O32
1stDisplSlabC
1stDisplSlabE
1stDisplSpanD12
2stDisplSlabC
2stDisplSlabE
2stDisplSpanD12
Load [kN/m²]
Displacement [mm]

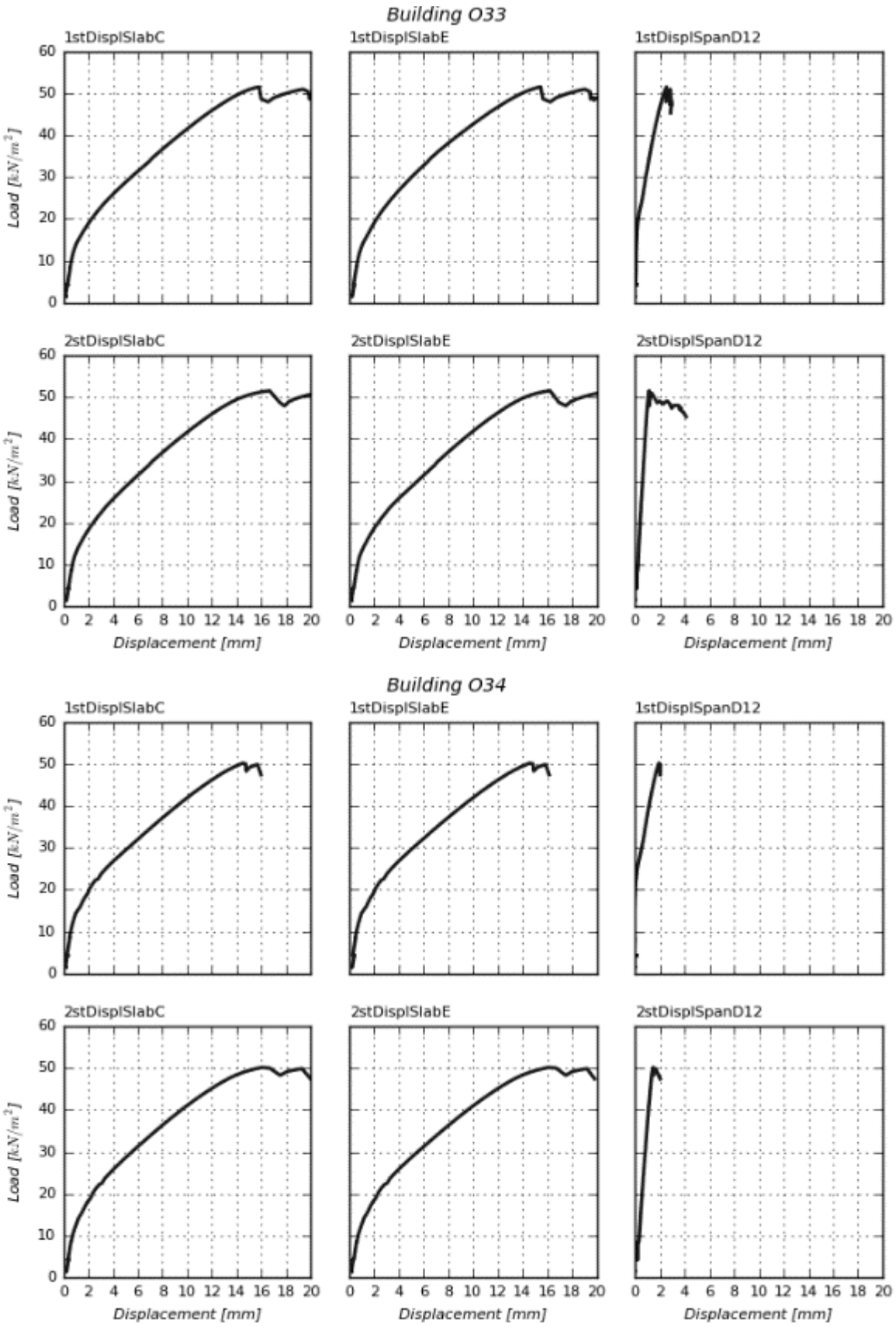
Building O33
1stDisplSlabC
1stDisplSlabE
1stDisplSpanD12
2stDisplSlabC
2stDisplSlabE
2stDisplSpanD12
Load [kN/m²]
Displacement [mm]
Building O34
1stDisplSlabC
1stDisplSlabE
1stDisplSpanD12
2stDisplSlabC
2stDisplSlabE
2stDisplSpanD12
Load [kN/m²]
Displacement [mm]

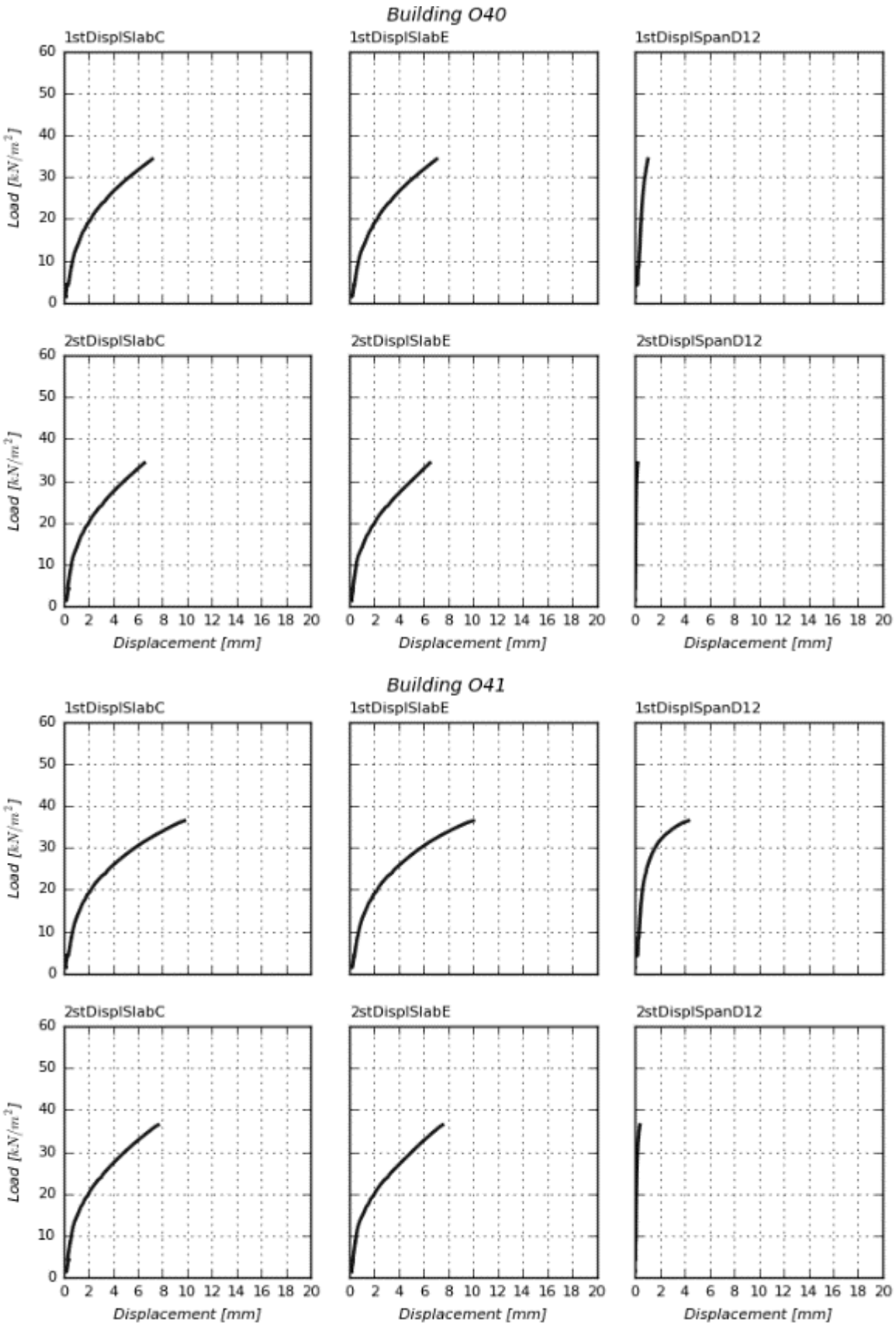
Building O40
1stDisplSlabC
1stDisplSlabE
1stDisplSpanD12
2stDisplSlabC
2stDisplSlabE
2stDisplSpanD12
Load [kN/m²]
Displacement [mm]
Building O41
1stDisplSlabC
1stDisplSlabE
1stDisplSpanD12
2stDisplSlabC
2stDisplSlabE
2stDisplSpanD12
Load [kN/m²]
Displacement [mm]

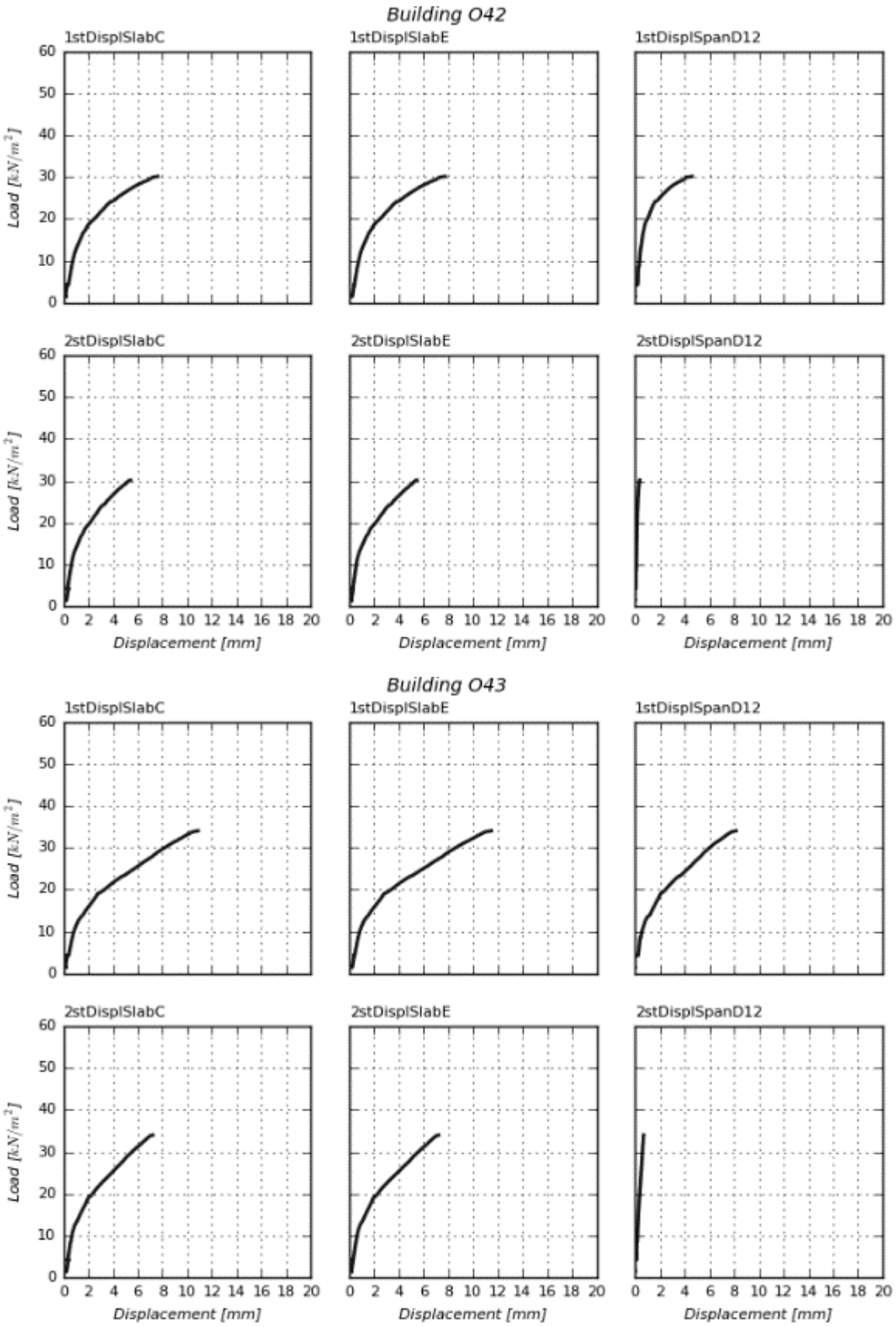
Building O42
1stDisplSlabC
1stDisplSlabE
1stDisplSpanD12
2stDisplSlabC
2stDisplSlabE
2stDisplSpanD12
Load [kN/m²]
Displacement [mm]
Building O43
1stDisplSlabC
1stDisplSlabE
1stDisplSpanD12
2stDisplSlabC
2stDisplSlabE
2stDisplSpanD12
Load [kN/m²]
Displacement [mm]

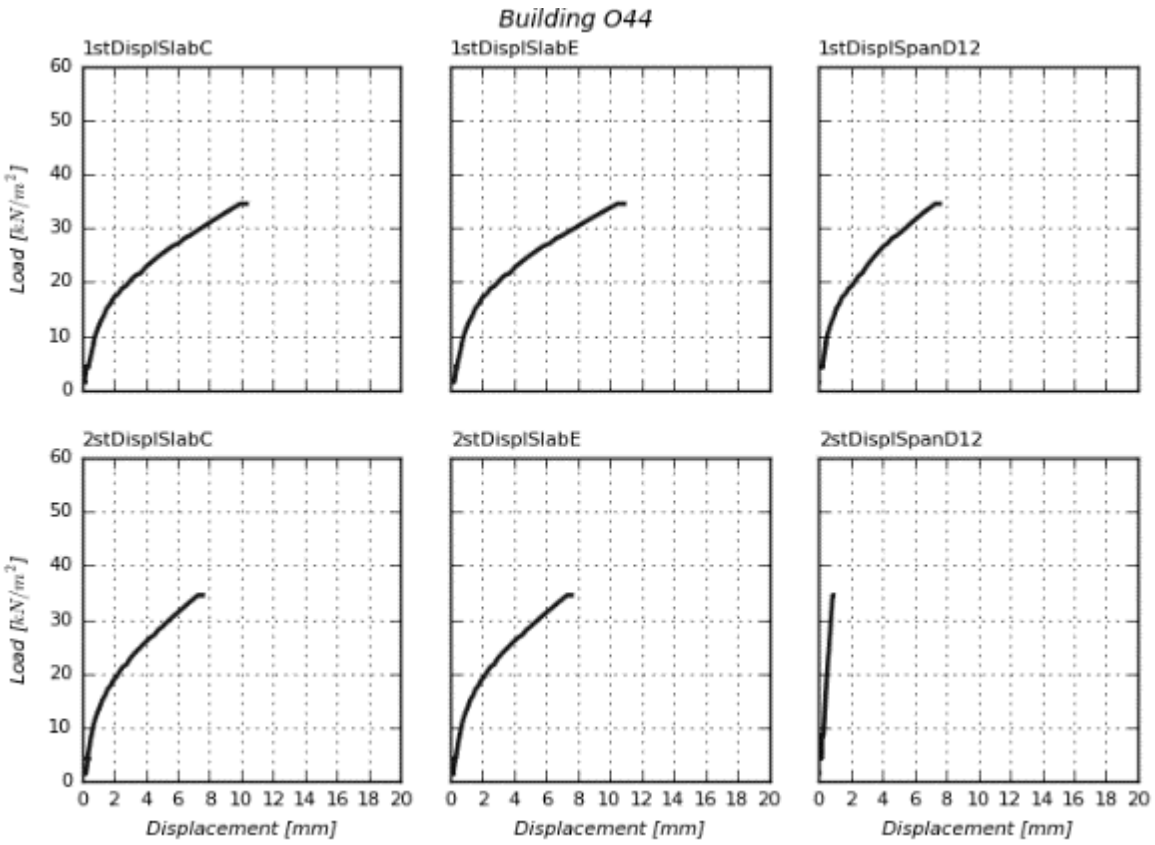
Building O44
1stDisplSlabC
1stDisplSlabE
1stDisplSpanD12
2stDisplSlabC
2stDisplSlabE
2stDisplSpanD12
Load [kN/m²]
Displacement [mm]
0
10
20
30
40
50
60
0 2 4 6 8 10 12 14 16 18 20

A4 – Load response diagrams for crack openings in critical slabs and walls

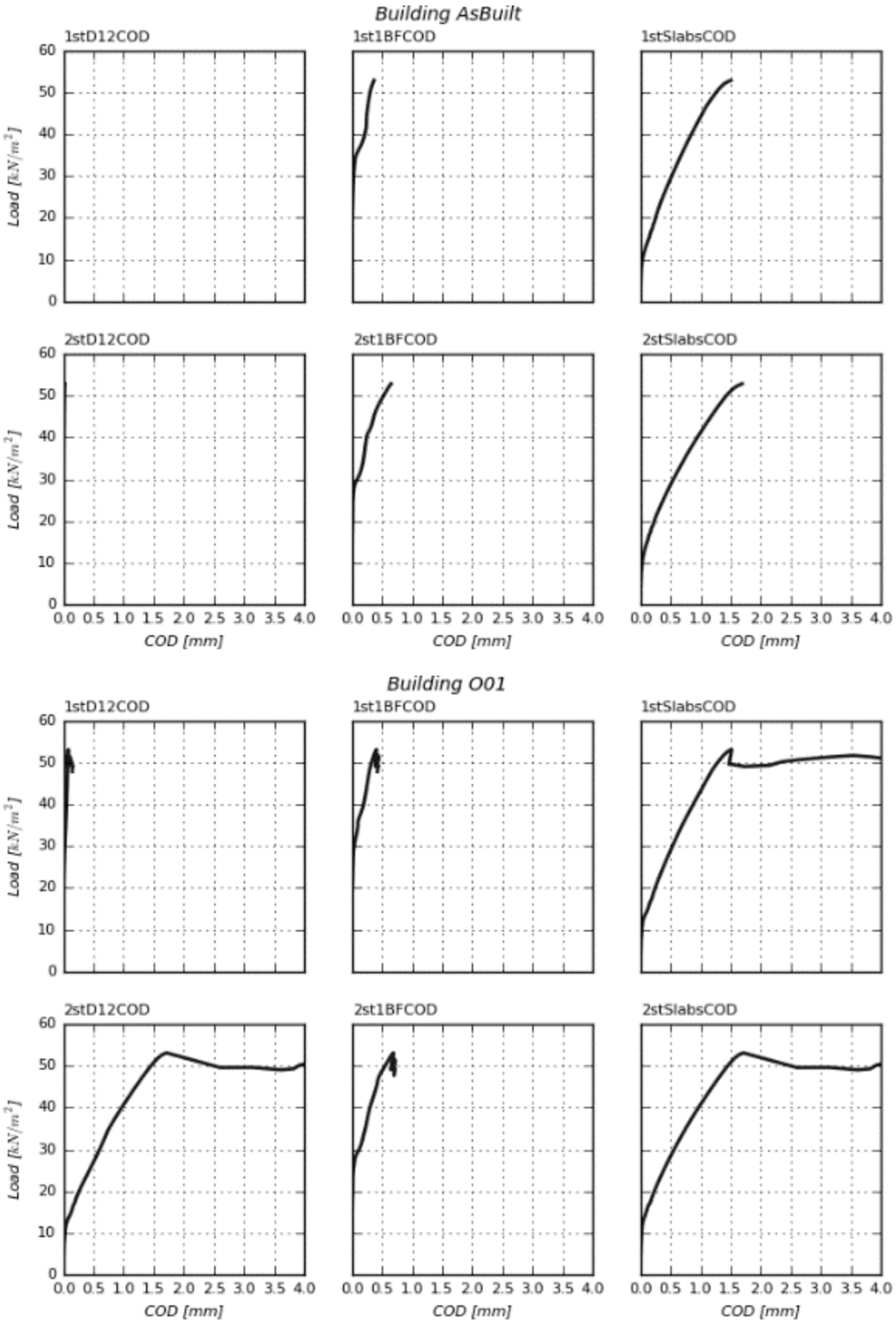

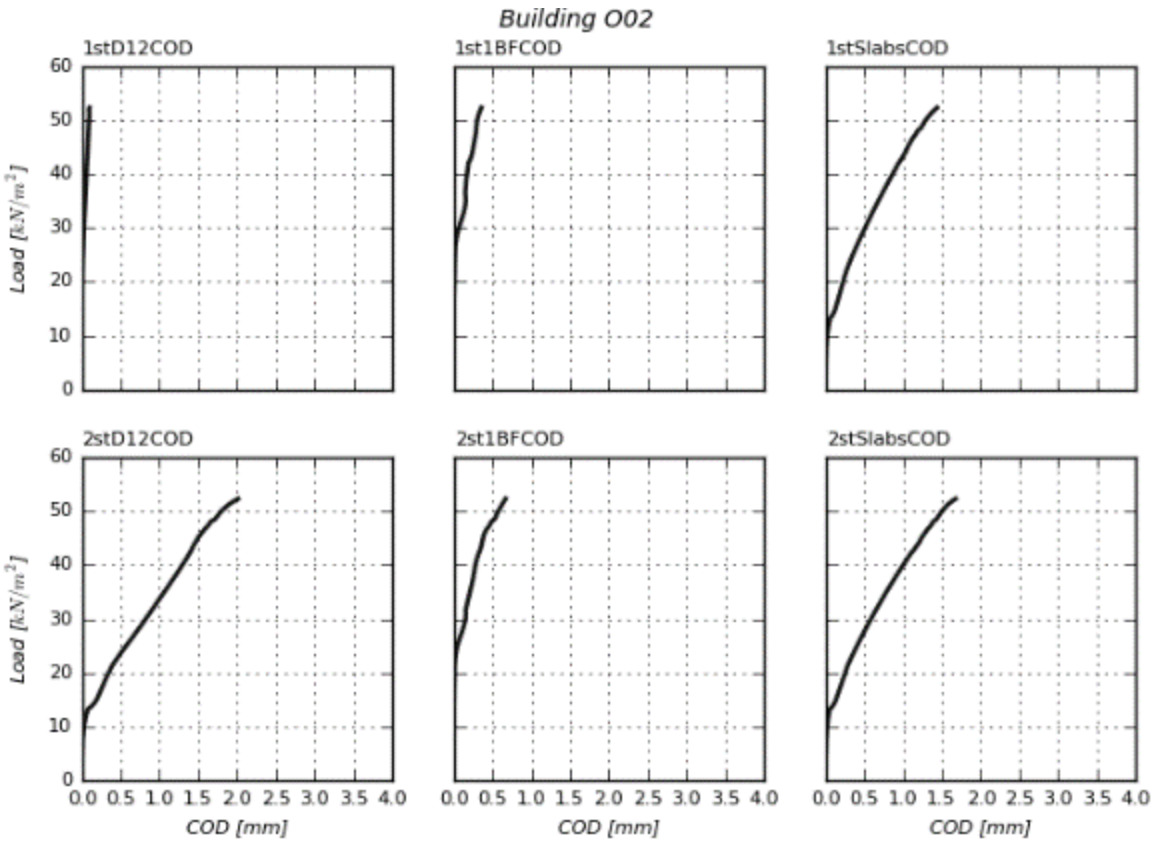
Building O02
1stD12COD
1st1BFCOD
1stSlabsCOD
2stD12COD
2st1BFCOD
2stSlabsCOD
Load [kN/m²]
COD [mm]
0 10 20 30 40 50 60
0.0 0.5 1.0 1.5 2.0 2.5 3.0 3.5 4.0

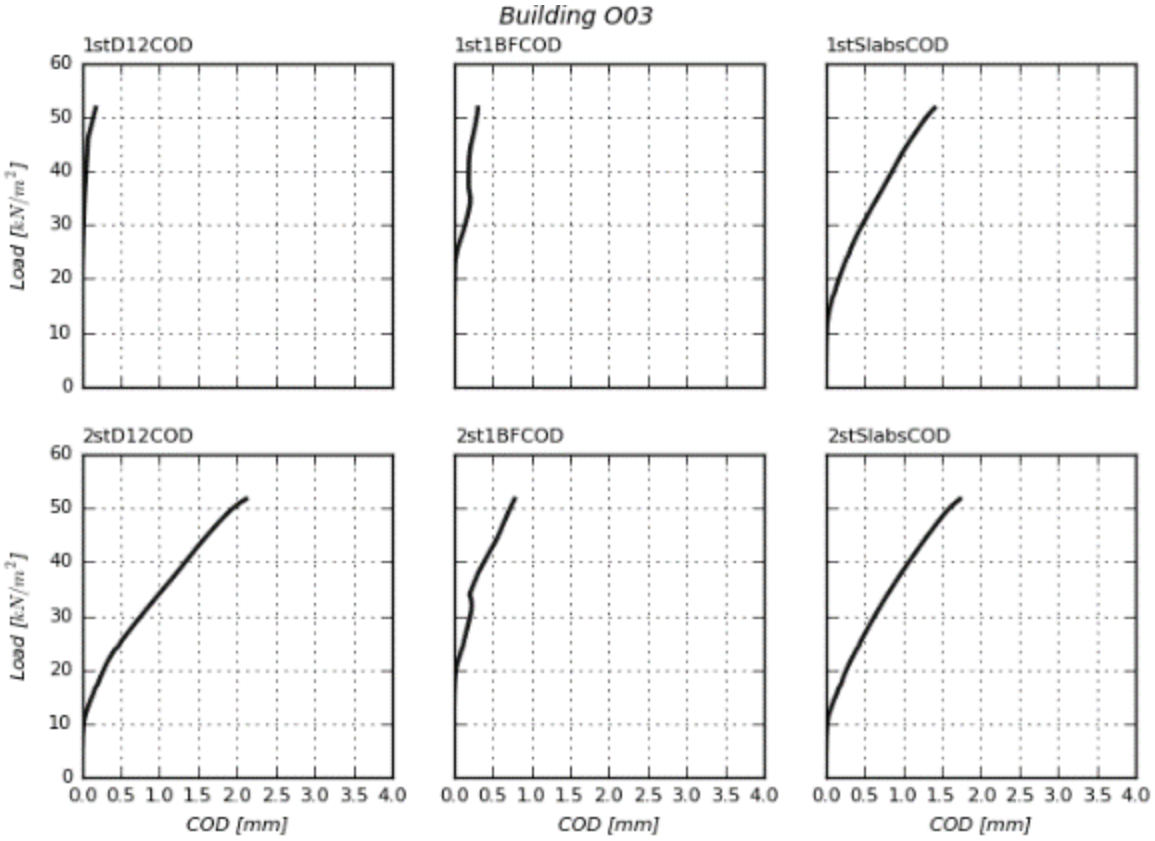
Building O03
1stD12COD
1st1BFCOD
1stSlabsCOD
2stD12COD
2st1BFCOD
2stSlabsCOD
Load [kN/m²]
COD [mm]
0 10 20 30 40 50 60
0.0 0.5 1.0 1.5 2.0 2.5 3.0 3.5 4.0

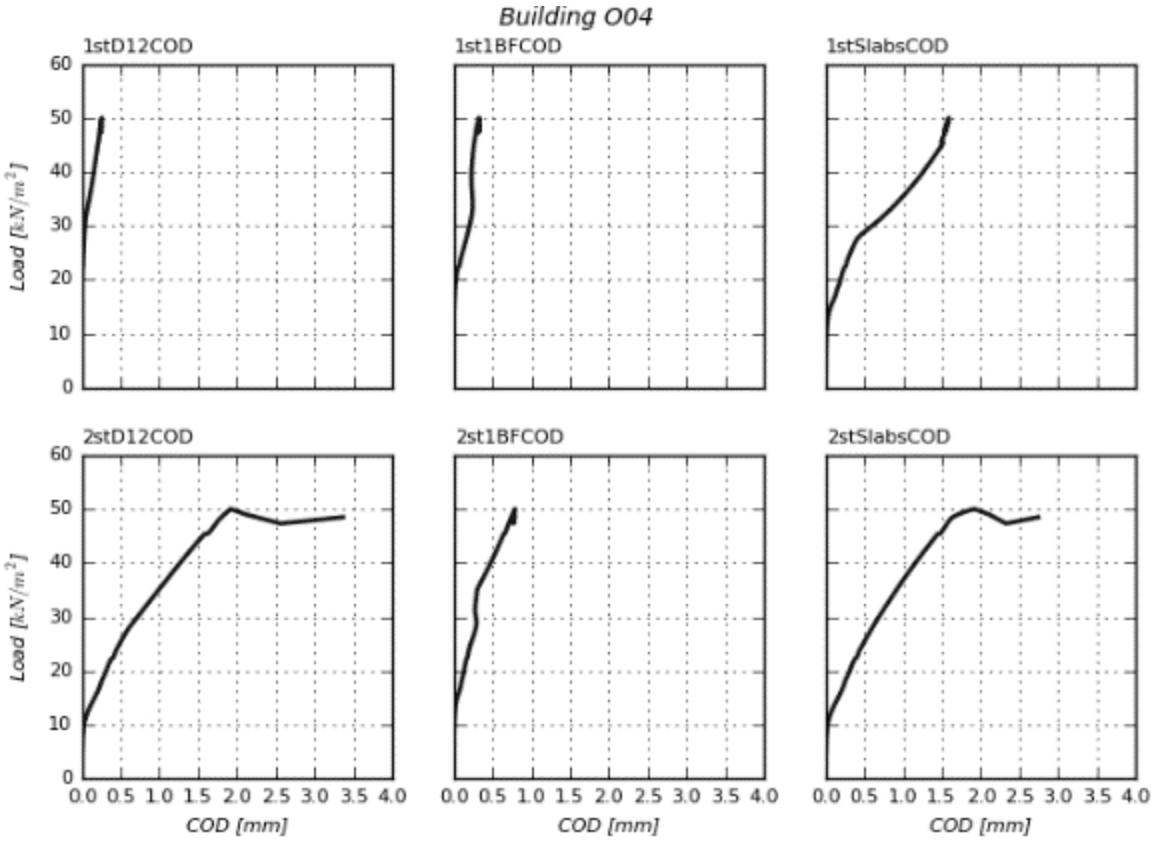
Building O04
1stD12COD
1st1BFCOD
1stSlabsCOD
2stD12COD
2st1BFCOD
2stSlabsCOD
Load [kN/m²]
COD [mm]

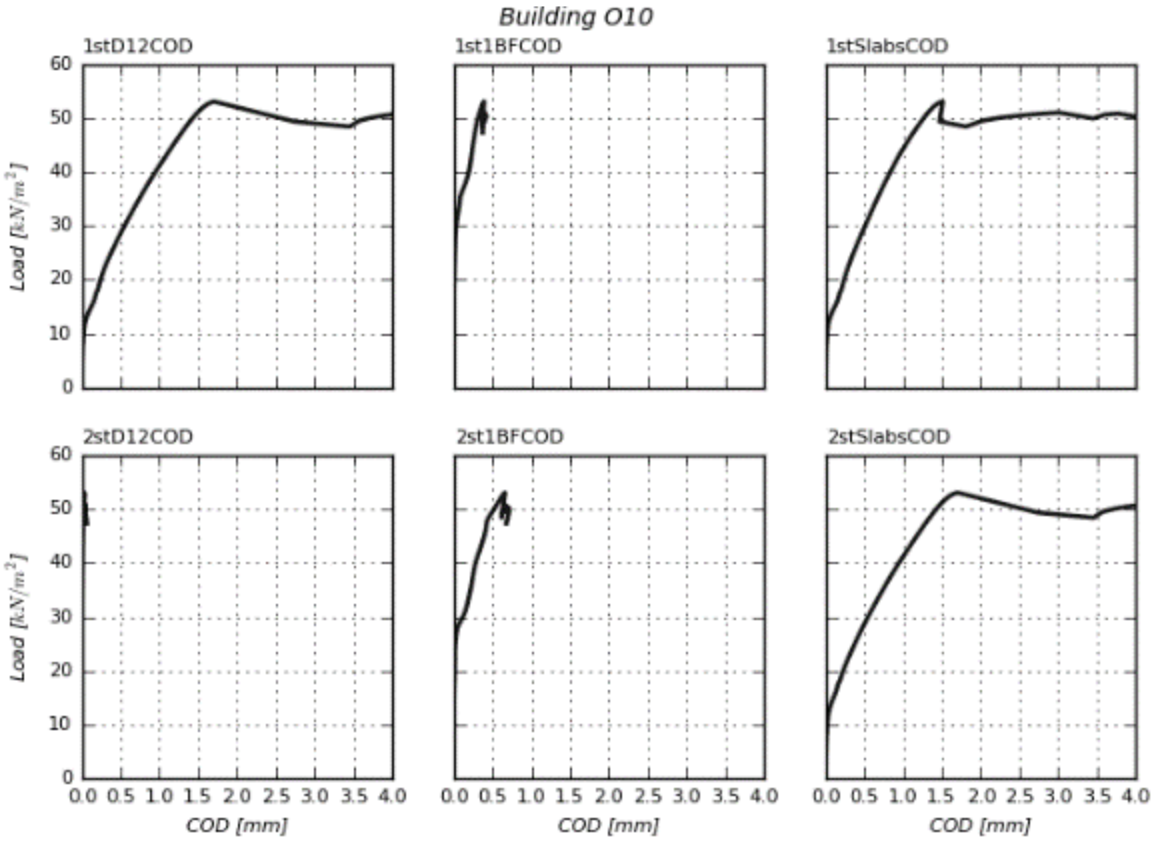
Building O10
1stD12COD
1st1BFCOD
1stSlabsCOD
2stD12COD
2st1BFCOD
2stSlabsCOD
Load [kN/m²]
COD [mm]

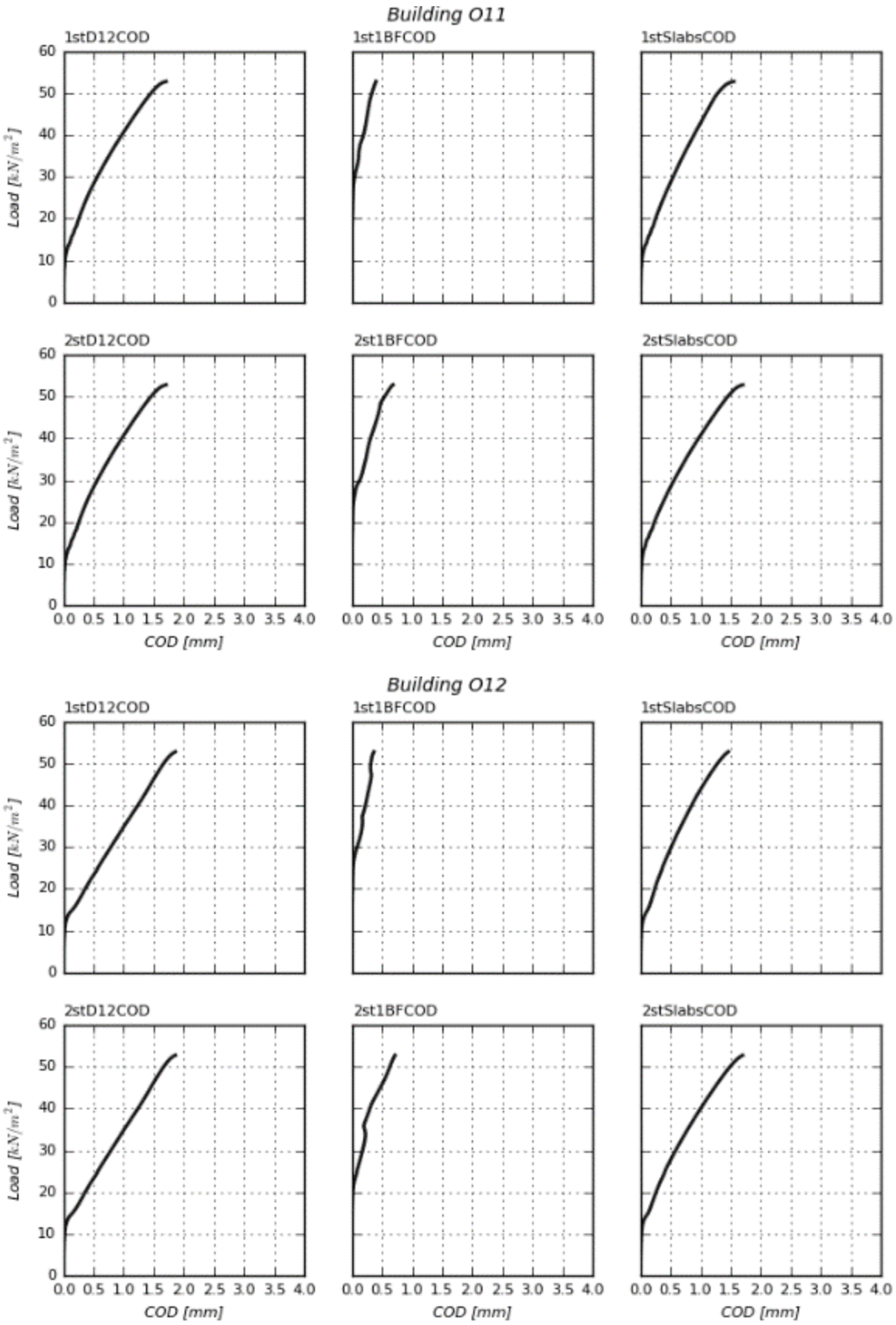
Building O11
1stD12COD
1st1BFCOD
1stSlabsCOD
2stD12COD
2st1BFCOD
2stSlabsCOD
Load [kN/m²]
COD [mm]
Building O12
1stD12COD
1st1BFCOD
1stSlabsCOD
2stD12COD
2st1BFCOD
2stSlabsCOD
Load [kN/m²]
COD [mm]

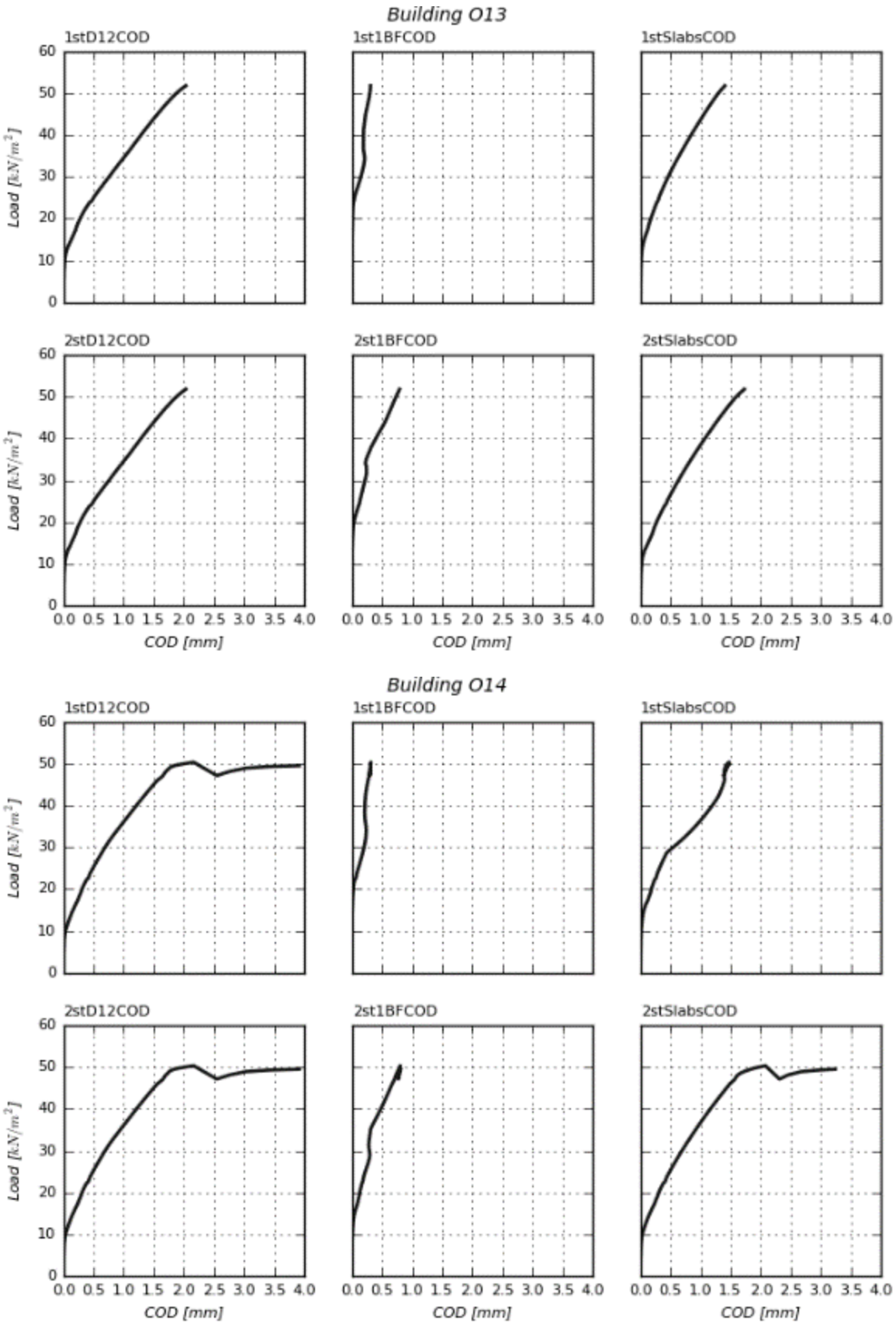
Building O13
1stD12COD
1st1BFCOD
1stSlabsCOD
2stD12COD
2st1BFCOD
2stSlabsCOD
Load [kN/m²]
COD [mm]
Building O14
1stD12COD
1st1BFCOD
1stSlabsCOD
2stD12COD
2st1BFCOD
2stSlabsCOD
Load [kN/m²]
COD [mm]

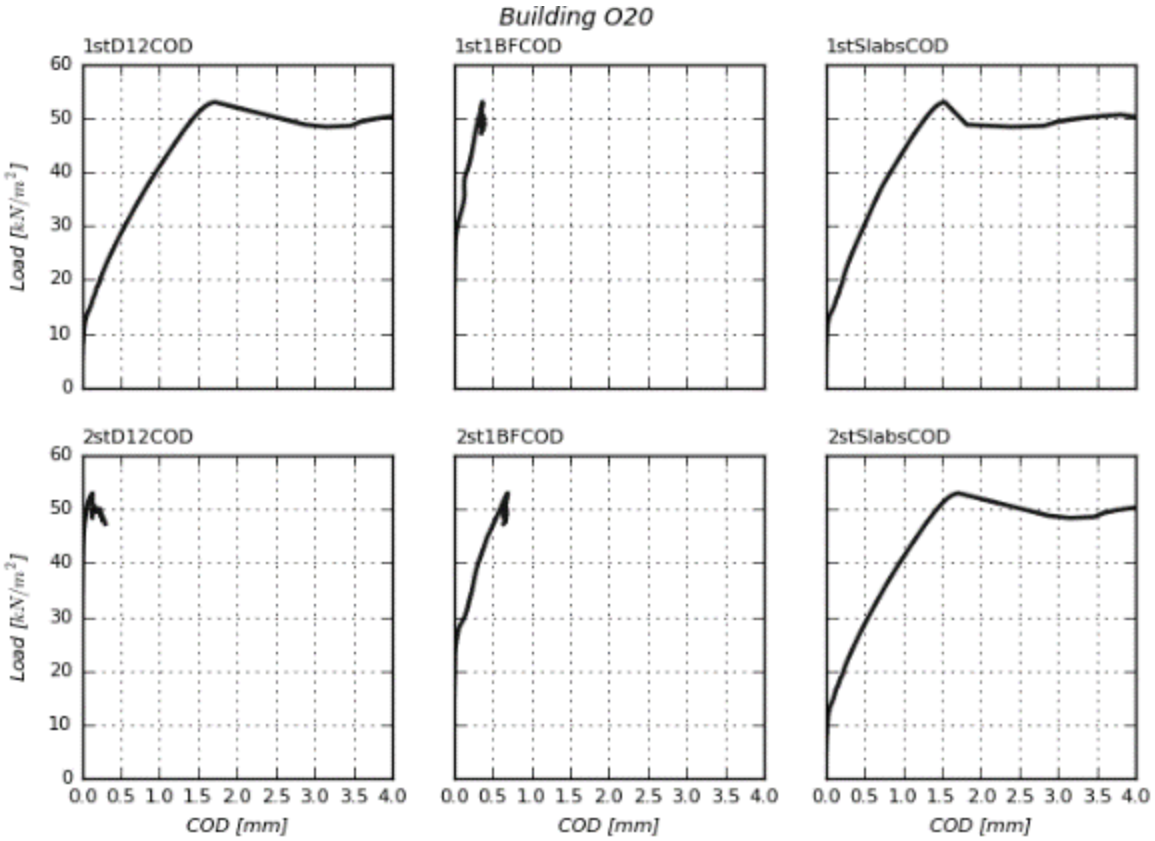
Building O20
1stD12COD
1st1BFCOD
1stSlabsCOD
2stD12COD
2st1BFCOD
2stSlabsCOD
Load [kN/m²]
COD [mm]

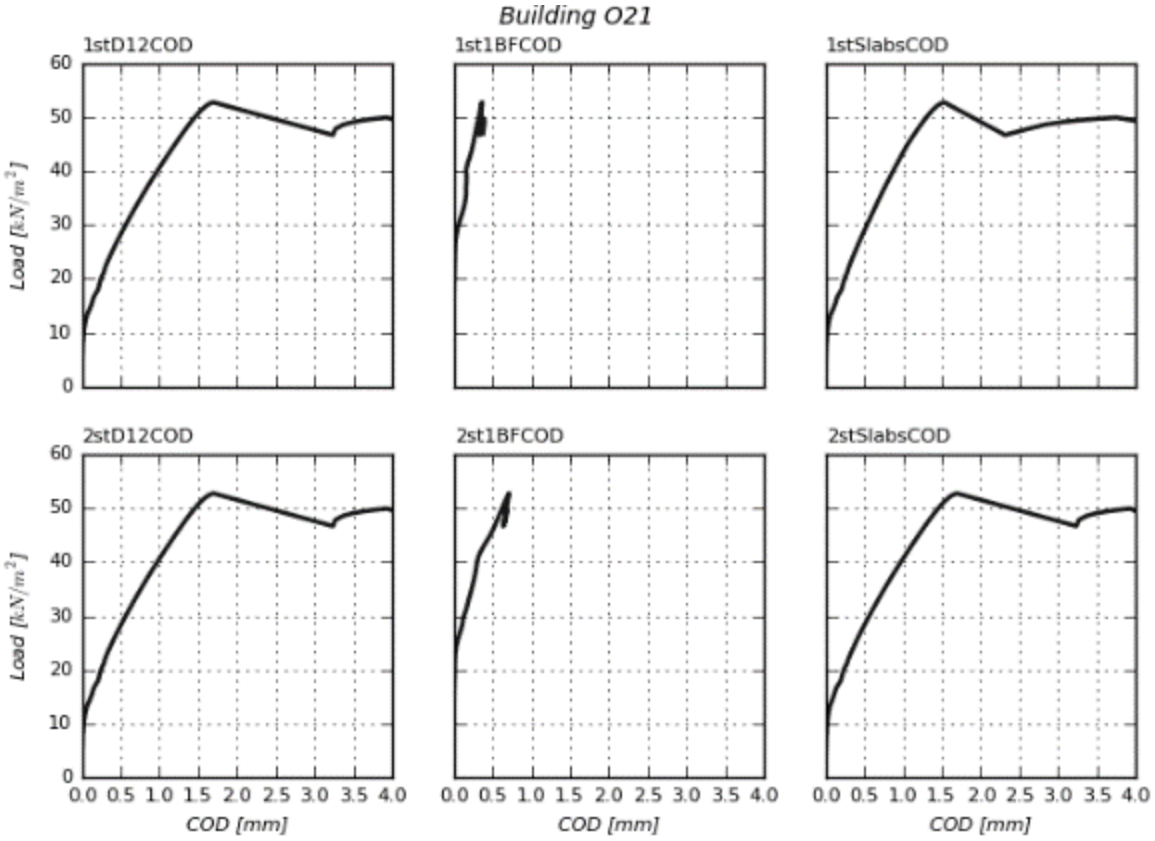
Building O21
1stD12COD
1st1BFCOD
1stSlabsCOD
2stD12COD
2st1BFCOD
2stSlabsCOD
Load [kN/m²]
COD [mm]

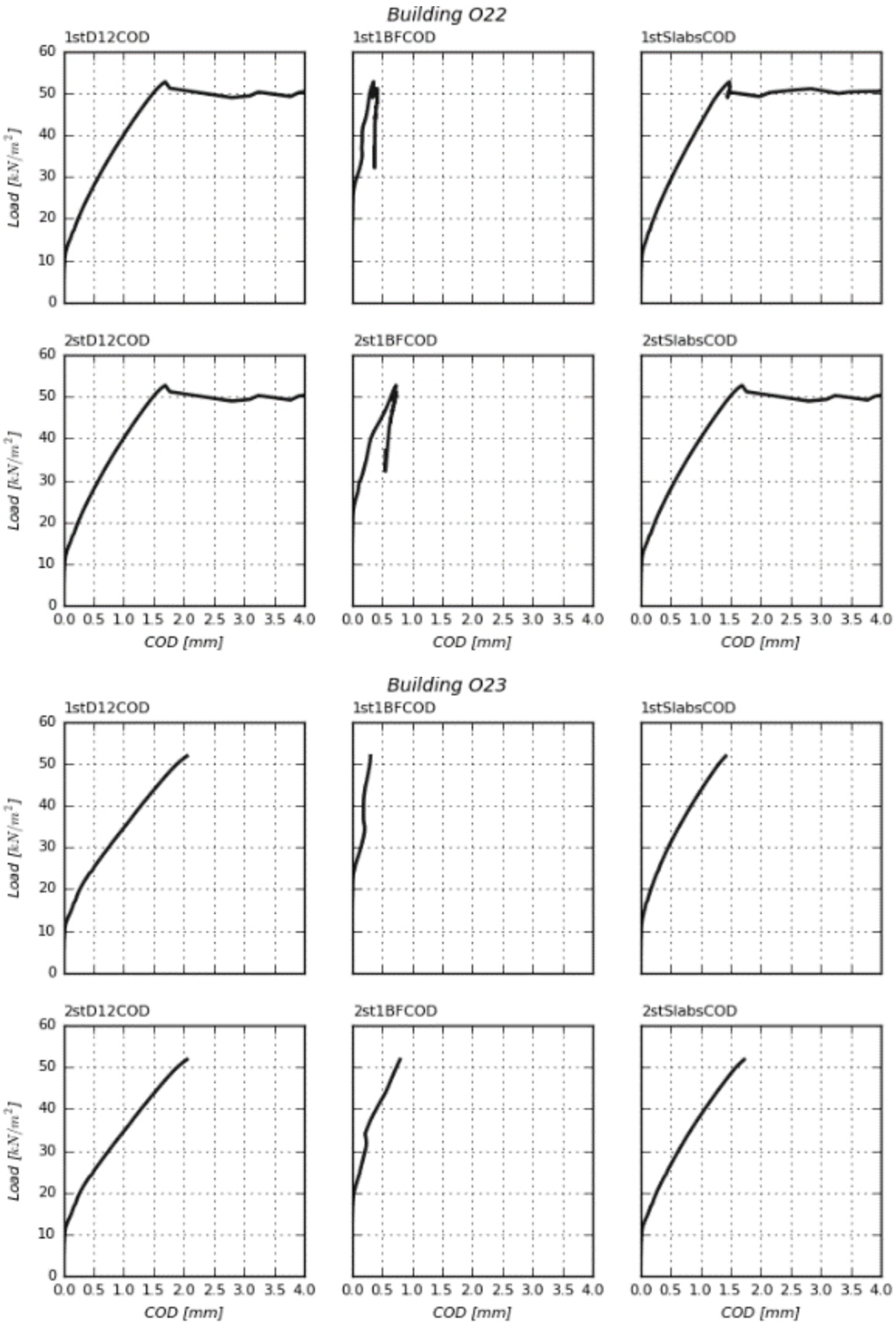
Building O22
1stD12COD
1st1BFCOD
1stSlabsCOD
2stD12COD
2st1BFCOD
2stSlabsCOD
Load [kN/m²]
COD [mm]
Building O23
1stD12COD
1st1BFCOD
1stSlabsCOD
2stD12COD
2st1BFCOD
2stSlabsCOD
Load [kN/m²]
COD [mm]

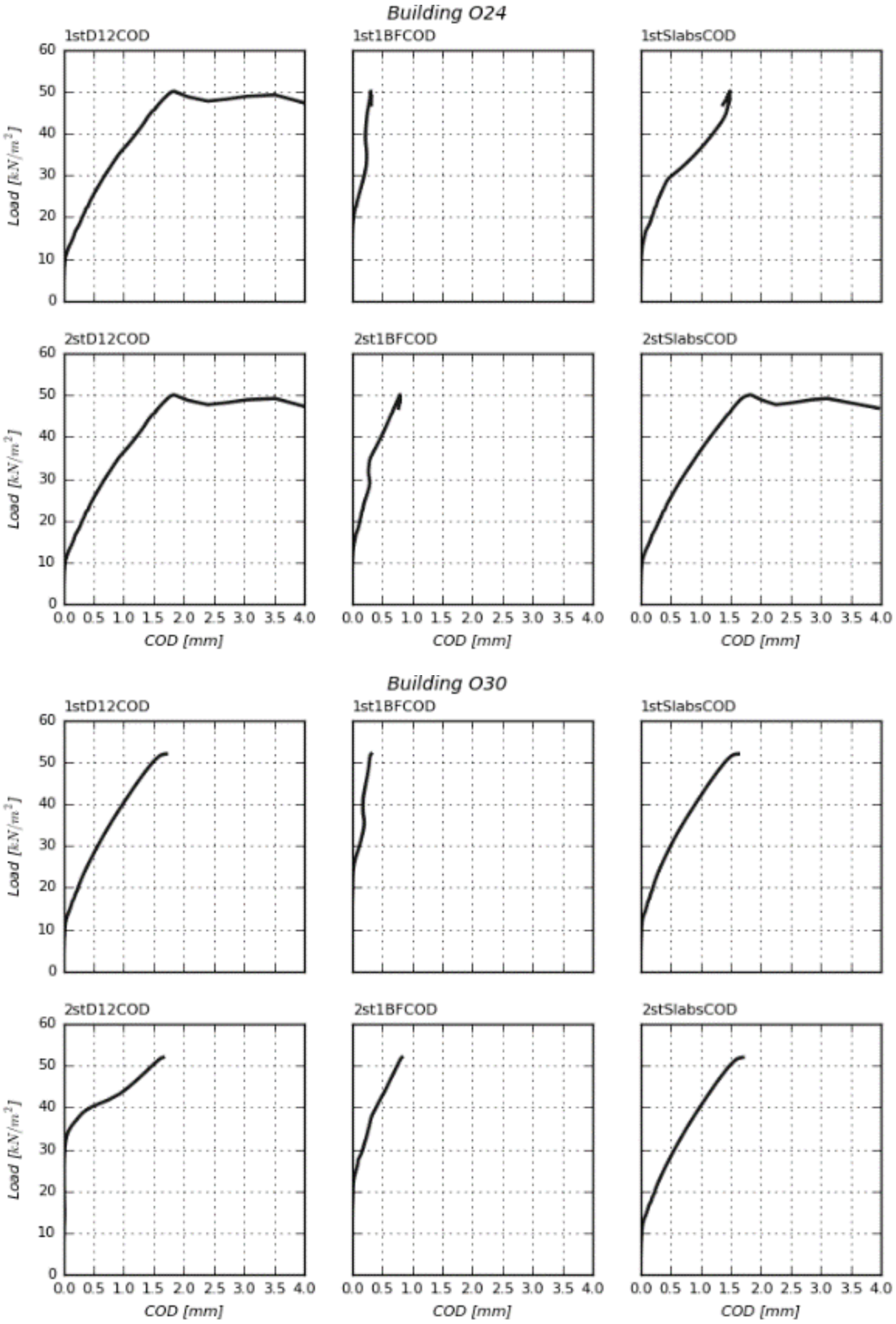
Building O24
1stD12COD
1st1BFCOD
1stSlabsCOD
2stD12COD
2st1BFCOD
2stSlabsCOD
Load [kN/m²]
COD [mm]
Building O30
1stD12COD
1st1BFCOD
1stSlabsCOD
2stD12COD
2st1BFCOD
2stSlabsCOD
Load [kN/m²]
COD [mm]

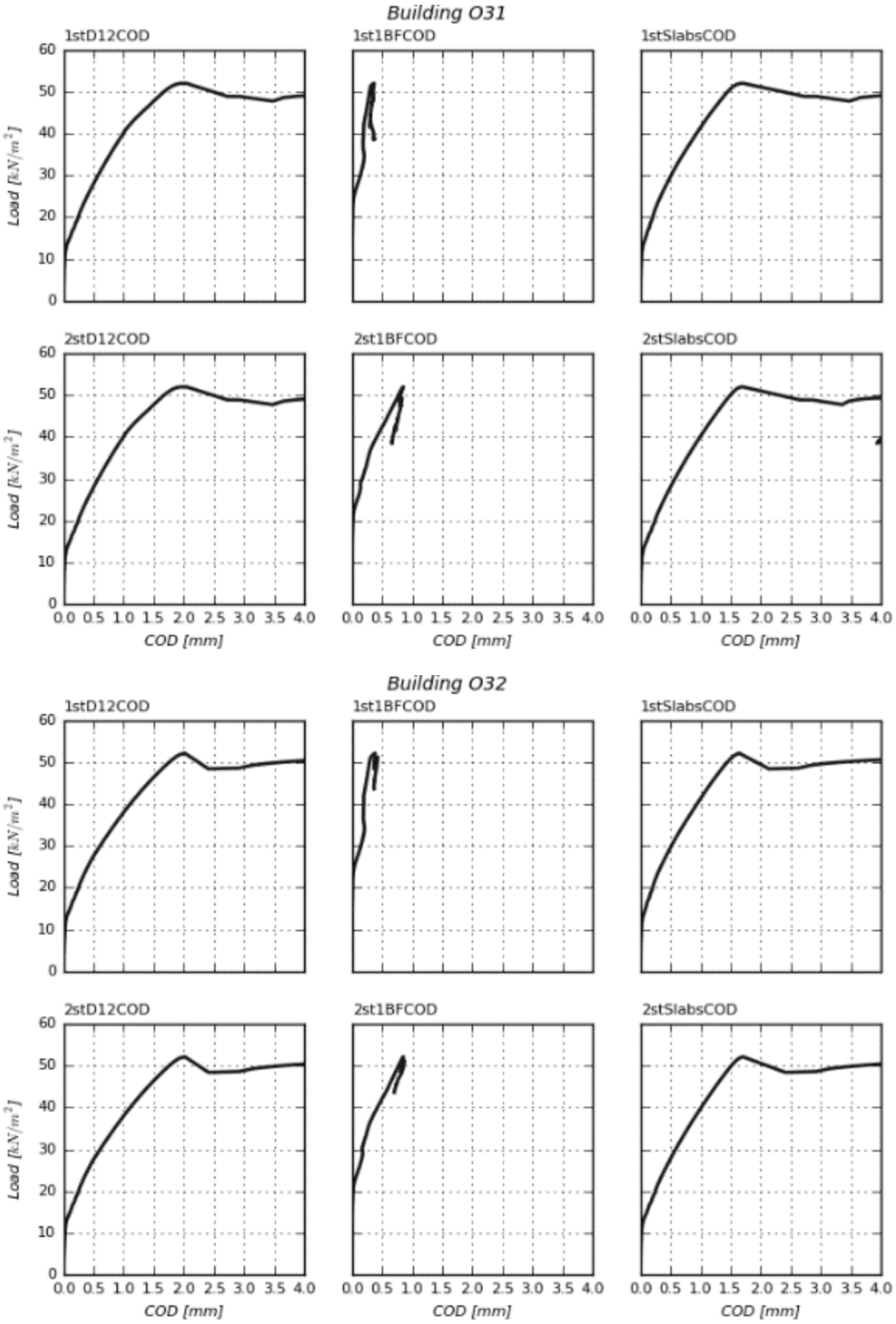
Building O31
1stD12COD
1st1BFCOD
1stSlabsCOD
2stD12COD
2st1BFCOD
2stSlabsCOD
Load [kN/m²]
COD [mm]
Building O32
1stD12COD
1st1BFCOD
1stSlabsCOD
2stD12COD
2st1BFCOD
2stSlabsCOD
Load [kN/m²]
COD [mm]

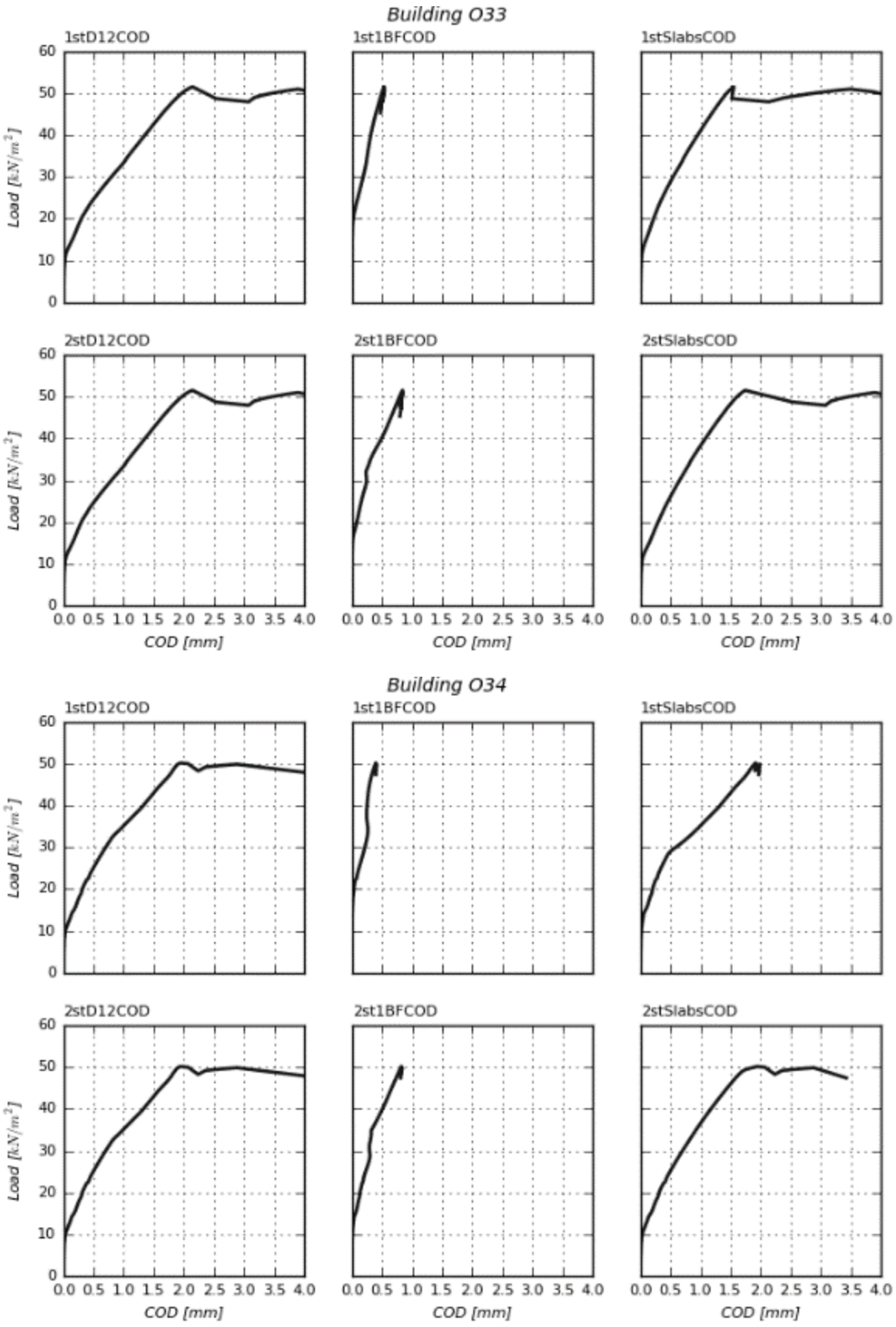
Building O33
1stD12COD
1st1BFCOD
1stSlabsCOD
2stD12COD
2st1BFCOD
2stSlabsCOD
Load [kN/m²]
COD [mm]
Building O34
1stD12COD
1st1BFCOD
1stSlabsCOD
2stD12COD
2st1BFCOD
2stSlabsCOD
Load [kN/m²]
COD [mm]

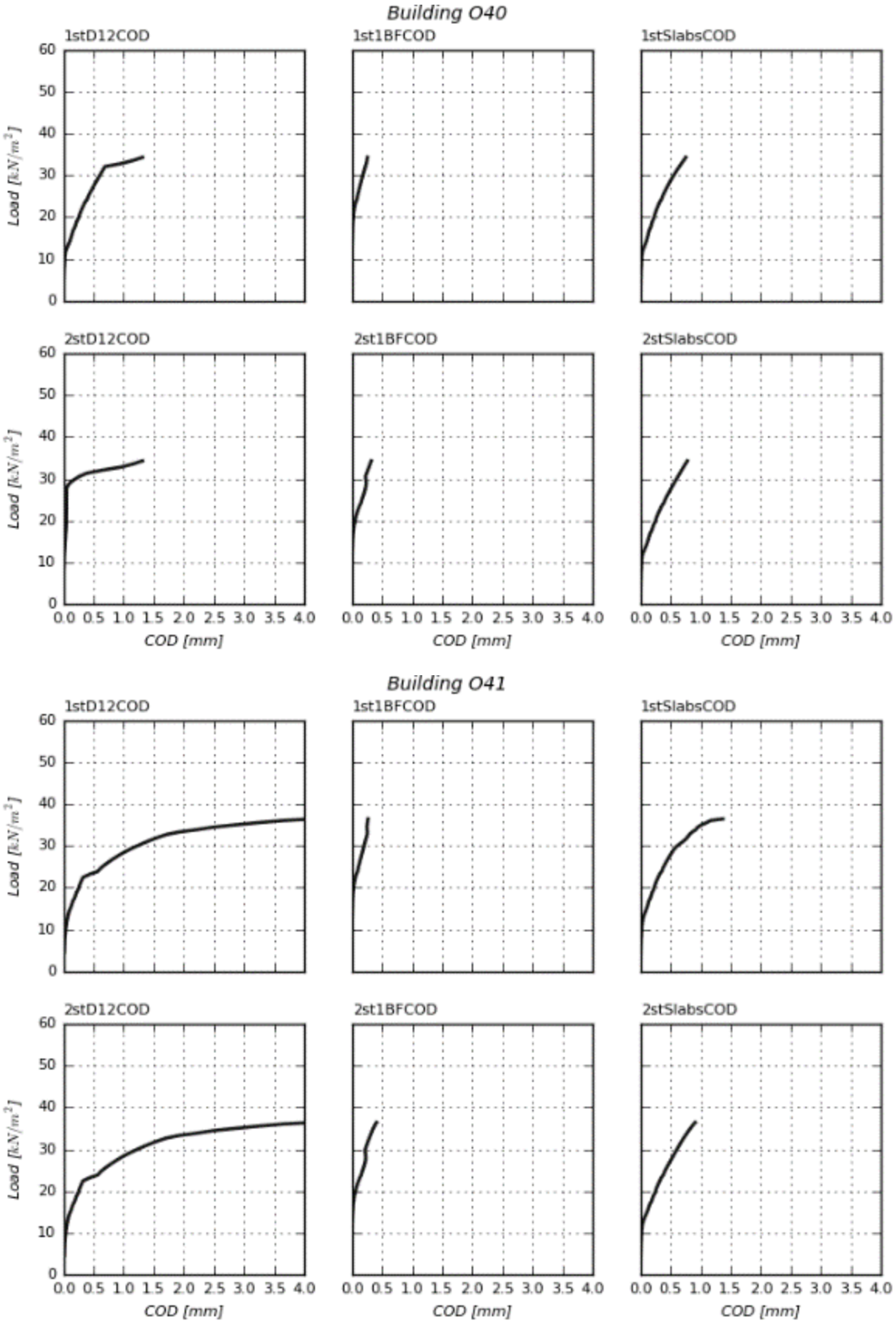
Building O40
1stD12COD
1st1BFCOD
1stSlabsCOD
2stD12COD
2st1BFCOD
2stSlabsCOD
Load [kN/m²]
COD [mm]
Building O41
1stD12COD
1st1BFCOD
1stSlabsCOD
2stD12COD
2st1BFCOD
2stSlabsCOD
Load [kN/m²]
COD [mm]

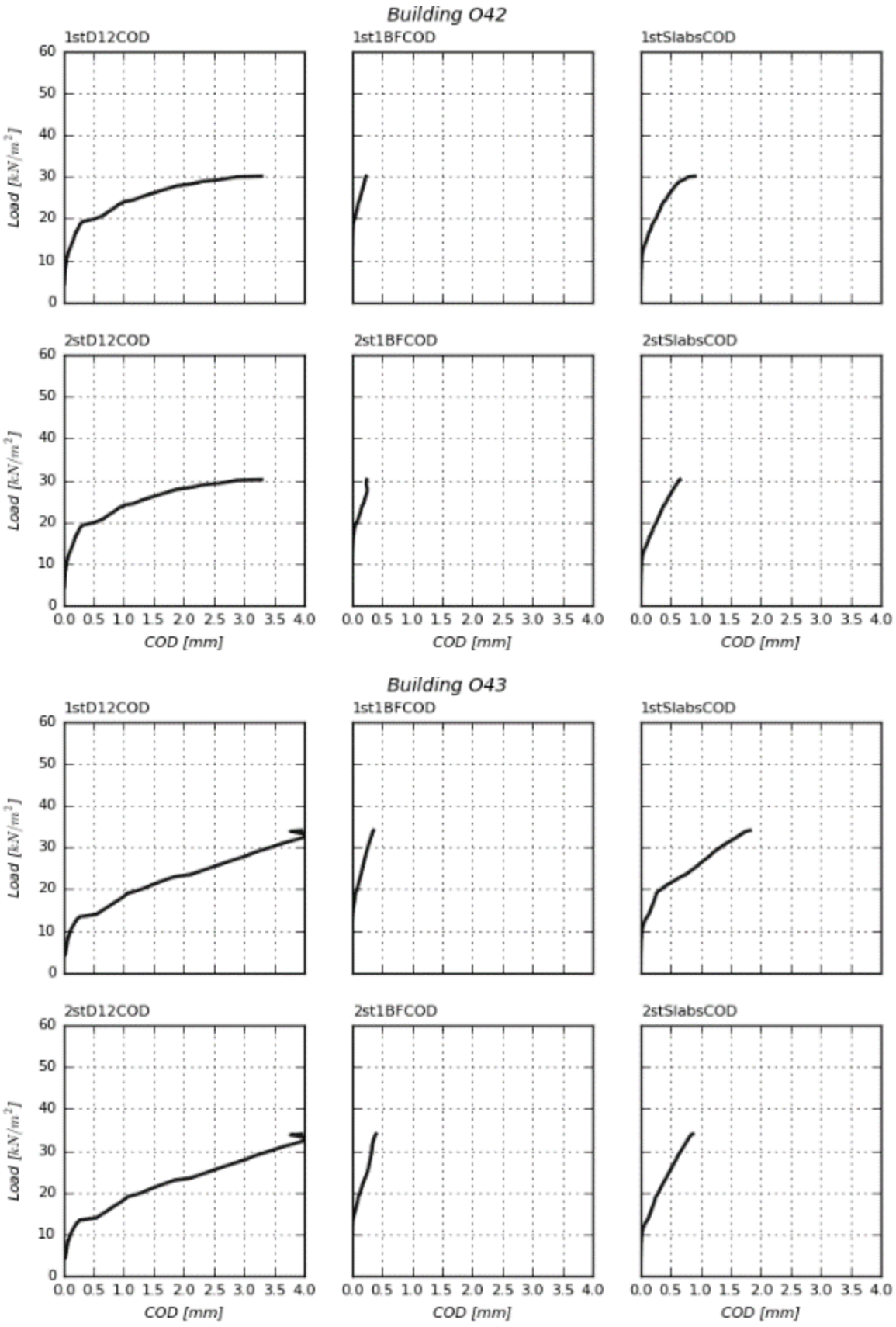
Building O42
1stD12COD
1st1BFCOD
1stSlabsCOD
2stD12COD
2st1BFCOD
2stSlabsCOD
Load [kN/m²]
COD [mm]
Building O43
1stD12COD
1st1BFCOD
1stSlabsCOD
2stD12COD
2st1BFCOD
2stSlabsCOD
Load [kN/m²]
COD [mm]

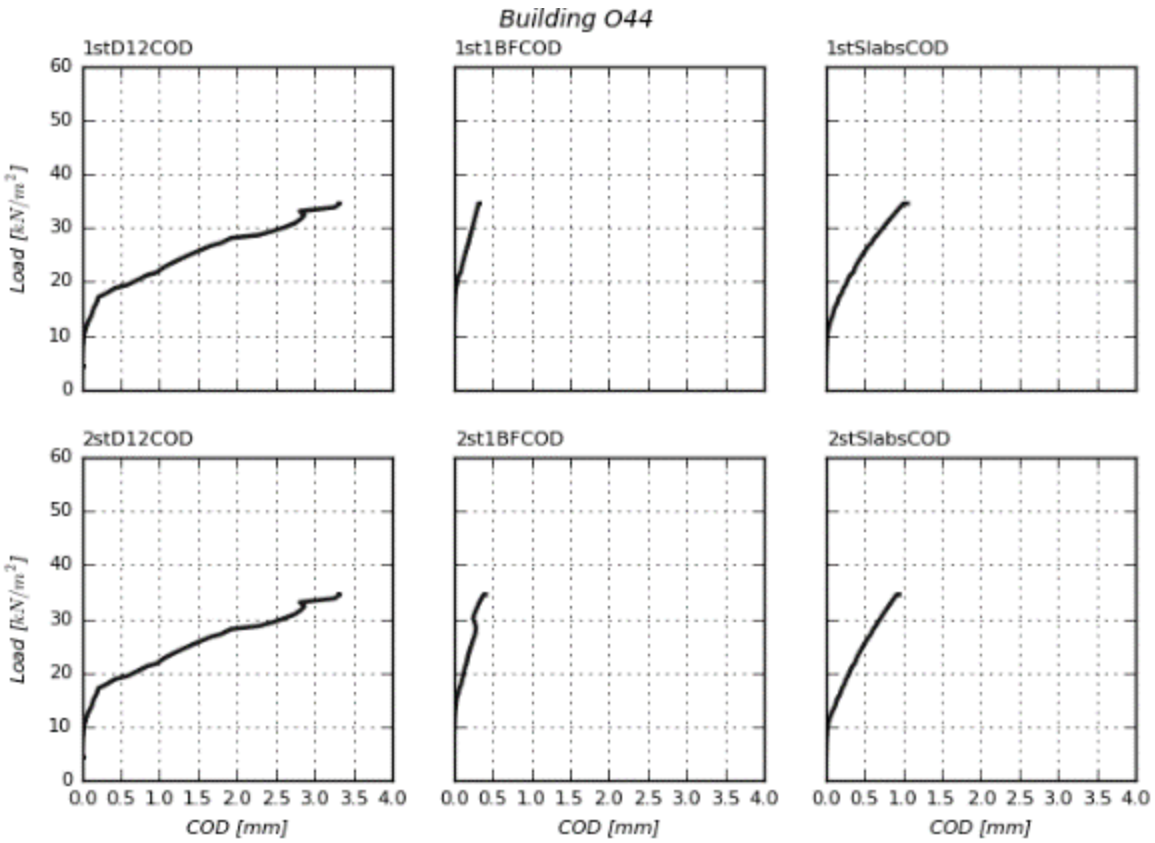
Building O44
1stD12COD
1st1BFCOD
1stSlabsCOD
2stD12COD
2st1BFCOD
2stSlabsCOD
Load [kN/m²]
COD [mm]
0
10
20
30
40
50
60
0.0 0.5 1.0 1.5 2.0 2.5 3.0 3.5 4.0

A5 – Load response diagrams for concrete compressive strain in critical walls

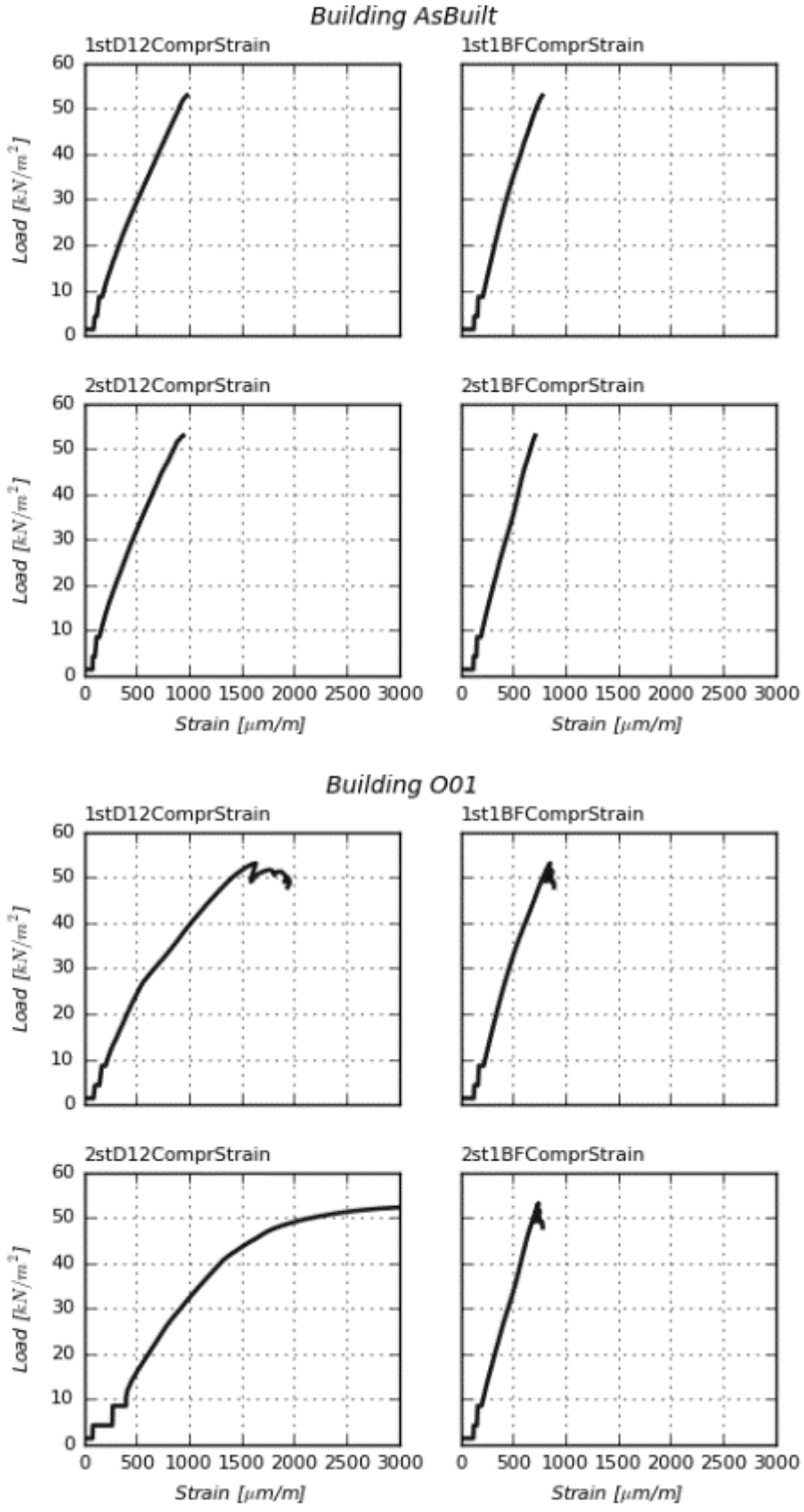

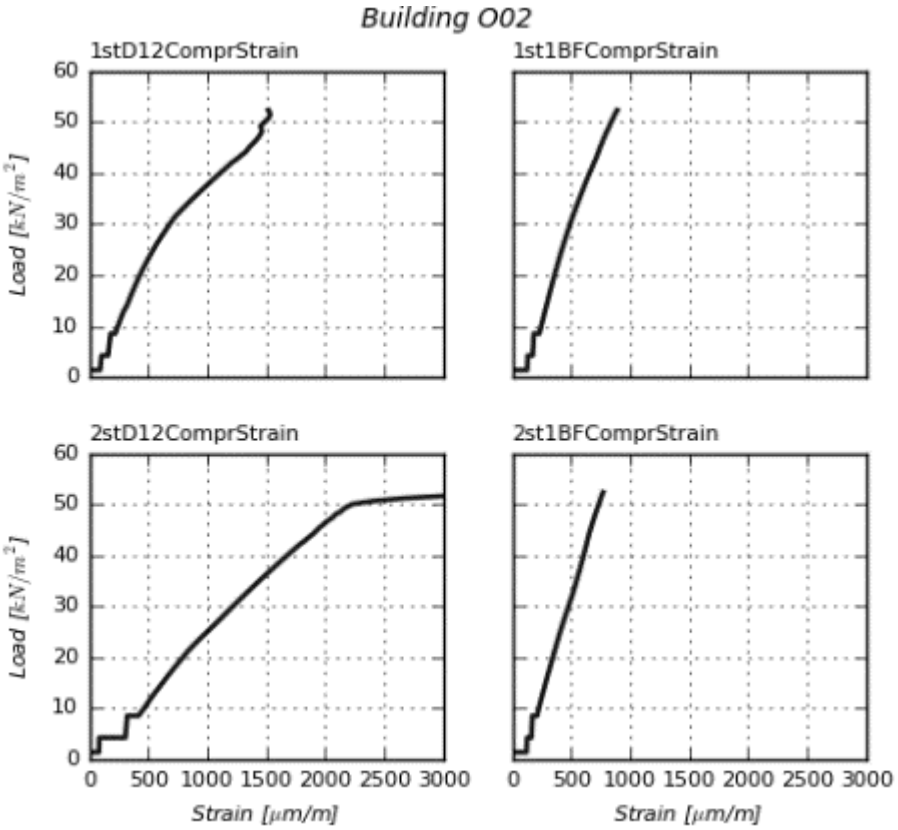
Building O02
1stD12ComprStrain
1st1BFComprStrain
2stD12ComprStrain
2st1BFComprStrain
Load [kN/m²]
Strain [μm/m]
0
10
20
30
40
50
60
0 500 1000 1500 2000 2500 3000

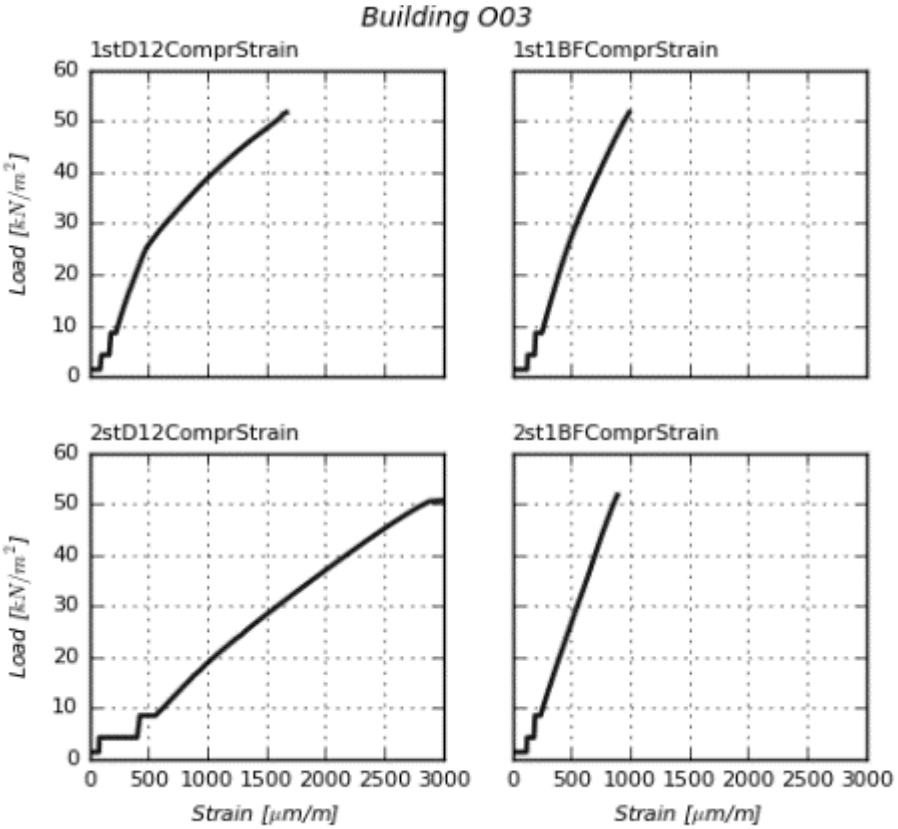
Building O03
1stD12ComprStrain
1st1BFComprStrain
2stD12ComprStrain
2st1BFComprStrain
Load [kN/m²]
Strain [μm/m]
0
10
20
30
40
50
60
0 500 1000 1500 2000 2500 3000

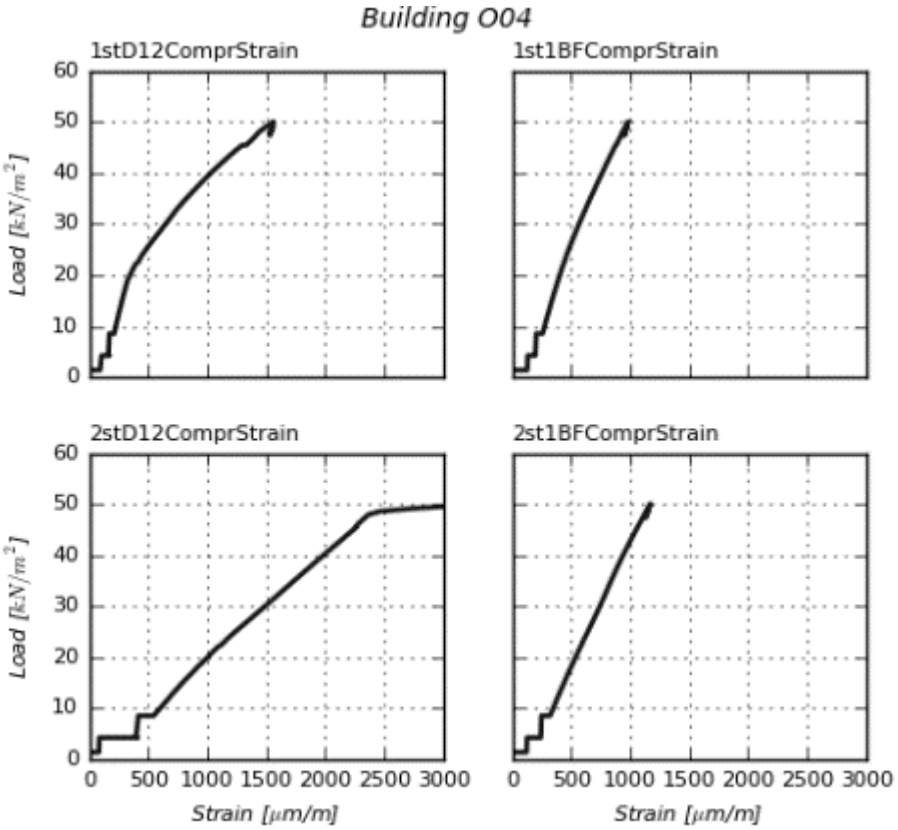
Building O04
1stD12ComprStrain
1st1BFComprStrain
2stD12ComprStrain
2st1BFComprStrain
Load [kN/m²]
Strain [μm/m]
0
10
20
30
40
50
60
0 500 1000 1500 2000 2500 3000

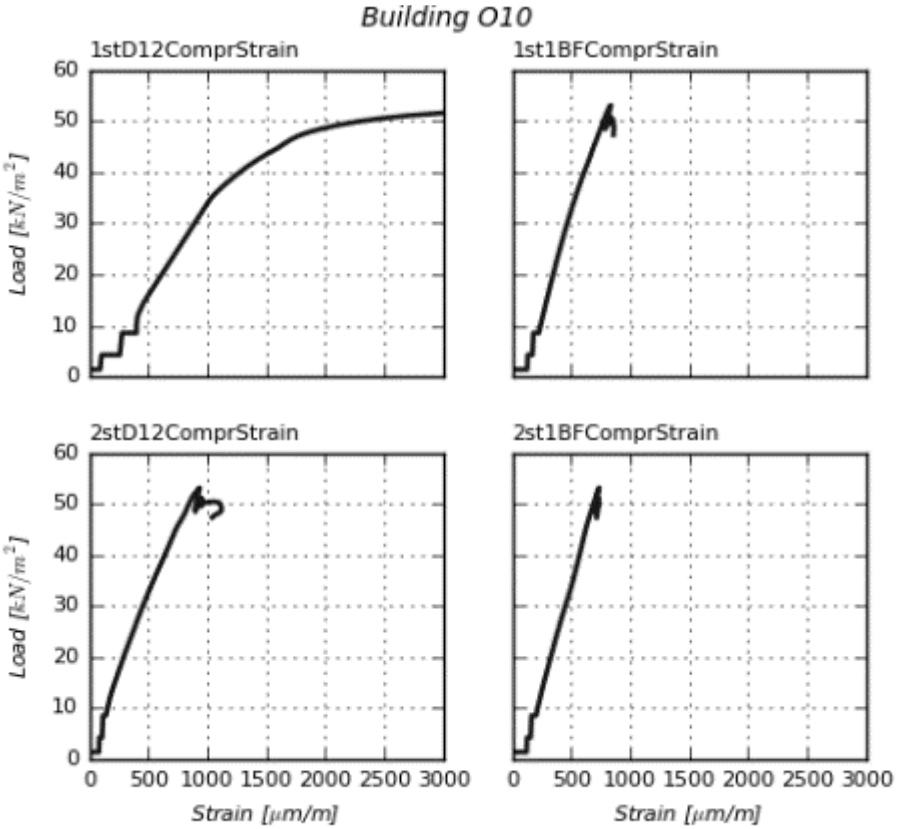
Building O10
1stD12ComprStrain
1st1BFComprStrain
2stD12ComprStrain
2st1BFComprStrain
Load [kN/m²]
Strain [μm/m]
0
10
20
30
40
50
60
0 500 1000 1500 2000 2500 3000

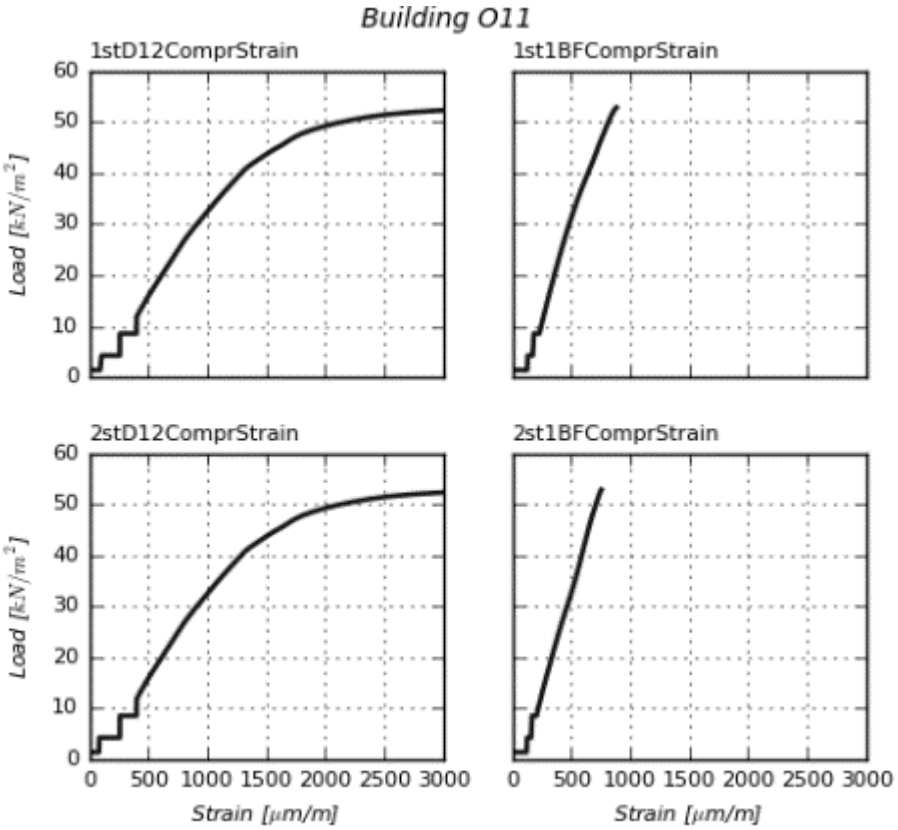
Building O11
1stD12ComprStrain
1st1BFComprStrain
2stD12ComprStrain
2st1BFComprStrain
Load [kN/m²]
Strain [μm/m]
0
10
20
30
40
50
60
0 500 1000 1500 2000 2500 3000

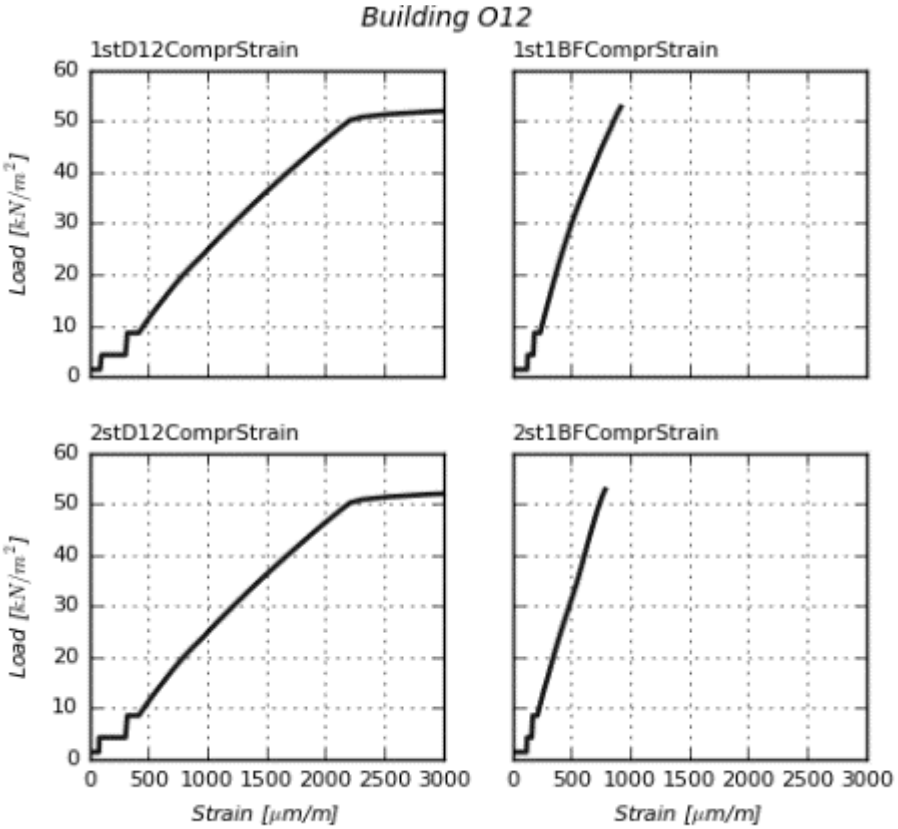
Building O12
1stD12ComprStrain
1st1BFComprStrain
2stD12ComprStrain
2st1BFComprStrain
Load [kN/m²]
Strain [μm/m]
0
10
20
30
40
50
60
0 500 1000 1500 2000 2500 3000

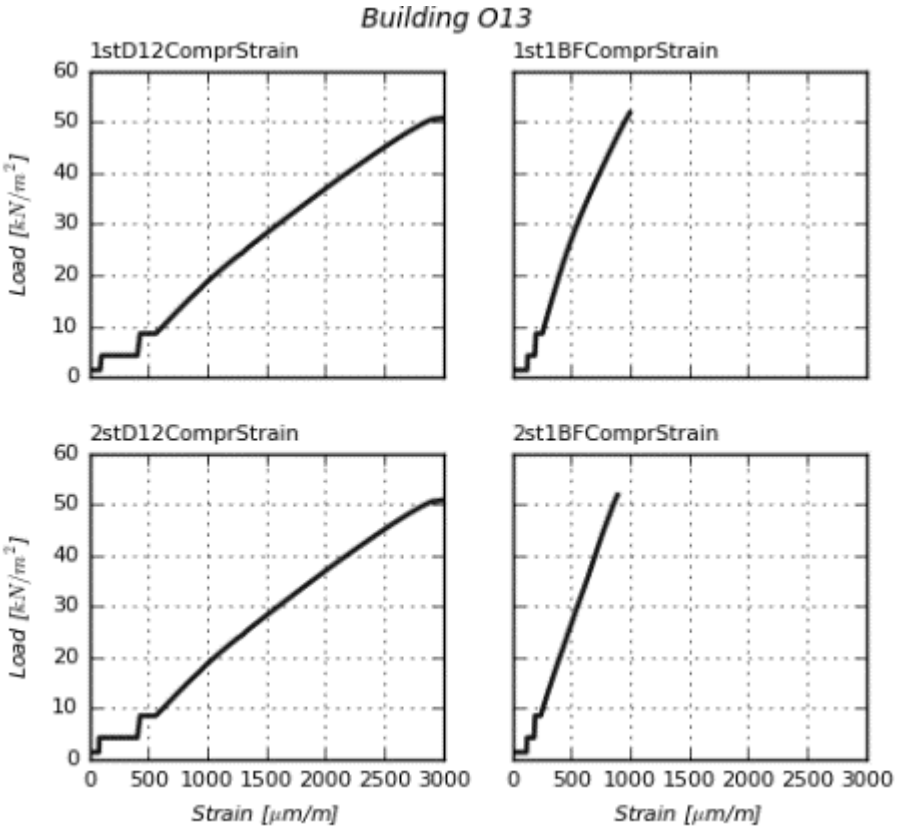
Building O13
1stD12ComprStrain
1st1BFComprStrain
2stD12ComprStrain
2st1BFComprStrain
Load [kN/m²]
Strain [μm/m]
0
10
20
30
40
50
60
0 500 1000 1500 2000 2500 3000

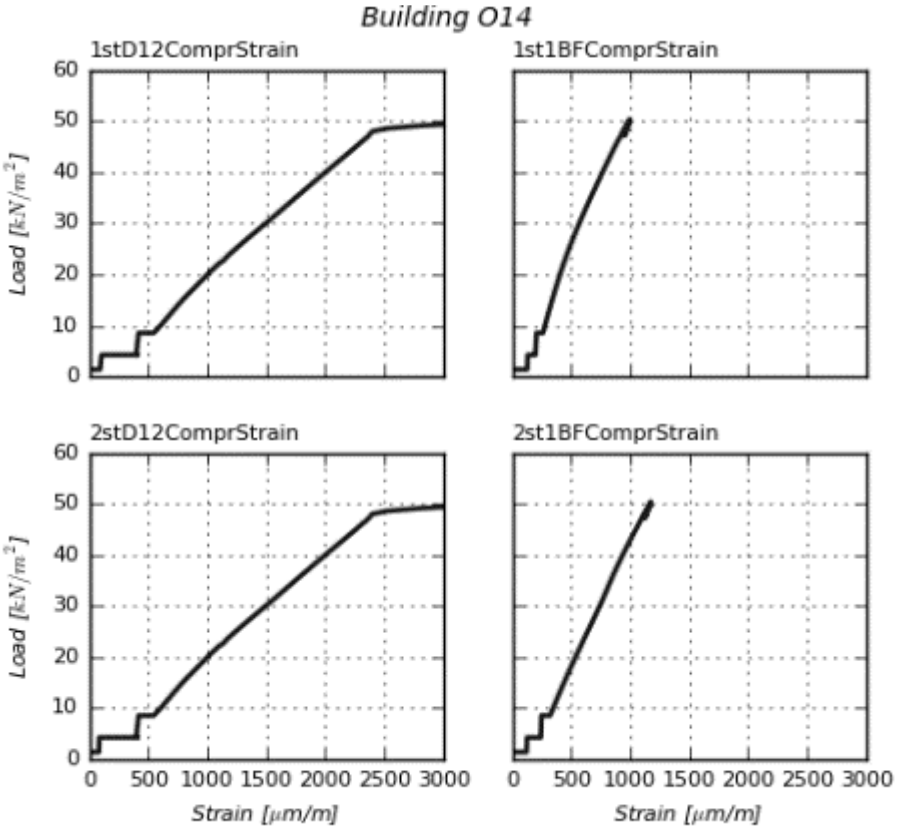
Building O14
1stD12ComprStrain
1st1BFComprStrain
2stD12ComprStrain
2st1BFComprStrain
Load [kN/m²]
Strain [μm/m]
0
10
20
30
40
50
60
0 500 1000 1500 2000 2500 3000

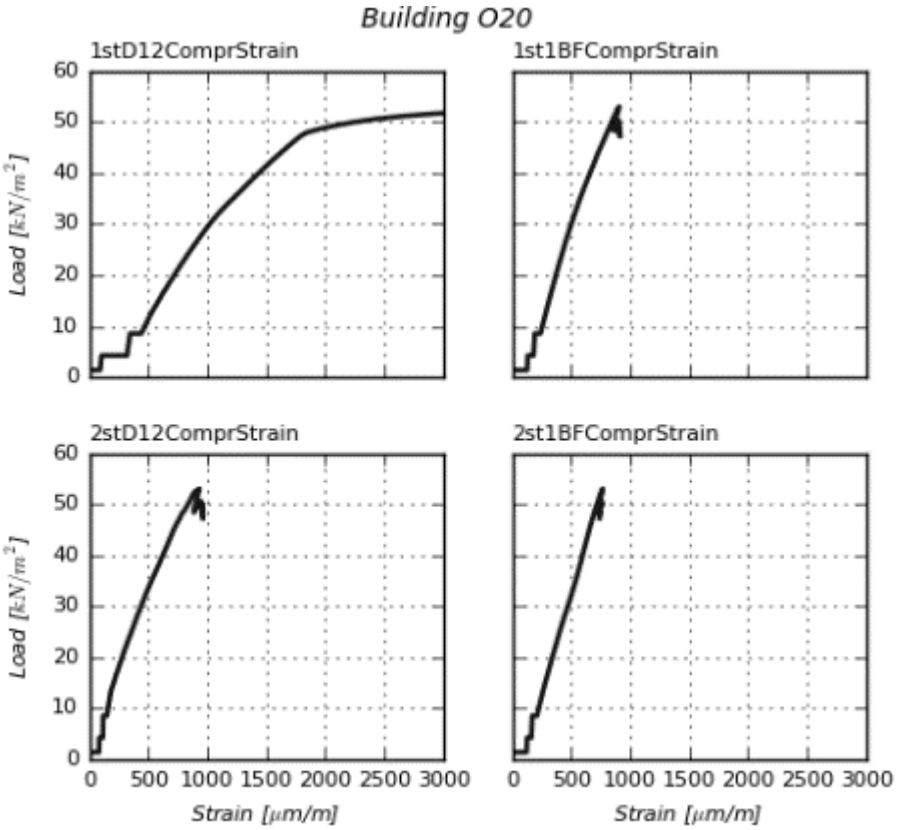
Building O20
1stD12ComprStrain
1st1BFComprStrain
2stD12ComprStrain
2st1BFComprStrain
Load [kN/m²]
Strain [μm/m]
0
10
20
30
40
50
60
0 500 1000 1500 2000 2500 3000

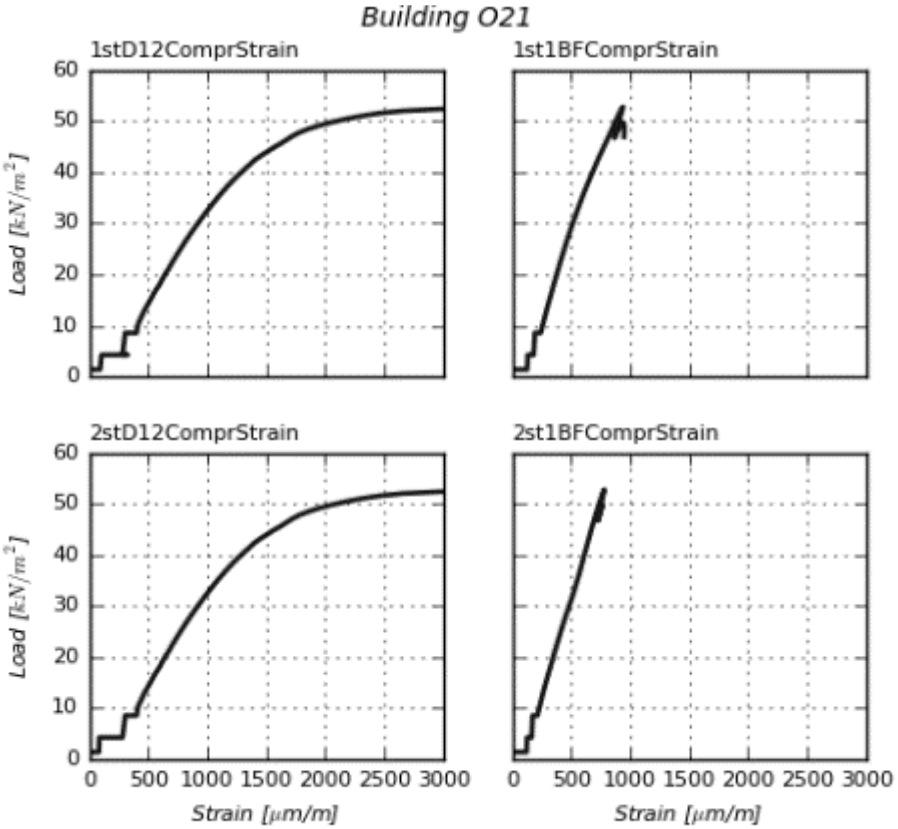
Building O21
1stD12ComprStrain
1st1BFComprStrain
2stD12ComprStrain
2st1BFComprStrain
Load [kN/m²]
Strain [μm/m]
0
10
20
30
40
50
60
0 500 1000 1500 2000 2500 3000

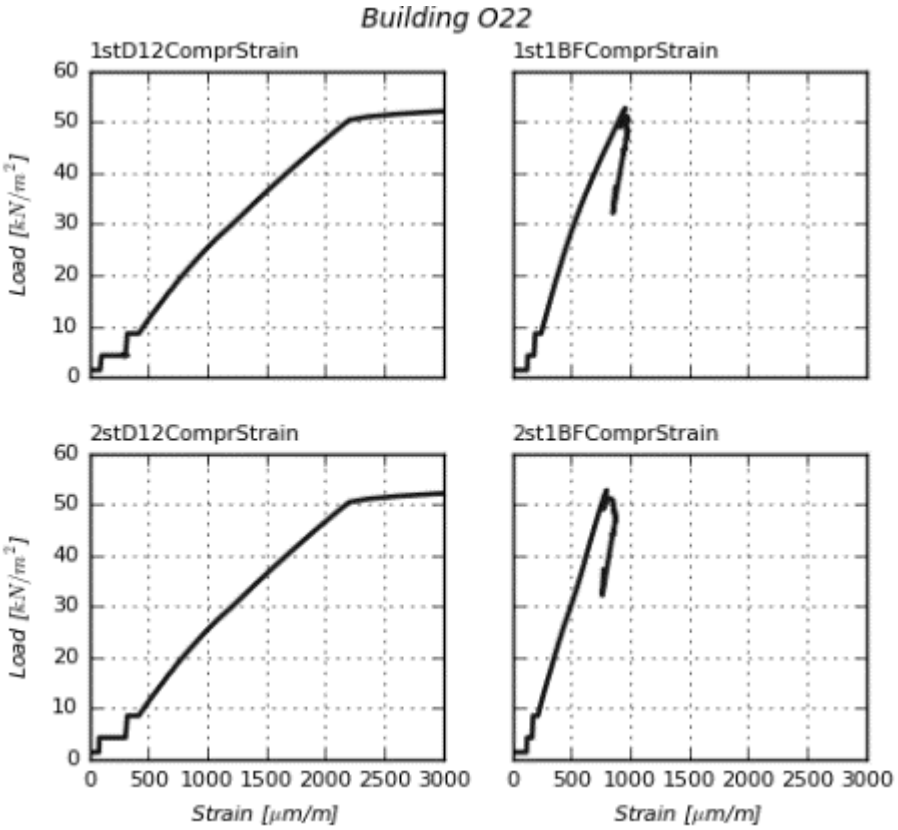
Building O22
1stD12ComprStrain
1st1BFComprStrain
2stD12ComprStrain
2st1BFComprStrain
Load [kN/m²]
Strain [μm/m]
0
10
20
30
40
50
60
0 500 1000 1500 2000 2500 3000

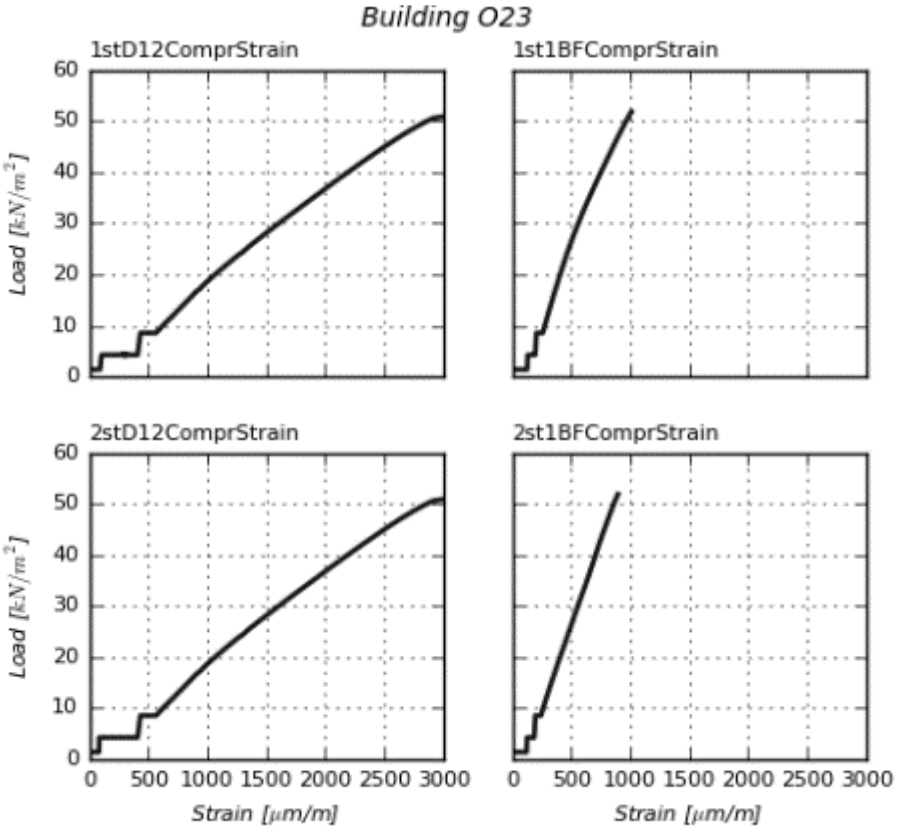
Building O23
1stD12ComprStrain
1st1BFComprStrain
2stD12ComprStrain
2st1BFComprStrain
Load [kN/m²]
Strain [μm/m]
0
10
20
30
40
50
60
0 500 1000 1500 2000 2500 3000

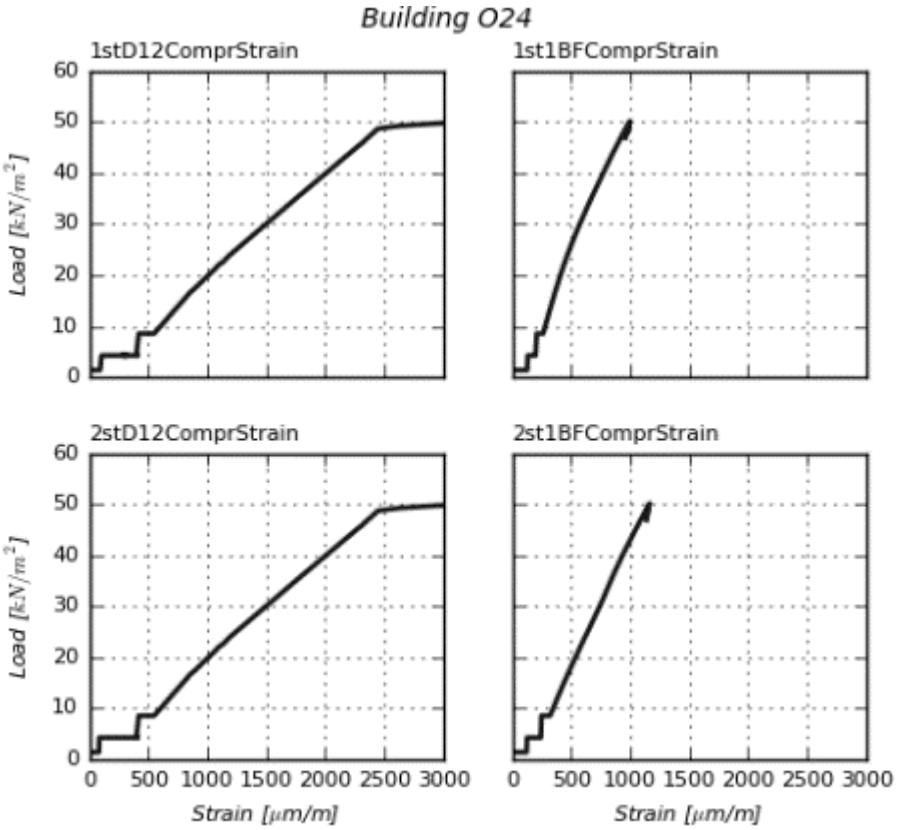
Building O24
1stD12ComprStrain
1st1BFComprStrain
2stD12ComprStrain
2st1BFComprStrain
Load [kN/m²]
Strain [μm/m]
0
10
20
30
40
50
60
0 500 1000 1500 2000 2500 3000

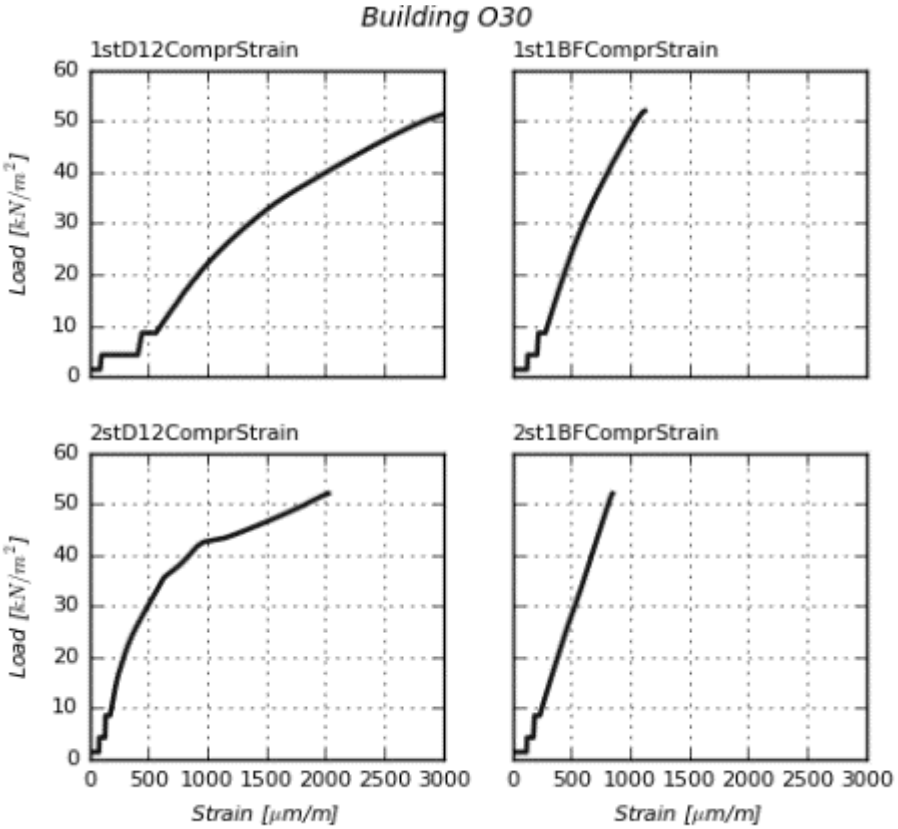
Building O30
1stD12ComprStrain
1st1BFComprStrain
2stD12ComprStrain
2st1BFComprStrain
Load [kN/m²]
Strain [μm/m]
0
10
20
30
40
50
60
0 500 1000 1500 2000 2500 3000

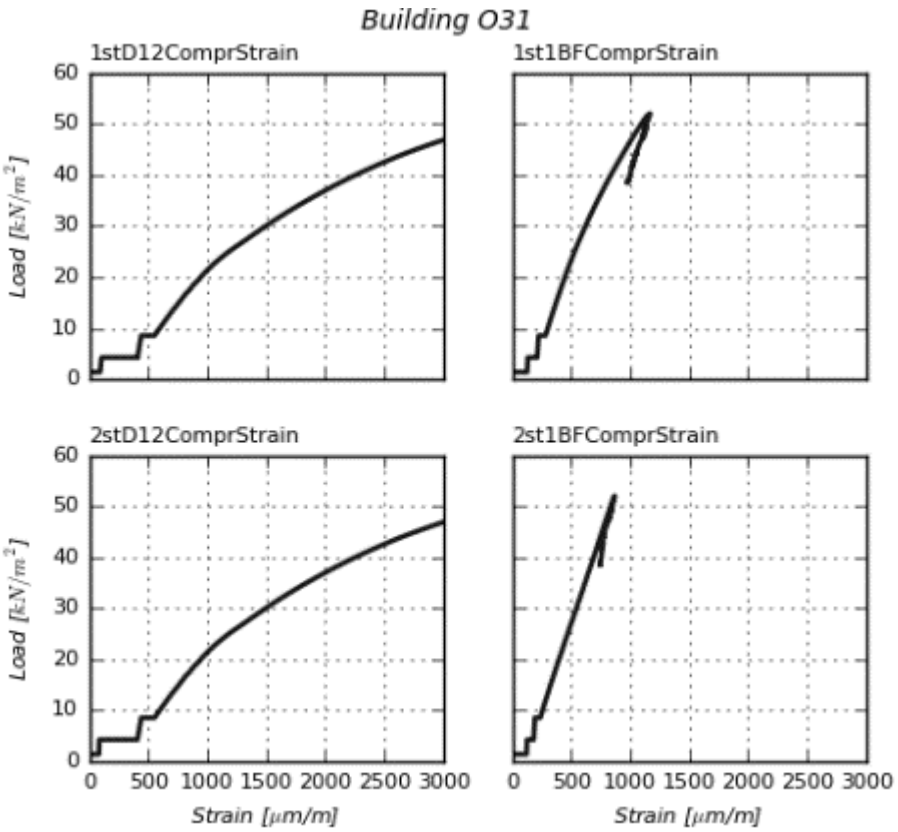
Building O31
1stD12ComprStrain
1st1BFComprStrain
2stD12ComprStrain
2st1BFComprStrain
Load [kN/m²]
Strain [μm/m]
0
10
20
30
40
50
60
0 500 1000 1500 2000 2500 3000

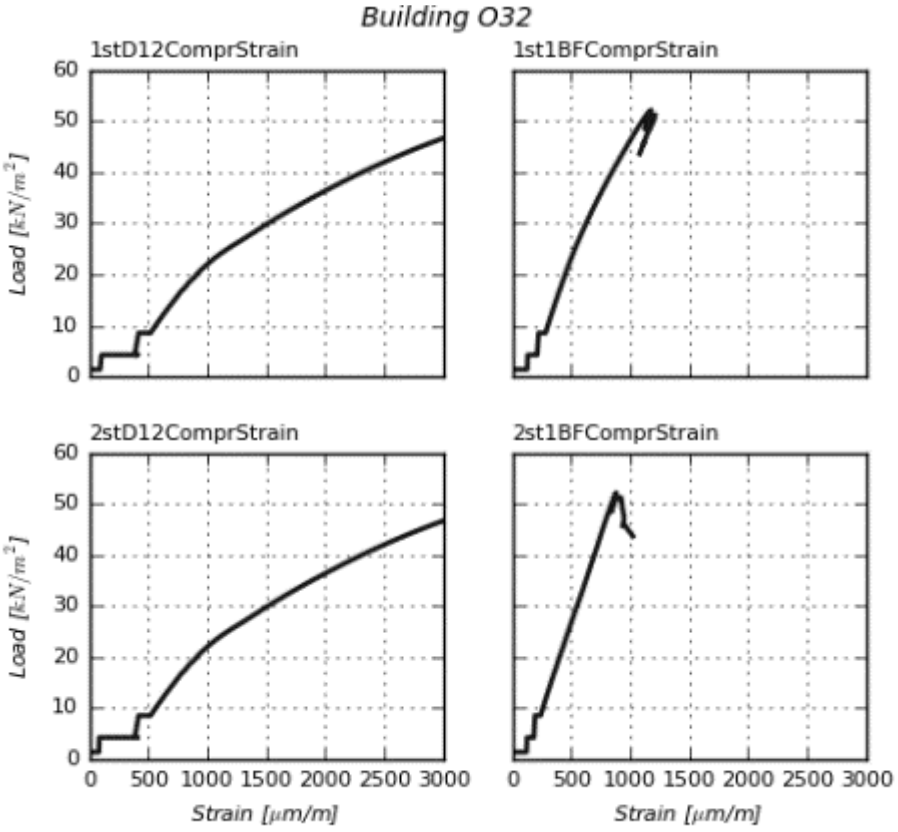
Building O32
1stD12ComprStrain
1st1BFComprStrain
2stD12ComprStrain
2st1BFComprStrain
Load [kN/m²]
Strain [μm/m]
0
10
20
30
40
50
60
0 500 1000 1500 2000 2500 3000

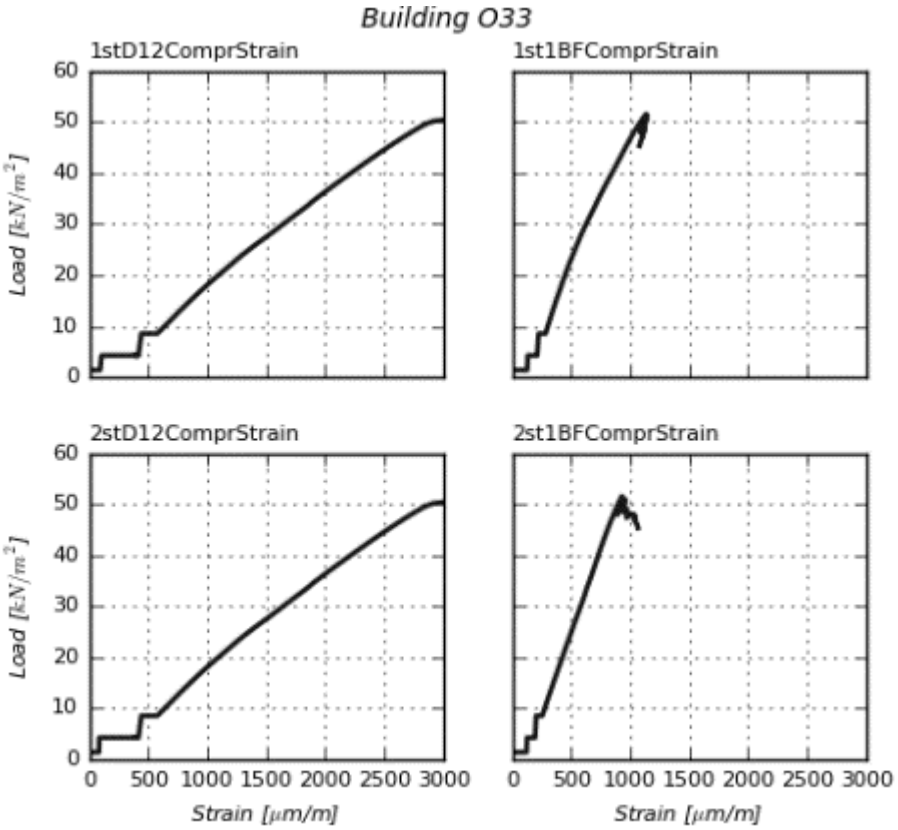
Building O33
1stD12ComprStrain
1st1BFComprStrain
2stD12ComprStrain
2st1BFComprStrain
Load [kN/m²]
Strain [μm/m]
0
10
20
30
40
50
60
0 500 1000 1500 2000 2500 3000

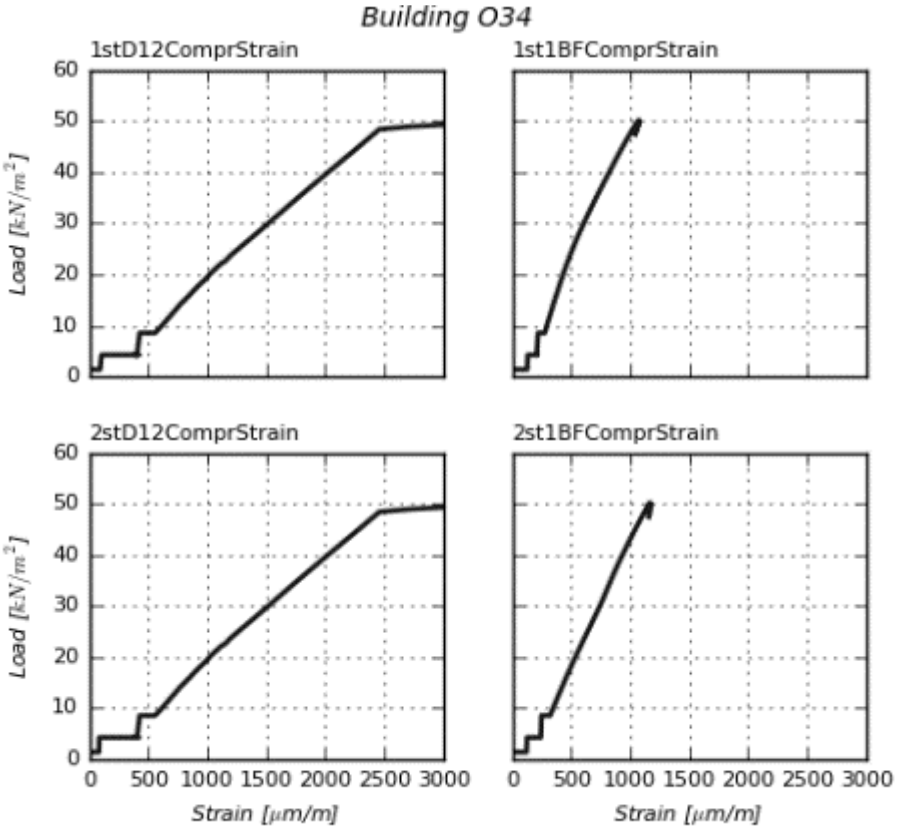
Building O34
1stD12ComprStrain
1st1BFComprStrain
2stD12ComprStrain
2st1BFComprStrain
Load [kN/m²]
Strain [μm/m]
0
10
20
30
40
50
60
0 500 1000 1500 2000 2500 3000

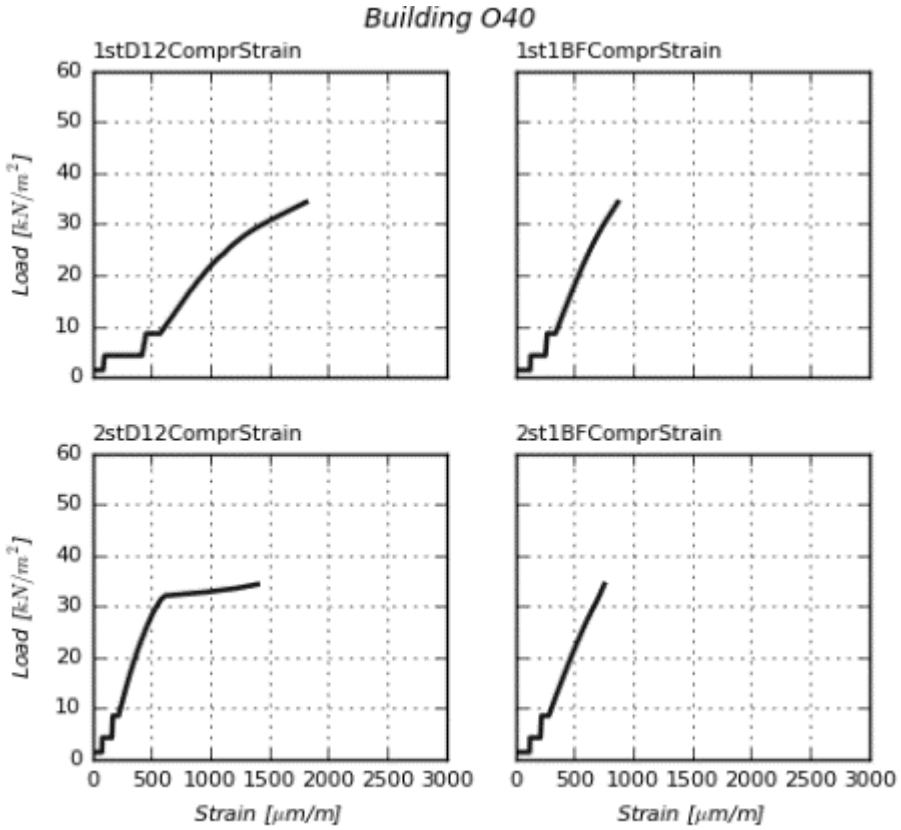
Building O40
1stD12ComprStrain
1st1BFComprStrain
2stD12ComprStrain
2st1BFComprStrain
Load [kN/m²]
Strain [μm/m]
0
10
20
30
40
50
60
0 500 1000 1500 2000 2500 3000

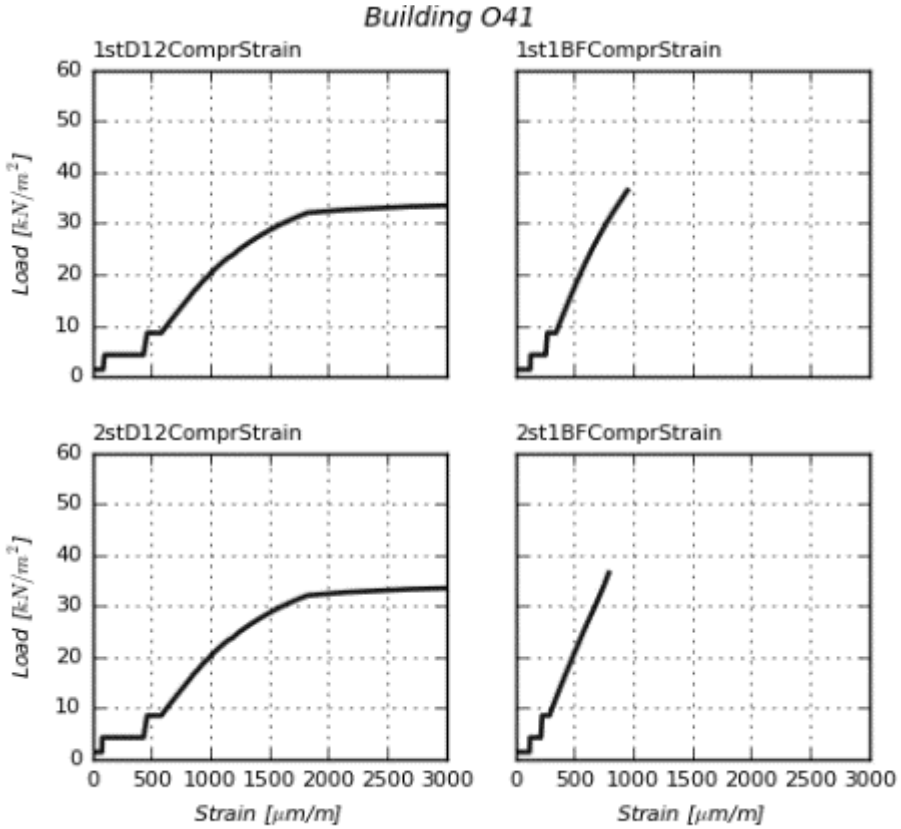
Building O41
1stD12ComprStrain
1st1BFComprStrain
2stD12ComprStrain
2st1BFComprStrain
Load [kN/m²]
Strain [μm/m]
0
10
20
30
40
50
60
0 500 1000 1500 2000 2500 3000

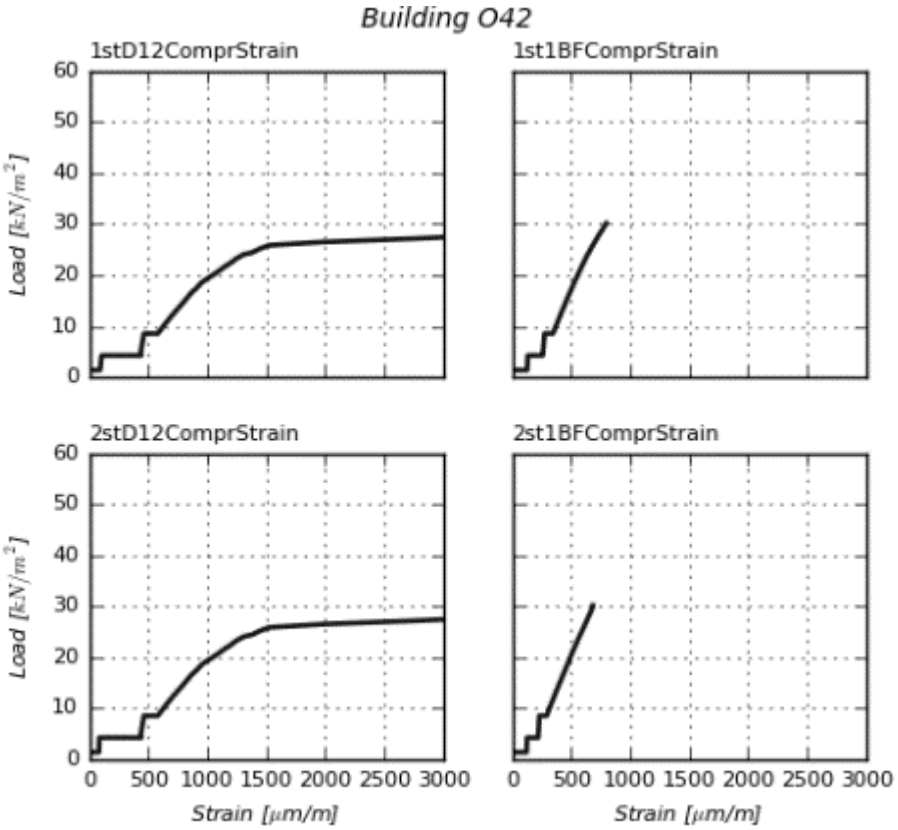
Building O42
1stD12ComprStrain
1st1BFComprStrain
2stD12ComprStrain
2st1BFComprStrain
Load [kN/m²]
Strain [μm/m]
0
10
20
30
40
50
60
0 500 1000 1500 2000 2500 3000

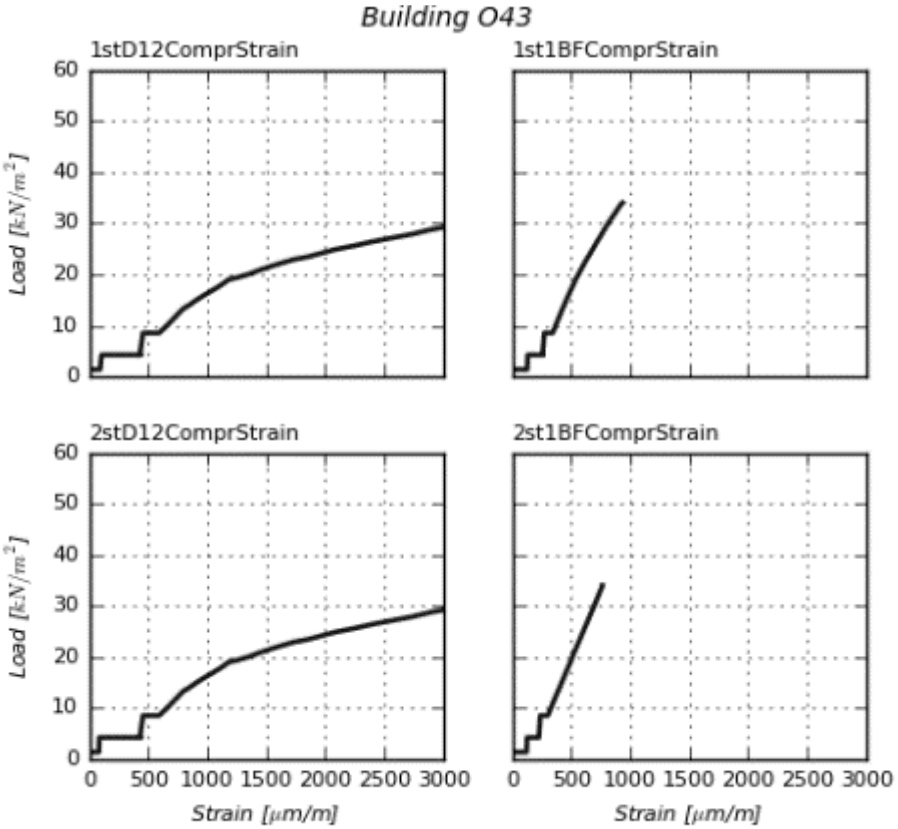
Building O43
1stD12ComprStrain
1st1BFComprStrain
2stD12ComprStrain
2st1BFComprStrain
Load [kN/m²]
Strain [μm/m]
0
10
20
30
40
50
60
0 500 1000 1500 2000 2500 3000

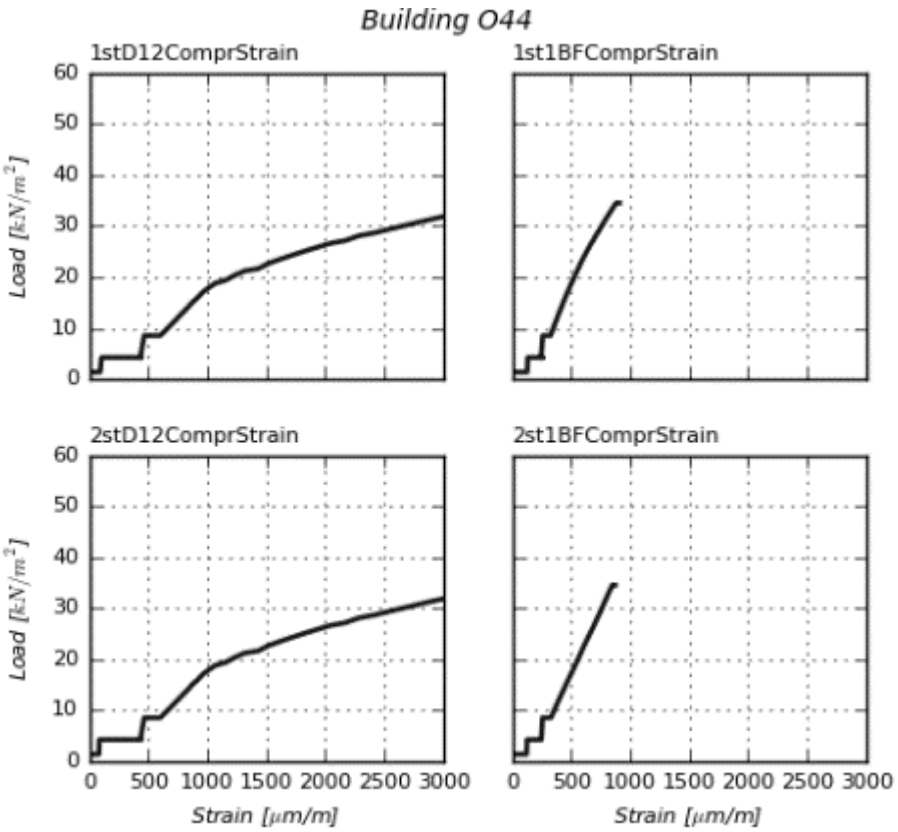
Building O44
1stD12ComprStrain
1st1BFComprStrain
2stD12ComprStrain
2st1BFComprStrain
Load [kN/m²]
Strain [μm/m]
0
10
20
30
40
50
60
0
500
1000
1500
2000
2500
3000

A6 – Load response diagrams for tensile reinforcement in walls and slabs

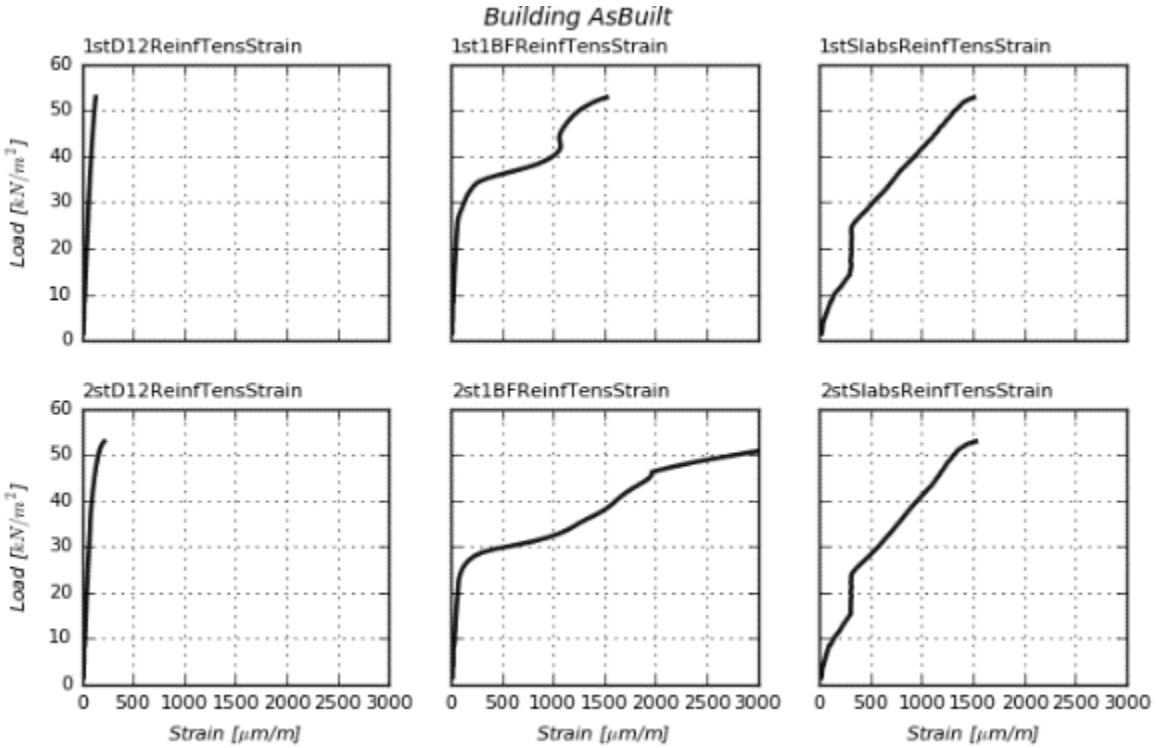

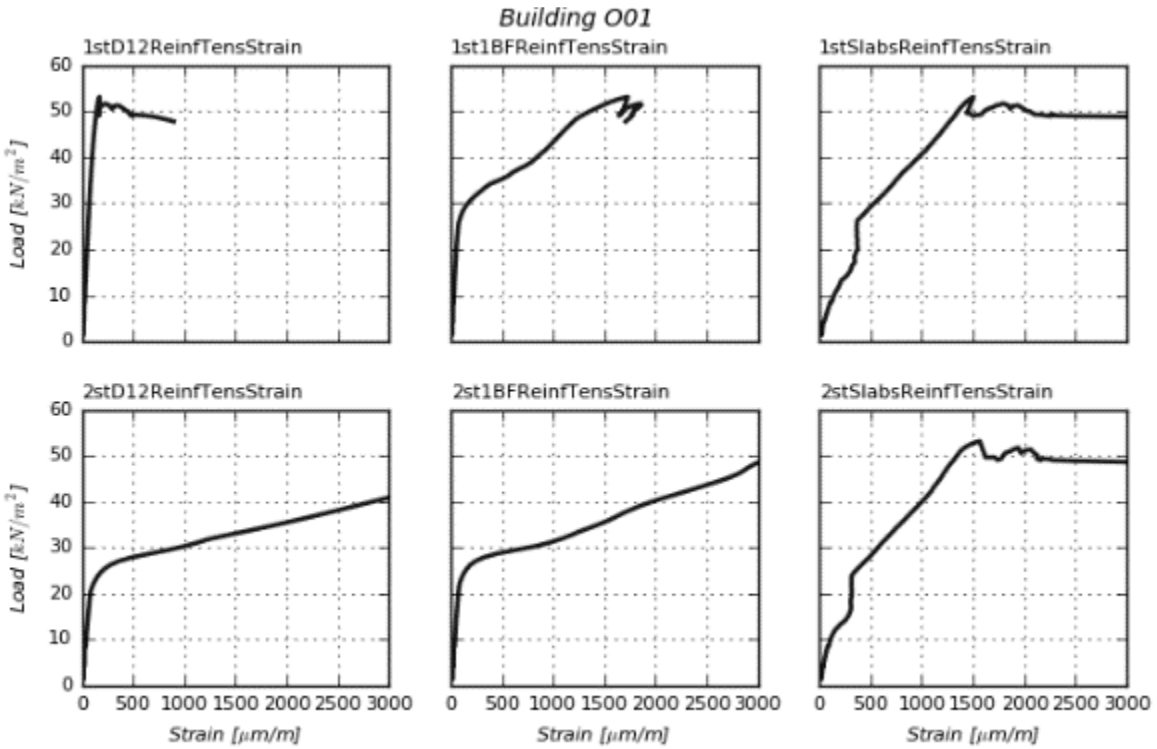

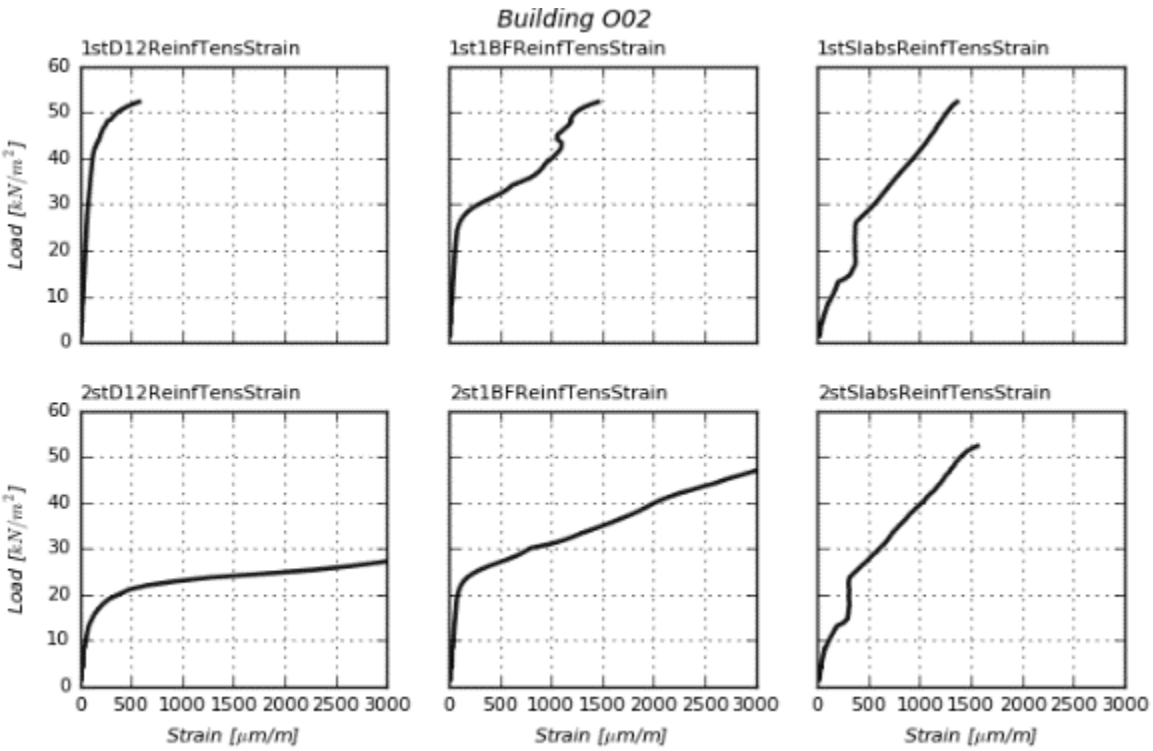
Building O02
1stD12ReinfTensStrain
1st1BFReinfTensStrain
1stSlabsReinfTensStrain
2stD12ReinfTensStrain
2st1BFReinfTensStrain
2stSlabsReinfTensStrain
Load [kN/m²]
Strain [μm/m]
0
10
20
30
40
50
60
0
500
1000
1500
2000
2500
3000

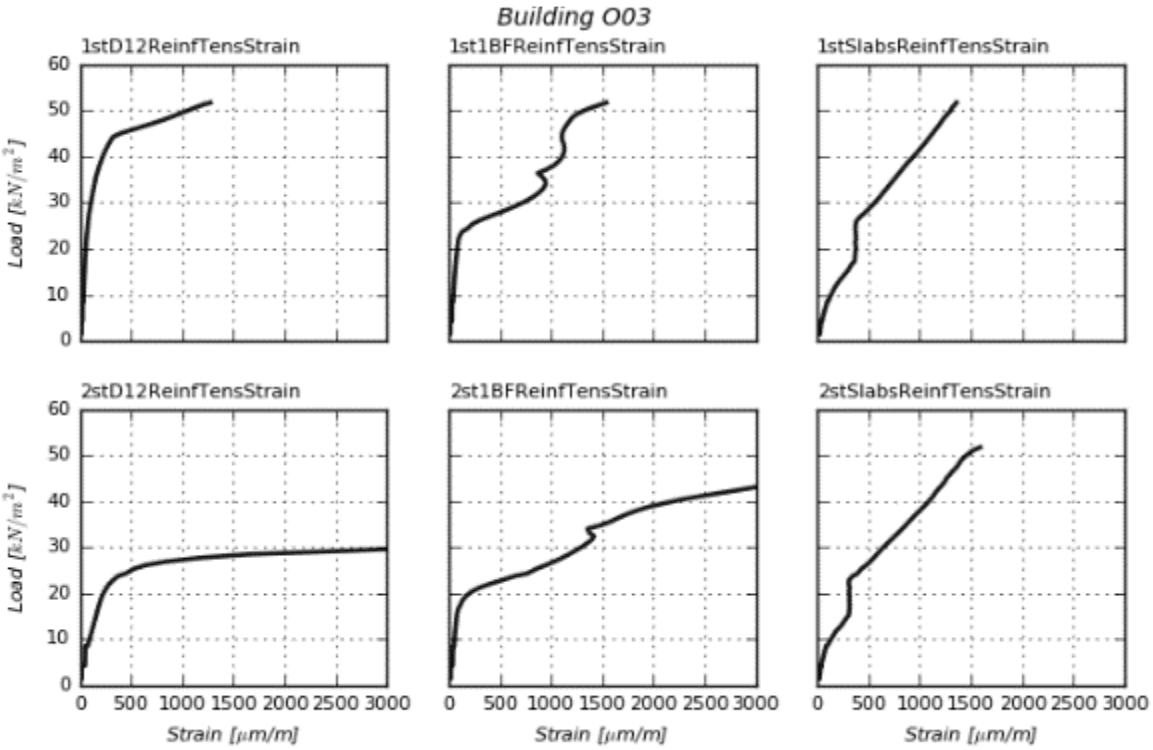
Building O03
1stD12ReinfTensStrain
1st1BFReinfTensStrain
1stSlabsReinfTensStrain
2stD12ReinfTensStrain
2st1BFReinfTensStrain
2stSlabsReinfTensStrain
Load [kN/m²]
Strain [μm/m]
0
10
20
30
40
50
60
0
500
1000
1500
2000
2500
3000

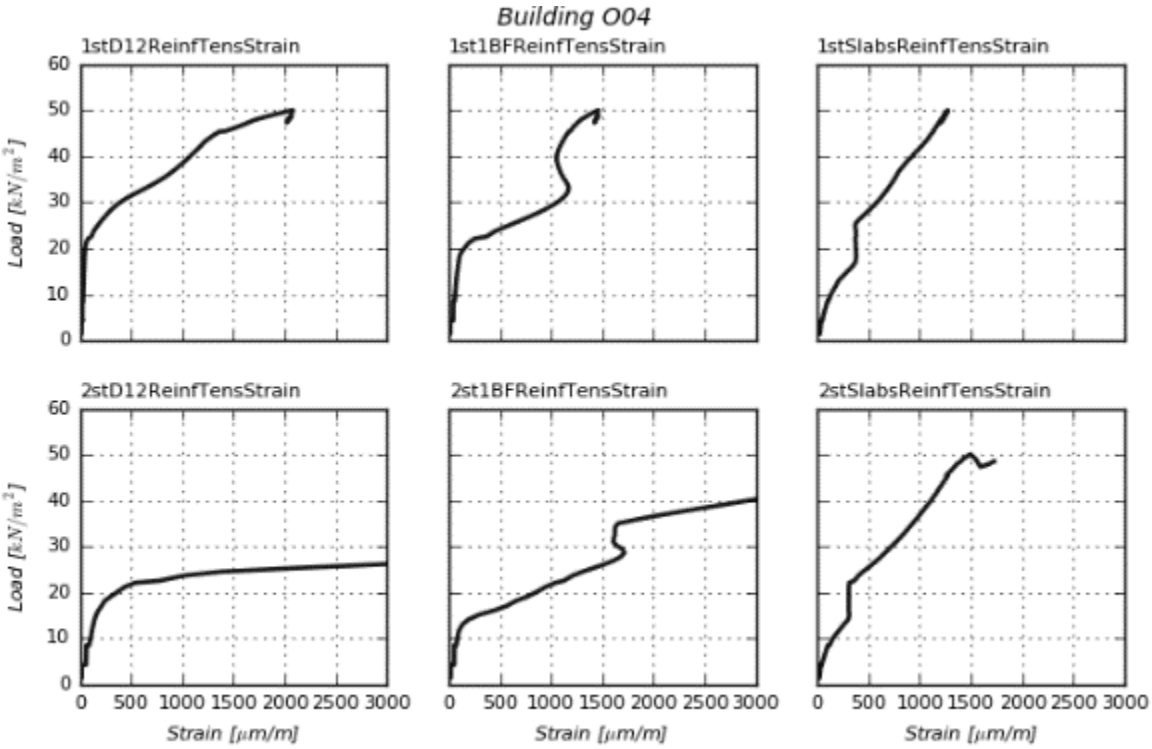
Building O04
1stD12ReinfTensStrain
1st1BFReinfTensStrain
1stSlabsReinfTensStrain
2stD12ReinfTensStrain
2st1BFReinfTensStrain
2stSlabsReinfTensStrain
Load [kN/m²]
Strain [μm/m]
0
10
20
30
40
50
60
0 500 1000 1500 2000 2500 3000

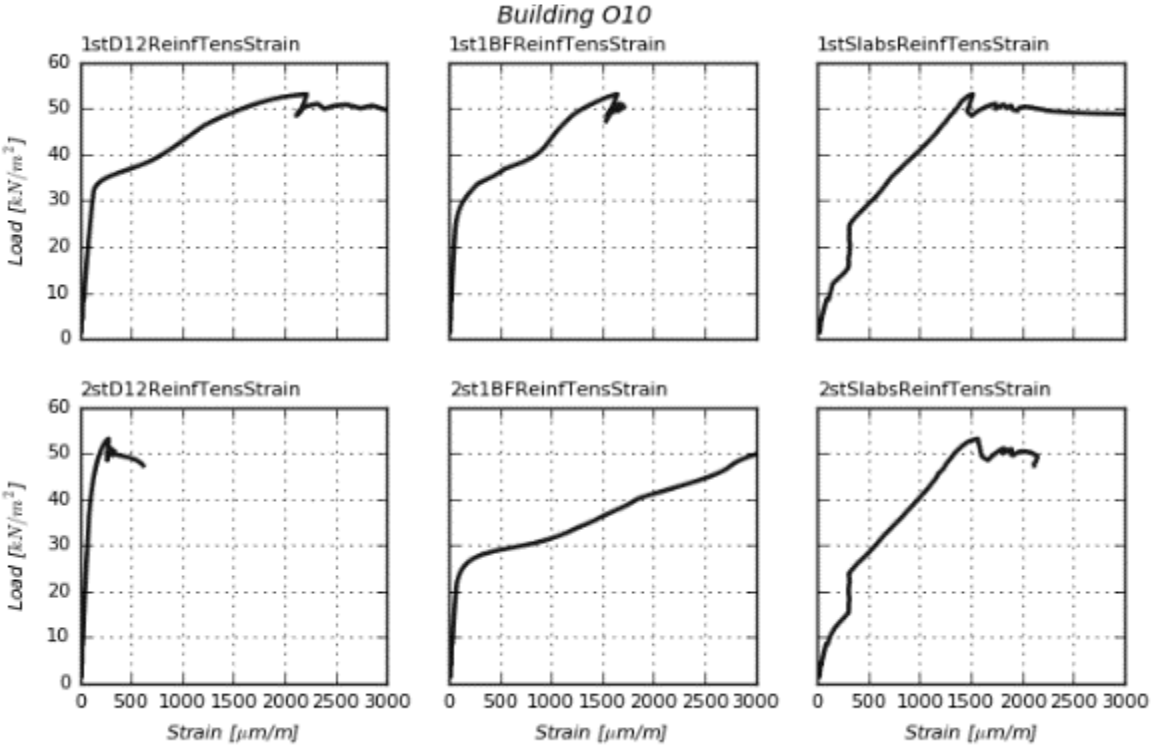
Building O10
1stD12ReinfTensStrain
1st1BFReinfTensStrain
1stSlabsReinfTensStrain
2stD12ReinfTensStrain
2st1BFReinfTensStrain
2stSlabsReinfTensStrain
Load [kN/m²]
Strain [μm/m]
0
10
20
30
40
50
60
0 500 1000 1500 2000 2500 3000

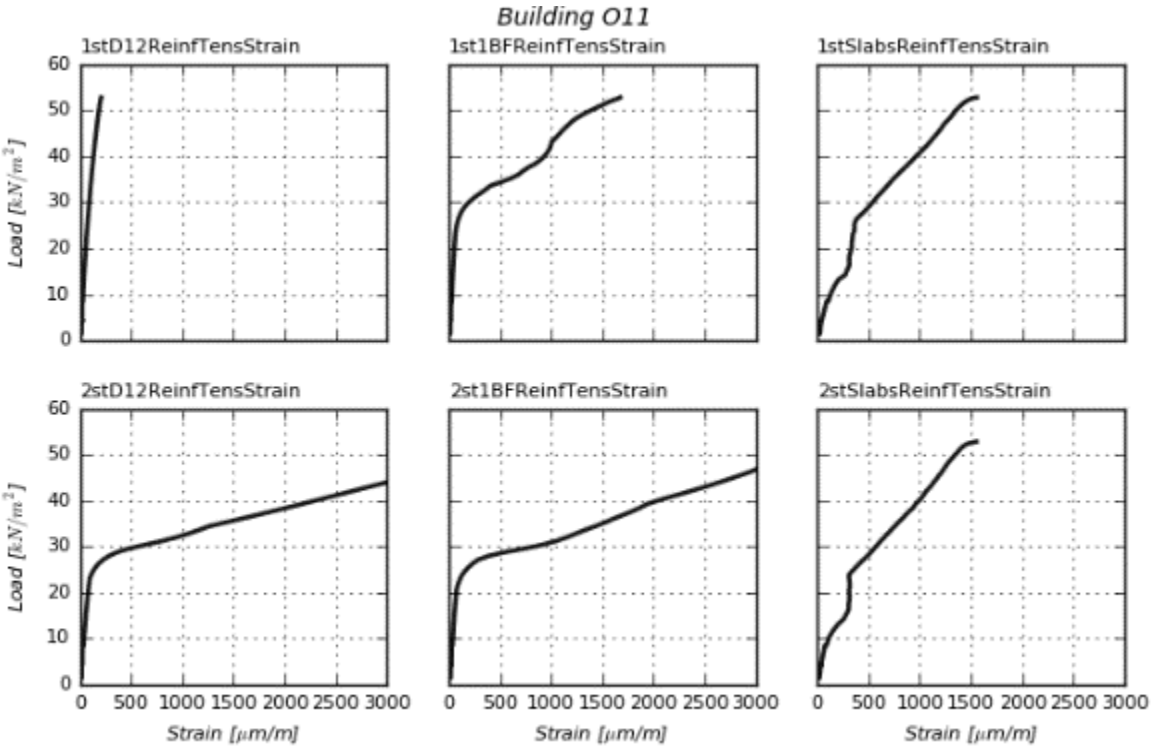
Building O11
1stD12ReinfTensStrain
1st1BFReinfTensStrain
1stSlabsReinfTensStrain
2stD12ReinfTensStrain
2st1BFReinfTensStrain
2stSlabsReinfTensStrain
Load [kN/m²]
Strain [μm/m]
0
10
20
30
40
50
60
0 500 1000 1500 2000 2500 3000

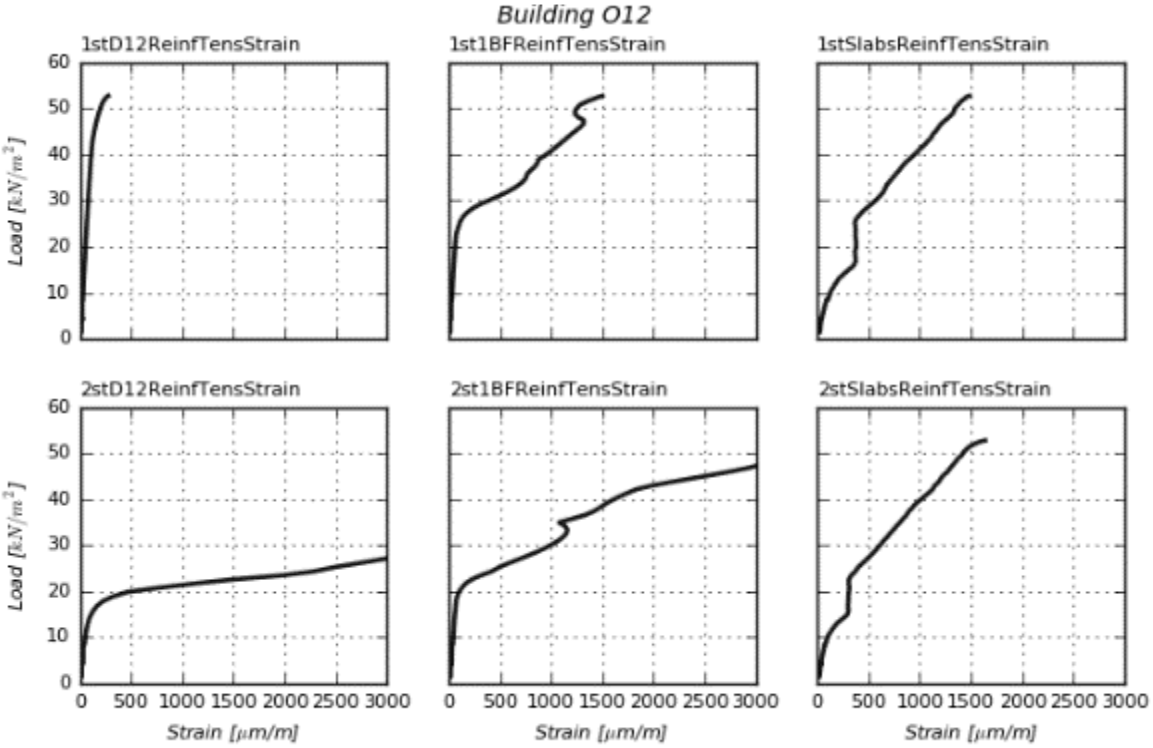
Building O12
1stD12ReinfTensStrain
1st1BFReinfTensStrain
1stSlabsReinfTensStrain
2stD12ReinfTensStrain
2st1BFReinfTensStrain
2stSlabsReinfTensStrain
Load [kN/m²]
Strain [μm/m]
0
10
20
30
40
50
60
0 500 1000 1500 2000 2500 3000

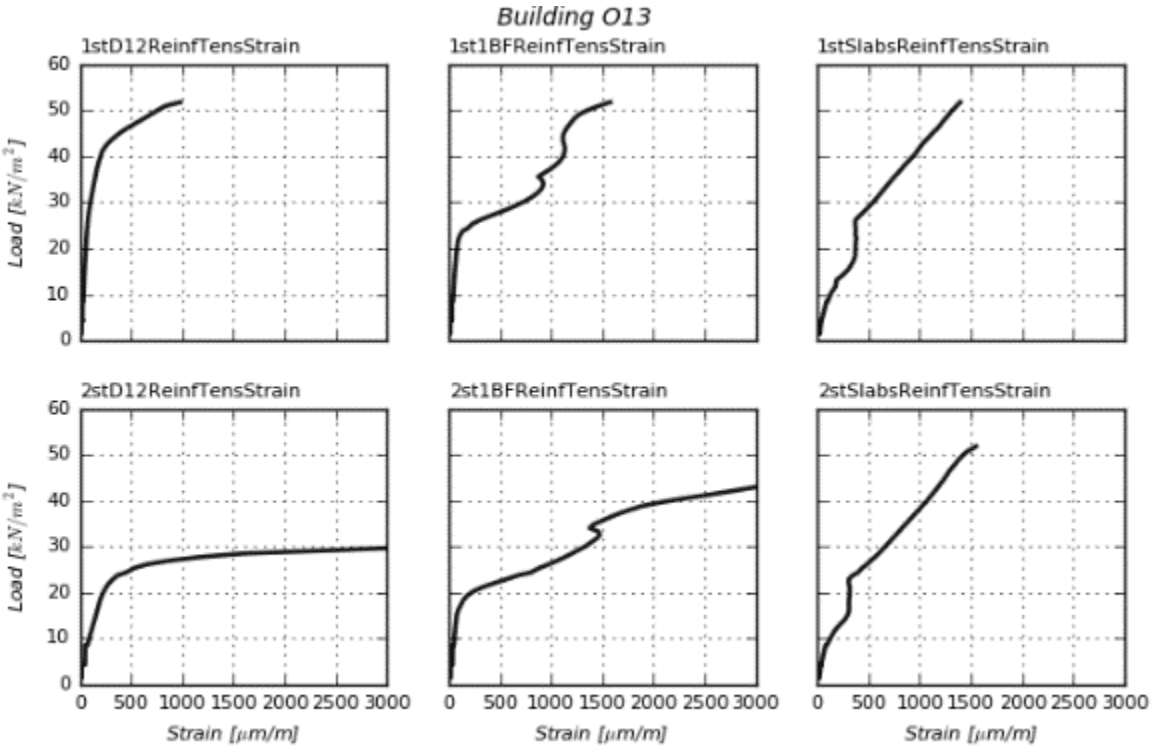
Building O13
1stD12ReinfTensStrain
1st1BFReinfTensStrain
1stSlabsReinfTensStrain
2stD12ReinfTensStrain
2st1BFReinfTensStrain
2stSlabsReinfTensStrain
Load [kN/m²]
Strain [μm/m]
0
10
20
30
40
50
60
0
500
1000
1500
2000
2500
3000

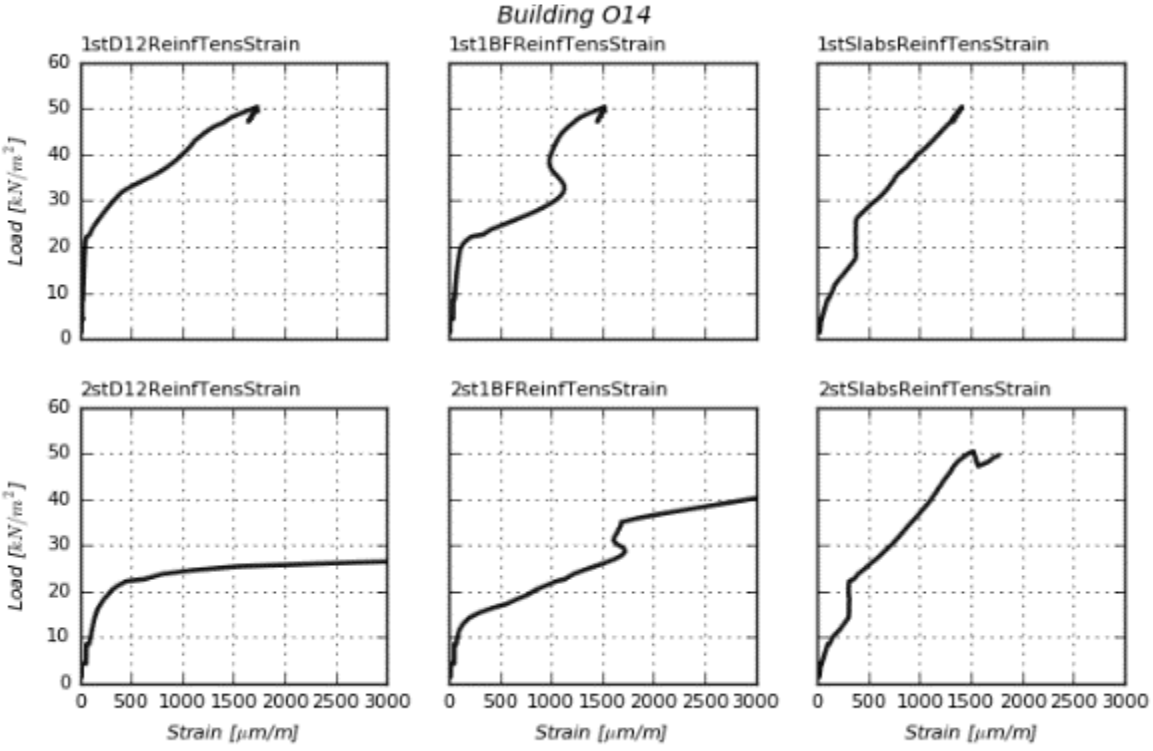
Building O14
1stD12ReinfTensStrain
1st1BFReinfTensStrain
1stSlabsReinfTensStrain
2stD12ReinfTensStrain
2st1BFReinfTensStrain
2stSlabsReinfTensStrain
Load [kN/m²]
Strain [μm/m]
0
10
20
30
40
50
60
0
500
1000
1500
2000
2500
3000

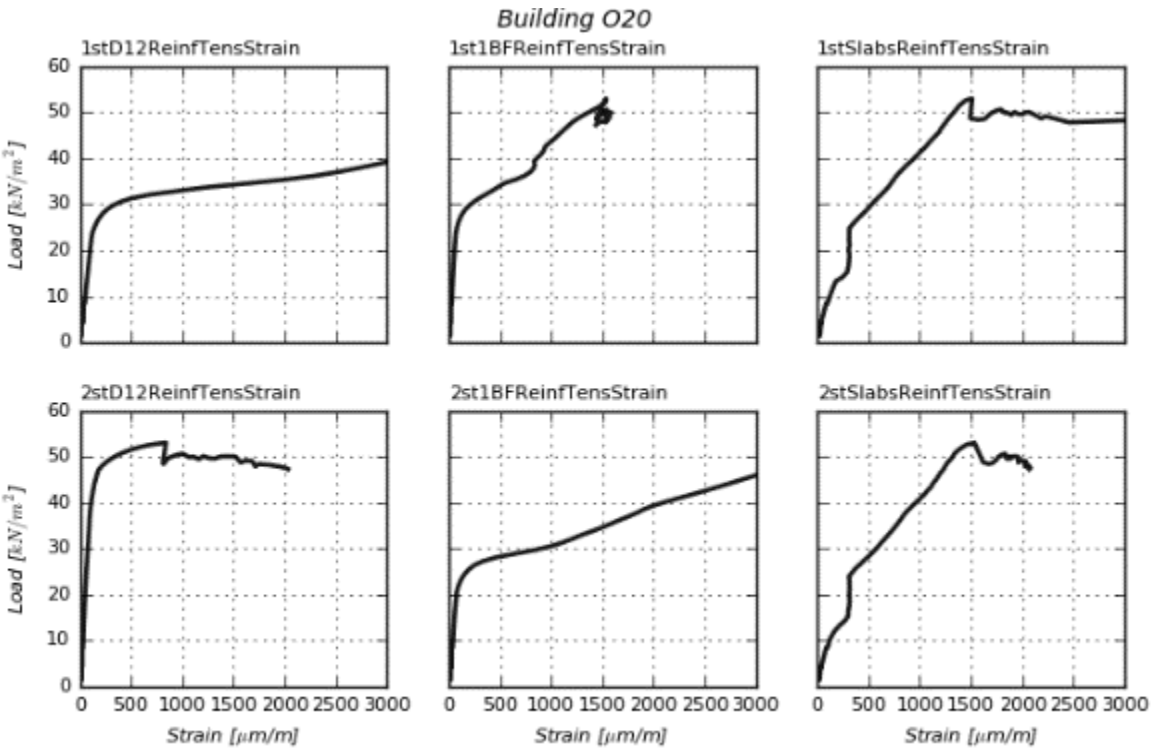
Building O20
1stD12ReinfTensStrain
1st1BFReinfTensStrain
1stSlabsReinfTensStrain
2stD12ReinfTensStrain
2st1BFReinfTensStrain
2stSlabsReinfTensStrain
Load [kN/m²]
Strain [μm/m]
0
10
20
30
40
50
60
0 500 1000 1500 2000 2500 3000

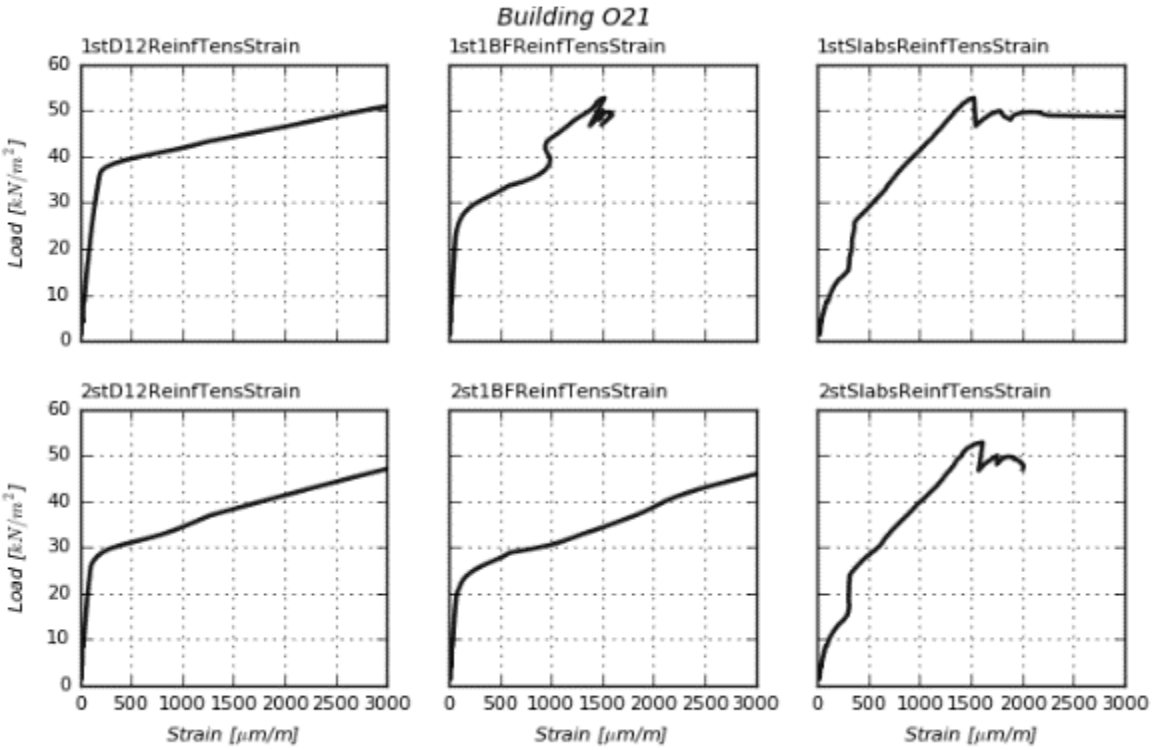
Building O21
1stD12ReinfTensStrain
1st1BFReinfTensStrain
1stSlabsReinfTensStrain
2stD12ReinfTensStrain
2st1BFReinfTensStrain
2stSlabsReinfTensStrain
Load [kN/m²]
Strain [μm/m]
0
10
20
30
40
50
60
0 500 1000 1500 2000 2500 3000

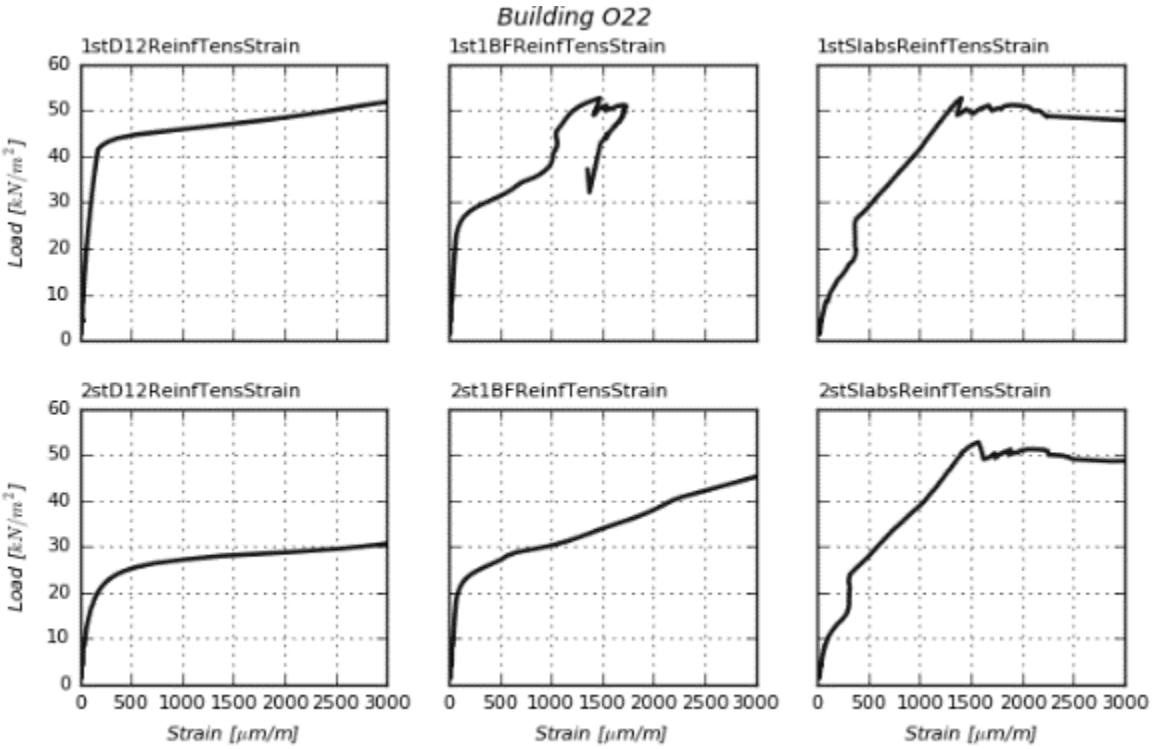
Building O22
1stD12ReinfTensStrain
1st1BFReinfTensStrain
1stSlabsReinfTensStrain
2stD12ReinfTensStrain
2st1BFReinfTensStrain
2stSlabsReinfTensStrain
Load [kN/m²]
Strain [μm/m]
0
10
20
30
40
50
60
0
500
1000
1500
2000
2500
3000

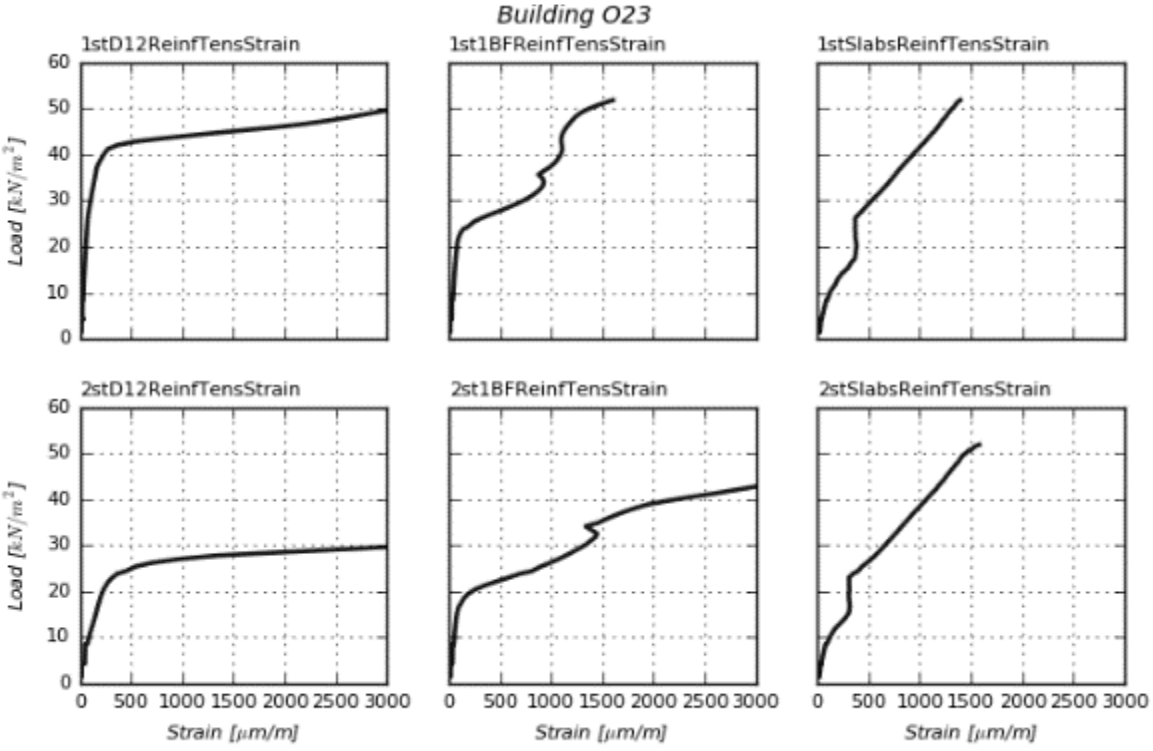
Building O23
1stD12ReinfTensStrain
1st1BFReinfTensStrain
1stSlabsReinfTensStrain
2stD12ReinfTensStrain
2st1BFReinfTensStrain
2stSlabsReinfTensStrain
Load [kN/m²]
Strain [μm/m]
0
10
20
30
40
50
60
0
500
1000
1500
2000
2500
3000

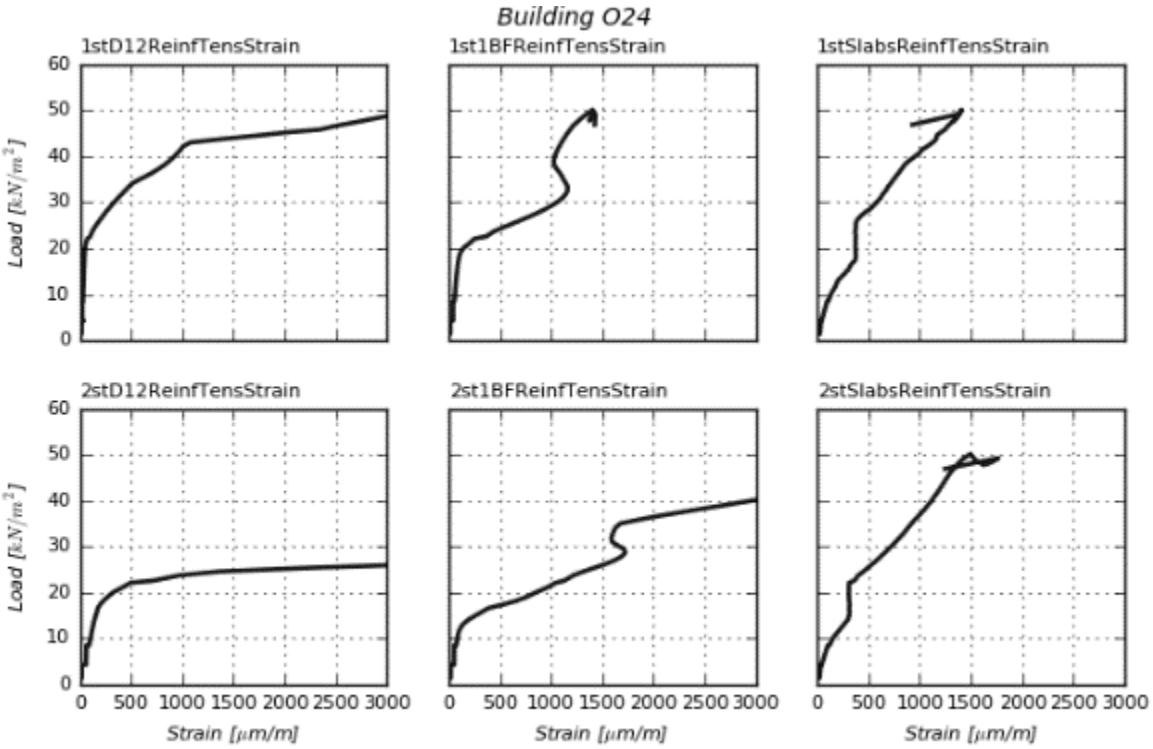
Building O24
1stD12ReinfTensStrain
1st1BFReinfTensStrain
1stSlabsReinfTensStrain
2stD12ReinfTensStrain
2st1BFReinfTensStrain
2stSlabsReinfTensStrain
Load [kN/m²]
Strain [μm/m]
0
10
20
30
40
50
60
0 500 1000 1500 2000 2500 3000

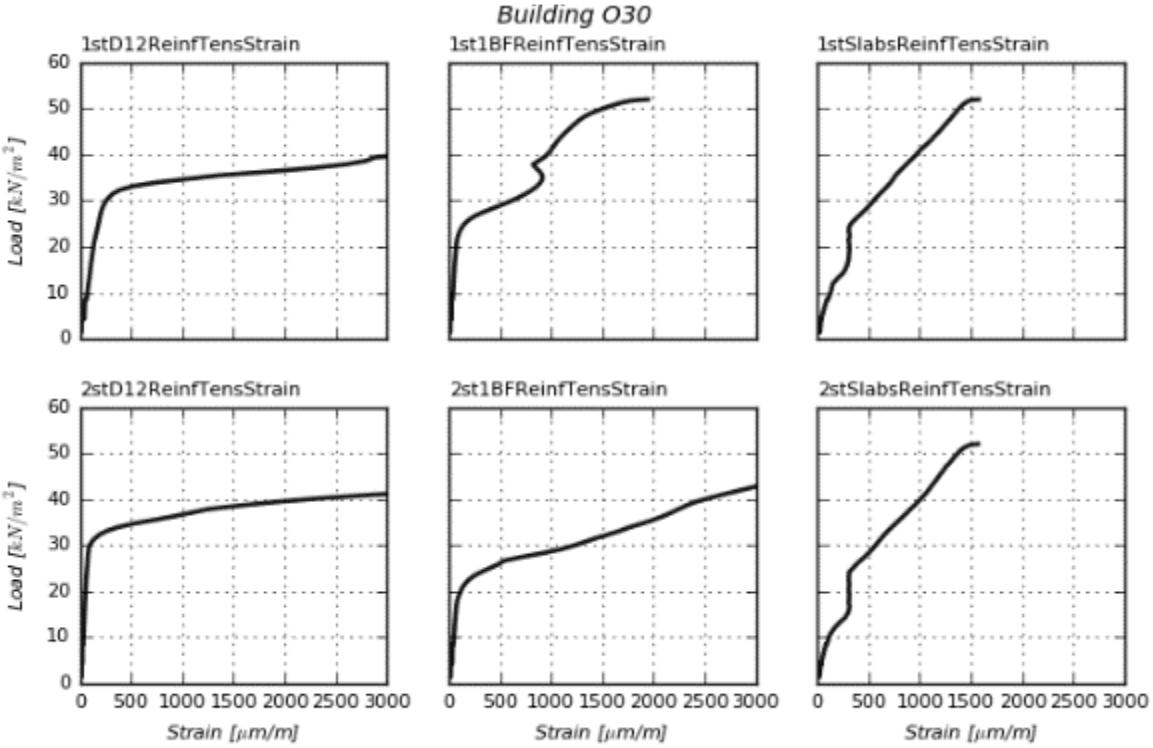
Building O30
1stD12ReinfTensStrain
1st1BFReinfTensStrain
1stSlabsReinfTensStrain
2stD12ReinfTensStrain
2st1BFReinfTensStrain
2stSlabsReinfTensStrain
Load [kN/m²]
Strain [μm/m]
0
10
20
30
40
50
60
0 500 1000 1500 2000 2500 3000

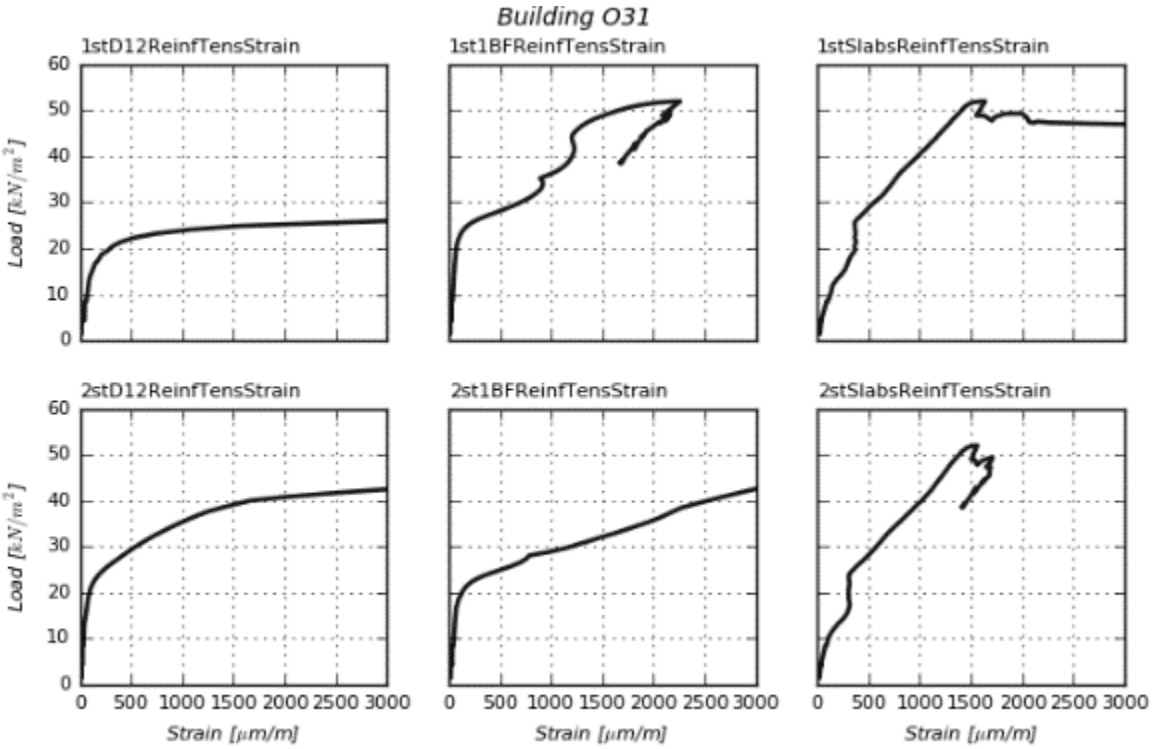
Building O31
1stD12ReinfTensStrain
1st1BFReinfTensStrain
1stSlabsReinfTensStrain
2stD12ReinfTensStrain
2st1BFReinfTensStrain
2stSlabsReinfTensStrain
Load [kN/m²]
Strain [μm/m]
0
10
20
30
40
50
60
0
500
1000
1500
2000
2500
3000

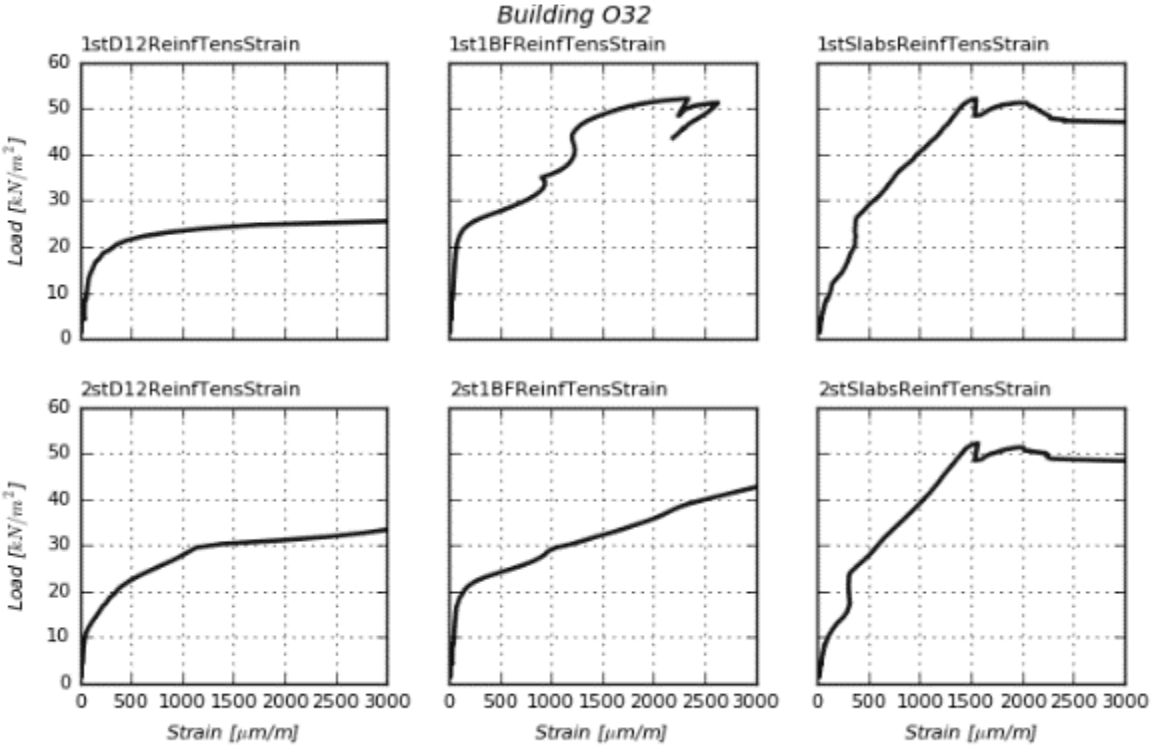
Building O32
1stD12ReinfTensStrain
1st1BFReinfTensStrain
1stSlabsReinfTensStrain
2stD12ReinfTensStrain
2st1BFReinfTensStrain
2stSlabsReinfTensStrain
Load [kN/m²]
Strain [μm/m]
0
10
20
30
40
50
60
0
500
1000
1500
2000
2500
3000

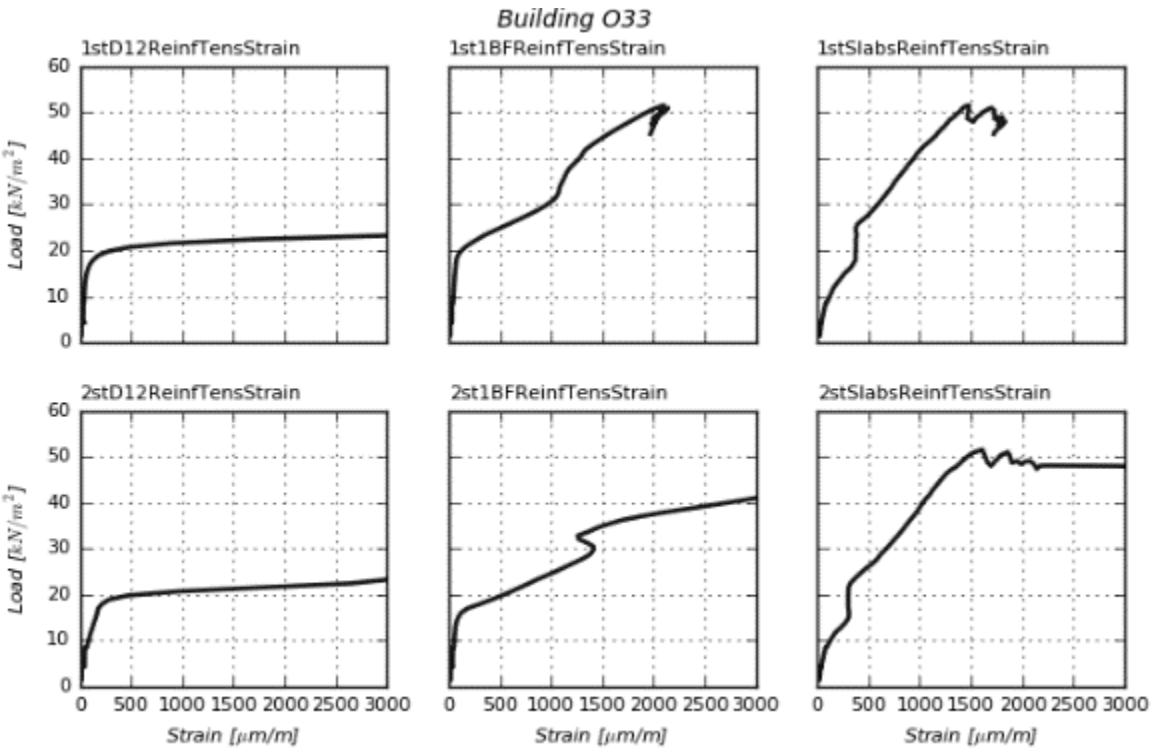
Building O33
1stD12ReinfTensStrain
1st1BFReinfTensStrain
1stSlabsReinfTensStrain
2stD12ReinfTensStrain
2st1BFReinfTensStrain
2stSlabsReinfTensStrain
Load [kN/m²]
Strain [μm/m]
0
10
20
30
40
50
60
0 500 1000 1500 2000 2500 3000

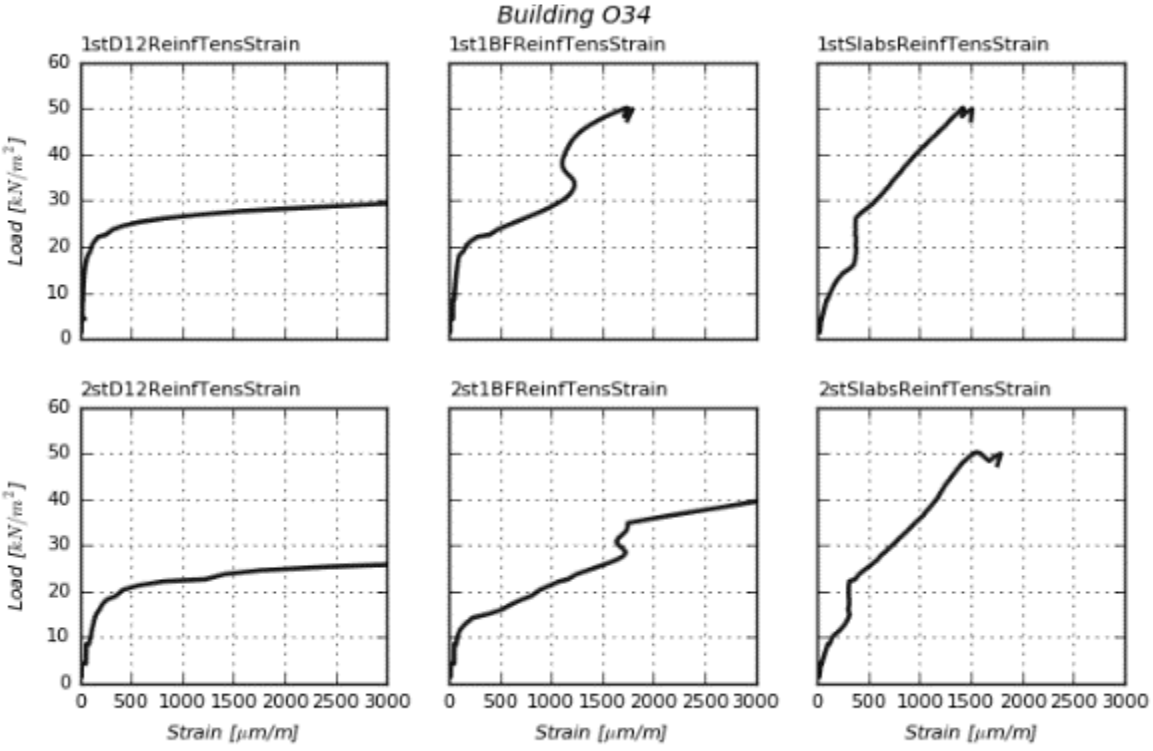
Building O34
1stD12ReinfTensStrain
1st1BFReinfTensStrain
1stSlabsReinfTensStrain
2stD12ReinfTensStrain
2st1BFReinfTensStrain
2stSlabsReinfTensStrain
Load [kN/m²]
Strain [μm/m]
0
10
20
30
40
50
60
0 500 1000 1500 2000 2500 3000

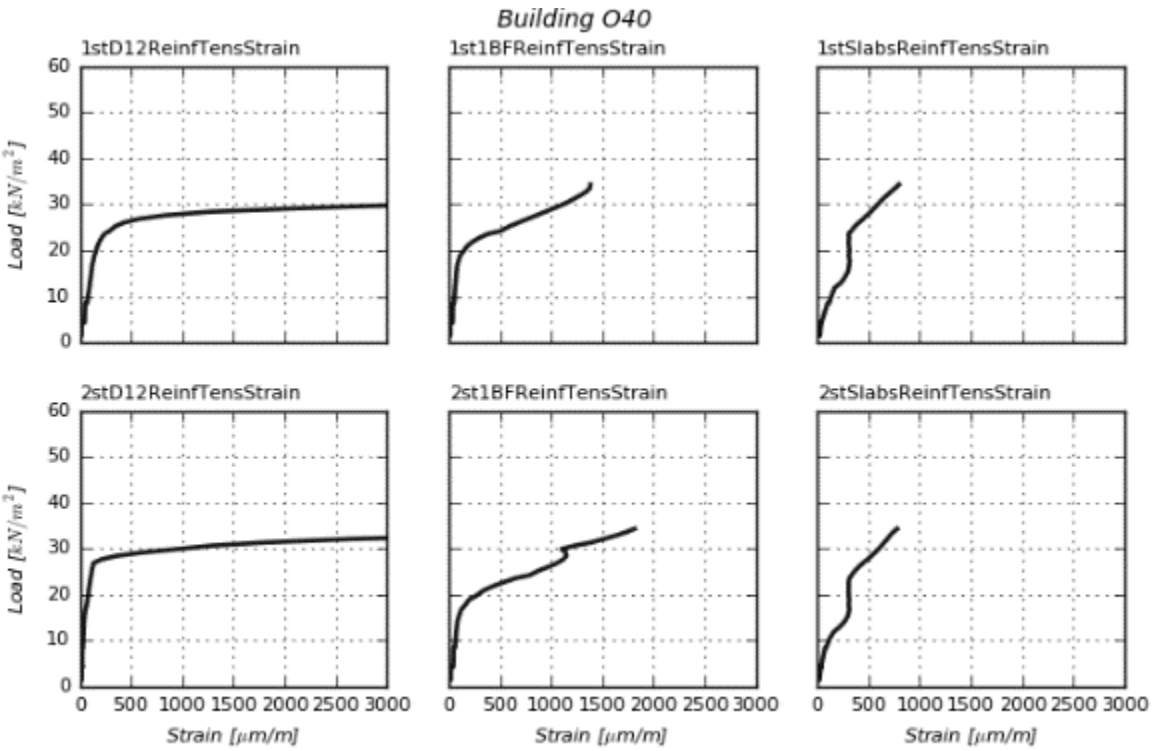
Building O40
1stD12ReinfTensStrain
1st1BFReinfTensStrain
1stSlabsReinfTensStrain
2stD12ReinfTensStrain
2st1BFReinfTensStrain
2stSlabsReinfTensStrain
Load [kN/m²]
Strain [μm/m]
0
10
20
30
40
50
60
0
500
1000
1500
2000
2500
3000

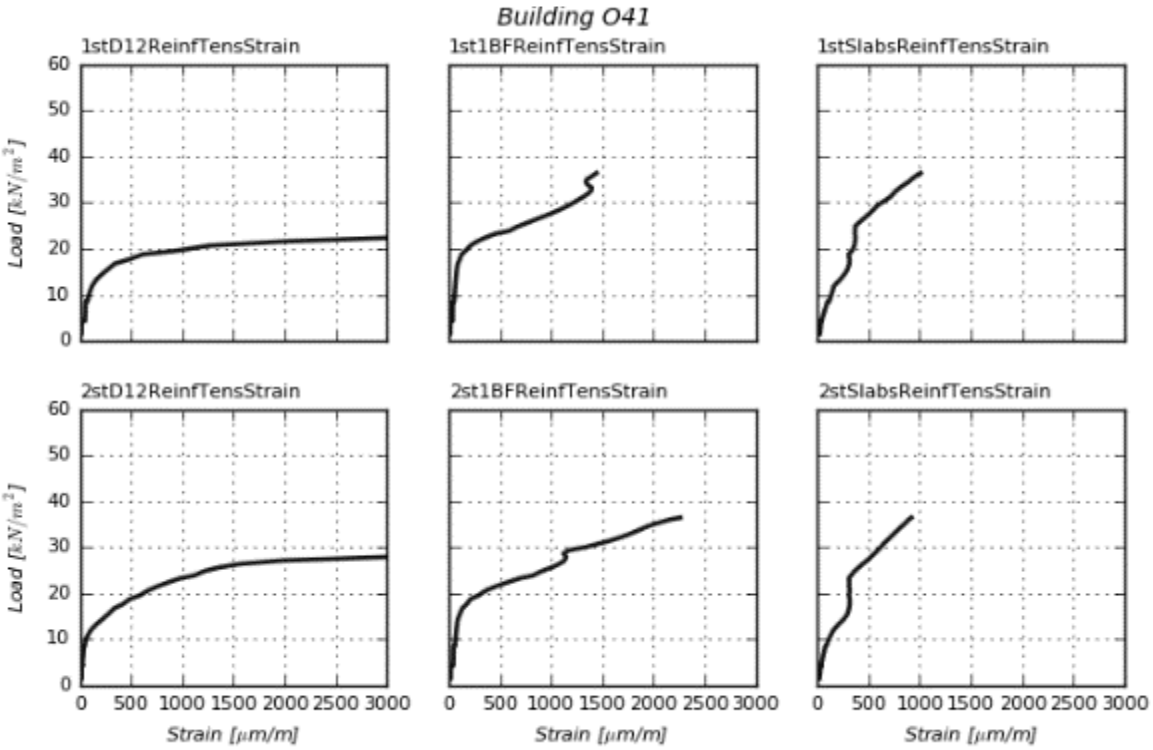
Building O41
1stD12ReinfTensStrain
1st1BFReinfTensStrain
1stSlabsReinfTensStrain
2stD12ReinfTensStrain
2st1BFReinfTensStrain
2stSlabsReinfTensStrain
Load [kN/m²]
Strain [μm/m]
0
10
20
30
40
50
60
0
500
1000
1500
2000
2500
3000

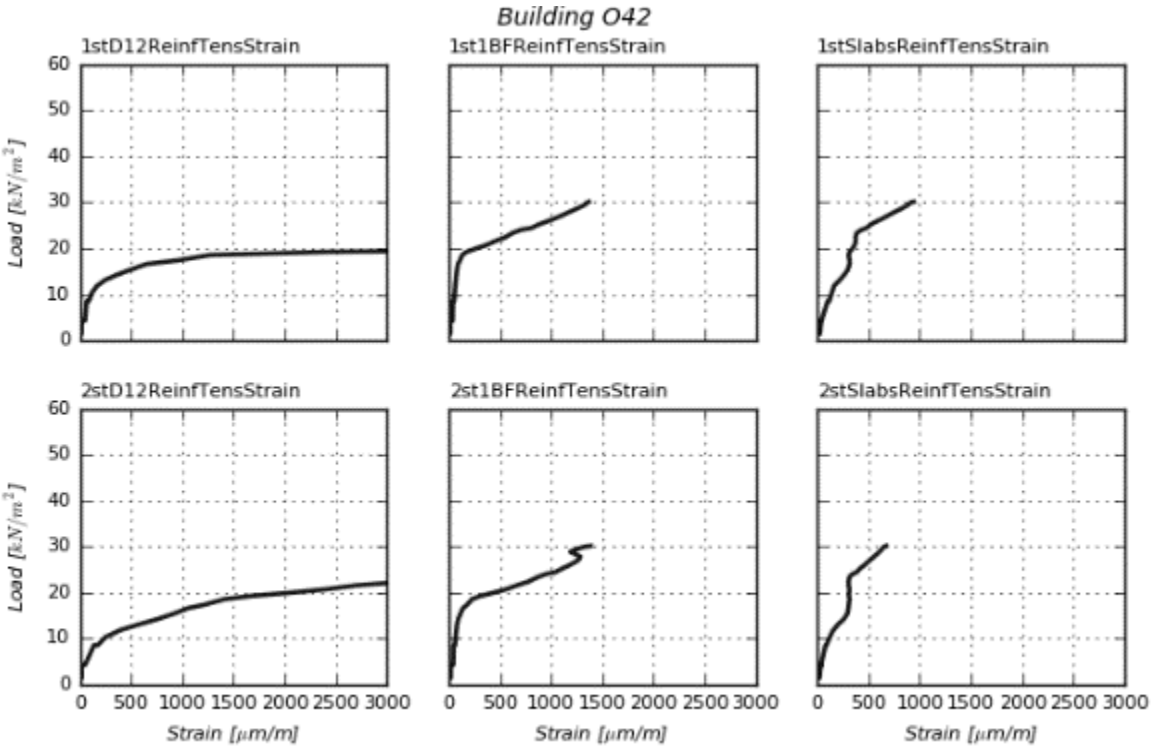
Building O42
1stD12ReinfTensStrain
1st1BFReinfTensStrain
1stSlabsReinfTensStrain
2stD12ReinfTensStrain
2st1BFReinfTensStrain
2stSlabsReinfTensStrain
Load [kN/m²]
Strain [μm/m]
0
10
20
30
40
50
60
0 500 1000 1500 2000 2500 3000

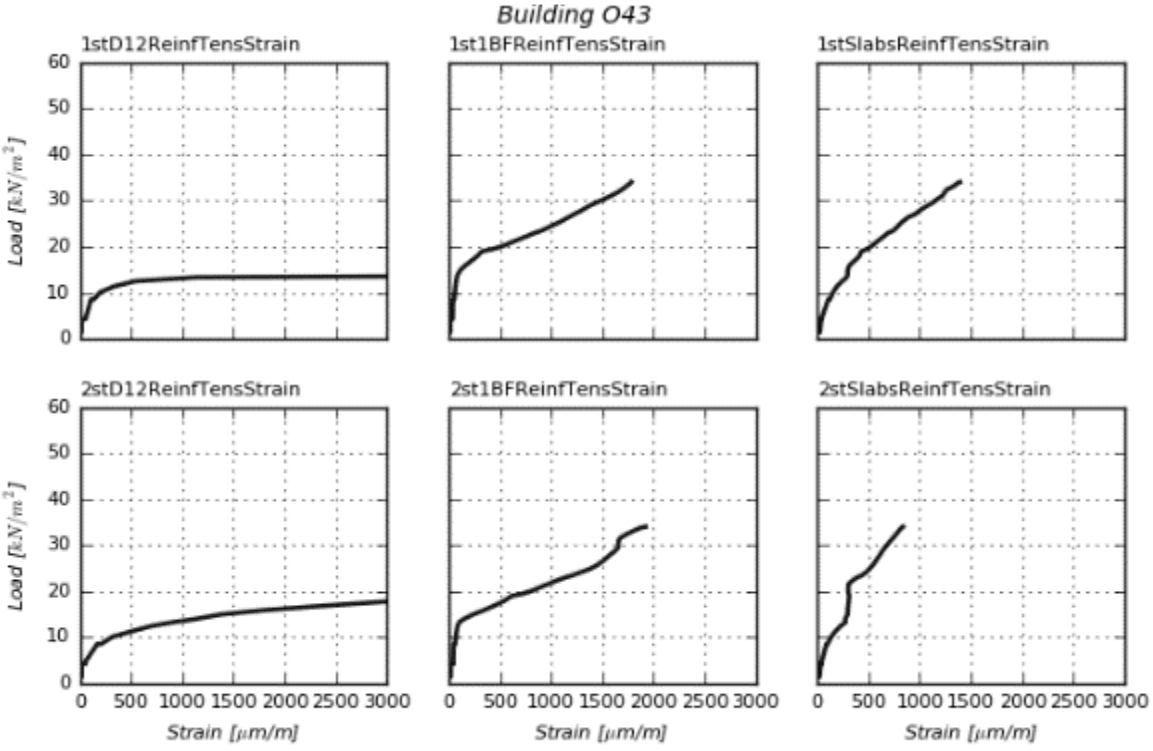
Building O43
1stD12ReinfTensStrain
1st1BFReinfTensStrain
1stSlabsReinfTensStrain
2stD12ReinfTensStrain
2st1BFReinfTensStrain
2stSlabsReinfTensStrain
Load [kN/m²]
Strain [μm/m]
0
10
20
30
40
50
60
0 500 1000 1500 2000 2500 3000

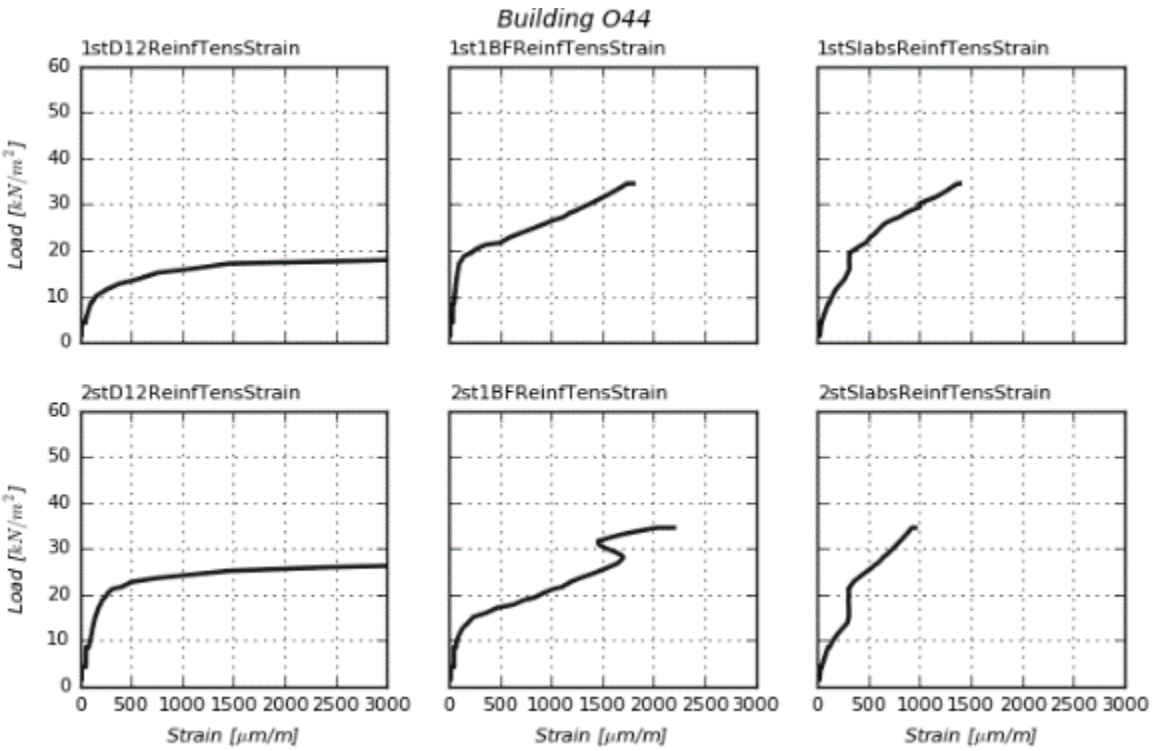
Building O44
1stD12ReinfTensStrain
1st1BFReinfTensStrain
1stSlabsReinfTensStrain
2stD12ReinfTensStrain
2st1BFReinfTensStrain
2stSlabsReinfTensStrain
Load [kN/m²]
Strain [μm/m]
0
10
20
30
40
50
60
0
500
1000
1500
2000
2500
3000

A7 – Building original plans and reinforcement details

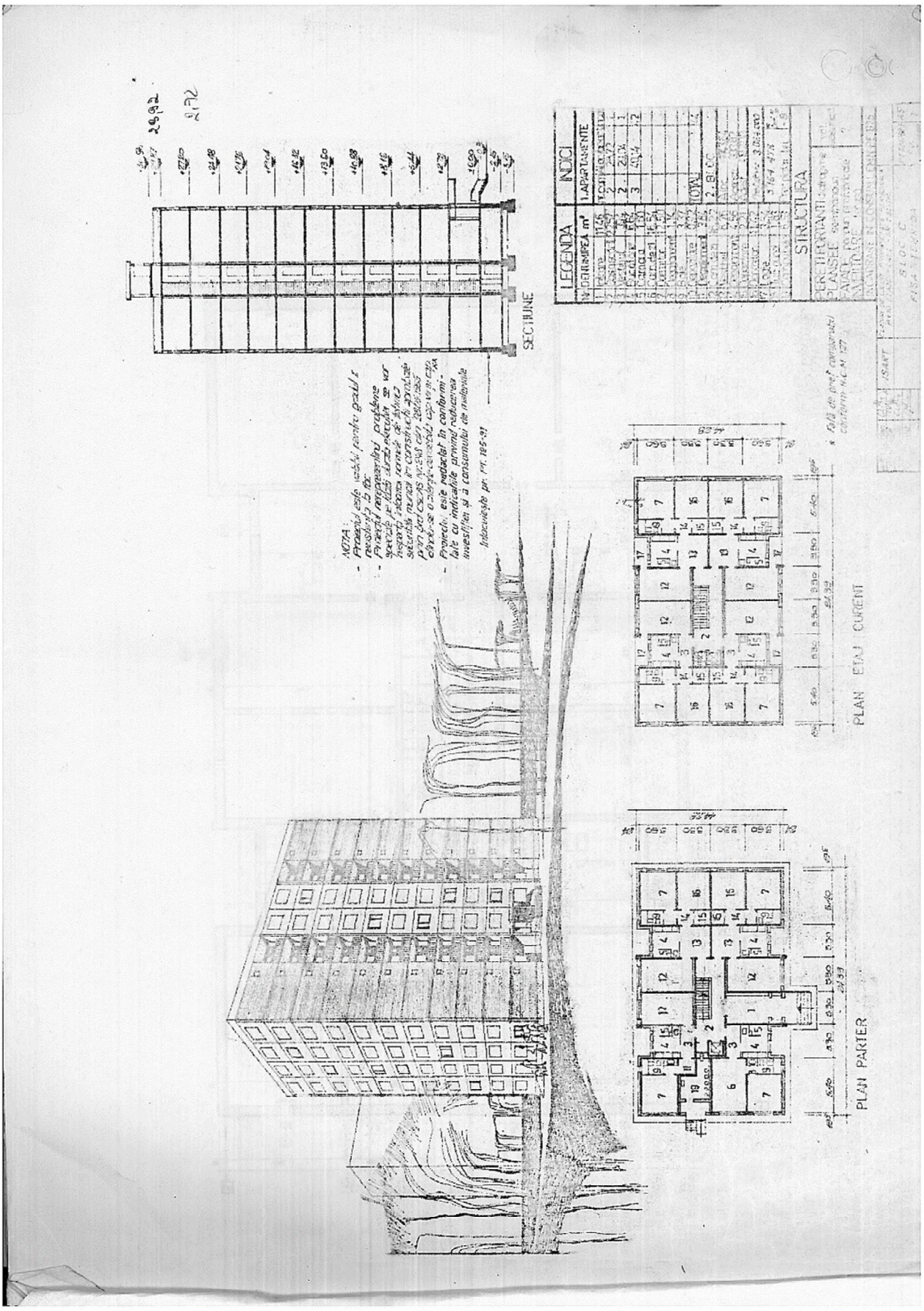

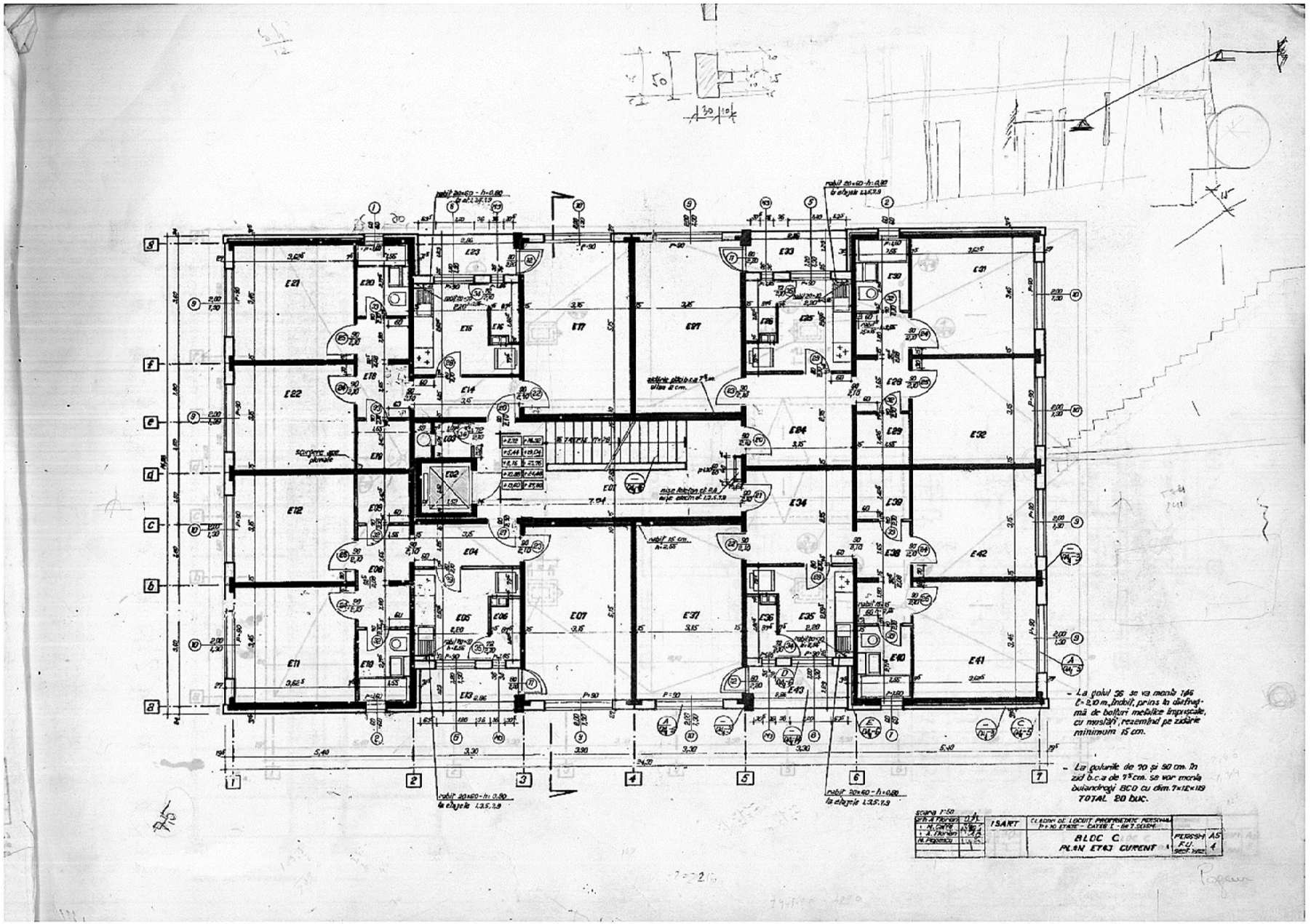
- La golul 36 se va monta 1#5 L= 2,10 m, îndoit, prins în diafragmă de bolțuri metalice înșurubate, cu mastic, rezemat pe zăbrele minimum 15 cm.
- La golurile de 70 și 90 cm. în zid b.c.a de 75 cm. se vor monta buiandrugi BCO cu dim. 7×12×19 TOTAL 80 buc.
ISART
BLOC C
PLAN ET#3 CURENT

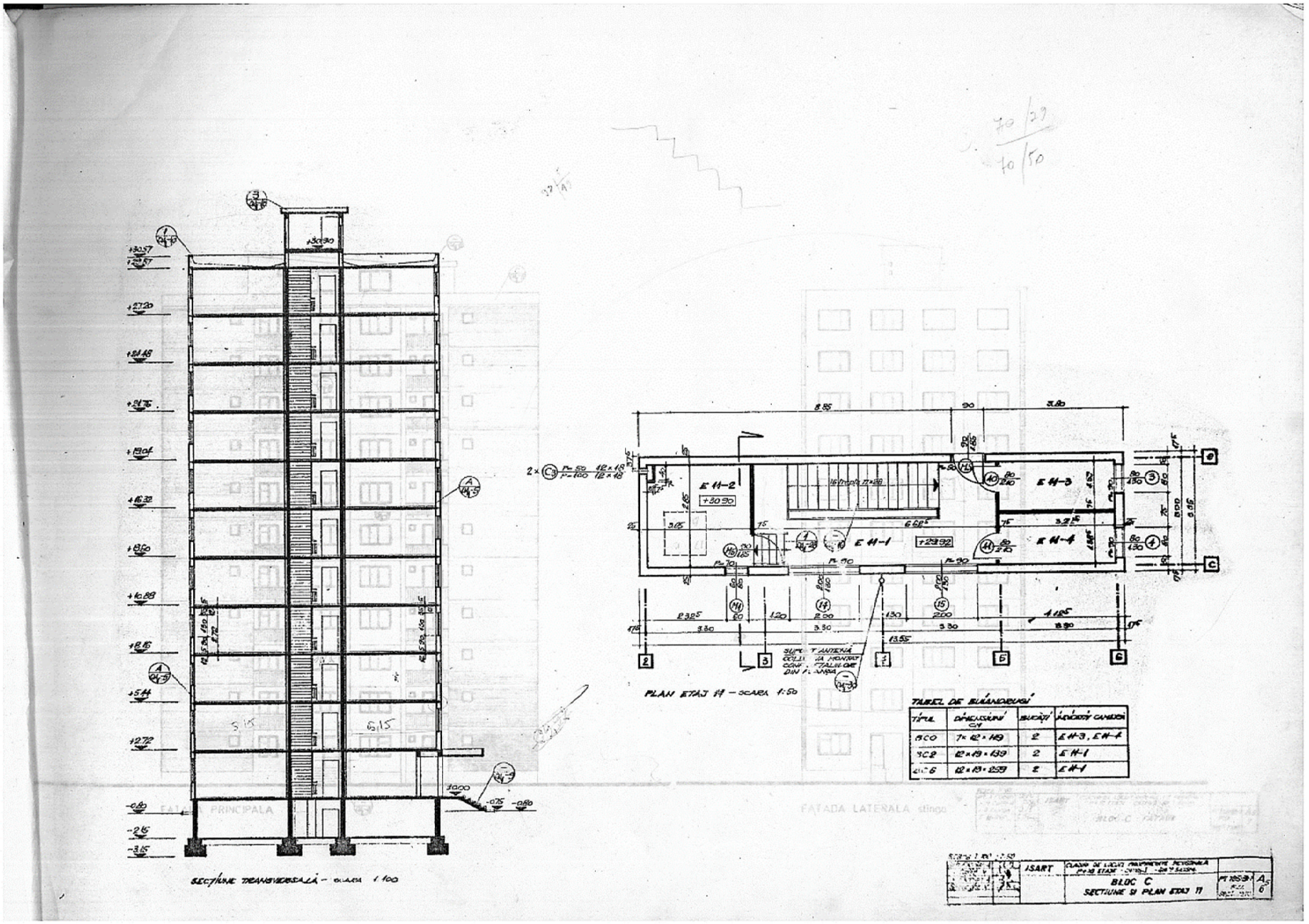
SECȚIUNE TRANSVERSALĂ – SCARA 1:100
PLAN ETAJ 11 – SCARA 1:50
TABEL DE ELEMENTE
BLOC C
SECȚIUNE ȘI PLAN ETAJ 11
ISART

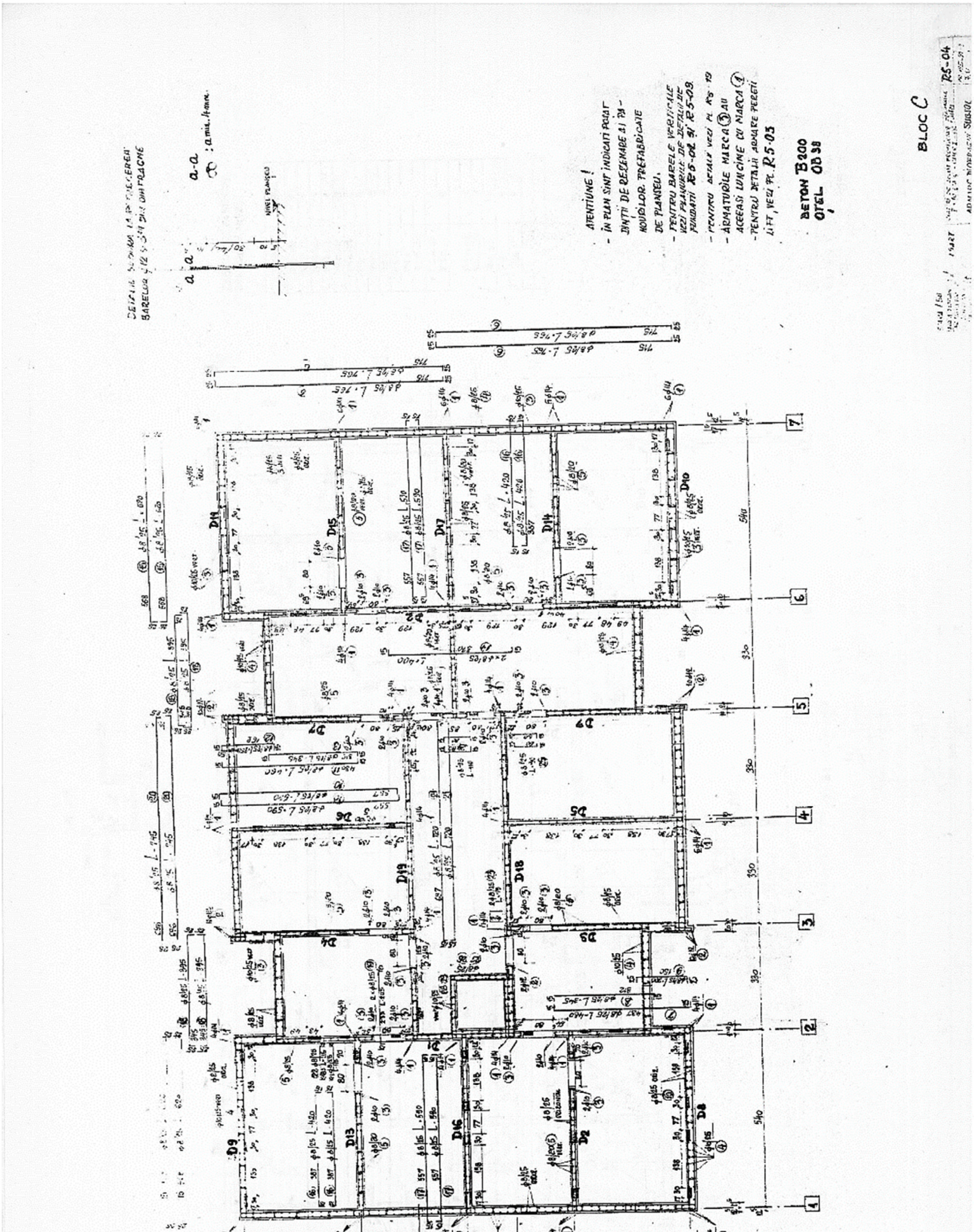
ATENȚIUNE !
BETON B200
OTEL OB38
BLOC C
RS-04

Secțiune 1-1

Detalii buiandrugi – goluri trecere

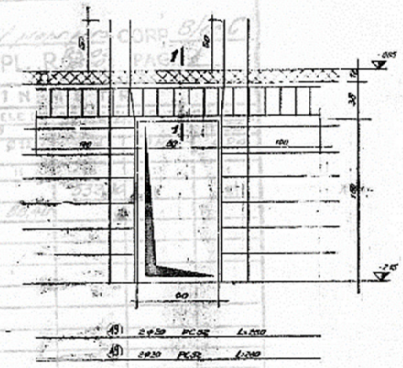

Goluri în pereți exteriori

Secțiune 2-2

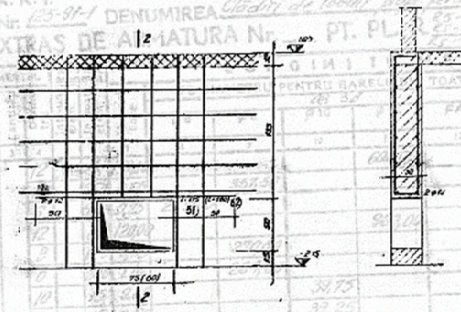

Goluri instalații în pereți interiori

Secțiune 3-3

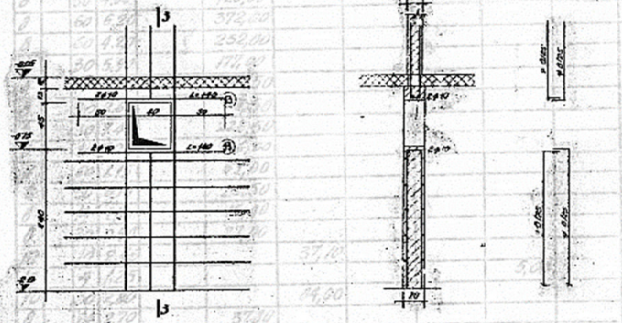

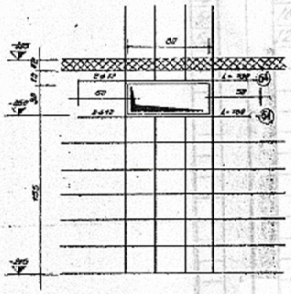

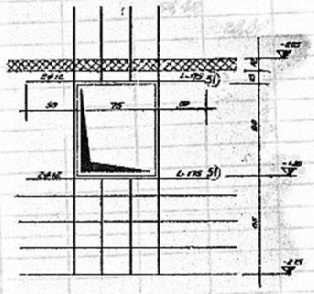

OB 38

BLOC C

ISANI

R5-19

Detalii armare diafragme subsol

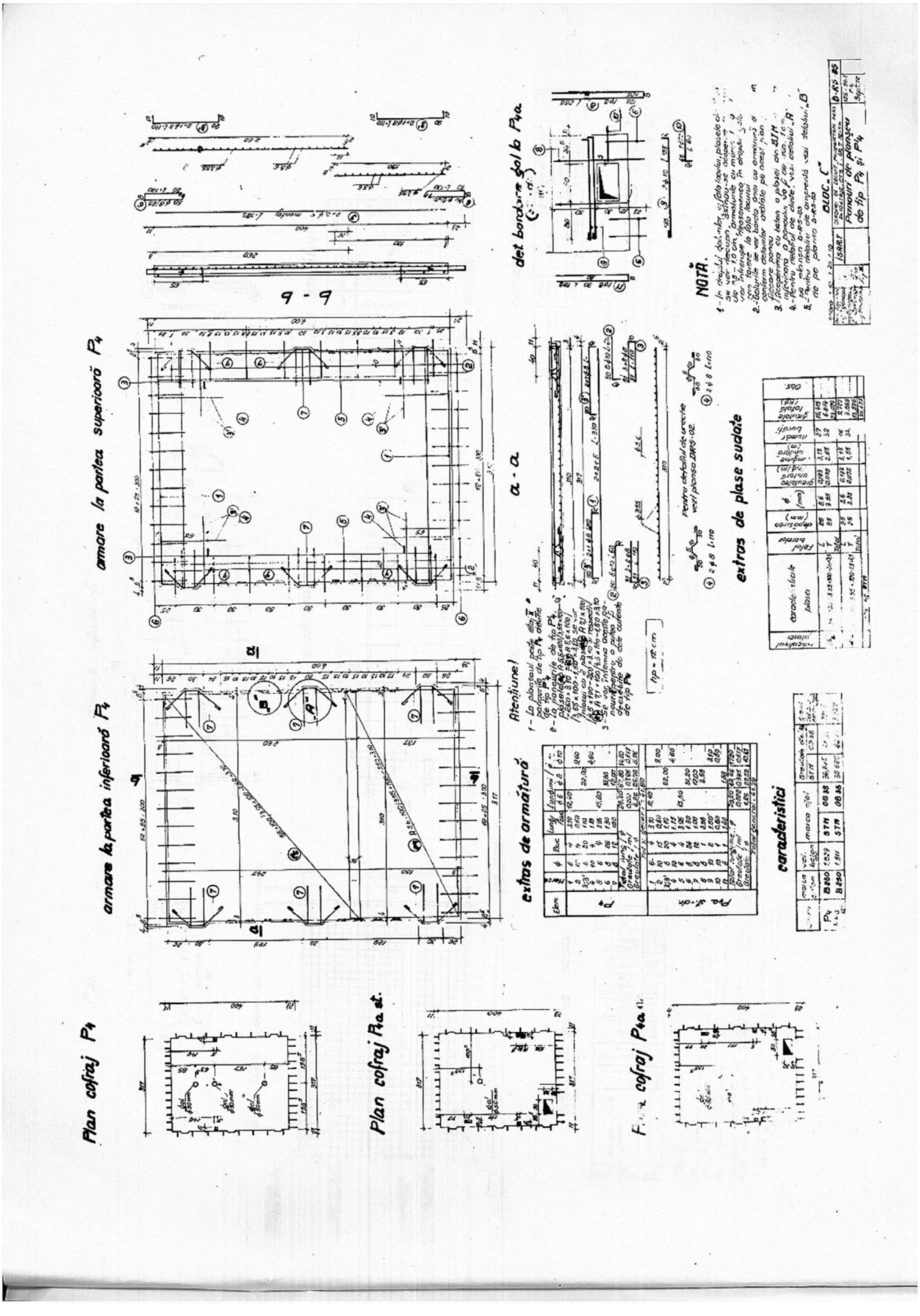
Plan cofraj P4
Plan cofraj P4a st.
Plan cofraj P4a dr.
armare la partea inferioară P4
armare la partea superioară P4
extras de armătură
caracteristici
a - a
b - b
det bordare gol la P4a
extras de plase sudate
Atenţiune!
NOTĂ.
BLOC "C"
Panouri de planşeu de tip P4 şi P4a

PANOU EXTERIOR F2

SECȚIUNE A-A

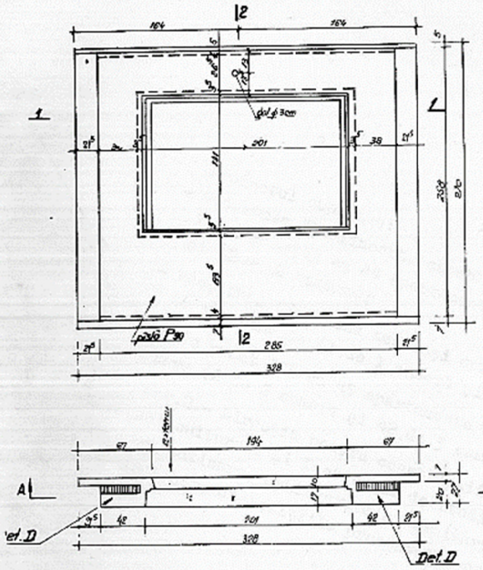

SECȚIUNE 2-2

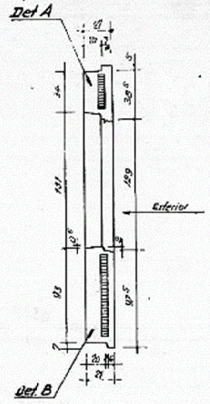

ARMARE STRAT INTERIOR

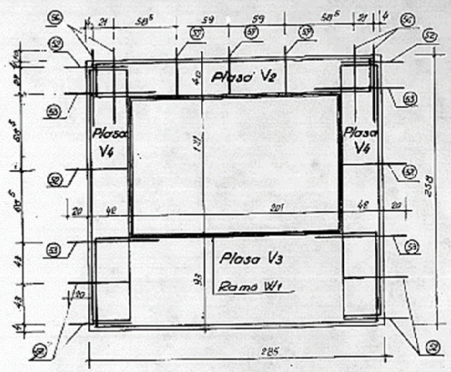

ARMARE STRAT EXTERIOR

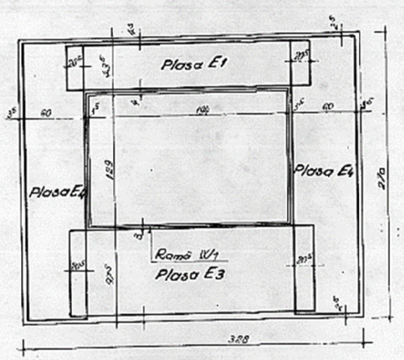

EXTRAS DE ARMĂTURĂ

Plasa sau marca	Buc	Greutate pe diametre				
		STM	OB 38			
		φ3	φ6	φ8	φ10	φ12
Plasa V2	1		1,22		6,30	
" " V3	1		2,38	1,92	6,30	
" " V4	2		2,28	7,60		
Bara 52	8				3,20	
" " 55	4				2,60	
" " 56	4					5,68
" " 57	3		0,69			
Plasa E1	1	1,49				
" " E3	1	2,85				
" " E4	2	6,80				
Ramă W1	1		1,73	5,43		
Greutate totală φ		11,14	5,20	14,95	18,40	5,68
Greutate totală		58,47 kg				

CARACTERISTICI

Denumire element	Volum beton	Greutate element	Greutate oțel	Pîslă P90	Marcă beton	Marcă oțel
	m^3	Kg	Kg	m^2		
Panou F2	1,33	3450	58,47	4,289	B 250	OB 38 și STM

NOTĂ

Pentru detaliile A, B, D vezi planșa Nr. D-R5-14
Pentru detaliile de plase vezi planșa Nr. D-R5-15

BLOC „C"

		ISART	CLĂDIRI DE LOCUINȚE ...	D-R5-13
		Scara 1:20	BLOC C PANOU FAȚADĂ F2	185-91-1 FU Sept. 1992